

Improved Synthesis and Enhanced Reactivity of *X*-BODIPYs

by

Travis Lee Lundrigan

Submitted in partial fulfilment of the requirements
for the degree of Doctor of Philosophy

at

Dalhousie University
Halifax, Nova Scotia
December 2017

TABLE OF CONTENTS

List of Tables	vi
List of Figures	vii
List of Schemes.....	ix
Abstract.....	xi
List of Abbreviations and Symbols Used	xii
Acknowledgements.....	xiv
Chapter 1 – Introduction	1
1.1 – Structure and Properties of Dipyrrinato Ligands	1
1.2 – Synthesis of Dipyrrins.....	2
1.3 – Dipyrrinato Complexes	4
1.4 – Structure and Properties of <i>F</i> -BODIPY Dyes.....	5
1.5 – <i>F</i> -BODIPY Synthesis.....	6
1.6 – Boron Substitution of BODIPY Dyes	7
1.7 – Thesis Overview.....	8
Chapter 2 – Improved Synthesis of <i>F</i> -BODIPYs	9
2.1 – Background	9
2.2 – Project Goals	13
2.3 – Results and Discussion.....	14
2.3.1 – Development of Synthetic Methodology	14
2.3.2 – Synthesis of bis(<i>F</i> -BODIPY)s	21
2.4 - Conclusions.....	26
Chapter 3 – <i>Cl</i> -BODIPYs	27
3.1 – General Background.....	27
3.2 – Project Goals	31
3.3 – Results and Discussion.....	32
3.3.1 – Synthesis of <i>Cl</i> -BODIPYs	32
3.3.2 – Reactivity of <i>Cl</i> -BODIPYs	36
3.3.3 – Conversion of <i>F</i> -BODIPY to <i>Cl</i> -BODIPY	40
3.3.4 – Using <i>Cl</i> -BODIPY as a Synthetic Intermediate.....	47
3.3.5 – Synthesis of Chiral <i>O</i> -BODIPYs	53
3.3.6 – Chiroptical Properties of Chiral Compounds.....	61

3.3.7 – Comparison of Spectroscopical Properties	68
3.4 – Conclusions	70
Chapter 4 – Activation and Deprotection of <i>F</i> -BODIPYs.....	72
4.1 – General Background.....	72
4.2 – Project Goals	73
4.3 – Results and Discussion.....	74
4.3.1 – Deprotection of <i>F</i> -BODIPYs using <i>X</i> -BODIPY intermediates	74
4.3.2 – Activation and deprotection of <i>F</i> -BODIPYs using BF ₃ •OEt ₂	82
4.4 – Conclusions	95
Chapter 5 – Experimental	97
5.1 – General Experimental.....	97
5.1.1 General Procedure for Emission Measurements	98
5.2 – Synthesis of Compounds.....	98
1,3,5,7-Tetramethyl-2-octyl-8- <i>H</i> -4-bora-3a,4a-diaza- <i>s</i> -indacene (1BF ₂).....	99
1,3,5,7-Tetramethyl-2-ethyl-8- <i>H</i> -4-bora-3a,4a-diaza- <i>s</i> -indacene (2BF ₂).....	99
1,3,5,7-Tetramethyl-2,6-diethyl-8- <i>H</i> -4-bora-3a,4a-diaza- <i>s</i> -indacene (3BF ₂).....	100
1,3,5,7-Tetramethyl-2,6-diethyl-8-phenyl-4-bora-3a,4a-diaza- <i>s</i> - indacene (5BF ₂).....	101
3-Methyl-1,5,7-triethyl-2-ethylcarboxylato-8- <i>H</i> -4-bora-3a,4a-diaza- <i>s</i> - indacene (6BF ₂).....	102
1,3,6-Trimethyl-2-(2-methoxy-2-oxoethyl)-7-ethyl-8- <i>H</i> -4,4'-difluoro- bora-3a,4a-diaza- <i>s</i> -indacene (7BF ₂).....	103
8-Phenyl-4-bora-3a,4a-diaza- <i>s</i> -indacene (8BF ₂)	104
1,7-Bis(5-((<i>Z</i>)-(4-ethyl-3,5-dimethyl-2 <i>H</i> -pyrrol-2-ylidene)methyl)-2,4- dimethyl-1 <i>H</i> -pyrrol-3-yl)hexane dihydrobromide (12•2HBr).....	104
1,7-Bis(1,3,5,7-tetramethyl-2-ethyl-8- <i>H</i> -4-bora-3a,4a-diaza- <i>s</i> - indacene)hexane (12BF ₂).....	106
1,7-Bis(5-((<i>Z</i>)-(4-ethyl-3,5-dimethyl-2 <i>H</i> -pyrrol-2-ylidene)methyl)-2,4- dimethyl-1 <i>H</i> -pyrrol-3-yl)heptane dihydrobromide (15•2HBr).....	106
1,7-Bis(1,3,5,7-tetramethyl-2-ethyl-8- <i>H</i> -4-bora-3a,4a-diaza- <i>s</i> - indacene)heptane (15BF ₂).....	108
1,3,5,7-Tetramethyl-2,6-diethyl-8-phenyl-4,4'-dichloro-bora-3a,4a- diaza- <i>s</i> -indacene (3BCl ₂)	108
1,3,5,7-Tetramethyl-2,6-diethyl-8- <i>H</i> -4,4'-dimethoxy-bora-3a,4a-diaza- <i>s</i> -indacene (3B(OMe) ₂)	111

1,3,5,7-Tetramethyl-2,6-diethyl-8-phenyl-4,4'-dimethoxy-bora-3a,4a-diaza- <i>s</i> -indacene (5B(OMe) ₂)	111
1,3,5,7-Tetramethyl-2,6-diethyl-8- <i>H</i> -4,4'-diphenyl-bora-3a,4a-diaza- <i>s</i> -indacene (3BPh ₂).....	112
1,3,5,7-Tetramethyl-2,6-diethyl-8- <i>H</i> -4,4'-diethyl-bora-3a,4a-diaza- <i>s</i> -indacene (3BEt ₂)	113
1,3,5,7-Tetramethyl-2,6-diethyl-8-phenyl-4,4'-diethyl-bora-3a,4a-diaza- <i>s</i> -indacene (5BEt ₂).....	114
1,3,5,7-Tetramethyl-2,6-diethyl-8- <i>H</i> -4,4'-dimethoxy-bora-3a,4a-diaza- <i>s</i> -indacene (3 ¹¹ B(OMe) ₂)	114
1,3,5,7-Tetramethyl-2,6-diethyl-8- <i>H</i> -4,4'-difluoro-bora-3a,4a-diaza- <i>s</i> -indacene (3 ¹¹ BF ₂).....	115
1,3,5,7-Tetramethyl-2-ethyl-8- <i>H</i> -4,4'-diethyl-bora-3a,4a-diaza- <i>s</i> -indacene (2BEt ₂)	116
1,3,6-Trimethyl-2-(2-methoxy-2-oxoethyl)-7-ethyl-8- <i>H</i> -4,4'-diethyl-bora-3a,4a-diaza- <i>s</i> -indacene (7BEt ₂)	116
8-Phenyl-4,4'-diethyl-bora-3a,4a-diaza- <i>s</i> -indacene (8BEt ₂)	117
1,3,5,7-Tetramethyl-2,6-diethyl-8- <i>H</i> -4,4'-[propane-1,3-bis(olate)]-bora-3a,4a-diaza- <i>s</i> -indacene (17)	117
1,3,5,7-Tetramethyl-2,6-diethyl-8- <i>H</i> -4,4'-[(1,1'-binaphthalene)-2,2'-bis(olate)]-bora-3a,4a-diaza- <i>s</i> -indacene (18)	118
1,3,5,7-Tetramethyl-2,6-diethyl-8- <i>H</i> -4,4'-[(1,1'-binaphthalene)-2,2'-bis(olate)]-bora-3a,4a-diaza- <i>s</i> -indacene (19)	119
1,3,5,7-Tetramethyl-2,6-diethyl-8-phenyl-4,4'-[(1,1'-binaphthalene)-2,2'-bis(olate)]-bora-3a,4a-diaza- <i>s</i> -indacene (20)	120
1,3,5,7-Tetramethyl-2,6-diethyl-8-phenyl-4,4'-[(1,1'-binaphthalene)-2,2'-bis(olate)]-bora-3a,4a-diaza- <i>s</i> -indacene (21)	121
(<i>Z</i>)-3-Ethyl-5-((4-ethyl-3,5-dimethyl-2 <i>H</i> -pyrrol-2-ylidene)methyl)-2,4-dimethyl-1 <i>H</i> -pyrrole hydrochloride (3HCl).....	122
(<i>Z</i>)-2-((4-Ethyl-3,5-dimethyl-2 <i>H</i> -pyrrol-2-ylidene)methyl)-3,5-dimethyl-1 <i>H</i> -pyrrole hydrochloride (2HCl).....	122
(<i>Z</i>)-2-((3,5-Dimethyl-2 <i>H</i> -pyrrol-2-ylidene)methyl)-3,5-dimethyl-1 <i>H</i> -pyrrole hydrochloride (4HCl)	123
(<i>Z</i>)-3-Ethyl-5-((4-ethyl-3,5-dimethyl-2 <i>H</i> -pyrrol-2-ylidene)(phenyl)methyl)-2,4-dimethyl-1 <i>H</i> -pyrrole hydrochloride (5HCl)	123
(<i>Z</i>)-1-(2-((4-Heptanoyl-3,5-dimethyl-1 <i>H</i> -pyrrol-2-yl)methylene)-3,5-dimethyl-2 <i>H</i> -pyrrol-4-yl)heptan-1-one hydrochloride (22HCl)	124

(Z)-1-(2-((4-Acetyl-3,5-dimethyl-1 <i>H</i> -pyrrol-2-yl)(phenyl)methylene)-3,5-dimethyl-2 <i>H</i> -pyrrol-4-yl)ethanone hydrochloride (23HCl)	124
(Z)-Ethyl 2-((3,4-dimethyl-1 <i>H</i> -pyrrol-2-yl)methylene)-3-ethyl-5-methyl-2 <i>H</i> -pyrrole-4-carboxylate hydrobromide (24HBr)	125
1,3,5,7-Tetramethyl-2,6-diethyl-8- <i>H</i> -4,4'-dibromo-bora-3a,4a-diaza- <i>s</i> -indacene (3BBr ₂)	125
(Z)-3-Ethyl-5-((4-ethyl-3,5-dimethyl-2 <i>H</i> -pyrrol-2-ylidene)methyl)-2,4-dimethyl-1 <i>H</i> -pyrrole tetrafluoroborate (3HBF ₄)	126
(Z)-2-((4-Ethyl-3,5-dimethyl-2 <i>H</i> -pyrrol-2-ylidene)methyl)-3,5-dimethyl-1 <i>H</i> -pyrrole tetrafluoroborate (2HBF ₄)	127
(Z)-2-((3,5-Dimethyl-2 <i>H</i> -pyrrol-2-ylidene)methyl)-3,5-dimethyl-1 <i>H</i> -pyrrole tetrafluoroborate (4HBF ₄)	127
(Z)-3-Ethyl-5-((4-ethyl-3,5-dimethyl-2 <i>H</i> -pyrrol-2-ylidene)(phenyl)methyl)-2,4-dimethyl-1 <i>H</i> -pyrrole tetrafluoroborate (5HBF ₄)	128
(Z)-2-(Phenyl(2 <i>H</i> -pyrrol-2-ylidene)methyl)-1 <i>H</i> -pyrrole tetrafluoroborate (8HBF ₄)	128
(Z)-3-Ethyl-5-((4-ethyl-3,5-dimethyl-2 <i>H</i> -pyrrol-2-ylidene)methyl)-2,4-dimethyl-1 <i>H</i> -pyrrole hydrobromide (3HBr)	129
Chapter 6 – Conclusions	130
6.1 – Conclusions	130
References	132
Appendix A: X-ray Analysis Data	137
Appendix B: NMR Data for Synthesized Compounds	140

List of Tables

Table 1: Ratio of dipyrin to F-BODIPY with varying equiv of $\text{BF}_3 \cdot \text{OEt}_2$	12
Table 2: Synthesis of F-BODIPYs via dipyrinato lithium salts using 1 equiv $\text{BF}_3 \cdot \text{OEt}_2$	18
Table 3: Summary of F-BODIPY 3BF_2 and Cl-BODIPY 3BCl_2 reactivity	39
Table 4: ^{11}B NMR chemical shift data for the spectrum in Figure 5.	44
Table 5: Synthesis of C-BODIPYs from F-BODIPYs using Cl-BODIPY intermediates	51
Table 6: Synthesis of chiral O-BODIPYs by substitution at boron atom	61
Table 7: Spectroscopic data of chiral BODIPY compounds	65
Table 8: Molar ellipticities of chiral BODIPY compounds 18-21	67
Table 9: Conversion of F-BODIPYs to dipyrin HCl salts	78
Table 10: Conversion of F-BODIPYs to dipyrin HBF_4 salts	85

List of Figures

Figure 1: Numbering system for dipyrrens (left) and BODIPYs (right) according to IUPAC.....	1
Figure 2: Constitutional isomers of bis(dipyrrens)s	10
Figure 3: Resonance structures of the β -diketiminato anion	27
Figure 4: ^{11}B NMR stack-plot revealing the conversion of F-BODIPY to Cl-BODIPY. Bottom = F-BODIPY 3BF_2 ; middle = F-BODIPY 3BF_2 and Cl-BODIPY 3BCl_2 after the addition of 0.5 equiv BCl_3 to the solution of 3BF_2 ; top = only Cl-BODIPY 3BCl_2 present after the addition of 1.0 equiv BCl_3	42
Figure 5: ^{11}B NMR spectrum showing the crude reaction mixture corresponding to Scheme 23, revealing the formation of boron trihalide by-products	44
Figure 6: Chiral F-BODIPYs incorporating homochirality via the meso-position.....	54
Figure 7: Chiral BODIPYs isolated using chiral resolution	55
Figure 8: CD spectra of compounds 18 (blue), 19 (red) and (S)-BINOL (inset) in CH_2Cl_2	63
Figure 9: Isolated section of CD spectra of 18/19 (top), UV/Vis spectrum of 18 (bottom).....	64
Figure 10: CD spectra of compounds 20 and 21.....	65
Figure 11: Comparison of CD spectra between compounds 19, 21 and (S)-BINOL at the same concentration (1.3×10^{-5} M).	67
Figure 12: Comparison of normalized UV-vis data of various analogues of compound 3.....	68
Figure 13: Comparison of normalized emission data of various analogues of compound 3.....	70
Figure 14: Proposed mechanism of Cl-BODIPY deprotection.....	76
Figure 15: ^{11}B NMR of 3BBr_2 in CDCl_3	81
Figure 16: ^{11}B NMR of 3HBF_4 in CDCl_3	83
Figure 17: Ellipsoid diagram (50%, H atoms omitted) of 2HBF_4	86
Figure 18: Proposed activation of F-BODIPYs of BF_3	89
Figure 19: Variable temperature ^{11}B NMR spectra B-E of 3BF_2 and $\text{BF}_3 \cdot \text{OEt}_2$. Spectrum A overlays the NMR spectra for 3BF_2 and $\text{BF}_3 \cdot \text{OEt}_2$, separately, at room temperature. All spectra were obtained using CDCl_3 as the solvent.	91
Figure 20: Variable temperature ^{19}F NMR spectra B-F of 3BF_2 and $\text{BF}_3 \cdot \text{OEt}_2$. Spectrum A overlays the NMR spectra for 3BF_2 and $\text{BF}_3 \cdot \text{OEt}_2$, separately, at room temperature. All spectra were obtained using CDCl_3 as the solvent.	92

Figure 21: Proposed mechanism for the deprotection of F-BODIPYs using
BF₃•OEt₂ 94

List of Schemes

Scheme 1: MacDonald coupling reaction to form dipyrrens.....	3
Scheme 2: Acid-catalyzed synthesis of dipyrrens	3
Scheme 3: Synthesis of dipyrrens through the oxidation of dipyrromethanes	4
Scheme 4: General dipyrrenato complexation.....	5
Scheme 5: Synthesis of F-BODIPYs. Top = starting from isolated dipyrren. Bottom = starting from α -free pyrrole and forming the dipyrren in situ	7
Scheme 6: Synthesis of 1 and 1BF ₂ from hydrobromide salt 1HBr	11
Scheme 7: Synthesis of scrambled F-BODIPYs from unsymmetrical dipyrren 2HBr	13
Scheme 8: Synthesis of lithium complex.....	14
Scheme 9: Initial trials of F-BODIPY synthesis using dipyrrenato lithium salts.....	15
Scheme 10: Synthesis of F-BODIPY from HBr salt of dipyrren	16
Scheme 11: Synthesis of F-BODIPY via in situ trapping of dipyrren	20
Scheme 12:: Synthesis of bis(dipyrren) salt 12•2HBr.....	22
Scheme 13: Synthesis of bis(dipyrren) salt 15•2HBr	23
Scheme 14: Synthesis of bis(F-BODIPY)s from dipyrrenato dilithium salts	24
Scheme 15: Attempted synthesis of monocomplexed bis(dipyrrenato) species.....	25
Scheme 16: Synthesis of β -diketiminato boron dihalide complexes	28
Scheme 17: Synthesis of first BODIPY containing a chloro substituent on boron	29
Scheme 18: Synthesis of first O-BODIPYs using BBr ₃	29
Scheme 19: Synthesis of boronium cations	31
Scheme 20: Synthesis of Cl-BODIPYs via dipyrrenato lithium salts	33
Scheme 21: Synthesis of Cl-BODIPYs from free-base dipyrrens.....	36
Scheme 22: Synthesis of C- and O-BODIPYs from Cl-BODIPYs	37
Scheme 23: Conversion of F-BODIPY to Cl-BODIPY	41
Scheme 24: Conversion of F-BODIPY to Cl-BODIPY in diethyl ether	44
Scheme 25: Synthesis of ¹¹ B labelled F-BODIPY	46
Scheme 26: Potential pathways I and II for F-BODIPY to Cl-BODIPY conversion.....	46
Scheme 27: Synthesis of O-BODIPY (3B(OMe) ₂) and C-BODIPY (3BEt ₂) from F- BODIPY (3BF ₂) using a Cl-BODIPY intermediate generated in situ	49
Scheme 28: Preparation of cyclic O-BODIPY 17	53
Scheme 29: Synthesis of racemic O-BODIPY	57

Scheme 30: Chiral O-BODIPYs developed by de la Moya.....	57
Scheme 31: Synthesis of chiral O-BODIPY 18 using (R)-BINOL.	60
Scheme 32: F-BODIPY deprotection strategies using microwave-assisted conditions ...	73
Scheme 33: Deprotection of Cl-BODIPY with water.....	76
Scheme 34: Deprotection of F-BODIPYs using Cl-BODIPY intermediate.....	77
Scheme 35: Synthesis of a Br-BODIPY	82
Scheme 36: Deprotection of F-BODIPYs with BF ₃ •OEt ₂ and water	85
Scheme 37: Exchange of BF ₄ ⁻ counter-ion with Br ⁻	88
Scheme 38: Synthesis of C-BODIPY from activated F-BODIPY.....	89
Scheme 39: Deprotection of labelled F-BODIPY affording an unlabelled HBF ₄ salt	93

Abstract

F-BODIPYs are most known for their high thermal and photochemical stability, being quite chemically robust and having tunable fluorescence properties. This thesis focuses on three general areas of BODIPY chemistry: the synthesis of *F*-BODIPYs; substitution at the boron centre; and deprotection of BODIPY compounds to afford the parent dipyrin after removal of the boron centre.

An improved methodology for the synthesis of *F*-BODIPYs from dipyrins and bis(dipyrin)s has been developed. This strategy employs lithium salts of dipyrins as intermediates that are then treated with only 1 equiv of boron trifluoride diethyl etherate to obtain the corresponding *F*-BODIPYs. This scalable route to *F*-BODIPYs renders high yields with a facile purification process involving merely filtration of the reaction mixture through Celite in many cases.

The first *Cl*-BODIPYs have been synthesized in high yields from the reaction of dipyrins with boron trichloride under air- and moisture-free conditions. These are a new class of BODIPY that enable extremely facile substitution at boron compared to their analogous *F*-BODIPYs, opening up a new pathway to BODIPYs functionalized at boron. Another method for the synthesis of *Cl*-BODIPYs has also been developed, starting from the *F*-BODIPY and simply treating it with boron trichloride. *Cl*-BODIPYs are exploited as synthetic intermediates generated in situ for the overall conversion of *F*-BODIPYs to *O*- and *C*-BODIPYs in high overall yields using a mild one-pot procedure. This route enables *F*-BODIPYs to be transformed into derivatives that are not accessible via the direct route and has led to the formation of chiral *O*-BODIPYs and the study of their spectroscopic properties.

The reactivity of *F*-BODIPYs with various boron trihalides has been investigated and has shown that activation occurs. The treatment of the activated *F*-BODIPY with a nucleophile affects facile substitution at boron; however, using water as the nucleophile promotes deprotective removal of the $-\text{BF}_2$ moiety and thereby desirable production of the corresponding parent dipyrin salt in quantitative yield under extremely mild conditions.

List of Abbreviations and Symbols Used

APCI:	Atmospheric-pressure chemical ionization
BINOL:	1,1'-Bi-2-naphthol
BODIPY:	Borondifluoride dipyrinato
brs:	Broad singlet
CD:	Circular dichroism
CPL:	Circularly polarized luminescence
d:	Doublet
DDQ:	2,2-dichloro-5,6-dicyano-1,4-benzoquinone
ECD:	Electronic circular dichroism
EI:	Positive ion detected electron impact ionization
Equiv:	Equivalents
ESI:	Electrospray ionization
Et:	Ethyl
h:	Hour
HRMS:	High resolution mass spectrometry
IUPAC:	International Union of Pure and Applied Chemistry
<i>J</i> :	Coupling constant
LiHMDS:	Lithium hexamethyldisilazide
m:	Multiplet
MHz:	Megahertz
min:	Minutes
MS:	Mass spectrometry
<i>m/z</i> :	Mass-to-charge ratio

NMR:	Nuclear magnetic resonance
OMe:	Methoxy
ppm:	Parts per million
q:	Quartet
s:	Singlet
t:	Triplet
THF:	Tetrahydrofuran
TOFMS:	Time-of-flight mass spectrometry
UV-vis:	Ultraviolet-visible
δ :	Chemical shift
$[\Theta]$:	Molar ellipticity
ϵ :	Molar extinction coefficient

Acknowledgements

I would like to begin by thanking my supervisor Dr. Alison Thompson. I am truly grateful for her endless guidance and support throughout my academic career. She was always willing to carefully push us to reach our academic potentials and was always eager to support any endeavours we wished to pursue. I have learned so much from her as both a leader and an educator, as I have shaped many of my own teaching philosophies from working alongside her in a classroom setting. I am thankful to my committee members, Dr. Norman Schepp, Dr. Robert White and Dr. Bruce Grindley for their aid and guidance throughout my degree.

I would like to acknowledge several researchers from Dalhousie for their contributions to this work over the years: Dr. Mike Lumsden for help with NMR experiments; Xiao Feng for running the mass spectrometry; Dr. T. Stanley Cameron for providing the X-ray crystal structures; Dr. Stephen Bearne for allowing us to use his circular dichroism spectrophotometer; and all of the support staff from the Dalhousie University Department of Chemistry. I am grateful for the financial support provided Dr. Thompson, the Killam Trusts and the National Science and Engineering Research Council of Canada.

I also wish to thank the former and current members of the Thompson research group as a much of the work presented in this thesis was a result of the collaborative effort between all group members: Dr. Sarah Crawford, Dr. Md. Imam Uddin, Dr. Estelle Marchal, Dr. Deborah Smithen, Dr. Carlotta Figliola, Dr. Jennifer Melanson, Dr. Brandon Groves, Cassandra Hawco, Katie Lund, Michael Beh, Sarah Greening, as well as the many undergraduate volunteers that I have been able to work with. Finally, I would like to thank Gaia Aish for her continuous support and encouragement every step of the way during this entire degree.

Chapter 1 – Introduction

1.1 – Structure and Properties of Dipyrinato Ligands

Dipyrrens (dipyrromethenes) are fully conjugated planar molecules formally consisting of a pyrrole attached to an azafulvene. Dipyrrens contain 12- π -electrons that are delocalized across the dipyririn such that structural data shows that the two pyrrolyl units are equivalent when identically substituted. Dipyrrens were first reported by Piloty in 1914.¹ The guidelines for the nomenclature of dipyrrens (Figure 1) was established by IUPAC in 1987.² However, it is more indicative to refer to the 1- and 9- positions as the α -positions, the 2-, 3-, 7- and 8- positions as the β -positions and the 5-position as the meso position, taken from terminology used to label pyrroles and porphyrins, respectively. The numbering system for 4,4-difluoro-4-bora-3a,4a-diaza-s-indacenes (BODIPYs) is quite different from the dipyrrens; counting from 1-8 and starting on a β -position and going around the molecule, including the boron centre in the numbering. However, the use of α -, β - and meso-terms is consistent for describing both dipyrrens and BODIPYs.

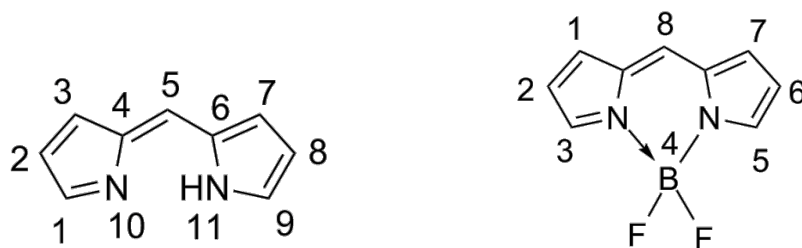


Figure 1: Numbering system for dipyrrens (left) and BODIPYs (right) according to IUPAC

The nature and extent of substitution around the dipyririn skeleton determines the consequent stability of the compound. Studies have shown³ that the fully unsubstituted

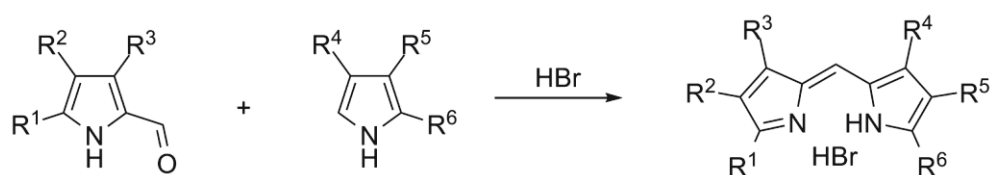
dipyrin is unstable in solution at temperatures above -40 °C due to the ability of the unsubstituted positions to undergo nucleophilic and electrophilic attack.^{4,5,6} Alkyl substituents at the 1-, 2-, 3-, -7, -8 and -9 positions enhance the stability of dipyrins. Dipyrins that are unsubstituted at the 5-position (meso) are typically unstable as free-bases,⁷ meaning that the ability to manipulate the dipyrin under air is compromised. Therefore, dipyrins are traditionally isolated as hydrobromide salts. However, aryl substituents at the meso-position increase the stability of dipyrins. Indeed, meso-aryl substituents allow for the isolation of unsubstituted dipyrins as air-stable compounds and also enhance the stability of radical cations formed from the resulting dipyrins, making them more suitable than 5-unsubstituted dipyrins for optoelectrochemical applications.⁸

X-ray crystallographic analysis of free-base dipyrins and their salts reveals essentially planar molecules with the nitrogen atoms arranged in the (*Z*)-*syn*-type arrangement.⁹ The planarity of the dipyrin unit arises from the intramolecular hydrogen bonding system, the conjugative planarization, and the dispersion forces between the sheets of molecules stacked parallel to one another at van der Waal distances of 3.4-4.0 Å.¹⁰

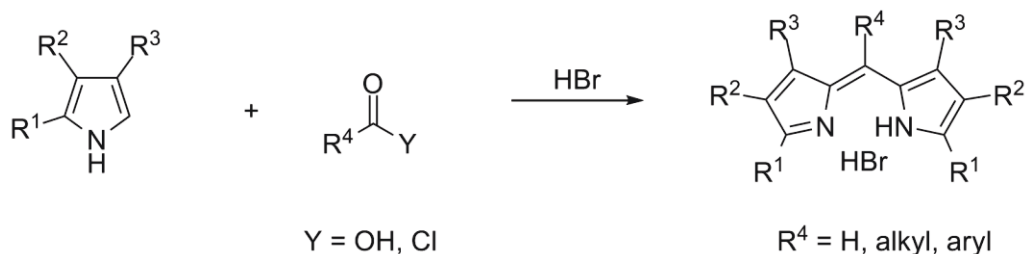
1.2 – Synthesis of Dipyrins

The synthesis of dipyrins was originally developed to provide precursors for the preparation of porphyrins. The synthesis of dipyrins typically involves the coupling of two pyrroles at the α -positions, through a methine carbon atom, to form a fully conjugated system. One route to achieve such a skeleton involves an acid-catalyzed condensation of a 2-formyl pyrrole with a pyrrole that is unsubstituted in the α -position,

to thus yield a meso-unsubstituted dipyrin. MacDonald developed this simple one-step procedure for the purpose of porphyrin synthesis and the method has since been used for the widespread synthesis of meso-unsubstituted symmetric or asymmetric dipyrins.¹¹⁻¹⁴ This procedure, for dipyrins, typically involves the use of hydrobromic acid due to the ease of crystallization of the corresponding hydrobromide salts. Use of the MacDonald coupling is the most common approach for preparing asymmetric dipyrins because it relies upon the reaction of complementary functionalities on the two pyrroles and thus unsymmetrical dipyrins are easily produced. Yields are generally quite high for these reactions, but can be hindered by the purification process which usually relies upon precipitation of the product from the reaction mixture. The synthesis of symmetric meso-substituted dipyrins can be achieved by the condensation of two equiv of an α -unsubstituted pyrrole with a carboxylic acid or an acid halide (Scheme 2).¹¹⁻¹⁴

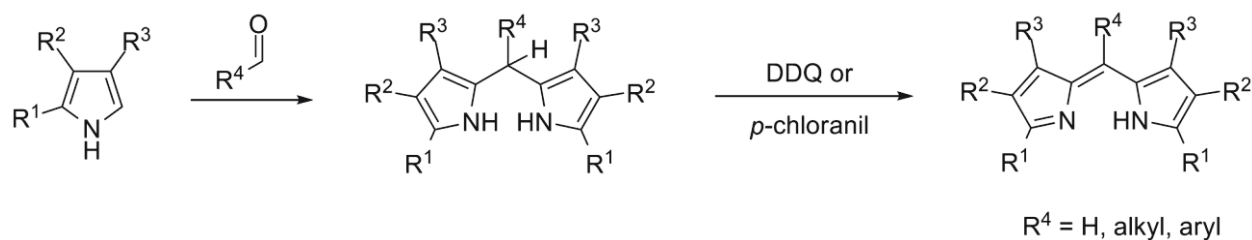


Scheme 1: MacDonald coupling reaction to form dipyrins



Scheme 2: Acid-catalyzed synthesis of dipyrins

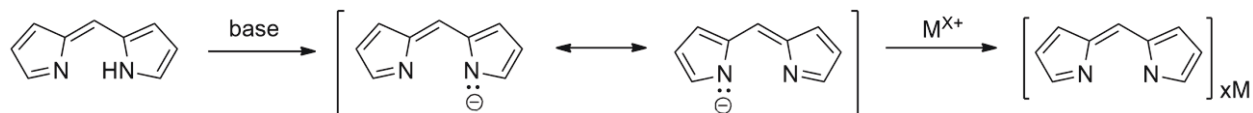
Other methods to synthesize dipyrrens involve, first, the condensation of two equiv of an α -unsubstituted pyrrole with an aldehyde to form a dipyrromethane (Scheme 3), and is a strategy generally used for the synthesis of meso-substituted dipyrrens. The resulting dipyrromethane is then oxidized to form a dipyrin, using an oxidizing agent such as 2,2-dichloro-5,6-dicyano-1,4-benzoquinone (DDQ) or *p*-chloranil.¹⁵⁻¹⁶



Scheme 3: Synthesis of dipyrrens through the oxidation of dipyrromethanes

1.3 – Dipyrinato Complexes

Dipyrrens are historically noted to be difficult to manipulate and purify and have often been converted to dipyrinato metal complexes prior to synthetic modification.⁷ The *NH* hydrogen atom of a dipyrin can be removed under basic conditions to give the monoanionic species that is stabilized by resonance, and the dipyrin can thus act as a bidentate ligand. The complexes generated from dipyrin ligands and metal ions are often neutral and can be purified using conventional chromatography (Scheme 4), as long as acidic conditions are avoided.¹⁷⁻¹⁸ While a wide variety of synthetic modifications can be carried out on the resulting dipyrinato complexes, conditions to induce decomplexation have to be avoided.⁷



Scheme 4: General dipyrinato complexation

Dipyrinato-metal complexes have been reported for M^+ species such as thallium(I)¹⁹ and rhodium(I);²⁰ M^{2+} species such as calcium(II),²¹ manganese(II),²² cobalt(II),²³ zinc(II),²³ nickel(II),²³ copper(II),²³ palladium(II),²⁴ cadmium(II),²⁴ and mercury(II);²⁴ and M^{3+} species such as iron(III),²⁵ cobalt(III)²⁵ and thallium(III).¹⁹ The geometry of the dipyrinato complex depends on several factors, such as the electronic structure of the metal, the available orbitals for bonding, and the conformational requirements of the ligand. Dipyrinato metal(II) complexes typically exhibit a tetrahedral geometry, excluding Pd(II) which exhibits square planar geometry.²⁴ Dipyrinato metal(III) complexes such as with Fe(III) and Co(III) exhibit octahedral geometries.²⁵ The dipyrinato ligands adopt a (*Z*)-*syn*-type configuration, and so the ligand is coordinated to the metal ion in a chelating κ^2 manner.

1.4 – Structure and Properties of *F*-BODIPY Dyes

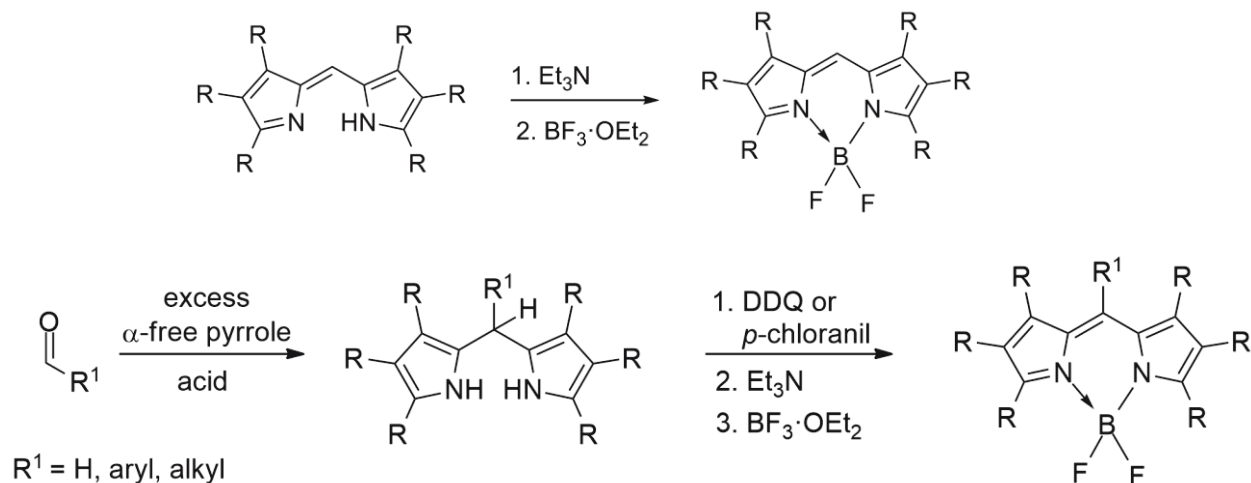
The most common dipyrinato complexes are the boron difluoride complexes, properly named 4,4-difluoro-4-bora-3a,4a-diaza-*s*-indacene, but referred to as *F*-BODIPYs²⁶ (Figure 1) hereafter. These complexes were first reported in 1968 by Treibs and Kreuzer.²⁷ *F*-BODIPYs tend to be strongly visible-absorbing molecules that emit

relatively sharp fluorescence peaks with very high quantum yields. *F*-BODIPYs are chemically robust and highly stable, allowing for simple purification procedures. They are nearly insensitive to the pH and polarity of their environment, in terms of their absorbance/emission, and are reasonably stable to physiological conditions.³ The structure of the BODIPY may be modified through the pyrrole core,²⁸ the meso position²⁹ and the substituents at the boron centre,³⁰ enabling tunable fluorescence properties, making these compounds useful for labelling proteins³¹ and DNA.³² *F*-BODIPY dyes have multiple applications in chemistry and biology due to their photoelectronic properties. For example, they have been used as fluorescent switches,³³ chemosensors³⁴ and as laser dyes.² They can also be used in the study of reaction dynamics, as well as in the study of the structure and function of biological systems such as monosaccharides,³⁵ lipid membranes and proteins.³¹

1.5 – *F*-BODIPY Synthesis

F-BODIPYs can be synthesized using several traditional methods. The simplest route is to start with the requisite dipyrin salt and to first treat the compound with excess triethylamine.³ The reaction mixture is then treated with excess boron trifluoride diethyl etherate and the *F*-BODIPY complex is formed (Scheme 5, top). Often, the dipyrin is formed *in situ* and then converted to the *F*-BODIPY,³⁶ such as when synthesizing meso-substituted *F*-BODIPYs. In this case, the first step involves the treatment of an aldehyde with excess pyrrole under acidic conditions to yield the dipyrromethane which is then oxidized using DDQ or *p*-chloranil, as stated earlier (Scheme 3), forming the dipyrin *in situ*. The dipyrin is then treated with excess triethylamine and boron trifluoride diethyl

etherate in order to yield the *F*-BODIPY (Scheme 5, bottom). The resulting *F*-BODIPYs are neutral complexes that are generally purified using conventional chromatography over silica.



Scheme 5: Synthesis of *F*-BODIPYs. Top = starting from isolated dipyrin. Bottom = starting from α -free pyrrole and forming the dipyrin in situ

1.6 – Boron Substitution of BODIPY Dyes

Recent reports as regards to *F*-BODIPYs have shown that substitution of the fluorine atoms at the boron centre is feasible, affording *B*-alkyl,³⁷ *B*-aryl,³⁷ *B*-alkynyl³⁸ and *B*-alkoxy³⁹ derivatives, often under harsh conditions. Varying the boron substituents often affects the optical properties of the BODIPY dyes and is simply another form of BODIPY modification that allows tuning of the fluorescence properties. Despite the many substitutions at boron performed, before the work reported herein there had never been an example of an isolated *X*-BODIPY of the heavier halogens, i.e. where $X \neq \text{F}$.

1.7 – Thesis Overview

Given the broad utility of BODIPYs, this thesis focuses on the development of new methods by which to synthesize and modify these boron complexes of dipyrrens. To this effect, Chapter 2 describes an approach by which to efficiently synthesize *F*-BODIPYs using an improved methodology. Chapter 3 builds upon the previous chapter's work, describing the synthesis and reactivity of BODIPYs featuring heavier atoms at boron. This work delves into the vastly unexplored area of *X*-BODIPYs where $X \neq F$, focusing on a new class of BODIPYs and their utility in the formation of BODIPY derivatives. Chapter 4 describes efforts to activate *F*-BODIPYs at the boron centre in order to facilitate decomplexation, thus returning the parent dipyrren ligand in an effective manner.

Chapter 2 – Improved Synthesis of *F*-BODIPYs

2.1 – Background

Compounds containing the *F*-BODIPY framework are known for their high thermal and photochemical stability, chemical robustness, and chemically tunable fluorescence properties, making them a highly desirable synthetic target.⁷ As mentioned earlier, *F*-BODIPYs are generally synthesized by trapping a dipyrin as its BF₂ complex, through a reaction with BF₃•OEt₂ and Et₃N. According to all literature reports published before the onset of this thesis work,³ all syntheses of *F*-BODIPYs require an excess of an amine base and an excess of BF₃•OEt₂.

Bis(dipyrin)s consist of two dipyrin units linked between the α - or β -positions of the central pyrrolic rings. They can be classified into three types of constitutional isomers, depending on their connectivity (Figure 2). Due to the large number of reported *F*-BODIPYs, it was quite surprising to discover that there were so few known examples of bis(*F*-BODIPY)s. There are two reported examples of meso-H α -linked bis(*F*-BODIPY)s⁴⁰ where the alkyl substituents about the BODIPY core are varied, along with a closely related example containing a meso-phenyl substituent. The bis(*F*-BODIPY)s are of importance as the photophysical properties of these compounds deviate from those of the monomers, including increased Stokes shifts, reduced fluorescent lifetimes and could potentially form BODIPY aggregates with different properties than the monomer. The Thompson group attempted⁴¹ to synthesize bis(*F*-BODIPY)s using traditional methods involving excess Et₃N and BF₃•OEt₂. However, these reactions resulted in complex

mixtures that could not be satisfactorily purified. Previous reports regarding bis(*F*-BODIPY)s have described similar difficulties.⁴⁰ Given these challenges it is clear that the traditional methods for *F*-BODIPY formation are failing in these cases, and that a new methodology is required.

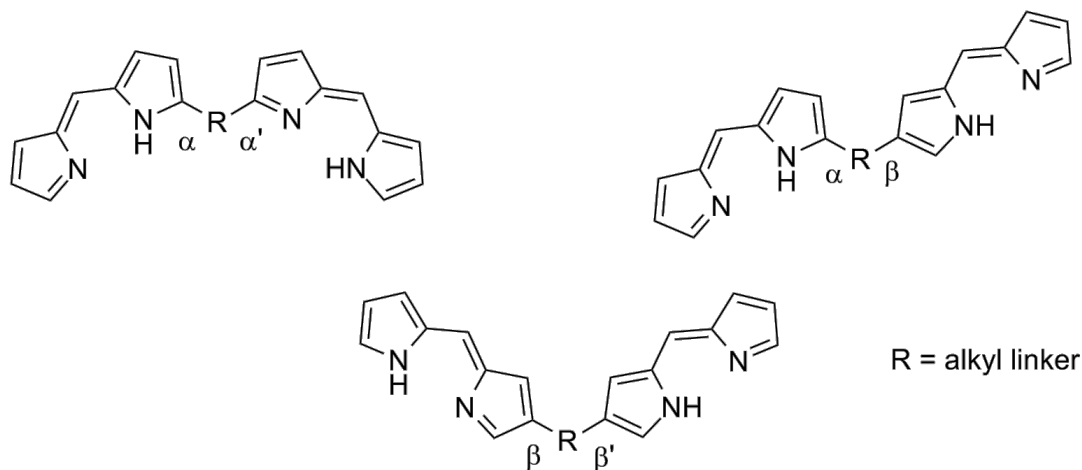
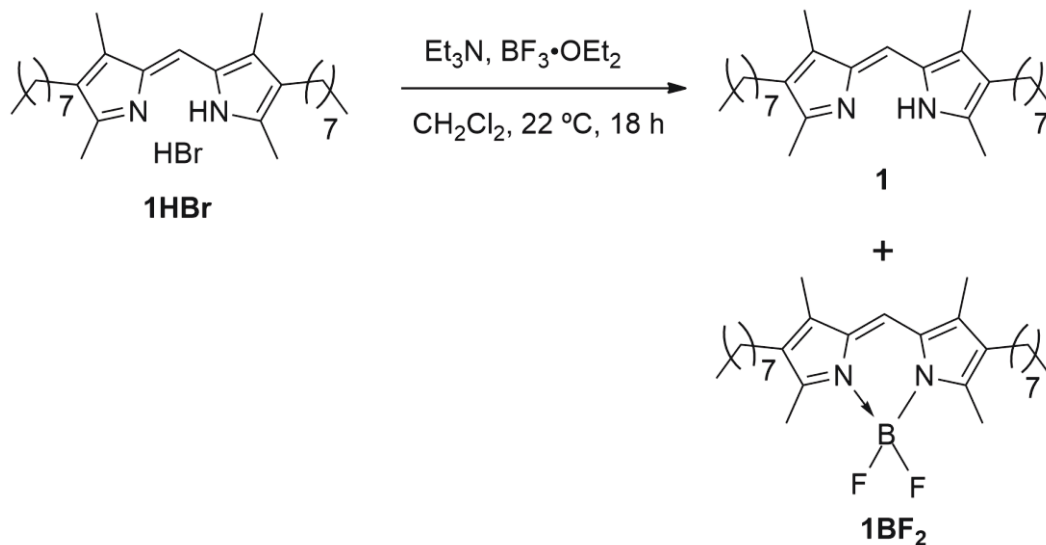


Figure 2: Constitutional isomers of bis(dipyrrins)

Previous work in the Thompson group⁴¹ involved the investigation of the formation of *F*-BODIPYs to optimize the reaction conditions for eventual application toward the synthesis of bis(*F*-BODIPY)s. Work with a simple alkyl-substituted dipyrrin hydrobromide salt (**1HBr**, Scheme 6) was carried out with the goal being to find the ratio of $\text{Et}_3\text{N}:\text{BF}_3\cdot\text{OEt}_2$ at which the greatest conversion of dipyrrin to its corresponding *F*-BODIPY would be achieved. The hope was that these conditions could be applied to the synthesis of bis(*F*-BODIPY)s. When the dipyrrin HBr salt was treated with $\text{BF}_3\cdot\text{OEt}_2$ alone, no reaction occurred; therefore, the amine base was required for the observed reactivity. The outcomes of the reactions were analyzed using ^1H NMR spectroscopic analysis of the crude reaction mixtures after work-up to monitor the integral values of the

peaks corresponding to the meso-H signals for each species. This allowed the crude ratio of free-base to *F*-BODIPY to be determined for each of the reactions.



Scheme 6: Synthesis of **1** and **1BF₂** from hydrobromide salt **1HBr**

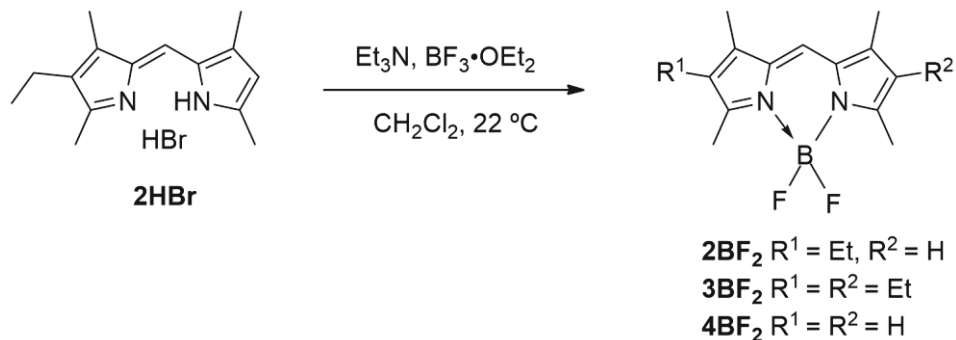
When equal equiv of $\text{BF}_3 \cdot \text{OEt}_2$ and Et_3N were used (Table 1, entry 6), almost equal amounts of **1** and **1BF₂** were observed in the product mixture. It was only when the equiv of $\text{BF}_3 \cdot \text{OEt}_2$ exceeded the equiv of Et_3N that the desired product, **1BF₂**, began to form in large proportions (Table 1, entries 7 and 8). In fact, using 9 equiv of $\text{BF}_3 \cdot \text{OEt}_2$ and 6 equiv of Et_3N ensured that **1HBr** was converted solely to **1BF₂** (Table 1, entry 8): these are indeed the conditions routinely reported and used³⁷ for the formation of *F*-BODIPYs from dipyrin HBr salts. The reason(s) for the requirement of the 9:6 $\text{BF}_3 \cdot \text{OEt}_2$: Et_3N ratio to achieve high yields of *F*-BODIPYs remain(s) unclear.⁴²

Entry	Equiv BF ₃ •OEt ₂	Equiv Et ₃ N	Ratio of Products (1:1BF ₂)
1	1	6	1:0
2	2	6	33:1
3	3	6	7.7:1
4	4	6	4.7:1
5	5	6	2.4:1
6	6	6	1.2:1
7	7	6	0.2:1
8	9	6	0:1

Table 1: Ratio of dipyrin to *F*-BODIPY with varying equiv of BF₃•OEt₂

Other previous work in the Thompson group revealed that the traditional procedure for the synthesis of *F*-BODIPYs has often suffered from irreproducible results when working with unsymmetrical dipyrin hydrobromide salts.⁴¹ Indeed, when the synthesis of *F*-BODIPY **2BF₂** (Scheme 7) from the unsymmetrical hydrobromide salt (**2HBr**) was attempted, an unexpected mixture of three products was produced. Attempts to optimize the reaction conditions continuously led to the same three products which were only separable via recrystallization. The products obtained were the expected unsymmetrical *F*-BODIPY (**2BF₂**), as well as two symmetrical *F*-BODIPYs (**3BF₂** and **4BF₂**) resulting from scrambling of the dipyrin during the synthesis of the BODIPY. It appears the scrambling occurs via conversion of the dipyrin to the corresponding α -free pyrrole and formyl pyrrole (or an equivalent synthon) in various combinations. This allows the pyrroles to react in situ to form both symmetric dipyrins, and these dipyrins then react to form the corresponding symmetrical *F*-BODIPYs. The resulting mixture

containing these *F*-BODIPYs was difficult to separate, making isolation of the desired complex problematic.

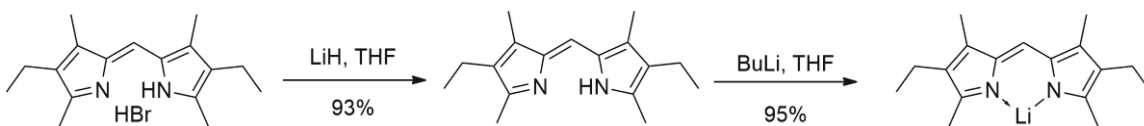


Scheme 7: Synthesis of scrambled *F*-BODIPYs from unsymmetrical dipyrin **2HBr**

2.2 – Project Goals

The aim of this project is to develop a new method for the synthesis of *F*-BODIPYs, one that will circumvent many of the synthetic challenges that are encountered when using the traditional method, as well as enhance yields and purification procedures to result in an overall increase in efficiency. As mentioned, problems arise during the formation of bis(*F*-BODIPY)s where very few successful examples have been reported.⁴⁰ It has also been shown that during the formation of *F*-BODIPYs from unsymmetrical dipyrins, there are often unwanted *F*-BODIPY by-products from the result of scrambling. Another problem can arise during the purification stage when using the traditional methodology. The use of excess Et₃N and BF₃·OEt₂ results in the formation of a large amount of a BF₃·Et₃N adduct, which can be easily removed using column chromatography. However, when performing a large scale synthesis of an *F*-BODIPY, the presence of this adduct makes product isolation difficult during both the extraction and column chromatography.

These problems highlight the need for the development of a new synthetic approach to *F*-BODIPYs, with a sharper focus on atom economy. To approach this challenge, the use of excess amine in the *F*-BODIPY formation was to be avoided, and thus a strategy requiring the need for formation of the dipyrinato anion prior to the addition of $\text{BF}_3 \cdot \text{OEt}_2$ was developed. The Thompson group has previously developed methodology for the synthesis and isolation of dipyrinato lithium salts using either *n*-BuLi⁴³ or LiHMDS (Scheme 8).⁴⁴ These dipyrinato lithium salts have been successfully employed as precursors to dipyrinato metal complexes, and it was conceived that they could also be used as efficient precursors for the formation of *F*-BODIPYs.



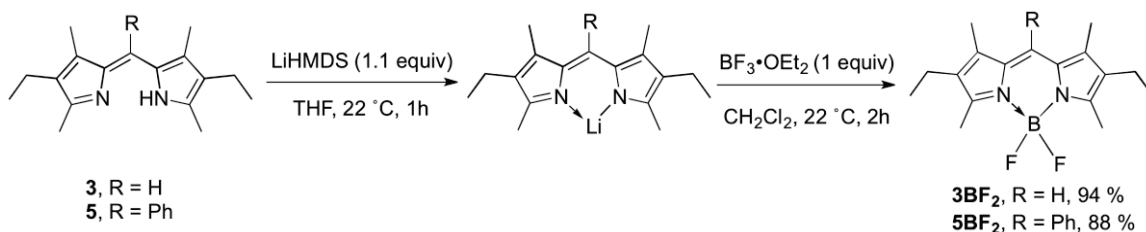
Scheme 8: Synthesis of lithium complex

2.3 – Results and Discussion

2.3.1 – Development of Synthetic Methodology

To investigate the use of dipyrinato lithium salts as precursors to *F*-BODIPYs, dipyrinato ligands that had been successfully converted to their lithium salts were initially used.⁴³ Two ligands were chosen, containing different meso-substitutions to demonstrate the scope of the strategy (Scheme 9) and any variances between the reactivity of the two ligand scaffolds. To form the lithium complexes, a solution of the dipyrin free-base in THF was reacted with a solution of 1.1 equiv LiHMDS, also in

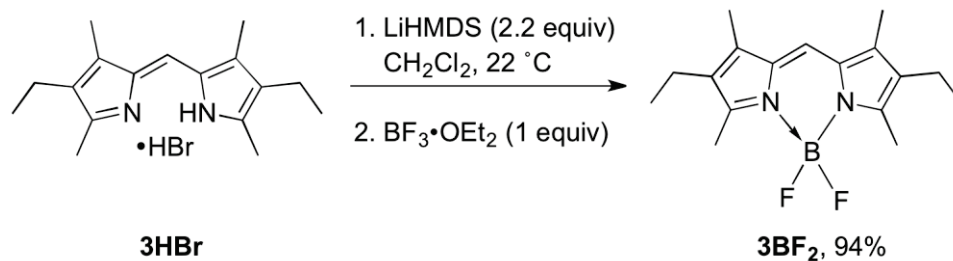
THF. The colour of the reaction mixture changed from orange to red upon the addition of LiHMDS. Upon completion of the reaction, the solvent was removed *in vacuo* and the resulting solid was washed with hexane to remove any unreacted free-base, as this material is soluble in hexanes. A slurry of this purified Li complex was then stirred in CH₂Cl₂ and one equiv of BF₃•OEt₂ was added drop-wise. The solution changed from yellow to orange, with a green fluorescent hue, upon the addition of BF₃•OEt₂. After two hours the reaction mixture was filtered through Celite, to remove any insoluble impurities, and the solvent was removed *in vacuo* to give the desired *F*-BODIPY as a red solid. These procedures were all completed with the use of a N₂-filled glovebox.



Scheme 9: Initial trials of *F*-BODIPY synthesis using dipyrroinato lithium salts

These initial trials were successful, resulting in high yields of the two *F*-BODIPYs. However, to improve efficiency further, the formation of a BF₂-complex was attempted from the initial HBr salt of the dipyrroin **3**, shown in Scheme 10. The HBr salt of the dipyrroin was dissolved in CH₂Cl₂ followed by the addition of 2.2 equiv of solid LiHMDS. The solution changed from yellow to dark red with the appearance of a red precipitate which corresponds to the dipyrroinato lithium salt, as this material is only partially soluble in CH₂Cl₂. The lithium salt precursor was not isolated and was instead directly used *in situ*. Following the formation of the Li salt, 1 equiv of BF₃•OEt₂ was

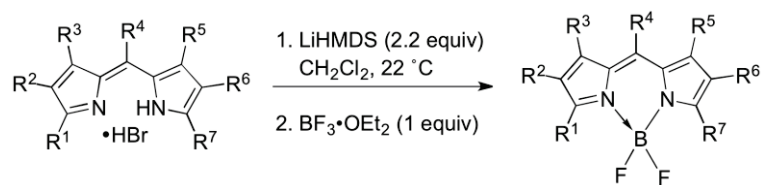
added drop-wise to the reaction mixture, resulting in an orange solution with a green fluorescent hue. The resulting solution was filtered through Celite to remove any insoluble by-products and then filtered through a pad of silica, eluting with CH_2Cl_2 , to provide the purified *F*-BODIPY product as a red solid. This experiment was successful, giving the required *F*-BODIPY in a high yield (**3BF₂**, 94%) and this new methodology showed promise for the general synthesis of *F*-BODIPYs.



Scheme 10: Synthesis of *F*-BODIPY from HBr salt of dipyrin

To demonstrate the utility of this newly developed methodology, a variety of *F*-BODIPYs including both meso-H and meso-phenyl substituents were synthesized. Various substitution patterns, including α -free, β -free and fully unsubstituted dipyrins were used, as well as conjugated alkanooate esters (Table 2). The dipyrin starting materials containing a meso-H substituent were prepared as HBr salts, as this is generally a more stable and isolable form of dipyrins. Meanwhile, the dipyrins containing a meso-aryl substituent were prepared as free-base dipyrins, as these compounds are stable and typically isolated as such. All ligands were tolerated by the new methodology and in all cases isolation of the desired product was facile, requiring simply filtration through a pad of Celite to produce yields generally >80%. Of significant importance is the synthesis of *F*-BODIPY **2BF₂** from unsymmetrical dipyrin **2HBr**. As noted earlier, the traditional

methodology used for the synthesis of **2BF₂** was unsuccessful as the formation of this product was accompanied by formation of the scrambled *F*-BODIPY by-products.⁴¹ However, synthesis of **2BF₂** using the new methodology (i.e. in-situ formation of the dipyrinato lithium salt, followed by 1 equiv of BF₃•OEt₂) resulted in 91% isolated yield of the desired *F*-BODIPY without the observation of any scrambled by-products.



Entry	BODIPY Product	Yield (%)
1	 1BF₂	quant ^a
2	 2BF₂	91 ^a
3	 3BF₂	94 ^a , 94 ^b
4	 5BF₂	88 ^{a,c}
5	 6BF₂	85 ^a
6	 7BF₂	81 ^a
7	 8BF₂	60 ^{a,c}

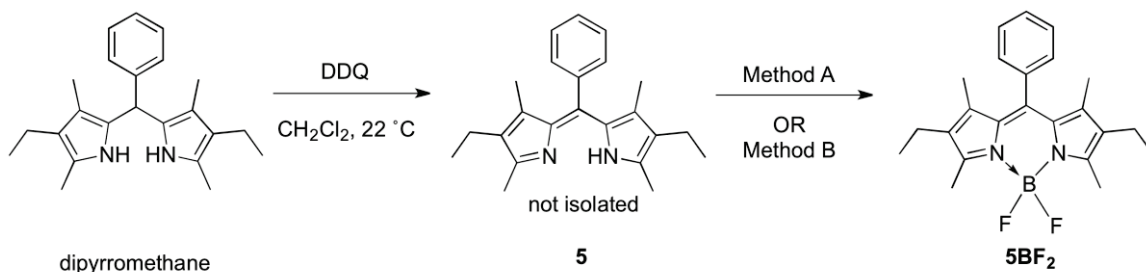
^aGlovebox, 50 mg scale. ^bInert atmosphere conditions outside of glovebox, 1 g scale. ^cPrepared from free-base starting material, and using 1.1 equiv LiHMDS

Table 2: Synthesis of *F*-BODIPYs via dipyrinato lithium salts using 1 equiv BF₃·OEt₂

To continue exploring this new methodology, it was important to determine the scalability of this reaction. The synthesis of *F*-BODIPYs using the traditional methodology³ calls for a large excess of both $\text{BF}_3 \cdot \text{OEt}_2$ and Et_3N . As mentioned previously, on small scale reactions this does not pose a significant problem. However, during large scale syntheses of *F*-BODIPYs (> 1 g), the $\text{BF}_3 \cdot \text{NEt}_3$ adduct is formed in significant quantities and can be difficult to remove from the reaction mixture.⁴⁵ However, the new methodology only requires one equiv of $\text{BF}_3 \cdot \text{OEt}_2$ and lacks the presence of Et_3N . Therefore, the previously observed $\text{BF}_3 \cdot \text{NEt}_3$ adduct is not produced and thus cannot impede the purification and isolation of the *F*-BODIPY products. The reaction for the synthesis of *F*-BODIPY **3BF₂** was scaled to 1 g, and performed outside of the glovebox under inert atmosphere using anhydrous conditions (Table 2, Entry 3). Purification for this compound required filtration through Celite to remove any insoluble impurities followed by filtration through a pad of silica, eluting with CH_2Cl_2 . The product was isolated in a 94% yield, demonstrating another advantage of this methodology over the traditional route (6 equiv NEt_3 , 9 equiv $\text{BF}_3 \cdot \text{OEt}_2$) for the synthesis of *F*-BODIPYs whereby the product was obtained in an 89% yield (1 g scale, purification required multiple aqueous extractions and column chromatography).

As previously introduced, a common approach for synthesizing *F*-BODIPYs involves the oxidation of a dipyrromethane, with DDQ, to form the free-base dipyrin which is trapped *in situ* as the *F*-BODIPY upon the addition of 6 equiv of Et_3N and 9 equiv of $\text{BF}_3 \cdot \text{OEt}_2$.³ The initial synthesis of **5BF₂** used this approach and the desired product was obtained in 50% yield from the corresponding dipyrromethane, after column chromatography (Scheme 11). It was necessary to compare the new methodology

involving 1 equiv of $\text{BF}_3 \cdot \text{OEt}_2$ to this traditional strategy, again starting from the corresponding dipyrromethane. Thus, one equiv of DDQ was added to a solution of the dipyrromethane in CH_2Cl_2 and the mixture was stirred for 4 hours. Upon oxidation to the free-base dipyrin (**5**), 3.3 equiv of a LiHMDS solution in hexanes was added drop-wise and the reaction mixture was stirred for an hour. While only 1.1 equiv of LiHMDS is necessary to react with the free-base dipyrin, the reduced hydroquinone form of DDQ is still present in the reaction mixture and can be deprotonated with LiHMDS. Therefore, an extra 2.2 equiv of LiHMDS is required to ensure deprotonation of the dipyrin and formation of the dipyrinato lithium salt. Then, just 1 equiv of $\text{BF}_3 \cdot \text{OEt}_2$ was added to the reaction mixture and stirring was continued for 3 hours. The reaction was performed under nitrogen and anhydrous conditions; the work-up required an acid/base wash followed by a simple filtration through a pad of silica to afford **5BF₂** in 52% yield on an 800 mg scale. The reaction was performed outside of the glovebox, again demonstrating the scalability and practicality of this methodology. Thus, the new methodology is easily merged with the standard approach used to synthesize *F*-BODIPYs from dipyrromethanes that bypasses the need to isolate and purify dipyrins or their HX salts.



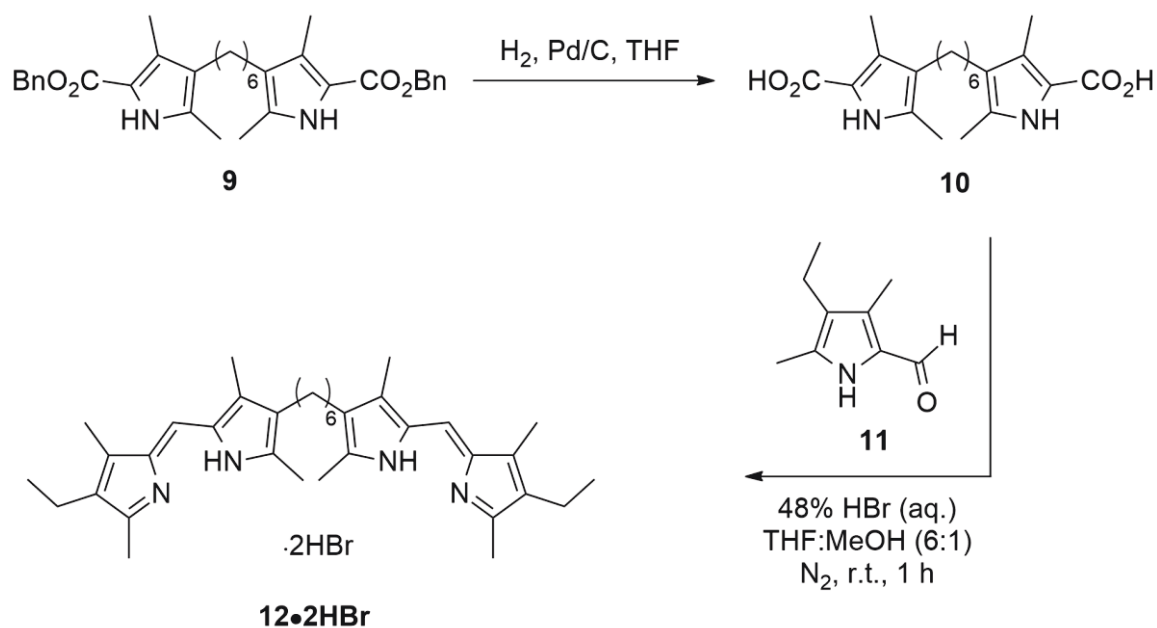
Method A: 6 equiv NEt_3 , 9 equiv $\text{BF}_3 \cdot \text{OEt}_2$, 50% after column chromatography

Method B: (a) 3.3 equiv LiHMDS; (b) 1 equiv $\text{BF}_3 \cdot \text{OEt}_2$, 52% after filtration through silica

Scheme 11: Synthesis of *F*-BODIPY via in situ trapping of dipyrin

2.3.2 – Synthesis of bis(*F*-BODIPY)s

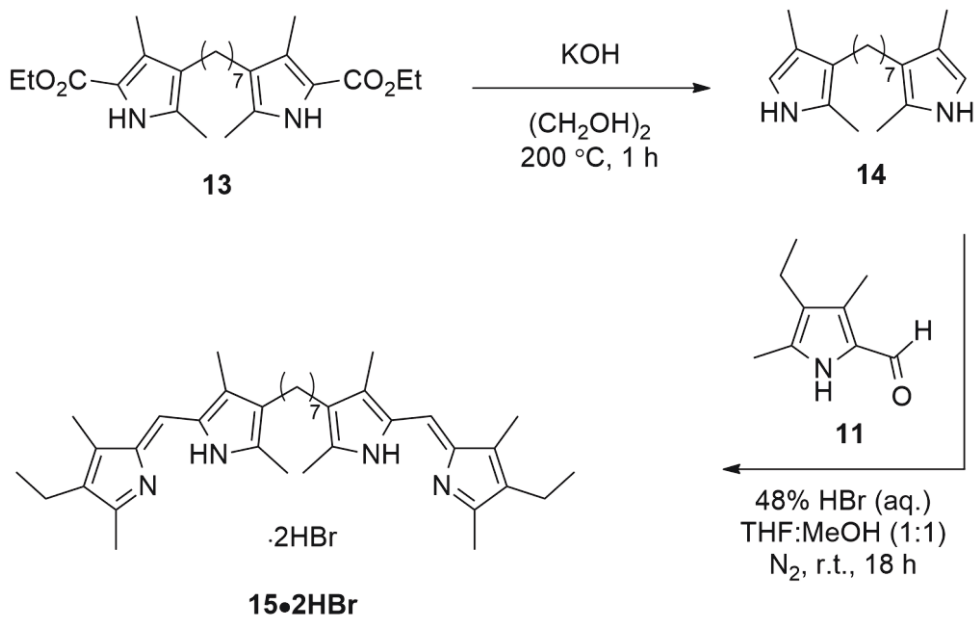
Given the success of this improved methodology for the formation of *F*-BODIPYs, the same conditions were applied to bis(dipyrrin)s in an attempt to synthesize bis(*F*-BODIPY)s in appreciable yields. To accomplish this, the bis(dipyrrin) starting materials were required. Thus, dibenzyl 4,4'-(hexane-1,7-diyl)bis(3,5-dimethyl-1*H*-pyrrole-2-carboxylate) (**9**)⁴⁶ was dissolved in THF, along with a drop of Et₃N (Scheme 12). 10% Pd/C was added to the solution which was then placed under an atmosphere of H₂. The reaction mixture was then stirred overnight. After hydrogenolysis of the benzyl groups, the Pd/C was removed via filtration over Celite and the solution was concentrated *in vacuo* to give **10** which was used in the next step without further purification. 2,4-Dimethyl-3-ethylpyrrole-5-carboxaldehyde (**11**)⁴⁷ was added to a solution of the preceding bis(pyrrole) **10** in methanol:THF under nitrogen. 48% aq. HBr was then added drop-wise and the reaction mixture was stirred at room temperature under nitrogen to allow MacDonald-type condensation to occur.³ The reaction mixture was concentrated *in vacuo* until only a small amount of solvent remained. Diethyl ether was then added until precipitation was complete. The precipitate was collected using filtration, then dissolved in dichloromethane and the solution dried over anhydrous Na₂SO₄. The solution was then concentrated *in vacuo* to give **12•2HBr** as a bright orange solid in a 92% yield over two steps.



Scheme 12:: Synthesis of bis(dipyririn) salt **12•2HBr**

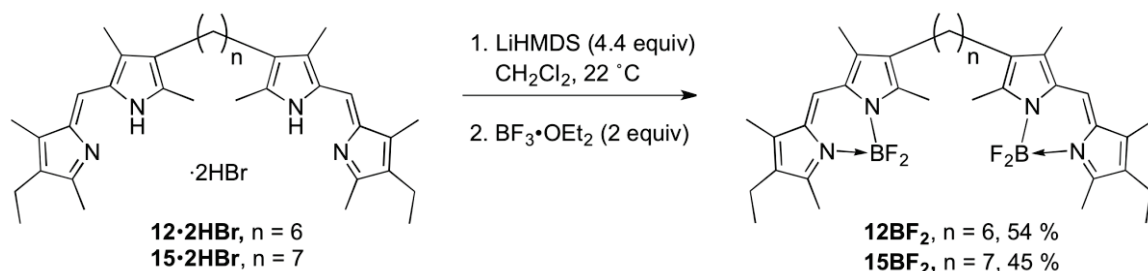
The synthesis of another bis(dipyririn) salt (**15•2HBr**) was achieved using a slightly different procedure (Scheme 13). Diethyl 4,4'-(heptane-1,7-diyl)bis(3,5-dimethyl-1*H*-pyrrole-2-carboxylate) (**13**)⁴⁶ was added to a suspension of potassium hydroxide in ethylene glycol and the reaction mixture was heated at 200 °C for 1 h. After cooling to room temperature, the reaction mixture was separated between ethyl acetate and water. The aqueous phase was extracted with ethyl acetate and the combined organic extracts were washed with water and brine, dried over anhydrous MgSO₄ and concentrated *in vacuo* to give 1,7-bis(2,4-dimethyl-1*H*-pyrrol-3-yl)heptane (**14**), which was used in the next step without further purification. From this point the synthesis followed a similar procedure as that used for **12**. 2,4-Dimethyl-3-ethyl pyrrole-5-carboxaldehyde (**11**)⁴⁷ was coupled to the preceding bis(pyrrole) using the MacDonald-

type coupling conditions. The desired bis(dipyrrin) (**15•2HBr**) was collected as a brown solid in a 67% yield over two steps.



Scheme 13: Synthesis of bis(dipyrrin) salt **15•2HBr**

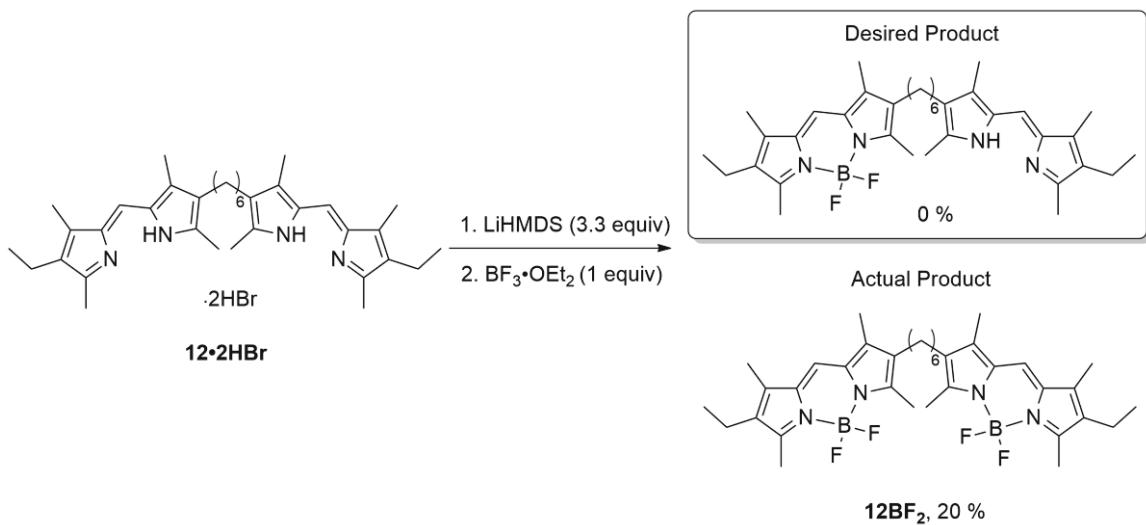
To solutions of the bis(dipyrrin) HBr salts **12•2HBr** and **15•2HBr** in CH_2Cl_2 , 4.4 equiv of LiHMDS in tetrahydrofuran was added drop-wise (Scheme 14). The reaction mixtures were stirred for 2 h to allow formation of the corresponding dilithium salts to occur. Solutions of 2 equiv of $\text{BF}_3\cdot\text{OEt}_2$ in CH_2Cl_2 were then added drop-wise, and the reaction mixtures were stirred for another 3 h. Upon completion, the reaction mixtures were filtered through Celite. The filtrate was then filtered through a pad of silica to give the desired bis(*F*-BODIPY)s **12BF₂** and **15BF₂** in isolated yields of 54% and 45%, respectively, significantly higher than those previously obtained for bis(*F*-BODIPY)s.⁴⁰



Scheme 14: Synthesis of bis(*F*-BODIPY)s from dipyrinato dilithium salts

The new methodology for the synthesis of *F*-BODIPY synthesis was tested on the bis(dipyrin)s for a variety of reasons. Historically the bis(BODIPY)s were synthesized in relatively low yields, so these ligands were chosen in an attempt to increase the yields of the corresponding bis(*F*-BODIPY)s. While this was successful, they were also chosen to test whether this methodology could be used to prepare a bis(dipyrinato) compound containing one free dipyrin unit and one *F*-BODIPY unit. The attempted synthesis was carried out in the exact same fashion, ideally preparing the mono-dipyrinato lithium salt which could then be converted to the *F*-BODIPY with 1 equiv of $\text{BF}_3 \cdot \text{OEt}_2$ (Scheme 15). The bis(dipyrin) **12·2HBr** was dissolved in CH_2Cl_2 and treated with 3.3 equiv of LiHMDS. The solution colour changed from orange to a yellow solution with red precipitate upon addition of the reagent. Then, 1 equiv of $\text{BF}_3 \cdot \text{OEt}_2$ was added drop-wise to the solution. The red precipitate disappeared and the solution became red in colour with a fluorescent hue. However, TLC for the reaction mixture showed that the product forming was simply the bis(BODIPY) and not the monocomplexed species as desired. The reaction mixture was filtered through Celite, washed with brine and dried with Na_2SO_4 . The remaining solution was concentrated in vacuo to give the crude material. Column chromatography was carried out on the material to separate the products and it was found that the only BODIPY-like species present was the bis(BODIPY) **12BF₂**

(20%) that was synthesized previously. It appears as though, once the bis(dipyrrin) reacts with the lithium reagent to form the first lithium salt, that new species is more reactive and the remaining LiHMDS in solution forms the second lithium salt on the same species, rather than react with a free molecule of bis(dipyrrin). This would explain why, during the *F*-BODIPY synthesis, the bis(BODIPY) was formed as opposed to the mono-complexed BODIPY. The reaction was attempted again but this time starting with the free-base bis(dipyrrin). The bis(dipyrrin) HBr salt was stirred in diethyl ether and treated with 48% NH₄OH to form the free-base bis(dipyrrin). The reason for doing so was to limit the amount of LiHMDS present in the reaction mixture. With the bis(dipyrrin) free-base in hand the material was dissolved in CH₂Cl₂ and treated with 1.1 equiv of LiHMDS. The red precipitate formed once more and was treated with 1 equiv of BF₃•OEt₂. However, the overall result was the same and only bis(BODIPY) **12BF₂** was isolated, this time in 22% yield. It appeared that using this methodology would not prove fruitful for the task at hand and thus efforts were put towards other feats.



Scheme 15: Attempted synthesis of monocomplexed bis(dipyrrinato) species

2.4 - Conclusions

In conclusion, an improved methodology for the formation of *F*-BODIPYs utilizing the lithium salt of the dipyrin and only 1 equiv of $\text{BF}_3 \cdot \text{OEt}_2$ has been developed.⁴¹ This strategy has significant benefits over traditional conditions for synthesizing *F*-BODIPYs (excess $\text{BF}_3 \cdot \text{OEt}_2$ and Et_3N), and widespread application toward the synthesis of these fluorescent compounds is anticipated. In the new methodology, Et_3N is not required and therefore a $\text{BF}_3 \cdot \text{NEt}_3$ adduct by-product is not formed: filtration through Celite suffices for the purification of most *F*-BODIPYs prepared using this efficient methodology. The strategy may be applied to the isolated free-base dipyrin or HBr salts, or to the approach involving trapping the dipyrin *in situ* once it has formed via oxidation of the corresponding dipyrromethane. Indeed, using the new strategy for the synthesis of *F*-BODIPYs via *in situ* trapping of dipyrins, themselves formed after oxidation of dipyrromethanes, gives comparable yields and simpler purification requirements than the usual approach. The new methodology avoids the synthesis of scrambled by-products in the formation of unsymmetrical *F*-BODIPYs. Furthermore, using this new methodology, bis(*F*-BODIPY)s were synthesized in yields appreciably higher than have previously been attained and involve the use of extremely efficient purification procedures.

Chapter 3 – *Cl*-BODIPYs

3.1 – General Background

As described earlier in this thesis, the NH hydrogen atom of a dipyrin can be deprotonated to give the monoanionic species that is stabilized through resonance. A compound that has a similar *N,N*-bidentate framework to the dipyrin ligand is the β -diketimine (Nacnac, Figure 3) which also forms a monoanionic ligand via deprotonation.⁴⁸ The Nacnac abbreviation is a modification of the abbreviation used for acetylacetonate (acac) as nacnac ligands are the diimine analogues of the acetylacetonate ligands. β -Diketiminato ligands are isoelectronic to cyclopentadienyl anions thus attracting much attention as spectator ligands. Nacnac ligands strongly coordinate to metal centres, and the reactivities of metal centres can be tuned by changing the steric and electronic properties of the substituents at the nitrogen atoms of the nacnac construct.

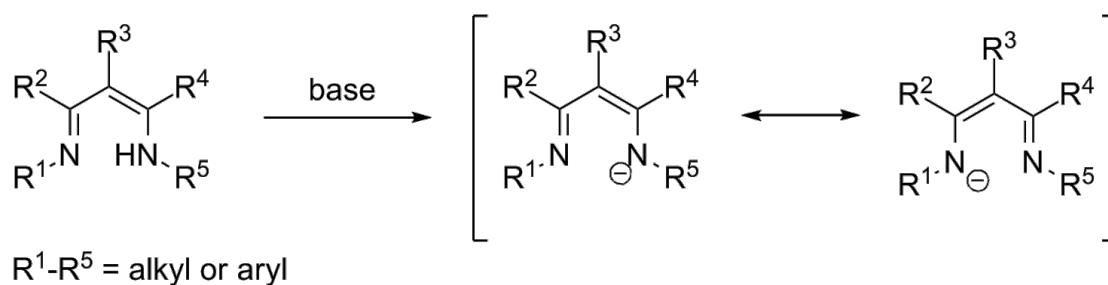
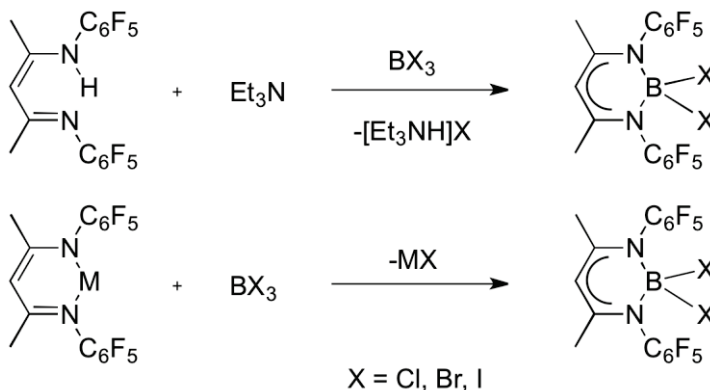


Figure 3: Major contributing resonance structures of the β -diketiminato anion

The Cowley group has reported the synthesis of boron dihalide complexes of β -diketimines.⁴⁹ Several methods have been employed to synthesize such complexes, including a dehydrohalogenation method as shown in Scheme 16 (top), where the aminoimine is treated with Et_3N and the appropriate boron trihalide. This particular

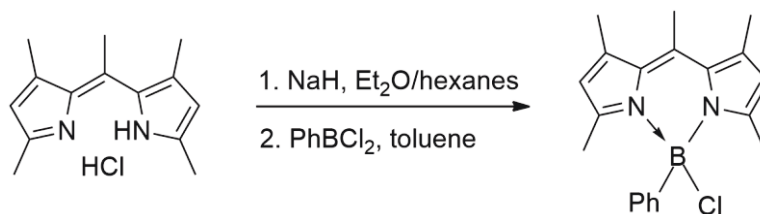
method is very similar to that traditionally used for the formation of *F*-BODIPYs, as discussed in Chapter 2 of this thesis. However, this method had limited success for synthesizing boron dihalide complexes of β -diketimines. While the dehydrohalogenation reactions resulted in the formation of the desired complexes, the products were contaminated with the Lewis acid-base complex $\text{Et}_3\text{N}\cdot\text{BX}_3$. As such, salt metathesis was employed, involving lithium, sodium and tin complexes of the β -diketiminato, rather than the free-base aminoimines (Scheme 16, bottom). Again, this method had limited success due to contamination of the products with unidentified impurities. Although the use of both synthetic routes has resulted in difficulties when applied to the β -diketimines, these strategies have been successfully employed for the synthesis of *F*-BODIPYs. Due to the similarity of the β -diketimine and the dipyrin, it is possible that methodologies used for preparing β -diketiminato complexes could be applied the synthesis of *X*-BODIPYs with other halides besides fluorine.



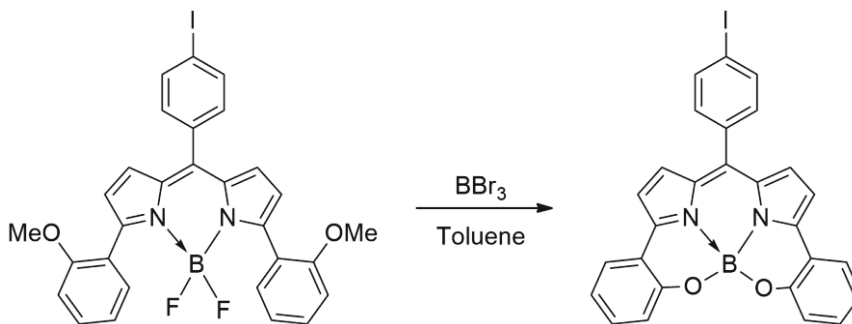
Scheme 16: Synthesis of β -diketiminato boron dihalide complexes

Prior to the work conducted as part of this thesis research, there were no previous reports of dihalogen *X*-BODIPYs in the literature. However, there existed one reported

BODIPY analogue that contained one B-Cl bond. In this case a meso-methyl substituted dipyrinato sodium complex was treated with PhBCl₂ to produce the BODIPY complex bearing one chloride and one phenyl substituent at the boron centre (Scheme 17).⁵⁰ There are also reports of an *F*-BODIPY featuring a protected phenol in the α -position (Scheme 18). Treatment of this material with BBr₃⁵¹ resulted in the formation of the corresponding phenoxy *O*-BODIPY, potentially formed via in situ formation of a *Br*-BODIPY intermediate.



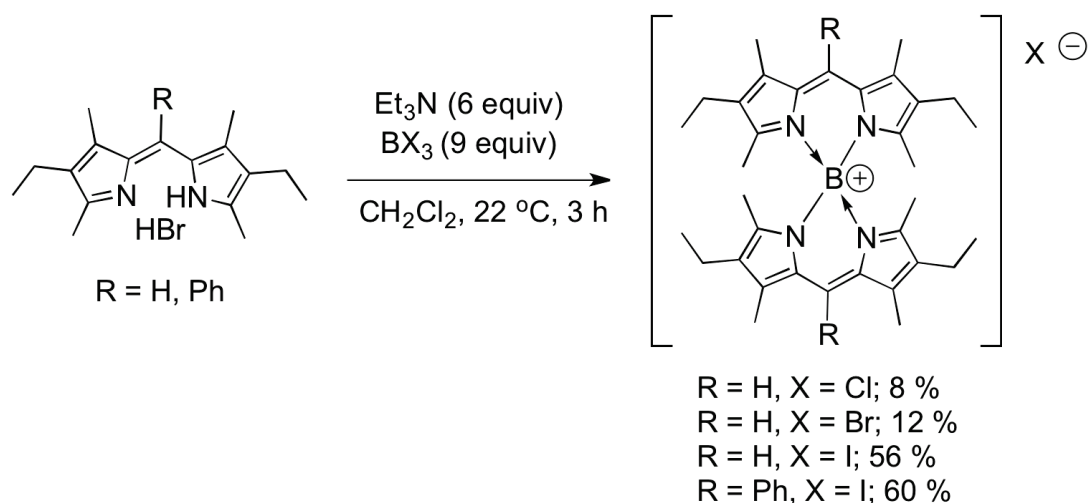
Scheme 17: Synthesis of first BODIPY containing a chloro substituent on boron



Scheme 18: Synthesis of first *O*-BODIPYs using BBr₃

Previous members of the Thompson group had attempted the synthesis of *X*-BODIPYs.⁵² At that time, the traditional *F*-BODIPY synthesis methodology using excess amounts of triethylamine and boron trifluoride was modified to incorporate use of the other boron trihalides. In this previous work, six equiv of triethylamine were added to a

solution of each dipyrin hydrobromide salt in CH_2Cl_2 (Scheme 19), followed by the addition of nine equiv of the boron trihalide as a 1.0 M solution in dichloromethane (BCl_3 and BBr_3), or as a solid (BI_3). The consequent deep red solutions were worked up via the addition of methanol, followed by an aqueous wash. The combined organic layers were dried over Na_2SO_4 , concentrated in vacuo and the resulting mixtures were purified over neutral alumina.⁵³ However, the desired heavier halogen *X*-BODIPY analogues were not isolated from the reaction mixtures. Characterization of the red, and not fluorescent, products revealed the first dipyrinato boronium cations, isolated with a counter-anion corresponding to the boron trihalide used, as shown in Scheme 19. The yields of the isolated compounds ranged from poor to moderate depending on the boron trihalide used. As the lability of the halogen leaving group increased ($\text{Cl} < \text{Br} < \text{I}$), the yield of the isolated boronium salt also increased. It is hypothesized that the relevant *X*-BODIPYs are formed in situ and simply decompose, and/or repropionate during the purification procedures. Since the iodo substituents are much better leaving groups than both bromo and chloro substituents, the boron centre of the *I*-BODIPY would be more susceptible to nucleophilic attack from another dipyrin ligand to result in the more stable boronium salts as the only isolable products of the reactions.



Scheme 19: Synthesis of boronium cations

3.2 – Project Goals

Studies involving BODIPY dyes have shown, in recent years, that substitution of the fluorine atoms at the boron centre is quite feasible. A variety of *C*- and *O*-BODIPY complexes have been synthesized, from *F*-BODIPYs, to afford *B*-alkyl,³⁷ *B*-aryl,³⁷ *B*-alkynyl³⁸ and *B*-alkoxy³⁹ derivatives. However, these substitutions are often achieved under harsh conditions, e.g., high temperatures, extended reaction times. Variation of the boron substituents can have a significant effect on the optical properties of the BODIPY dyes and is a valuable method of tuning the fluorescence properties of these complexes. Our goal became to prepare *X*-BODIPYs where $X \neq \text{F}$. Changing the substituent at the BODIPY boron centre from fluorine to the heavier halogens was anticipated to have a significant effect on the fluorescence properties of the resulting *X*-BODIPYs. The presence of the heavier halogens was expected to facilitate fluorescence quenching and enhance non-radiative decay pathways by increasing spin-orbit coupling. It was

postulated that the synthesis of *X*-BODIPYs ($X \neq F$), would allow for more facile substitutions at the boron centre. It is known that boron-halogen bond strengths decrease in the order $B-F \gg B-Cl > B-Br > B-I$; $B-F$ ($\Delta H_f^{298} = 766 \text{ kJ/mol}$) $> B-Cl$ ($\Delta H_f^{298} = 536 \text{ kJ/mol}$) $> B-Br$ ($\Delta H_f^{298} = 435 \text{ kJ/mol}$) $> B-I$ ($\Delta H_f^{298} = 384 \text{ kJ/mol}$).⁵⁴ Furthermore, *B-Cl*, *B-Br* and *B-I* bonds, respectively, in a BODIPY are expected to be increasingly much more labile than the equivalent *B-F* bond within an *F*-BODIPY. The lability of these substituents would potentially allow nucleophilic substitution at the boron atom to be more facile, with the hopes of providing a new synthetic route to complexes that were previously unattainable or synthetically challenging using the existing methodologies.

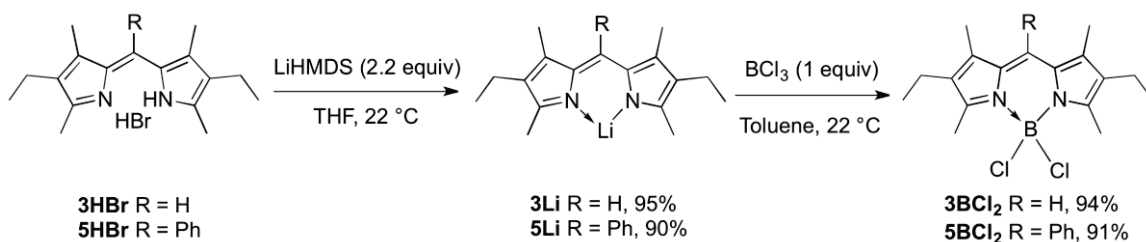
3.3 – Results and Discussion

3.3.1 – Synthesis of *Cl*-BODIPYs

Following the synthetic pathways used to prepare β -diketiminato boron dihalide complexes,⁴⁹ it was found that applying the dehydrohalogenation methodology to the formation of *X*-BODIPYs was unsuccessful. Given that treatment of dipyrin with triethylamine and boron trihalides, other than BF_3 , gave the corresponding boronium salts,⁵³ efforts were turned toward the use of the salt metathesis methodology described in Chapter 2 for the synthesis of *F*-BODIPYs. As such, dipyrinato lithium salts were selected as the initial precursors for the synthesis of *X*-BODIPYs ($X \neq F$). Due to the labile nature of the *B-X* bonds, it is apparent that these complexes should be most stable

under the air- and moisture-free conditions which are also required when handling the dipyrinato lithium salts.

Initial experiments aiming to synthesize the *X*-BODIPYs were completed with two dipyrin ligands, **3HBr** and **5HBr**, i.e., a meso-unsubstituted and a meso-substituted ligand. The lithium complexes of these dipyrins were synthesized using the same methods that have been discussed (Scheme 20). In this case the dipyrinato lithium complexes were isolated and purified, rather than formed *in situ*. Each lithium complex was then stirred as a slurry in toluene, being only partially soluble and forming a yellow suspension. One equiv of a solution of boron trichloride in hexanes was added drop-wise to the reaction mixture. Upon addition of BCl₃, the reaction mixtures instantly changed to a red-orange solution with a green fluorescent hue. The reaction mixtures were stirred for an hour before filtration over Celite. The filtrate was concentrated *in vacuo* to give the products as a red solid, without need for further purification. The *Cl*-BODIPYs **3BCl₂** and **5BCl₂** were thus formed in near-quantitative yields from the corresponding dipyrinato lithium salts.



Scheme 20: Synthesis of *Cl*-BODIPYs via dipyrinato lithium salts

These new BODIPY compounds, termed *Cl*-BODIPYs, were characterized using ¹H, ¹³C and ¹¹B NMR spectroscopy. The ¹¹B NMR spectra of the *Cl*-BODIPYs showed

the presence of a sharp singlet around 2.4 ppm which is downfield from the signal of the analogous *F*-BODIPYs: the ^{11}B NMR spectra of *F*-BODIPYs typically show a triplet at roughly 0.8 ppm. However, the masses of ions corresponding to **3BCl₂** and **5BCl₂** were not detected using either ESI or APCI mass spectrometry as the compounds did not survive the ionization techniques used. In each case, the only detectable ion corresponded to the free-base dipyrin, **3H⁺** or **5H⁺**, respectively, without the presence of the $-\text{BCl}_2$ moiety, suggesting that the material decomposed under the conditions used for ionization. As postulated earlier, the *Cl*-BODIPYs are stable under an inert atmosphere but are particularly sensitive to moisture and succumb to decomposition in the presence of water. The *Cl*-BODIPYs are also unstable to column chromatography (silica and alumina) and would decompose during any attempts to purify using this technique. It is presumed that the instability of these materials is due to the lability of the chloro substituents which are being replaced by the nucleophilic oxygen atoms of water and silica, ultimately leading to decomposition.

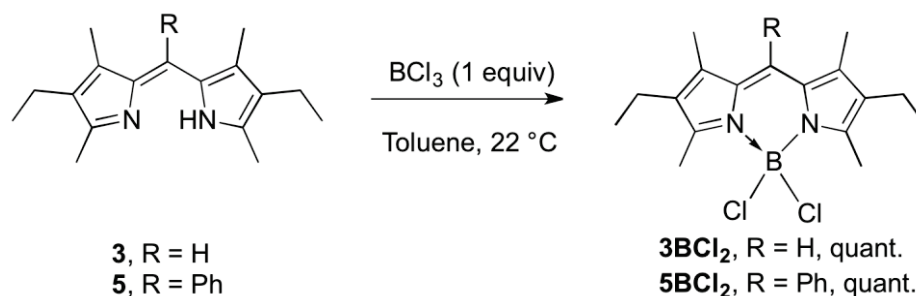
The *Cl*-BODIPYs exhibited significant fluorescence in solution. The quantum yield of a fluorescent material is defined as the ratio of the number of photons emitted and the number of photons absorbed, providing information about the emission efficiency of a given fluorophore. The quantum yields for compounds **3BCl₂** and **5BCl₂** were measured in CH_2Cl_2 and found to be $\Phi_{\text{F}} = 0.45$ and 0.40 , respectively, with emission at 546 nm for both compounds. While these quantum yields are substantially lower than those of the analogous *F*-BODIPYs (**3BF₂** and **5BF₂**, $\Phi_{\text{F}} = 0.91$ and 0.87 , respectively), the fluorescence exhibited by these *Cl*-BODIPYs is still significant.⁵³ The decrease in

fluorescence quantum yield for the *Cl*-BODIPYs is to be expected, as the heavier halogens promote fluorescence quenching.⁵⁵

With the successfully isolated *Cl*-BODIPYs in hand, the synthesis of the heavier halogen *X*-BODIPYs was attempted. The same dipyrinato lithium complexes were synthesized and treated with both BBr₃ and BI₃. However, these reactions were not as successful. In both cases, upon addition of the boron trihalide, the reaction mixture instantly became deep red and exhibited fluorescence, indicating that the *X*-BODIPYs may be present. However, the products could only be isolated in impure form, even after multiple attempts to purify them via solvent washes, crystallization and chromatography. The reaction was attempted using various solvents, including CH₂Cl₂ and THF, but toluene produced the most promising results based on the NMR data of the crude materials, as reactions conducted in these solvents resulted in the least number of impurities. The crude material was washed with hexanes and filtered over Celite. Further attempts to purify the materials included filtration over both a silica and an alumina plug. However, the instability of the products resulted in decomposition during these procedures, and loss of fluorescence.

While the synthesis of *Cl*-BODIPYs was very successful using the dipyrinato lithium complexes, it was decided to attempt the synthesis without first generating these precursors. When the hydrobromide salts of the dipyrins were mixed with boron trihalides, there was no reaction. Therefore, the hydrobromide salts, in a solution of diethyl ether, were converted to their free-base dipyrins through treatment with concentrated ammonium hydroxide (28%), followed by an aqueous wash and then drying over Na₂SO₄. Solutions of the free-base dipyrins (**3** and **5**) in toluene were then stirred

and treated with one equiv of BCl_3 (Scheme 21). Upon addition of the BCl_3 the reaction mixture changed from yellow in colour to a red-orange solution with a green fluorescent hue, again suggesting the formation of the *Cl*-BODIPYs. After 1 hour of stirring, the reaction mixtures were filtered over Celite, with the filtrate then being concentrated *in vacuo* to provide the products as red solids (quantitative isolated yields of both **3BCl₂** and **5BCl₂**). It should be noted that treating the free-base dipyrins with BBr_3 and BI_3 resulted in fluorescence yet again, but isolation of those *X*-BODIPYs was again unfruitful.



Scheme 21: Synthesis of *Cl*-BODIPYs from free-base dipyrins

3.3.2 – Reactivity of *Cl*-BODIPYs

Having explored the reactions of boron trihalides BCl_3 , BBr_3 , and BI_3 with dipyrins, attention was next turned to the reactivity of the new *Cl*-BODIPYs. Due to the difference in boron-halogen bond strengths between the B-F ($\Delta H_{f298} = 766$ kJ/mol) and B-Cl ($\Delta H_{f298} = 536$ kJ/mol) bond,⁵⁴ it was reasoned that the lability of the B-Cl bond would be much greater than that of the B-F bond. It was expected that substitution of halogen at the boron atom of *Cl*-BODIPYs would be much more facile than for the corresponding *F*-BODIPYs. To investigate the differences in reactivity, dialkyl, diaryl and dialkoxy BODIPYs were synthesized from the new *Cl*-BODIPYs (Scheme 22). The conditions

5BEt₂) were also synthesized from the *Cl*-BODIPYs. As EtMgBr was added to solutions of **3BCl₂** and **5BCl₂** in anhydrous diethyl ether, in each case an orange precipitate immediately formed and the solutions became red-orange. The reaction mixture was then washed with water and extracted with diethyl ether. The organic layer was dried over Na₂SO₄ and concentrated *in vacuo*. The products **3BEt₂** and **5BEt₂** were obtained as red crystalline solids in quantitative yields. The diaryl *C*-BODIPY **3BPh₂** was synthesized through the addition of PhLi to a solution of **3BCl₂** in anhydrous THF, resulting in an immediate colour change to dark red with a red fluorescent tinge. After 1 h the reaction mixture was filtered over Celite and the resulting filtrate was concentrated *in vacuo* to give a crude red-brown powder containing the desired product **3BPh₂** (50% isolated yield after column chromatography), as well as several other compounds in minor amounts, including the trisubstituted meso-phenyl derivative **5BPh₂**: it has been shown previously that when *B*-arylation reactions are carried out on meso-H *F*-BODIPYs, unwanted meso-substituted by-products are also produced.³⁷

Importantly, substitutions at the boron atom of **3BCl₂** and **5BCl₂** were achieved in quantitative yield using mild conditions (room temperature) and short reaction times (1-3 hours). The conditions reported for the synthesis of all compounds in Scheme 22 from **3BF₂** and **5BF₂** are significantly harsher, e.g., reflux temperatures, 18 hour reaction times. To enable a direct comparison of the relative reactivities of *Cl*-BODIPYs and *F*-BODIPYs, the conditions used to convert **3BCl₂** and **5BCl₂** to the analogues *O*- and *C*-BODIPYs were applied to **3BF₂** and **5BF₂**. When the corresponding *F*-BODIPY **3BF₂** was treated with the conditions used for the quantitative synthesis of *O*-BODIPYs from **3BCl₂**, only trace product was observed. This is unsurprising as reported procedures for

O-BODIPY synthesis starting from *F*-BODIPYs requires activation of the B-F bond with AlCl₃ followed by treatment with methanol³⁹ or, reported more recently, treatment with sodium methoxide at elevated temperature.³⁷ Using *Cl*-BODIPYs, rather than *F*-BODIPYs, is clearly more fruitful due to the higher yields, lower temperatures and shorter reaction times. In forming the diphenyl *C*-BODIPY, the *F*-BODIPY **3BF₂** was treated with PhLi under the same conditions that had been used to generate **3BPh₂** from the *Cl*-BODIPY **3BCl₂**. A mixture of **3BPh₂** and the corresponding meso-phenyl substituted derivative (**5BPh₂**) was thus generated in a 36% overall yield after an extended reaction time. Procedures for diaryl *C*-BODIPY synthesis are routinely carried out at room temperature with yields <50%.⁵⁶⁻⁵⁷ When *F*-BODIPY **3BF₂** was treated with the conditions that had been used to generate **3BEt₂** from **3BCl₂**, the diethyl *C*-BODIPY was produced in 67% yield. This yield was much lower than that obtained when starting from *Cl*-BODIPY **3BCl₂**. Reported procedures for the formation of dialkyl *C*-BODIPY starting from *F*-BODIPY demonstrate that reactions conducted at room temperature produce yields under 60%⁵⁷⁻⁵⁸ and that an elevated temperature is necessary to obtain high yields.³⁷

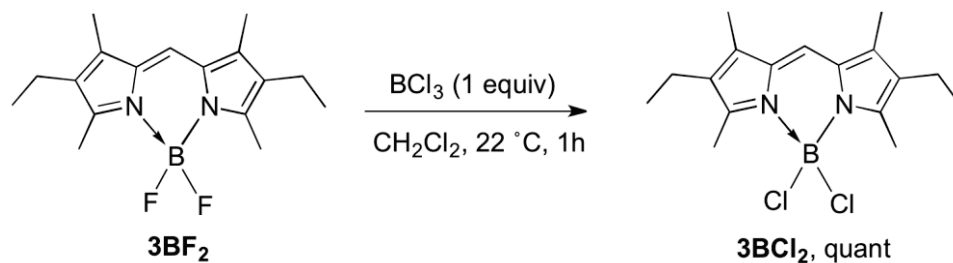
<i>B</i>-Substitution Conditions	<i>Cl</i>-BODIPY 3BCl₂	<i>F</i>-BODIPY 3BF₂
NaOMe, MeOH, 3 h, 22 °C	3B(OMe)₂ , quant	3B(OMe)₂ , No Reaction
PhLi, THF, 1 h, 22 °C	3BPh₂ , 50%	3BPh₂ and 5BPh₂ (1.0 : 0.2) after 24 h, 36%
EtMgBr, Et ₂ O, 3 h, 22 °C	3BEt₂ , quant	3BEt₂ , 67%

Table 3: Summary of *F*-BODIPY **3BF₂** and *Cl*-BODIPY **3BCl₂** reactivity

3.3.3 – Conversion of *F*-BODIPY to *Cl*-BODIPY

Originally the work with *Cl*-BODIPYs was focused on using the dipyrin free-base as the starting material.⁵³ However, many dipyrins are generally not isolated as a free-base due to instability, or simply as a consequence of the synthetic strategies used in their preparation. Dipyrins are often isolated as their HX salts, which happen to be unreactive with BCl₃. In some instances the dipyrin is not isolated after its formation via the oxidation of a dipyrromethane and is instead simply trapped *in-situ* with BF₃•OEt₂ to form the *F*-BODIPY.³ Therefore, the methodology described thus far for preparing *Cl*-BODIPYs from free-base dipyrins is rather limiting. As such, it became clear that an alternate route for the synthesis was required in order to make these compounds more accessible.

The *F*-BODIPY is the most common BODIPY construct, both in terms of synthetic use and commercial availability. Therefore, this construct was used as the source of the dipyrinato unit for the synthesis of *Cl*-BODIPYs. The *F*-BODIPY **3BF₂** was thus stirred in anhydrous CH₂Cl₂ at room temperature and the solution then treated with one equiv of BCl₃ (Scheme 23). The initial solution was bright orange with a green fluorescent hue: upon treatment with BCl₃ the solution immediately became deep purple in colour. The reaction mixture was stirred for 1 h and then filtered through Celite. The resulting solution was concentrated *in vacuo* to gratifyingly give a quantitative yield of complex **3BCl₂** as a pure solid, as identified through the comparison of characterization data with the known compound.⁵³



Scheme 23: Conversion of *F*-BODIPY to *Cl*-BODIPY

The reaction appeared to occur quite rapidly; therefore, attempts were made to monitor the reaction *via* ^{11}B NMR spectroscopy which revealed that as soon as the BCl_3 was introduced to the solution of *F*-BODIPY, the *Cl*-BODIPY formed before data acquisition could begin (< 2 mins). The reaction was then performed in an NMR tube, in the presence of controlled amounts of BCl_3 to enable the conversion of the *F*-BODIPY to the *Cl*-BODIPY to be monitored through noting changes in the ^{11}B resonances. A solution of *F*-BODIPY **3BF₂** in CD_2Cl_2 was placed in an NMR tube under an inert nitrogen atmosphere, and the sample was sealed with a septum. Aliquots of BCl_3 were added through the septum, as a 1.0 M solution in CH_2Cl_2 , and the sample was quickly shaken to ensure efficient mixing before NMR spectra were acquired. In each case, 128 scans were acquired within 2 mins of the BCl_3 addition. The results of these experiments are shown in Figure 4. The starting material *F*-BODIPY (**3BF₂**) appears as a triplet in the ^{11}B NMR spectra due to B-F coupling. As BCl_3 was added, the *F*-BODIPY triplet decreased in intensity and a singlet corresponding to the *Cl*-BODIPY appeared. After 0.5 equiv of BCl_3 had been added (Figure 4, middle) integration of the two signals revealed the two species to be present in essentially equal amounts, as expected. Upon the addition of 1.0 equiv BCl_3 , complete conversion to the *Cl*-BODIPY was observed, with only a

singlet apparent in the ^{11}B NMR spectrum. The NMR experiments demonstrate the clean conversion from 3BF_2 to 3BCl_2 .

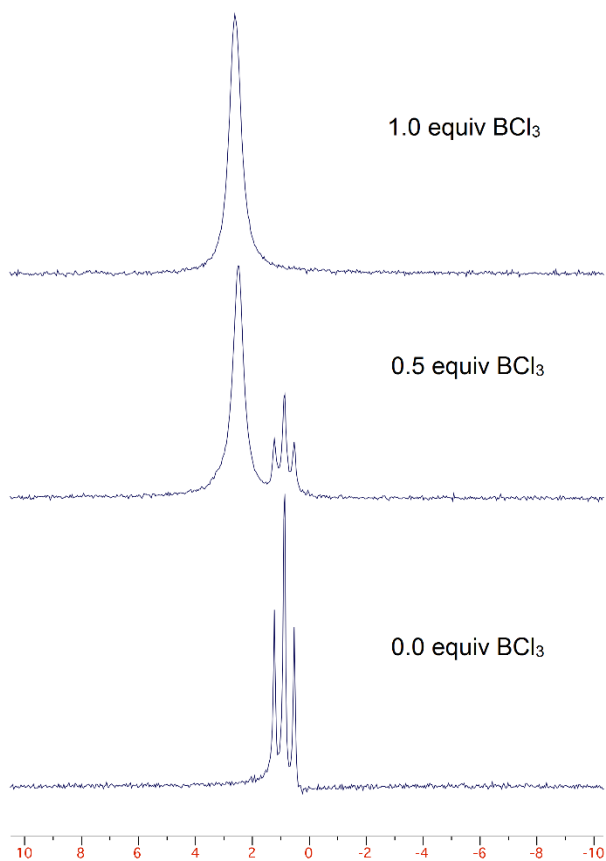
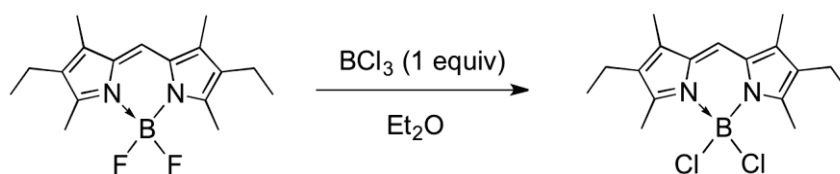


Figure 4: ^{11}B NMR stack-plot revealing the conversion of *F*-BODIPY to *Cl*-BODIPY. Bottom = *F*-BODIPY 3BF_2 ; middle = *F*-BODIPY 3BF_2 and *Cl*-BODIPY 3BCl_2 after the addition of 0.5 equiv BCl_3 to the solution of 3BF_2 ; top = only *Cl*-BODIPY 3BCl_2 present after the addition of 1.0 equiv BCl_3

The NMR experiment reported in Figure 4 shows complete conversion of the *F*-BODIPY to *Cl*-BODIPY with 1 equiv of BCl_3 . However, this led to questions regarding the mechanism that transforms the *F*-BODIPY to the *Cl*-BODIPY. The ^{11}B NMR spectrum of the product mixture shows the presence of the boron signal corresponding to a BODIPY, with no evidence of a boron-containing by-product, suggesting that the by-product must leave the solution as a gaseous substance. The mechanism of this

transformation could conceivably occur *via* two pathways. It is possible that the boron centre of the *F*-BODIPY is displaced by the boron atom of the BCl_3 . Alternatively, it is also possible that halogen exchange occurs between the $-\text{BF}_2$ moiety of the *F*-BODIPY and BCl_3 .⁵⁹⁻⁶⁰ Several experiments were performed to determine which mechanism is more plausible. Initially the conversion of 3BF_2 to 3BCl_2 was monitored using ^{11}B NMR spectroscopy once more, using 1 equiv of BCl_3 under an inert atmosphere. However, this time the experiment was conducted in anhydrous Et_2O in an attempt to trap any boron trihalide by-products in solution as their etherate adducts, e.g., $\text{BF}_2\text{Cl}\cdot\text{OEt}_2$, an expected by-product (Scheme 24). The resulting ^{11}B NMR spectrum obtained from this experiment is shown in Figure 5 and reveals the presence of a singlet corresponding to the *Cl*-BODIPY, a singlet corresponding to $\text{BF}_3\cdot\text{OEt}_2$, a triplet corresponding to $\text{BF}_2\text{Cl}\cdot\text{OEt}_2$, and a doublet corresponding to $\text{BFCl}_2\cdot\text{OEt}_2$ (Table 4). Indeed, every combination of fluoride- and chloride-containing boron trihalide BF_xCl_y ($x + y = 3$) was present and the ^{11}B NMR chemical shift values matched the literature values of the same etherates.⁶¹ It should be noted that the coupling constants for $\text{BFCl}_2\cdot\text{OEt}_2$ and $\text{BF}_2\text{Cl}\cdot\text{OEt}_2$ vary significantly, with values of 58.0 and 29.1, respectively. The reason for this disparity is due to the π bonding between the boron and fluorine atoms. As the fluorine atoms are replaced by less capable π bonding groups, the value of $^1J_{\text{B-F}}$ increases steadily, corresponding to an increase in the total π bonding per fluorine atom.⁶²

Overall, these results support the notion that halogen exchange occurs between the *F*-BODIPY and BCl_3 to liberate $\text{BF}_2\text{Cl}\cdot\text{OEt}_2$; however, it appears that the $\text{BF}_2\text{Cl}\cdot\text{OEt}_2$ species then undergoes further exchange of halogens until an equilibrium is formed between all possible boron trihalides.



Scheme 24: Conversion of *F*-BODIPY to *Cl*-BODIPY in diethyl ether

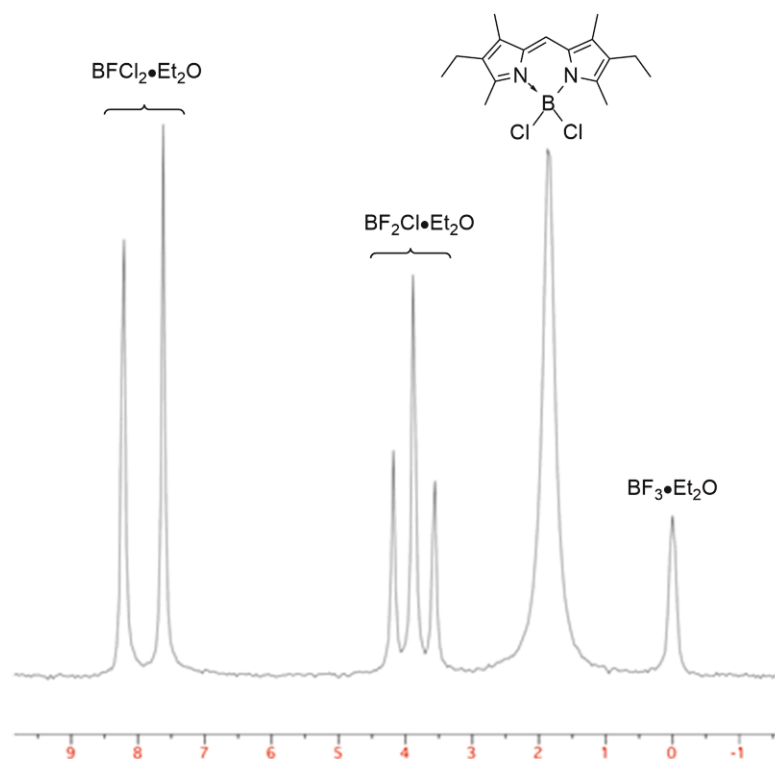
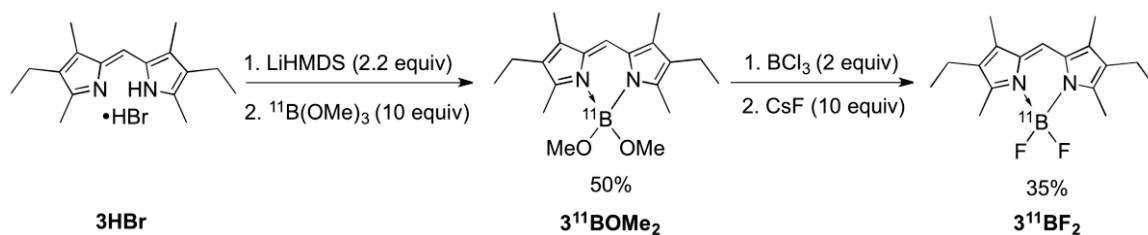


Figure 5: ^{11}B NMR spectrum showing the crude reaction mixture corresponding to Scheme 23, revealing the formation of boron trihalide by-products

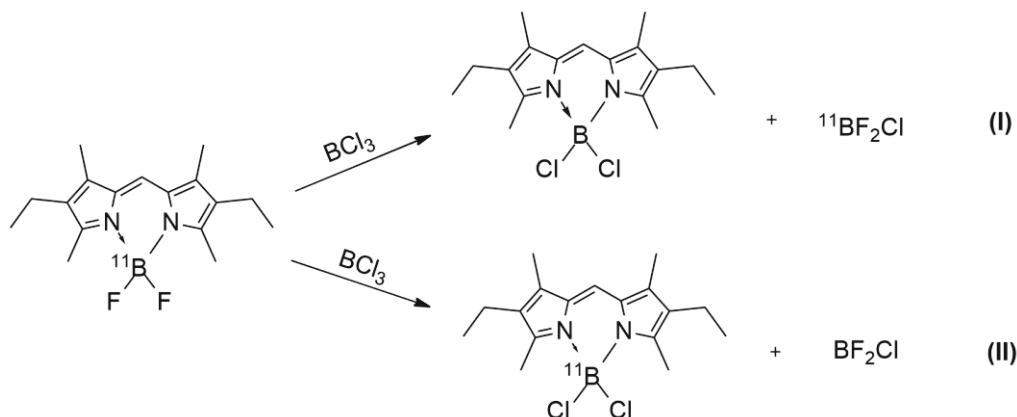
Compound	δ_{B} (ppm)	$^1J_{\text{B-F}}$ (Hz)
$\text{BF}_3 \cdot \text{OEt}_2$	0	--
3BCl_2	1.9	--
$\text{BF}_2\text{Cl} \cdot \text{OEt}_2$	3.9	29.1
$\text{BFCl}_2 \cdot \text{OEt}_2$	7.9	58.0

Table 4: ^{11}B NMR chemical shift data for the spectrum in Figure 5.

While this evidence certainly supports the notion that the mechanism for the transformation of *F*-BODIPYs into *Cl*-BODIPYs proceeds via halogen exchange, further experiments were required to solidify this claim. The next step was to prepare an *F*-BODIPY with an isotopically pure boron centre. With a labelled *F*-BODIPY, it would be possible to track the fate of the BODIPY boron centre in the conversion of the *F*-BODIPY to the *Cl*-BODIPY, to show whether or not the boron centre of the BODIPY remains in place thus supporting the claim of halogen exchange taking place. The easiest pathway to acquiring a labelled *F*-BODIPY would ideally be through the use of labelled $^{10}\text{BF}_3$ or $^{11}\text{BF}_3$, but attempts to procure this material were unfruitful. However, labelled ^{11}B trimethyl borate ($^{11}\text{B}(\text{OMe})_3$) was readily available and an alternative *F*-BODIPY synthesis was developed to incorporate this reagent (Scheme 25). The HBr salt **3HBr** was dissolved in anhydrous CH_2Cl_2 and treated with 2.2 equiv of LiHMDS, to form the lithium salt in-situ as the solution went from yellow to red with the appearance of a large amount of precipitate. To the reaction mixture, 10 equiv of $^{11}\text{B}(\text{OMe})_3$ was added and the precipitate dissolved as the solution went to deep red. The reaction mixture was washed with water, dried over Na_2SO_4 and concentrated in vacuo. The crude material was purified over alumina and the labelled *O*-BODIPY **3 $^{11}\text{B}(\text{OMe})_2$** was isolated in 50% yield. The next step required conversion of **3 $^{11}\text{B}(\text{OMe})_2$** to the labelled *F*-BODIPY. The *O*-BODIPY was thus dissolved in anhydrous CH_2Cl_2 and treated with 2 equiv of BCl_3 , followed by the addition of excess CsF. Upon completion of the reaction, the mixture was washed with water, dried over Na_2SO_4 and concentrated in vacuo. The crude product was purified over a pad of silica eluting with CH_2Cl_2 to afford the labelled *F*-BODIPY **3 $^{11}\text{BF}_2$** in 35% yield.



Scheme 25: Synthesis of ^{11}B labelled *F*-BODIPY



Scheme 26: Potential pathways **I** and **II** for *F*-BODIPY to *Cl*-BODIPY conversion

With the labelled *F*-BODIPY in hand (as confirmed using ^{10}B and ^{11}B spectroscopy), the aim was to convert this material to the *Cl*-BODIPY by treatment with BCl_3 , as achieved previously, and determine if the boron atom in the starting *F*-BODIPY is the same boron atom present in the resulting *Cl*-BODIPY (Scheme 26). Naturally occurring boron is composed of two stable isotopes, being ^{10}B and ^{11}B in an approximate ratio of 20:80.⁶³ Since the labelled *F*-BODIPY contained a ^{11}B enriched boron centre, the conversion from *F*- to *Cl*-BODIPY was to be monitored using both ^{10}B and ^{11}B NMR spectroscopy. The isotopically pure ^{11}B labelled *F*-BODIPY would not be observed using ^{10}B NMR spectroscopy; therefore, if the conversion of *F*-BODIPY to *Cl*-BODIPY occurs via halogen exchange, the resulting *Cl*-BODIPY should have the same labelled boron centre as the original *F*-BODIPY and thus present no signal in the ^{10}B NMR spectrum.

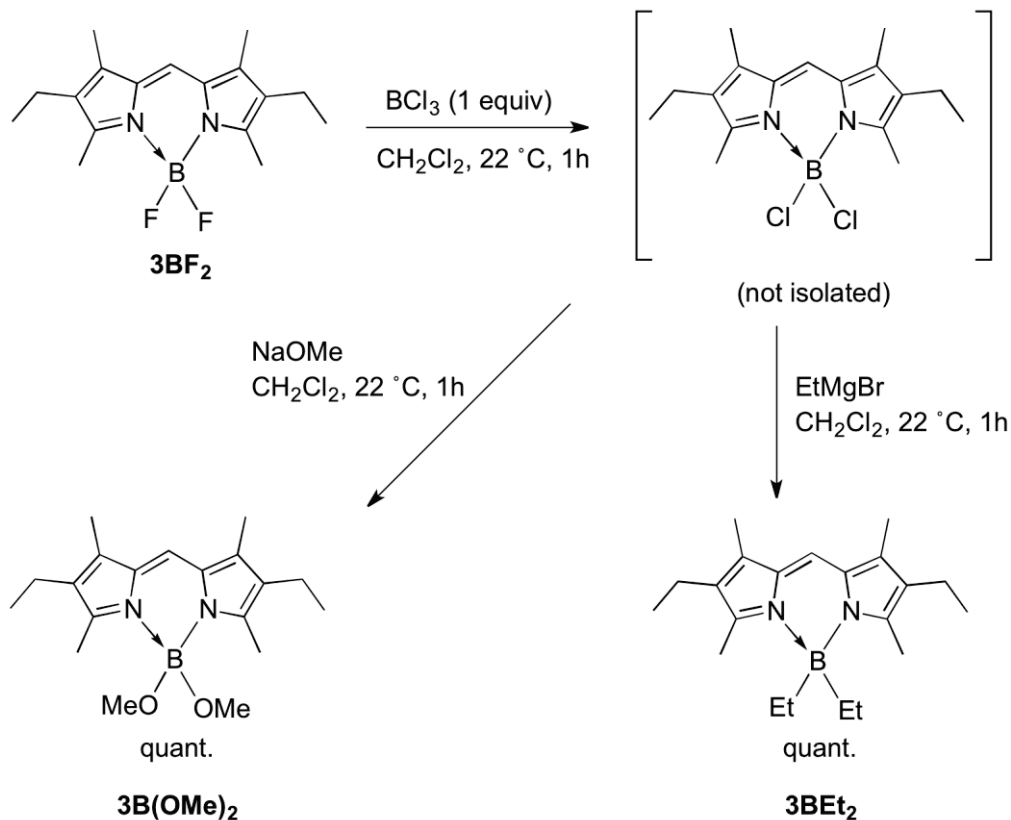
However, if the boron centre of the labelled *F*-BODIPY is displaced by the boron of the unlabelled BCl_3 , then a signal would appear in the ^{10}B NMR spectrum for the resulting *Cl*-BODIPY. To carry out this experiment under an inert atmosphere, the labelled ^{11}B *F*-BODIPY was dissolved in CD_2Cl_2 , and the solution placed in an NMR tube and sealed with a septum. A 1.0 M solution of BCl_3 in CH_2Cl_2 was then added through the septum and the sample was shaken to ensure mixing. As a control experiment, the unlabelled *F*-BODIPY was exposed to identical reaction conditions as those used for the substitution of the labelled *F*-BODIPY. The ^{10}B NMR spectrum of the product *Cl*-BODIPY for the unlabelled trial revealed the expected singlet, while the trial involving the labelled *F*-BODIPY revealed no ^{10}B signal, thereby supporting the previous indications that the *Cl*-BODIPY product contains the original labelled boron centre, and that the conversion of the *F*-BODIPY to the *Cl*-BODIPY occurs *via* halogen exchange.

3.3.4 – Using *Cl*-BODIPY as a Synthetic Intermediate

Having demonstrated that the *Cl*-BODIPY 3BCl_2 can easily be generated from its analogous *F*-BODIPY, the next step was to examine the utility of the *Cl*-BODIPY as a synthetic intermediate. The goal was to substitute at the boron centre once more, but starting from the *F*-BODIPY and proceeding via the *Cl*-BODIPY in a one-pot procedure. It has already been shown that substitutions at the boron atom of *Cl*-BODIPYs occur under mild conditions (Scheme 22). Therefore, it was a logical next step to try and prepare these known compounds using the *F*-BODIPY as a starting material. *F*-BODIPY 3BF_2 was thus treated with 1.0 equiv of BCl_3 in CH_2Cl_2 (Scheme 27) at room temperature. After 1 h, solid NaOMe was added to the solution under inert conditions and the reaction mixture was stirred for an hour. The solution was then washed with water

and extracted with CH₂Cl₂. The organic layer was dried over anhydrous Na₂SO₄ and concentrated *in vacuo*. The *O*-BODIPY **3B(OMe)₂** was thus isolated in a quantitative yield from **3BF₂**. As has been mentioned earlier in this chapter, to convert the *F*-BODIPY **3BF₂** directly to the dimethoxy *O*-BODIPY, the reaction requires elevated temperatures, typically reflux, and reaction times reaching 18 h.³⁷ Furthermore, when the *F*-BODIPY is treated directly with NaOMe at room temperature, only trace amounts of product are observed, supporting the discovery that the *Cl*-BODIPY intermediate is key to enabling substitution at the boron centre to proceed at room temperature under mild conditions. The *C*-BODIPY **3BEt₂** was also synthesized from *F*-BODIPY **3BF₂**, via the *Cl*-BODIPY intermediate. The initial formation of the *Cl*-BODIPY intermediate was carried out in the same fashion, and the solution was then treated with EtMgBr. Upon addition of the Grignard reagent the reaction mixture became bright orange rather than the dark purple colour of the *Cl*-BODIPY that had been formed *in-situ*. After an hour the reaction mixture was washed with water and brine, and extracted with CH₂Cl₂. The organic layer was dried over anhydrous Na₂SO₄ and the resulting solution concentrated *in vacuo* to give the *C*-BODIPY **3BEt₂** in a quantitative yield from **3BF₂**. It has been stated prior that treatment of *F*-BODIPY **3BF₂** with EtMgBr at room temperature results in the formation of **3BEt₂** (Table 3); however, the isolated product yield was 67% compared to the quantitative yield obtained when taking advantage of the *Cl*-BODIPY intermediate. Another benefit of using the *Cl*-BODIPY intermediate is that this strategy results in cleaner reactions. Column chromatography is required to purify the *C*-BODIPY **3BEt₂** prepared directly from the *F*-BODIPY at room temperature, but this is not necessary after

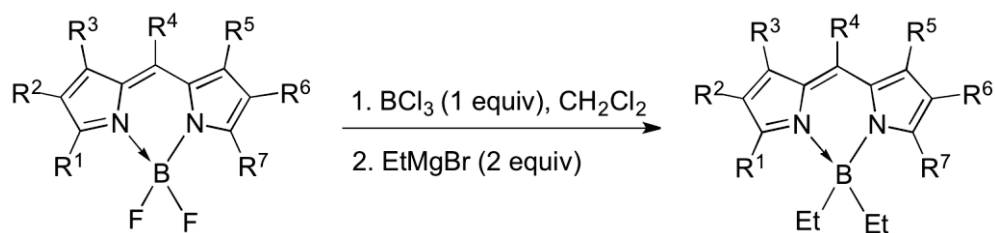
proceeding via the *Cl*-BODIPY: in the latter case, only a simple work-up consisting of an aqueous wash and drying of the organic phase is required.



Scheme 27: Synthesis of *O*-BODIPY (**3B(OMe)₂**) and *C*-BODIPY (**3BEt₂**) from *F*-BODIPY (**3BF₂**) using a *Cl*-BODIPY intermediate generated in situ

To demonstrate the utility of this one-pot procedure, it was necessary to expand the scope of the dipyrin ligands used (Table 5). Therefore, a variety of *F*-BODIPYs were converted to their analogous diethyl *C*-BODIPYs. The dipyrinato units of the BODIPYs used have various alkyl and ester substituents about the pyrrolic rings, and substitutions at the meso position, which are all common substituents about dipyrins. Entries 1-3 (Table 5) concern dipyrins that contain alkyl substituents around the pyrrolic rings, alongside both meso-H and meso-Ph substitution. Previous reactions of *F*-BODIPYs with

Grignard reagents have resulted in substitution at the meso position.³⁷ However, this was not observed when treating the *Cl*-BODIPY with the Grignard reagent and, instead, selective reaction at the boron centre occurred. Compound **7BEt₂** (Table 5, entry 4) contains a methyl alkanoate substituent, and this substrate was chosen to determine whether the Grignard reagent would preferentially react with the ester functionality or instead substitute at the boron centre. Some minor by-products formed from the reaction of the Grignard reagent with the ester functional group. However, these compounds were not isolated. The yield for the preparation of **7BEt₂** was only moderate at 75%, and the reaction mixture required filtration through a silica plug for pure **7BEt₂** to be obtained. Nevertheless, preferential reactivity of the Grignard with the boron centre, rather than the ester functionality, was clearly in evidence. Compound **8BEt₂** (Table 5, Entry 5) is completely unsubstituted on the pyrrolic rings, containing only a meso-Ph group, and was chosen to demonstrate the preferential reactivity of the Grignard reagent for substitution at boron as opposed to addition to the unsubstituted positions of the pyrrolic rings. A variety of *C*-BODIPYs were successfully prepared from *F*-BODIPYs in one pot via *Cl*-BODIPYs intermediates, and in high isolated yields. These yields are significantly higher than those generally found for the direct derivatization of *F*-BODIPYs under harsh conditions, demonstrating the overall efficiency of this new procedure.



Entry	BODIPY Product	Yield (%)
1		Quant.
2		Quant.
3		Quant.
4		75%
5		Quant.

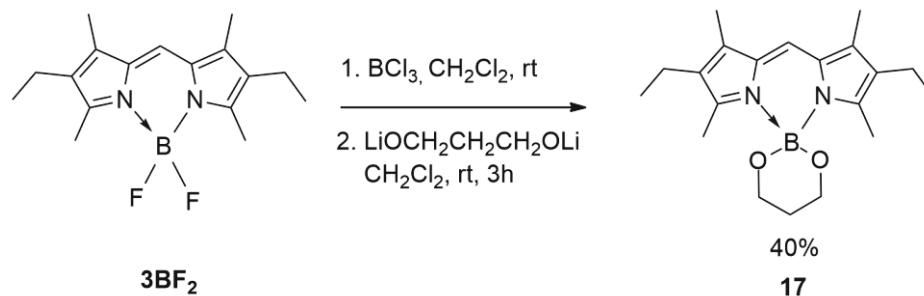
Table 5: Synthesis of *C*-BODIPYs from *F*-BODIPYs using *Cl*-BODIPY intermediates

To further demonstrate the advantageous use of *Cl*-BODIPYs as in situ intermediates, a transformation that has been previously unsuccessful for *F*-BODIPYs was attempted using a *Cl*-BODIPY. The reaction of a meso-aryl *F*-BODIPY with

alcohols in the presence of AlCl_3 has been reported to result in substitution at the boron centre to give a variety of *O*-BODIPYs: the reaction is believed to proceed via in situ formation of a chelate involving B-F-Al-F.³⁹ The Lewis acid activates the B-F bonds allowing a range of *O*-BODIPYs to be prepared in low-to-reasonable yields. These reactions were reported to not take place in the absence of AlCl_3 . The reactions proceeded well with alkyl and aryl alcohols, as well as with several diols to provide cyclic analogues. However, under these reported conditions, attempted substitution of the fluoro substituents with 1,3-propanediol did not provide the corresponding cyclic derivative at boron. Therefore, the methodology involving in situ generation of *Cl*-BODIPY was used to attempt to substitute 1,3-propanediol at the boron centre of an *F*-BODIPY.

The *F*-BODIPY **3BF₂** was reacted with 1 equiv BCl_3 in CH_2Cl_2 at room temperature, to form **3BCl₂** in situ (Scheme 28). In a separate flask, a stoichiometric amount of 1,3-propanediol was dissolved in CH_2Cl_2 at room temperature and reacted with 2 equiv of LiHMDS to form the lithium dialkoxide of 1,3-propanediol. The lithium dialkoxide solution became a slurry which was then added to the reaction mixture containing the *Cl*-BODIPY intermediate. The reaction was stirred for 3 hours. The solution was then washed with brine, dried over Na_2SO_4 and concentrated in vacuo. The crude material was purified over silica to give compound **17** in 40% yield for the two-step, one-pot transformation. The methodology used to perform this substitution at the boron centre was vastly different than the AlCl_3 method mentioned previously, but with good reason. Initial attempts to synthesize compound **17** began by reacting the *Cl*-BODIPY **3BCl₂** with 1,3-propanediol but this was unsuccessful and so the lithium

dialkoxide was used. Reaction of *F*-BODIPY **3BF₂** with the lithium dialkoxide was also attempted and this was unsuccessful, clearly demonstrating the advantage of proceeding via the *Cl*-BODIPY using the one-pot procedure.



Scheme 28: Preparation of cyclic *O*-BODIPY **17**

3.3.5 – Synthesis of Chiral *O*-BODIPYs

While the BODIPY chromophore is well known, most reported compounds of this type are achiral in nature. As such, the chiroptical properties of chiral derivatives have been largely neglected. However, in recent years, chemists have started to develop various BODIPY dyes containing chiral appendages to expand the use of BODIPYs as a chiral fluorophore in fields such as laser dyes, photodynamic therapy agents and a multitude of photonic devices.⁶⁴ The first chiral BODIPYs came from compounds containing chiral functional groups around the dipyrin core, typically containing a large chiral moiety in the meso position.⁶⁵⁻⁶⁷ The majority of these compounds were synthesised using a homochiral building block which was attached to a BODIPY to form the final product. For example, Daub and co-workers reported the synthesis of homochiral bis-BODIPY complexes that were prepared through the incorporation of chiral 1,1'-bi-2-naphthol (BINOL) moieties via the meso position of dipyrins (Figure 6,

left).⁶⁵ Another example was developed by Zhu et al. whereby enantiopure (*S*)-1-bromo-2-methylbutane was incorporated at the meso-position of a BODIPY core (Figure 6, right).⁶⁸ The purpose of the (*S*)-2-methylbutoxyl group was to increase solubility in conventional organic solvents. Zhu and co-workers ultimately developed a variety of chiral BODIPY-based donor- π -acceptor type polymers using a palladium-catalyzed Sonogashira polymerization. These polymers exhibit red fluorescent emission and have tunable band gaps making their photophysical and electrochemical properties sufficient for investigation in device-based applications.

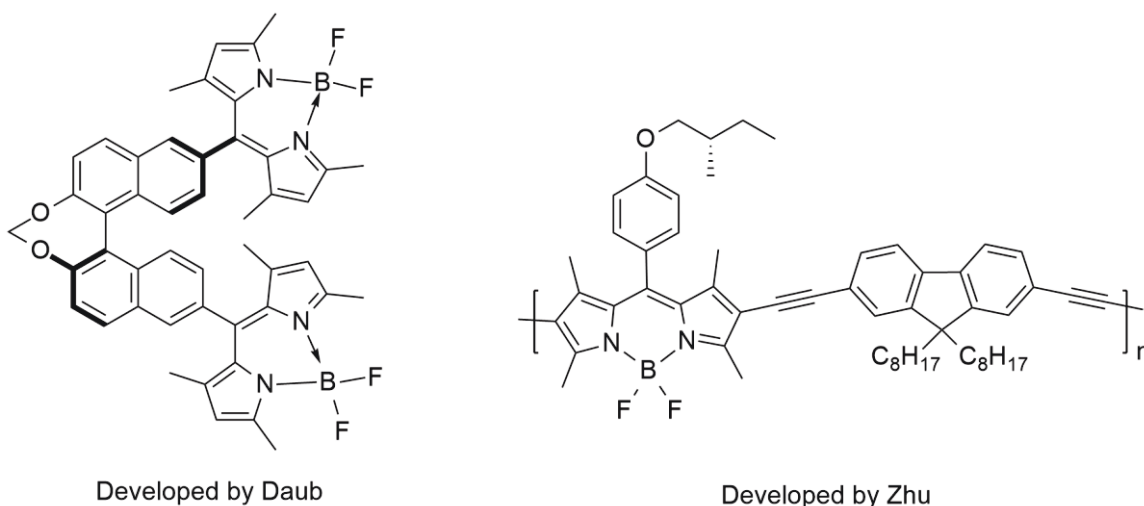


Figure 6: Chiral *F*-BODIPYs incorporating homochirality via the meso-position

While the use of homochiral appendages was successful in developing the first chiral BODIPYs, other researchers have isolated homochiral BODIPYs via chiral resolution methods. Ziessel and co-workers were the first to isolate a chiral BODIPY in this manner (Figure 7, left).⁶⁹ These researchers developed a BODIPY that undergoes dissymmetrization at the central boron atom due to the introduction of a formyl group on one pyrrole unit that renders the chelate unsymmetrical and stabilizes the configuration at

the boron centre via hydrogen bonding to the fluoro ligand. The BODIPY was synthesized as a racemate and resolution was achieved using chiral HPLC. Another variety of chiral BODIPYs that have been resolved using chiral HPLC are atropisomers such as those developed by the two groups of Akkaya and Hall (Figure 7, middle and right, respectively).^{64, 70} These types of stereoisomers exhibit axial chirality as a result of a nonplanar arrangement of different substituents on both sides of the chiral plane. The enantiopure species are configurationally stable and enable isolation, courtesy of the restricted rotation of a single bond on the chiral axis.

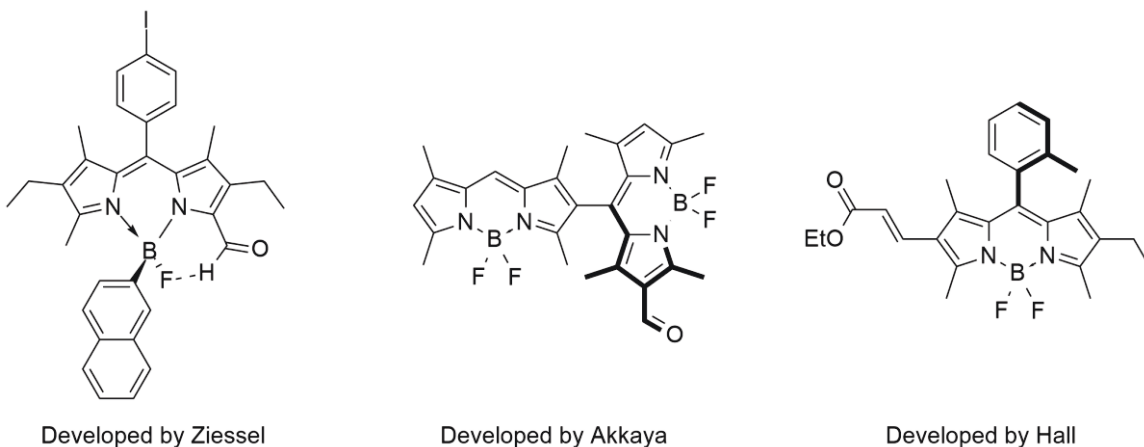
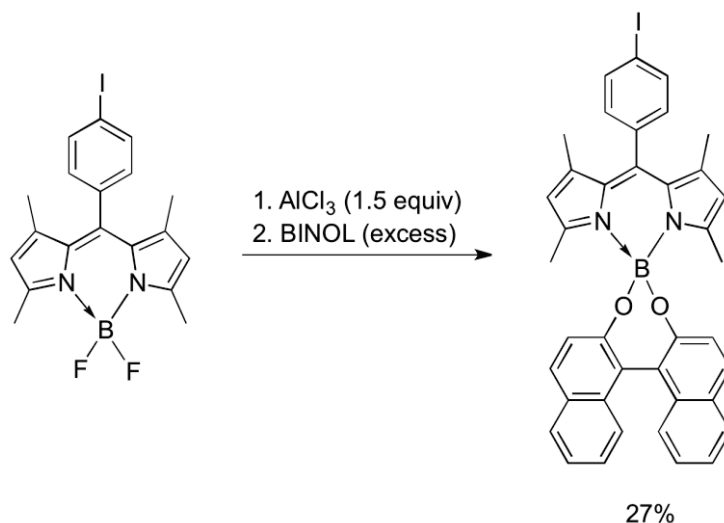


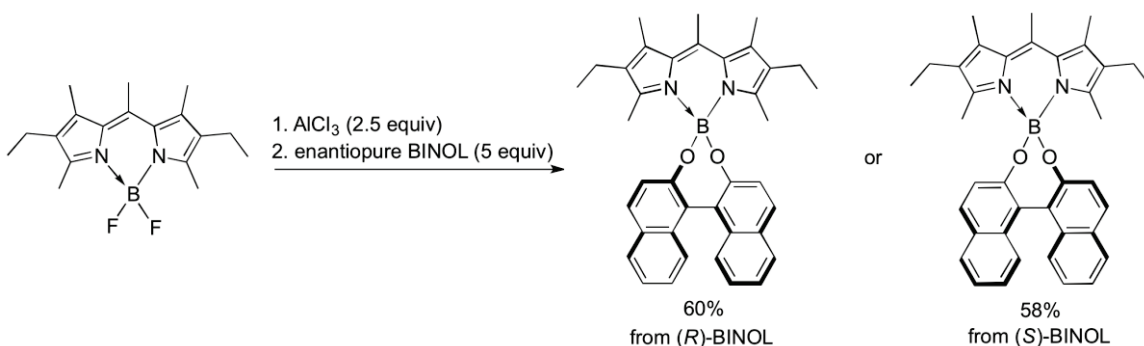
Figure 7: Chiral BODIPYs isolated using chiral resolution

The work developed by Tahtaoui and co-workers led to the synthesis of the first *O*-BODIPYs from *F*-BODIPYs.³⁹ These initial studies involved the activation of the B-F bond of the *F*-BODIPY with 1.5 equiv AlCl_3 , followed by treatment with excess amounts of alcohol which is then substituted onto the boron centre to give the *O*-BODIPY. One particular example involved the substitution of racemic BINOL on the boron centre to successfully provide a cyclic derivative in modest yield (Scheme 29). These studies

regarding the synthesis of *O*-BODIPYs have led to the discovery of chiral *O*-BODIPYs where the chirality is introduced at the boron centre, developed by de la Moya and co-workers.⁶⁷ These BODIPYs were prepared by substituting an enantiopure BINOL moiety at the boron centre of the previously achiral *F*-BODIPY chromophore (Scheme 30). To prepare these compounds, the starting material *F*-BODIPY was heated at reflux temperature with AlCl₃, under argon, and the reaction mixture then cooled to room temperature. Once cooled, a solution of 5 equiv of enantiopure BINOL in acetonitrile was added drop-wise to the reaction mixture. The solution was stirred at room temperature for another 6 hours. Upon completion of the reaction, the products were purified using column chromatography, and isolated in ~60% yield. These compounds exhibit interesting chiroptical properties in terms of their electronic circular dichroism (ECD) spectra, demonstrating that the designed chiral perturbation interferes with the BODIPY chromophore, at least in the ground state, suggesting it could interfere with the excited states of the BODIPY chromophore, thus leading to circularly polarized luminescence (CPL). CPL is the differential emission of right- and left-circularly polarized light by chiral luminescent systems. These data provide information about the general structure of the involved excited states, of use to applications focused on the improvement and potential development of multiple photonic tools (3D optical displays, optical storage, bio probes, etc.). These particular *O*-BODIPYs were the first reported molecules to exhibit CPL from achiral chromophores, upon direct absorption of visible light by the BODIPY itself.



Scheme 29: Synthesis of racemic *O*-BODIPY



Scheme 30: Chiral *O*-BODIPYs developed by de la Moya

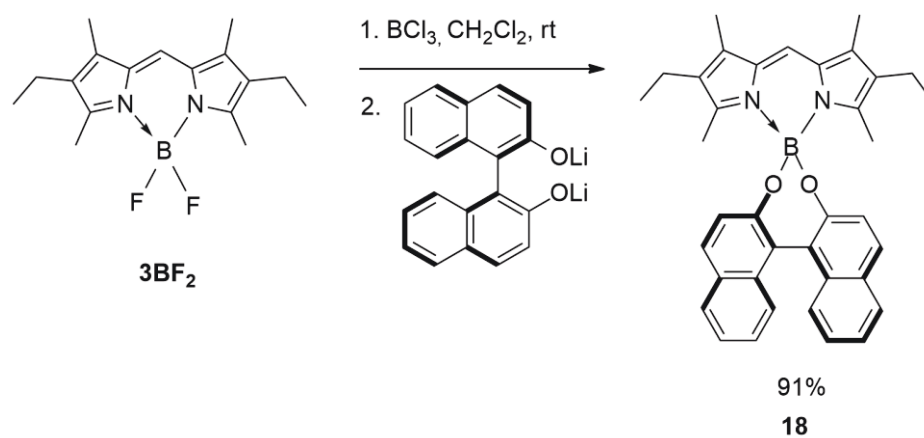
The synthetic routes for these various types of chiral BODIPYs include the attachment of a chiral appendage to the dipyrroin core, synthesis of a racemate that is later resolved using chiral resolution techniques and most recently the direct substitution of a chiral moiety at the central boron atom. Our interest lies in the most recent form of substitution at the boron centre to induce chirality via the use of a homochiral appendage. The use of *Cl*-BODIPYs for such a transformation has the potential to provide an efficient route to homochiral BODIPYs due to the ease of substitution at boron when

compared to analogous *F*-BODIPYS. While other groups have developed homochiral BODIPYS to study the various properties of these compounds, our interest in these specific compounds lies in the design of efficient methodologies for their synthesis. The present study focuses on using the chemistry of substitution at the boron centre, as shown previously in this thesis, to synthesize new homochiral BODIPYS in high yields and under mild reaction conditions.

The chemistry described hereafter was developed several years prior to the publications showing the first chiral *O*-BODIPYS and while this work has some features similar to those recently published by others, the scope of the reactions has the potential to be expanded further than in the published cases.⁶⁷ As demonstrated earlier in this thesis, work with *Cl*-BODIPYS revealed their tendency toward facile substitution at the boron centre. Therefore, the reaction of a *Cl*-BODIPY with a homochiral nucleophile to effect substitution at the boron centre was formally investigated as an intended synthetic route to create single enantiomers of BODIPYS that are chiral by virtue of a homochiral auxiliary at boron. Using a homochiral nucleophile to substitute at the boron centre allows an opportunity to introduce chirality at a late stage in the synthesis of the fluorescent species. The first homochiral appendages of choice were the two enantiomers of BINOL. Incorporating an enantiomerically pure BINOL into the BODIPY framework would allow us to investigate the chiroptical properties of the resulting homochiral BODIPYS.

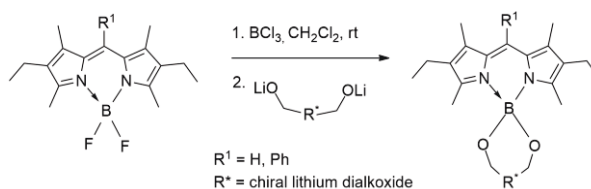
The preparation of these homochiral BODIPYS began with the reaction of a solution of **3BF₂** in CH₂Cl₂ at room temperature with 1 equiv of BCl₃, to result in the formation of **3BCl₂** in-situ, all under an inert N₂ atmosphere (Scheme 31). As with the synthesis of previous *O*-BODIPYS herein, such as compound **17** (Scheme 28), (*R*)-BINOL

was first converted to the corresponding dilithium alkoxide before reaction with **3BCl₂**. The lithium dialkoxy BINOL derivative (1 equiv) was added drop-wise to the solution of **3BCl₂** in CH₂Cl₂, in 1:1 stoichiometry. The solution of **3BCl₂** changed from purple to dark red upon the addition of the lithium dialkoxide solution. The reaction mixture was stirred for another hour and then washed with brine. The organic fraction was then dried over Na₂SO₄ and concentrated in vacuo. The crude reaction mixture was filtered through a pad of silica, eluting with CH₂Cl₂ to result in **18** as a red solid in a two-step, one-pot transformation and a 91% yield. The purity of **18** was such that chromatography was unnecessary. The same reaction was completed using (*S*)-BINOL to prepare enantiomeric **19** with similar success (Table 6). The methodology utilized by de la Moya, incorporating AlCl₃, for the synthesis of comparable compounds (Scheme 30) resulted in much lower isolated yields of roughly 60% after the requirement for further purification via column chromatography. The reaction conditions required reflux temperatures and reaction times over 6 hours, as well as the use of excess amounts of the BINOL reagent. Furthermore, the methodology presented in this thesis for the synthesis of these homochiral BODIPYs, utilizing the *Cl*-BODIPY intermediate, is performed with stoichiometric amounts of reagents, entirely at room temperature, and with shorter reaction times. Additionally, the yields were higher upon using the methodology involving *Cl*-BODIPY intermediates, with the desired homochiral compounds isolated in ~90% yields.



Scheme 31: Synthesis of chiral *O*-BODIPY **18** using (*R*)-BINOL.

With the successful synthesis of the first chiral pair of *O*-BODIPYs **18** and **19**, the scope of the reaction was expanded upon by varying both the *F*-BODIPY substrates as well as the homochiral nucleophiles to be substituted onto the boron centre. *F*-BODIPY **5BF₂** was the next substrate to be chosen as it contains a meso-Ph substituent. The pair of chiral *O*-BODIPYs **20** (incorporating (*R*)-BINOL) and **21** (incorporating (*S*)-BINOL) were successfully prepared in 90% yield (Table 6, entries 3 and 4), following the same methodology as used for **18** and **19**.



Entry	BODIPY Product	Yield (%)	
1		18	91 ^a
2		19	91 ^a
3		20	90 ^a
4		21	90 ^a

^aGlovebox, 50 mg scale.

Table 6: Synthesis of chiral *O*-BODIPYs by substitution at boron atom

3.3.6 – Chiroptical Properties of Chiral Compounds

With two pairs of chiral BODIPY compounds in hand it was important to measure the circular dichroism (CD) of these pairs, to determine the Cotton effects of the various chromophores. The Cotton effect is the characteristic change in circular dichroism in the

vicinity of the absorption band of the compound. The CD spectra of these compounds were acquired using a Jasco J-810 spectropolarimeter with a 2 mm cell and CH₂Cl₂ as the solvent. The molar ellipticities are recorded in units of degrees cm²dmol⁻¹. It should be noted that the spectropolarimeter uses a Xenon lamp with an ideal range of 190-850 nm. However, the data tends to become less accurate as the lamp heads below 225 nm and any data collected lower than this wavelength is omitted.

To examine the chiroptical activities of compounds **18** and **19**, the CD spectra of solutions of each of these compounds in CH₂Cl₂ were recorded. The CD spectra of solutions of **18** and **19** in CH₂Cl₂, each with concentration 2.7 x 10⁻⁵ M, exhibited Cotton effects with maxima at 238, 343 and 530 nm and were essentially mirror images of one another, as expected for a pair of enantiomers. The CD spectrum of a 4.9 x 10⁻⁵M solution of (*S*)-BINOL in CH₂Cl₂ was also recorded and can be seen as an inset in Figure 8. The BINOL ligand exhibits Cotton effects with maxima at 240 and 318 nm. Thus, the Cotton effects from compounds **18** and **19** below 350 nm are most heavily influenced by the BINOL moiety as is evident from the similar shapes of the curves in this region of the spectra. The enhanced CD activity at 343 nm is an induced circular dichroism generated by the BINOL. The complexed BINOL ligand shows much more prominent signals in the CD spectrum than the free BINOL ligand presumably is due to the increased rigidity of the BINOL moiety in the BODIPY compound, resulting in a lower dihedral angle between the 1,1'-binaphthalenes relative to the free BINOL ligand.⁷¹

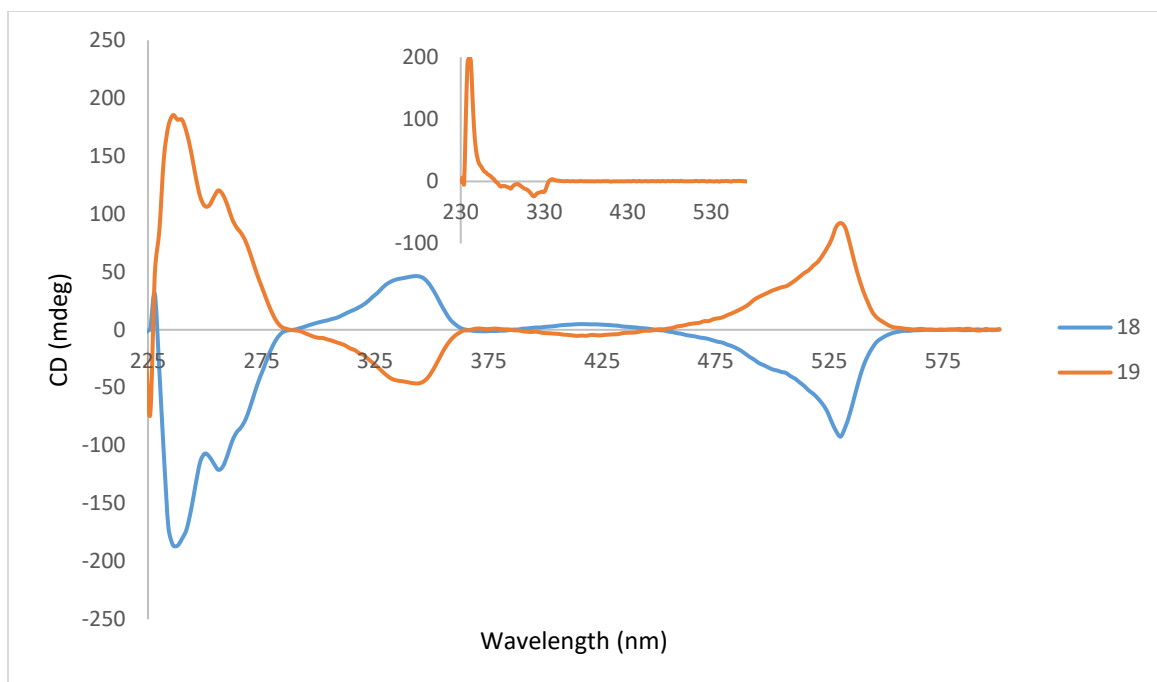


Figure 8: CD spectra of compounds **18** (blue), **19** (red) and (*S*)-BINOL (inset) in CH₂Cl₂.

The lowest energy CD signal in the visible range of the CD spectrum for **18** at 530 nm corresponds to the electronic transition from the ground to the first excited states ($S_0 \rightarrow S_1$ transition) of the BODIPY core, as shown in the UV/Vis absorbance spectrum (Figure 9).⁷² All samples in Figure 9 were run at a concentration of 2.7×10^{-5} M in CH₂Cl₂. The modest shoulder found at a slightly higher energy is attributed to out-of-plane vibrations of the aromatic skeleton. Compound **18** exhibits a negative Cotton effect, i.e. the optical rotation first decreases as the wavelength decreases and a positive effect if the reverse occurs. The strong Cotton effects for both **18** and **19** in the visible region of the spectra show that the chiral perturbation of the BINOL moiety is acting on the BODIPY chromophore, at least in the ground state. These results suggest that the BINOL moiety could also potentially act on the involved excited states of the BODIPY

chromophore, making these compounds potentially suitable for CPL as was the case with similar compounds reported in the literature.⁶⁷

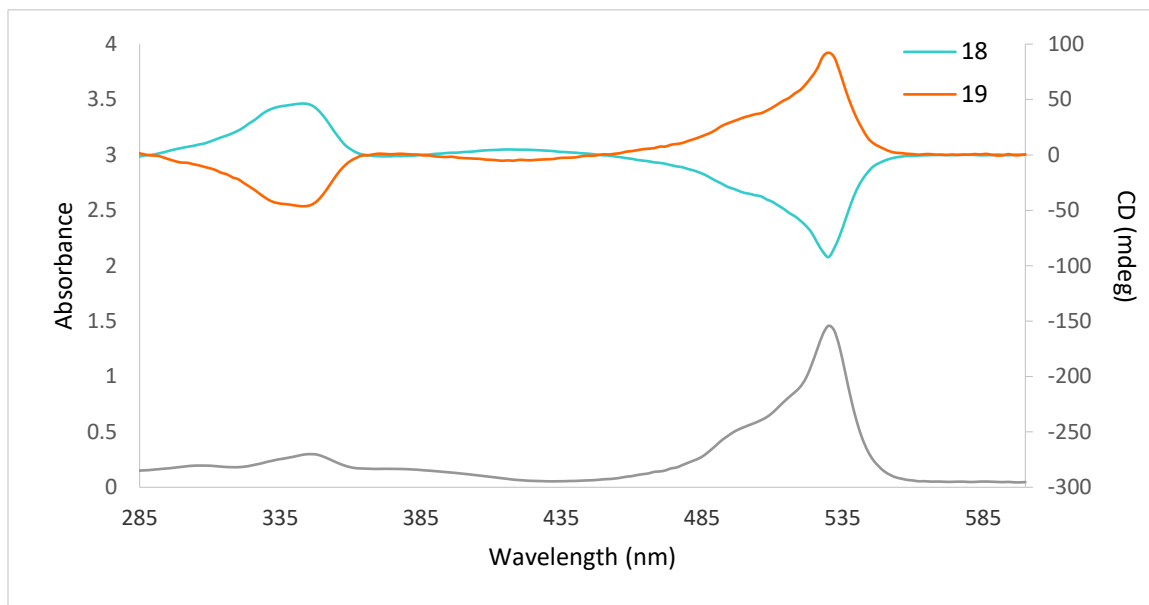


Figure 9: Isolated section of CD spectra of **18/19** (top), UV/Vis spectrum of **18** (bottom).

The chiroptical activities of compounds **20** and **21** were also investigated. The CD spectra of **20** and **21** exhibited Cotton effects with maxima at 242, 334 and 526 nm and were essentially mirror images of one another, as expected of the enantiomeric pair (Figure 10). The spectra were gathered with a sample concentration of 3.5×10^{-5} M. Similar to the pair of compounds **18** and **19**, the Cotton effects shown below 350 nm are most heavily influenced by the BINOL moiety (Figure 8). Again, it can be seen that the enhanced activity at 334 nm is due to an induced circular dichroism by the BINOL moiety. However, it should be noted that compared to compounds **18** and **19**, compounds **20** and **21** show weaker activity, particularly in the visible region of the spectrum. The area of the spectrum induced by the BINOL portion of the molecule still exhibits comparable CD activity to compounds **18** and **19**.

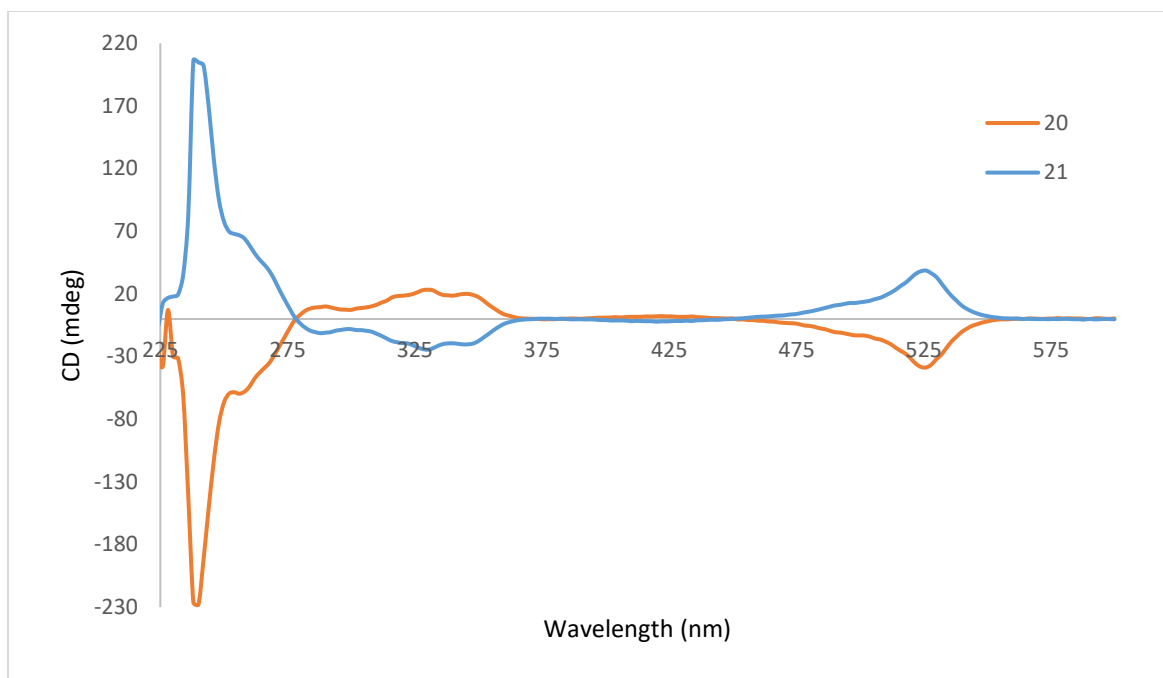


Figure 10: CD spectra of compounds **20** and **21**

Compound	λ_{abs} (nm)	ϵ_{abs} ($\text{M}^{-1}\text{cm}^{-1}$)	λ_{em} (nm)	$[\Theta]$ ($^{\circ}\text{cm}^2\text{dmol}^{-1}$)	Φ_{F}
3BF₂	531	87 000	538	--	0.91
5BF₂	525	81 000	533	--	0.88
3BCl₂	540	35 000	548	--	0.45
5BCl₂	533	30 000	547	--	0.40
18	530	32 000	536	3.4×10^5	0.13
19	530	32 000	536	-3.3×10^5	0.13
20	526	29 000	535	1.1×10^5	0.13
21	526	29 000	535	-1.3×10^5	0.13

Table 7: Spectroscopic data of chiral BODIPY compounds

The presence of the meso-Ph substituent in compounds **20** and **21** appears to play a factor in reducing the amount of chiral perturbation on the BODIPY chromophore by the BINOL ligand, which is surprising considering the molar absorptivity of the meso-H and meso-Ph compounds are quite comparable. The overlay of CD spectra from compounds **19** and **21**, comparing the meso-H and meso-Ph variants, shows the two samples run at the same concentration of 1.3×10^{-5} M (Figure 11). The CD spectrum of (*S*)-BINOL is also shown, so as to enable comparison to the free-ligand to the complexed variants, and is run at the same concentration of 1.3×10^{-5} M. The molar ellipticities at the peak wavelength of each Cotton effect can be found in Table 8. These results suggest that perhaps the B-O bonds of the meso-Ph compound (**21**) are longer than the meso-H compound (**19**) resulting in the BINOL moiety sitting further away from the BODIPY chromophore. This would allow for a decrease in the rigidity and an increase in the dihedral angle of the 1,1'-binaphthalenes in **21**, which would provide a lower intensity CD signal in the UV region as is shown in Figure 11. If the BINOL moiety truly is further from the BODIPY chromophore in **21**, it would also explain the decreased activity in the visible region due to a decrease in the chiral perturbation of the BODIPY chromophore by the BINOL ligand. It is abundantly clear that, compared to the CD activity of the free BINOL, the complexed species still show much stronger signals overall.

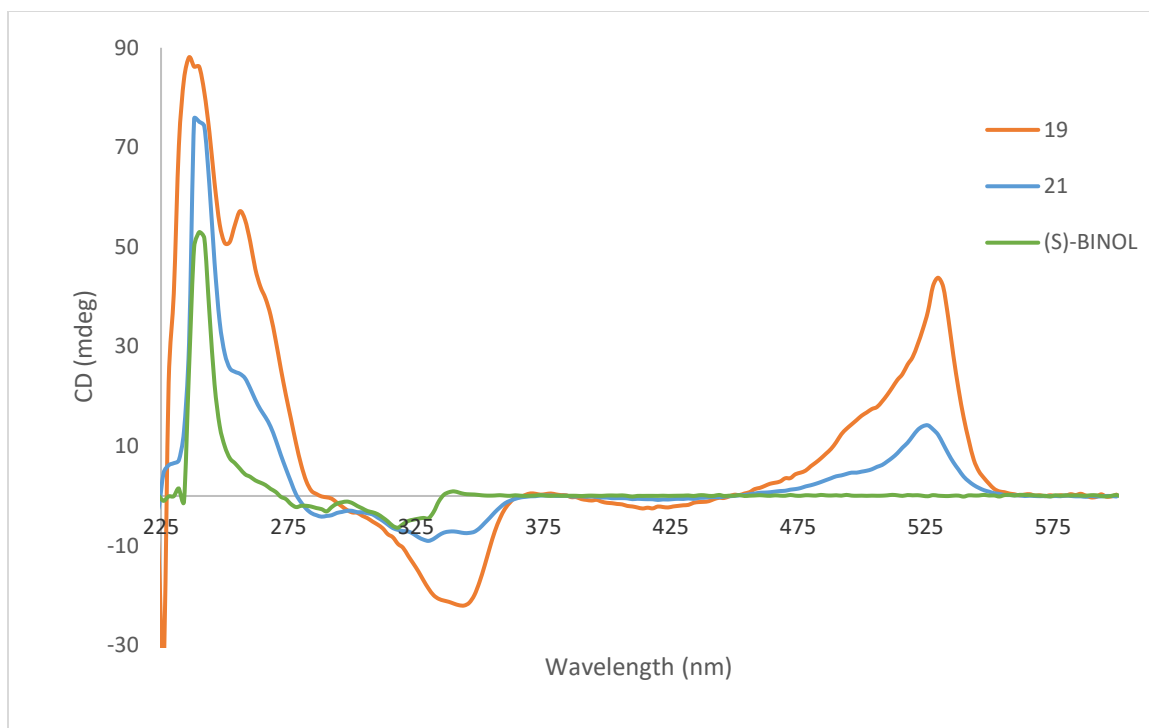


Figure 11: Comparison of CD spectra between compounds **19**, **21** and (*S*)-BINOL at the same concentration (1.3×10^{-5} M).

Compound	λ_{abs} (nm)	$[\Theta]$ ($^{\circ}\text{cm}^2\text{dmol}^{-1}$)
18	238; 343; 530	6.8×10^5 ; -1.7×10^5 ; 3.4×10^5
19	238; 343; 530	-6.6×10^5 ; 1.6×10^5 ; -3.3×10^5
20	242; 334; 526	5.8×10^5 ; -6.9×10^4 ; 1.1×10^5
21	242; 334; 526	-5.9×10^5 ; 7.1×10^4 ; -1.3×10^5
(S)-BINOL	240; 318	4.1×10^5 ; -4.9×10^4

Table 8: Molar ellipticities of chiral BODIPY compounds **18-21**.

3.3.7 – Comparison of Spectroscopical Properties

The absorbance spectrum of free-base dipyrin **3** is shown in Figure 12 and presents a λ_{\max} at 486 nm. Complexation to the $-\text{BF}_2$ moiety to provide **3BF₂** results in a bathochromic shift of the λ_{\max} to 531 nm. The reason for this shift is that the $-\text{BF}_2$ group acts as a linking bridge, providing an even more rigid delocalized π -system. The substitution of the fluorine atoms of **3BF₂** with the oxygen atoms of BINOL (**18**) results in virtually no change of the absorbance spectrum in the visible region. The only variance in the absorbance curves is the presence of new peaks in the UV region on account of the BINOL moiety. However, when the fluorine atoms of **3BF₂** are substituted with chlorine atoms to give **3BCl₂**, the λ_{\max} is once again bathochromically shifted to 540 nm and the absorbance band is much broader.

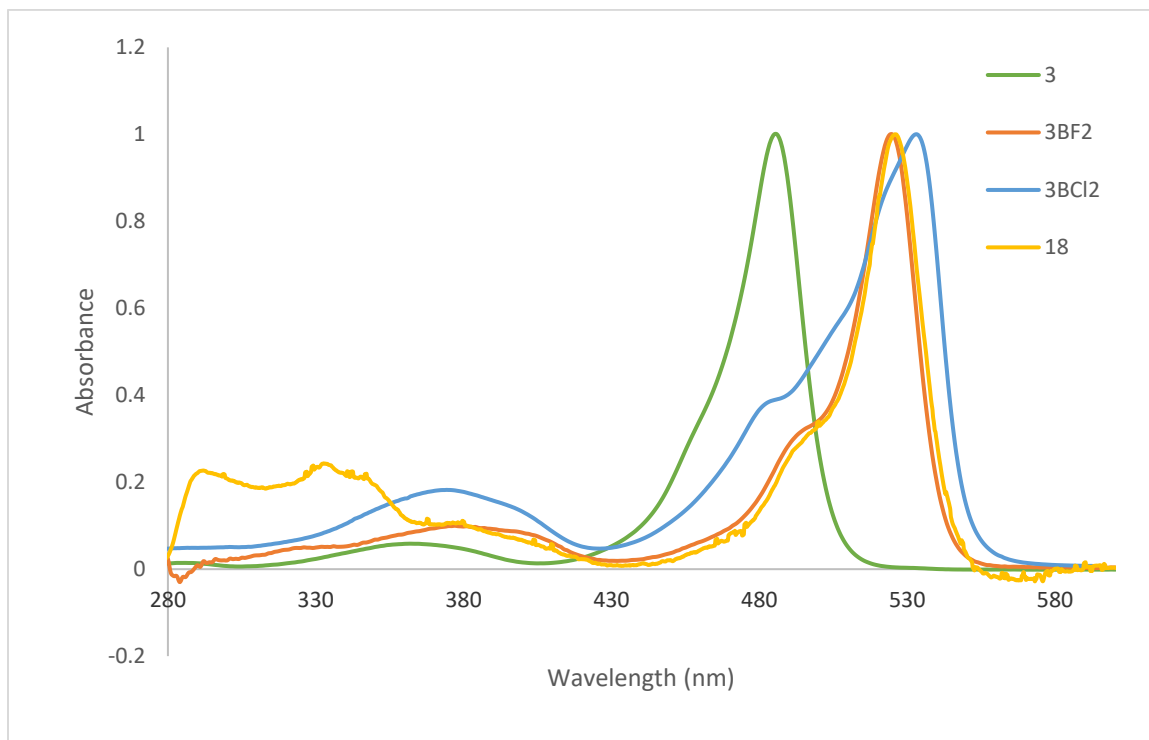


Figure 12: Comparison of normalized UV-vis data of various analogues of compound **3**.

The emission spectra of the BODIPY analogues of compound **3** were also obtained and are shown in Figure 13. The shape of each curve is essentially the mirror image of the $S_0 \rightarrow S_1$ absorption band found in the visible region of each curve in Figure 12, suggesting similar vibrational levels in both electronic states. Each fluorescent band is characterized by a small Stokes shift of 6-8 nm. The shape of the fluorescence band is also independent of the excitation wavelength which suggests that the emission is from the lowest vibrational level of the S_1 excited state, independent of the electron-vibrational level directly populated in the excitation process.⁷³ While the emission spectra appear similar, the quantum yields of the various BODIPYs varied greatly. Compound **3BF₂** had the greatest quantum yield of 0.91. However, conversion of the *F*-BODIPY to the *Cl*-BODIPY **3BCl₂** resulted in a quantum yield of 0.45. The reason for the sharp decrease in quantum yield is a result of the decrease in orbital overlap that occurs when substituting the fluorine atoms for chlorine. As mentioned earlier, the $-\text{BF}_2$ group of *F*-BODIPYs acts as a linker and enables a rigid delocalized π -system. With both boron and fluorine being second row elements, there is a better degree of orbital overlap between the atoms that allows for greater electron flow around the chromophore and thus an increase in emission. By introducing the chlorine atoms in place of the fluorine, the same degree of orbital overlap is not achieved which hinders the electron flow in the molecule resulting in lower emissions. The quantum yield for compound **18** is much lower than the other BODIPY analogues with $\Phi_F = 0.13$, as was expected.³⁹

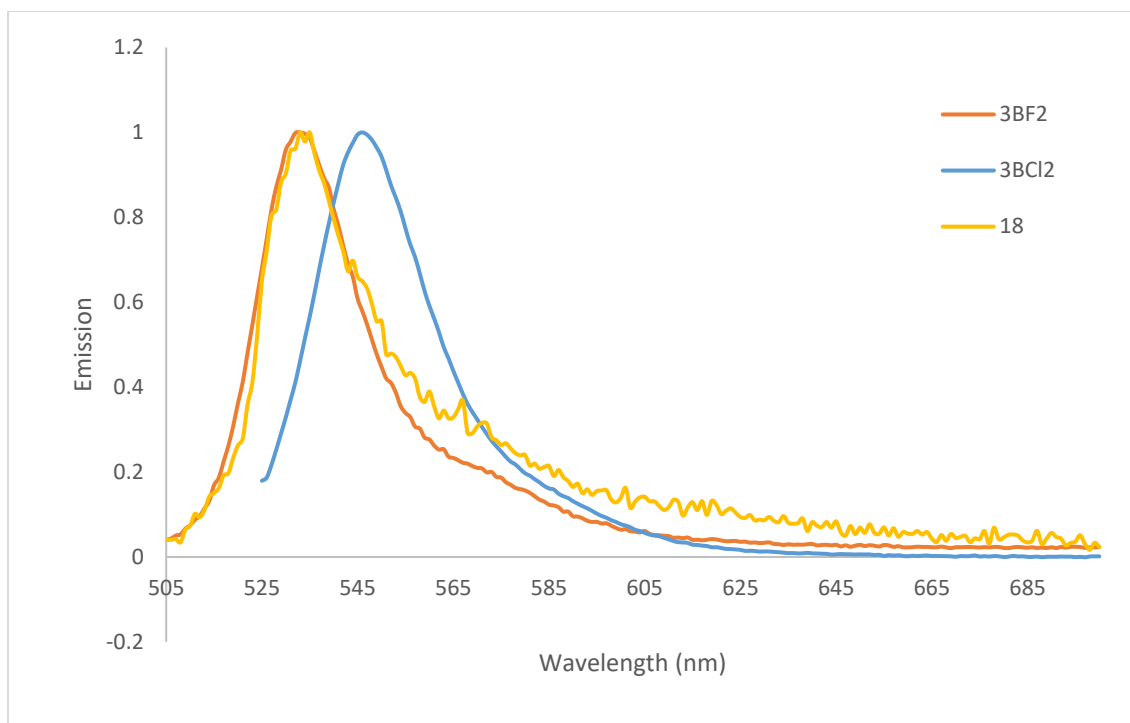


Figure 13: Comparison of normalized emission data of various analogues of compound **3**.

3.4 – Conclusions

In short, the first *Cl*-BODIPYs have been synthesized and are facile to substitute at boron, using mild conditions and short reaction times.⁵³ *Cl*-BODIPYs can be prepared from either the free-base dipyrin or the *F*-BODIPY.⁷⁴ It has been demonstrated that *Cl*-BODIPYs can be used in the preparation of BODIPY analogues that have been moderately difficult to prepare from the analogous *F*-BODIPY. The *Cl*-BODIPYs were also successfully used as a synthetic intermediate in a one-pot procedure for the formation of BODIPY derivatives with varying substituents at the boron centre, starting from the *F*-BODIPY. The one-pot conversion of *F*-BODIPYs to other BODIPYs was achieved in excellent yields, once again using mild reaction conditions and shorter reaction times than the traditional methods for substituting at the boron atom of *F*-

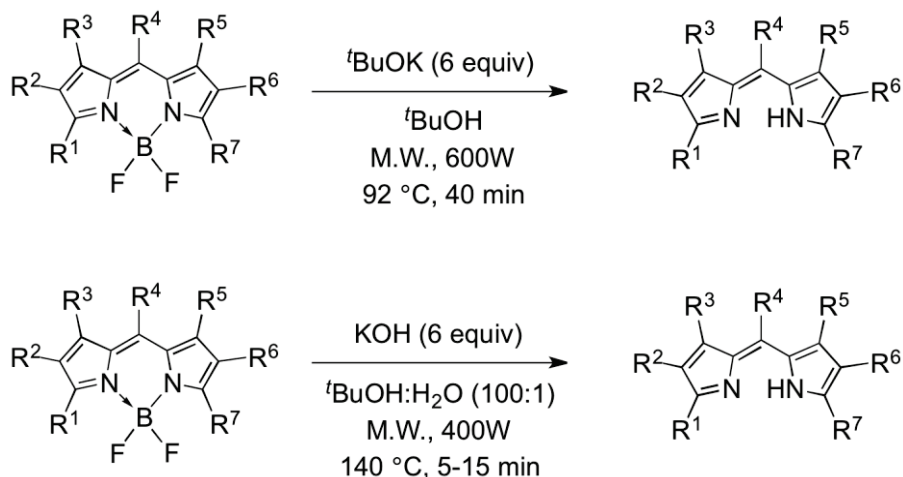
BODIPYs. This methodology was applied to the synthesis of homochiral BODIPYs featuring moieties at boron that effected stereochemical features by virtue of axial chirality. This method, involving generation and in situ substitution of *C**l*-BODIPYs, is higher yielding than reported methods, requires only stoichiometric amounts of the homochiral units and is conducted under mild conditions. Purification methods have also been simplified.

Chapter 4 – Activation and Deprotection of *F*-BODIPYs

4.1 – General Background

Countless BODIPYs have been synthesized and reported, yet until recently there was no clear way of removing the $-\text{BF}_2$ moiety from the dipyrinato ligand.³⁷ In many respects, the inability to remove the $-\text{BF}_2$ moiety from *F*-BODIPYs has not been troublesome as the *F*-BODIPY themselves have always been the synthetic targets, for use in a number of applications.³ However, the conversion of dipyrins to the corresponding *F*-BODIPYs can also be envisioned as a protecting group strategy, whereby the $-\text{BF}_2$ moiety acts as a protecting group for the parent dipyrin. *F*-BODIPYs are known to be more chemically robust than their dipyrin counterparts, and have been shown to undergo synthetic modifications at the dipyrinato core.⁷ An ideal scenario would involve the protection of the dipyrin as its more stable and easily purified *F*-BODIPY, which could then be chemically modified at the dipyrin core and then deprotected to give the desired dipyrin compound. However, to be a viable protecting group strategy, there must also be a feasible strategy to remove the $-\text{BF}_2$ moiety to provide the parent dipyrin. The Thompson group has published the first general methodology for the deprotection of *F*-BODIPYs using a microwave-assisted procedure involving 6 equiv of potassium tert-butoxide in tert-butanol in a sealed vessel at 92 °C for 40 minutes (Scheme 32).³⁷ These conditions resulted in good-to-excellent yields for a variety of substituted dipyrins. However, the Thompson group has since improved upon these reaction conditions by using potassium hydroxide, a mixture of tert-butanol/water as the solvent, and higher

temperatures for shorter reaction times.⁷⁵ The improved methodology also provided good-to-excellent yields, and for an even wider array of dipyrins.



Scheme 32: *F*-BODIPY deprotection strategies using microwave-assisted conditions

4.2 – Project Goals

While the deprotection strategies discussed thus far have been very successful, there are several limitations. The strategies presented are only successful when using microwave heating. A deprotection strategy would be much more useful and accessible if it could be accomplished using conventional heating or without the need for heat at all. Furthermore, the success of the current strategies depends entirely on the stability of the parent dipyrin in the free-base form under the rather harsh basic aqueous conditions. It is known that some dipyrins, specifically the meso-H variants, are generally unstable as their free-base which is why they are typically isolated as HX salts. Since the dipyrins that result from the deprotection strategies shown in Scheme 32 are isolated as their free-bases, that also means that column chromatography is required to purify these dipyrins which can also provide

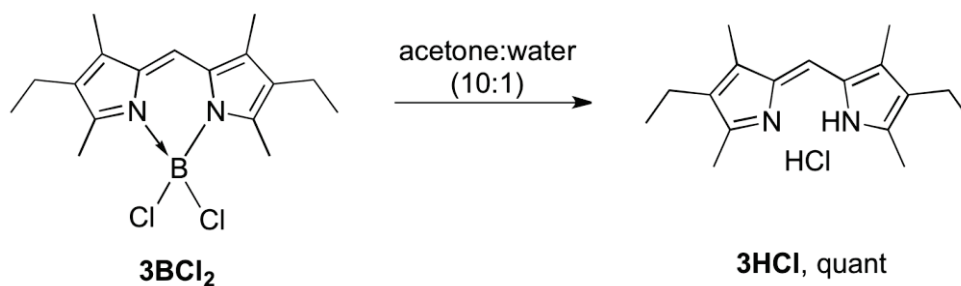
difficulties. Therefore, it would be beneficial to have a deprotection strategy for *F*-BODIPYs that can bypass some of these current limitations. In this vein, it was postulated that the inherent sensitivity to moisture of the *Cl*-BODIPYs would render feasible the use of this construct as an intermediate in the deprotection of *F*-BODIPYs.

4.3 – Results and Discussion

4.3.1 – Deprotection of *F*-BODIPYs using *X*-BODIPY intermediates

As has been stated previously in this thesis, work with *Cl*-BODIPYs revealed their sensitivity to air and moisture.⁵³ Therefore, the reaction of *Cl*-BODIPY with water acting as the nucleophile to substitute at the boron centre was formally investigated as an intended synthetic route by which to remove the boron atom from BODIPYs. The expected result of this reaction would be the generation of the dihydroxy *O*-BODIPY, which is known to be unstable.⁷⁶ It has been reported that these dihydroxy *O*-BODIPYs are sensitive to aqueous acidic conditions which results in the liberation of boric acid through decomposition of the *O*-BODIPY. This decomposition can be viewed as a deprotection strategy to obtain the dipyrin by removal of the boron centre. Initial attempts to investigate the reaction of a *Cl*-BODIPY with water began by preparing a solution of **3****BCl₂** in CH₂Cl₂ and adding excess (10 equiv) water to the reaction mixture in a drop-wise fashion. However, due to the poor solubility of the water in CH₂Cl₂, the reaction proceeded quite slowly and did not reach completion even after stirring overnight at reflux. The ¹H NMR spectrum of the mixture

showed the presence of several dipyrin-containing compounds, some of which still contained a boron centre as shown in the ^{11}B NMR spectrum. Purification was attempted using column chromatography; however, the majority of the by-products decomposed on the alumina leaving only the free-base dipyrin to be isolated in a 62% yield. While the deprotection was successful, a different approach was chosen in an attempt to increase the yield of the reaction. The reaction was repeated in a different solvent mixture in order to completely solubilize the water. Thus, *Cl*-BODIPY **3BCl₂** was dissolved in a solution of acetone/water in a 10:1 mixture. The reaction was stirred for an hour, during which time the solution changed from green/orange in colour, typical of a BODIPY, to a yellow solution, typical of a dipyrin as either a free-base or HX salt. The reaction mixture was diluted with water and extracted three times with CH_2Cl_2 . The combined organic layers were dried over Na_2SO_4 and concentrated in vacuo to give an orange powder. The resulting material was the HCl salt of the dipyrin obtained in a quantitative yield (Scheme 33). Up until this point, all deprotections of *F*-BODIPYs were accomplished under basic conditions which resulted in the isolation of the dipyrin as its free-base. However, using the *Cl*-BODIPYs, only the HCl salt of the dipyrin was present in quantitative yield. The benefit of isolating these materials as HCl salts is that they are generally more stable than their free-base analogues and due to their differing solubility properties, purification only requires a wash with ether rather than column chromatography. Ether dissolves any trace starting material remaining, leaving the dipyrin HCl salt as an orange solid.



Scheme 33: Deprotection of *Cl*-BODIPY with water

The proposed mechanism for this reaction suggests that one equiv of water acts as a nucleophile attacking the boron centre of the *Cl*-BODIPY, releasing a molecule of HCl in the process (Figure 14). The mono-chloro BODIPY would react with another equiv of water to give the dihydroxy *O*-BODIPY. One more equiv of water would then attack the boron centre of the *O*-BODIPY, resulting in the loss of boric acid and formation of the free-base dipyrin. The free-base dipyrin would react with the HCl formed in situ to give the HCl salt of the dipyrin.

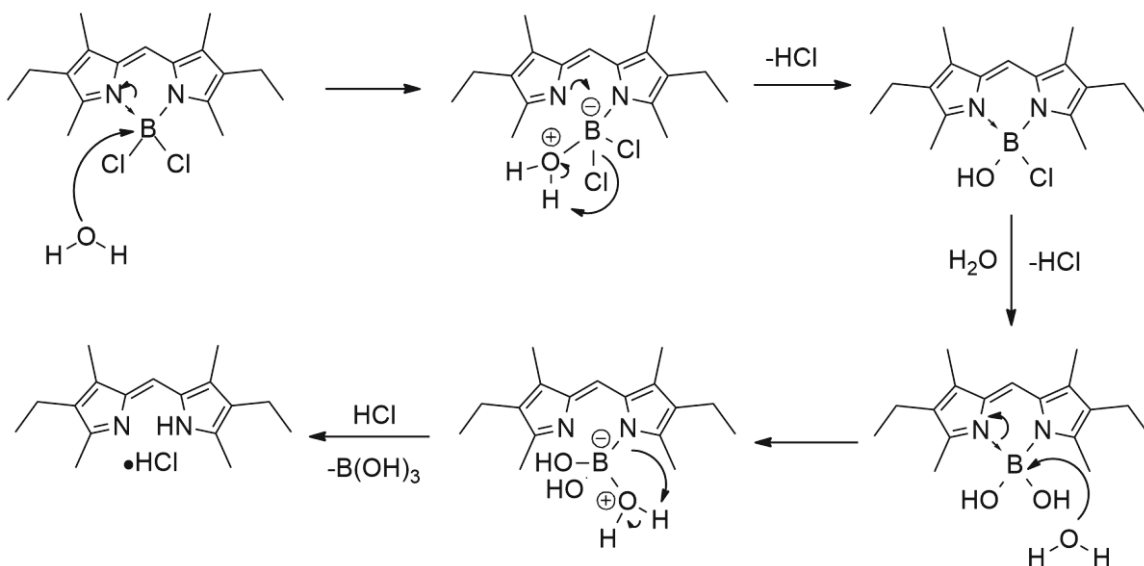
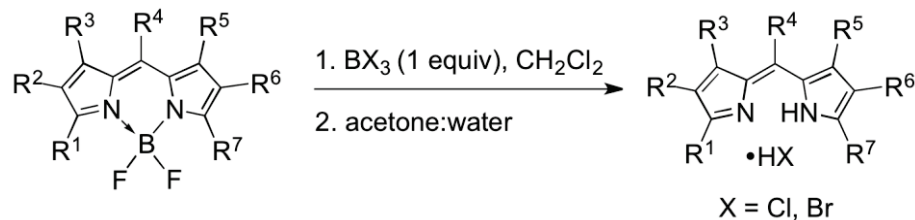
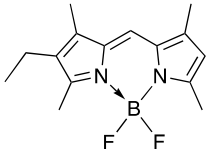
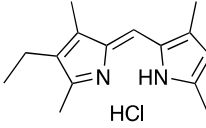
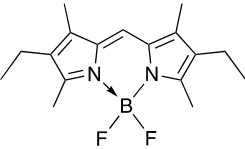
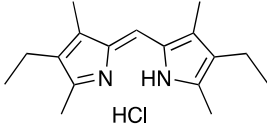
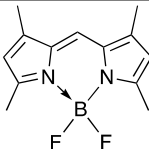
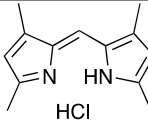
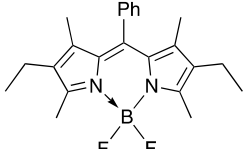
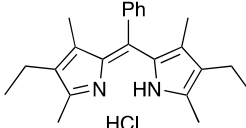
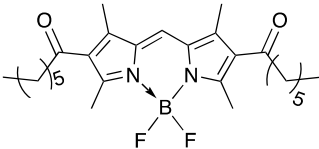
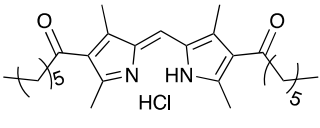
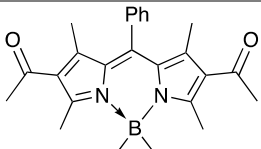
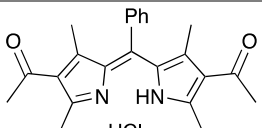
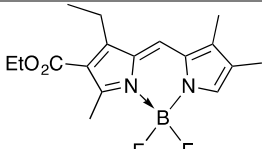
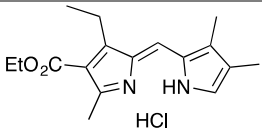


Figure 14: Proposed mechanism of *Cl*-BODIPY deprotection

With demonstration that *Cl*-BODIPY **3BCl₂** can be deprotected to provide the HCl salt of the dipyrin, the scope of the substrate was expanded in order to investigate the full utility of this methodology. Firstly, to improve the accessibility of this methodology, it was important to determine whether the deprotection strategy could work using *F*-BODIPY as the starting material and synthesizing the *Cl*-BODIPY in situ before deprotection. Reaction of *F*-BODIPY **3BF₂** in CH₂Cl₂ with BCl₃ (1 eq), under an inert atmosphere, achieved complete conversion to the *Cl*-BODIPY, as demonstrated previously.⁷⁴ The solvent was then removed in vacuo, still under inert conditions, and the remaining *Cl*-BODIPY was dissolved in acetone:water (10:1). The reaction mixture was stirred for an hour and upon aqueous work-up and extraction with CH₂Cl₂, the dipyrin HCl salt **3HCl** was afforded as an orange solid in quantitative yield (Table 9, entry 2). With the success of this reaction sequence, it has been demonstrated that *F*-BODIPY can be deprotected, in one-pot, to provide the dipyrin HCl salt under mild conditions using the *Cl*-BODIPY intermediate. A variety of *F*-BODIPYs with varying substituents were subjected to these deprotection conditions to explore the range of substrates with which this methodology is fruitful (Table 9).



Scheme 34: Deprotection of *F*-BODIPYs using *Cl*-BODIPY intermediate

Entry	<i>F</i> -BODIPY	Product	Isolated Yield (%)
1	 2BF₂	 2HCl	quant.
2	 3BF₂	 3HCl	quant. (quant.) ^a
3	 4BF₂	 4HCl	quant.
4	 5BF₂	 5HCl	quant.
5	 22BF₂	 22HCl	quant.
6	 23BF₂	 23HCl	quant.
7	 24BF₂	 24HCl	N/A (quant.) ^a

^aYields for the synthesis of HBr salt using BBr₃

Table 9: Conversion of *F*-BODIPYs to dipyrin HCl salts

The breadth of this mild deprotection strategy for the deprotection of *F*-BODIPY extends to a variety of functionalities around the dipyrin core (Table 9). Alkyl and keto substituents (Entries 1-6) were tolerated, and *F*-BODIPYs featuring a meso-phenyl group (Entries 4 and 6), were also converted to their HCl salts in quantitative yields. The *F*-BODIPY **24BF₂**, featuring an ester substituent, was successfully converted to the *Cl*-BODIPY. However, reaction with water to form the corresponding *O*-BODIPY was followed by complete decomposition of the material, rather than isolation of the dipyrin as its HCl salt. This result was surprising as there are several known examples of dipyrins containing conjugated ethyl esters that were formed as their HCl salts.^{35,36} While the exact dipyrin **24HCl** has never been reported in the literature, similar dipyrins have been isolated as their HCl salts. However, this dipyrin was successfully prepared as its HBr salt. Therefore, the focus of this deprotection strategy was directed towards preparing various HX salts rather than just the HCl salts.

It is known that HBr salts of dipyrins are more crystalline than other HX salts;⁷ therefore, it would be useful if this methodology for deprotection could also produce dipyrins as their HBr salts to increase the range of dipyrins for which this deprotection will be successful. Simply using BBr₃, in place of BCl₃, should result in the liberation of HBr during the reaction which will thus lead to dipyrin HBr salts. Initially, *F*-BODIPY **3BF₂** was subjected to the same reaction conditions mentioned above but with the addition of 1 equiv of BBr₃ instead of BCl₃. Upon addition of BBr₃, the reaction mixture changed from the green/orange colour typical of an *F*-BODIPY, to a dark red/purple solution with a fluorescent hue. Visually the solution was reminiscent of the in situ formation of a *Cl*-

BODIPY from an *F*-BODIPY. Using the altered protocol, compound **3BF₂** was successfully converted to the HBr salt **3HBr** in quantitative yield (Table 9, Entry 2, parentheses). With the success of this reaction, compound **24BF₂** was also subjected to the same reaction conditions involving BBr₃ and was also quantitatively converted to the HBr salt, **24HBr** (Table 9, Entry 7, parentheses). Given this result, it was hypothesized that the reaction of *F*-BODIPYs with BBr₃ will produce the corresponding *Br*-BODIPYs, despite the fact that previous attempts at isolating the *Br*-BODIPY were unsuccessful, albeit using a methodology involving lithium dipyrinato salts.⁵³ Therefore, the synthesis and isolation of *Br*-BODIPY, was revisited using the halogen exchange methodology starting with the *F*-BODIPY. The *F*-BODIPY **3BF₂** was dissolved in anhydrous CH₂Cl₂ under an inert atmosphere, treated with 1 equiv of BBr₃ and the mixture stirred for 1 h at room temperature. The solvent was removed in vacuo and the crude material was investigated using ¹H NMR and ¹¹B NMR spectroscopic experiments. According to the ¹H NMR spectrum, one major dipyrinato product had formed, along with some minor side products. The ¹¹B NMR spectrum also showed one major singlet, potentially corresponding to the *Br*-BODIPY, along with various minor boron containing impurities. It appeared as if purifying this material would once again be troublesome. The reaction was repeated in various solvents, including toluene and THF, but these trials still resulted in impure material. As mentioned previously, purification via chromatography is not an option for such unstable *X*-BODIPYs, and attempts to purify using solvent washes and crystallizations were unfruitful. However, when CCl₄ was used as the solvent, the result was the quantitative return of the *Br*-BODIPY **3BBr₂**, the first *Br*-BODIPY to be isolated (Scheme

35). Characterisation using ^{11}B NMR spectroscopy clearly revealed a singlet at -5.89 ppm, compared to the triplet at 0.76 ppm for the starting material *F*-BODIPY (Figure 15).

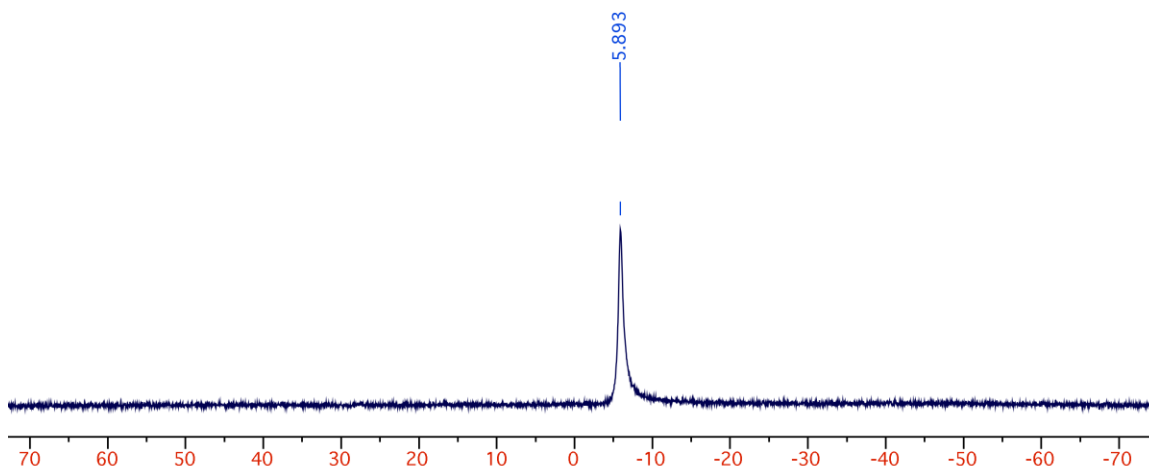
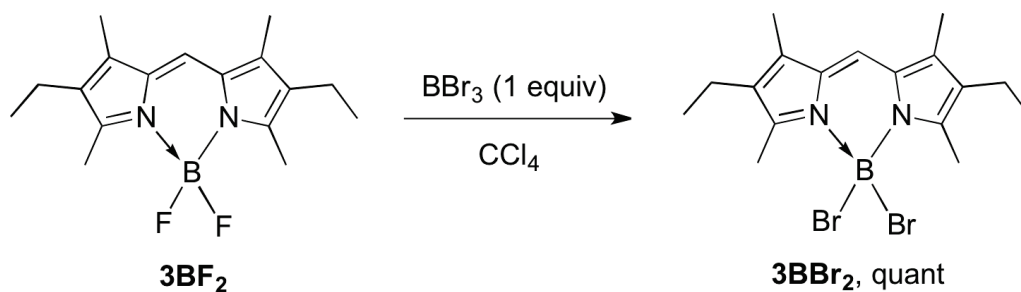


Figure 15: ^{11}B NMR of 3BBr_2 in CDCl_3

The isolation of this material supports the sentiment that the methodology by which to achieve deprotection, as described for 3BF_2 and 24BF_2 , occurs through the *Br*-BODIPY. It is a reasonable conclusion that reaction with water would then produce the unstable dihydroxy *O*-BODIPY, followed by decomposition to liberate the dipyrin as the HBr salt. It is not clear why CCl_4 was the best solvent for this reaction. However, work by Chen and co-workers has also shown that CCl_4 was the best solvent of choice when performing a halogenation reaction using BBr_3 .⁷⁷ Typically, CCl_4 is a useful solvent for halogenations involving free-radicals as CCl_4 does not easily undergo free-radical reactions due to the lack of C-H bonds. Even though neither this reaction, or the work by Chen, appear to be undergoing free-radical reactions, CCl_4 appears to play a role in the success of each halogenation.



Scheme 35: Synthesis of a *Br*-BODIPY

4.3.2 – Activation and deprotection of *F*-BODIPYs using $\text{BF}_3 \cdot \text{OEt}_2$

To continue exploring the reactions of *F*-BODIPYs with boron trihalides, attention was refocused to the fluoro analogue BF_3 . It is now known that treatment of *F*-BODIPYs with BX_3 ($X \neq \text{F}$) results in halogen exchange to provide the *X*-BODIPYs ($X = \text{Cl}, \text{Br}$) and that these materials can react with water to give the corresponding HX salts of the parent dipyrins. Therefore, we postulated that using BF_3 could react in a similar manner to potentially synthesize HF salts. The *F*-BODIPY 3BF_2 was dissolved in anhydrous CH_2Cl_2 and treated with $\text{BF}_3 \cdot \text{OEt}_2$ (1 equiv). The reaction mixture immediately changed from a fluorescent orange solution, characteristic of an *F*-BODIPY, to a fluorescent red/purple colour, which generally indicates an interaction/activation between the *F*-BODIPY and the added Lewis acid. The solvent was removed in vacuo under inert conditions and the resulting crude material was dissolved in a mixture of acetone/water as done previously. However, this reaction did not result in the formation of the dipyrin salt, and instead there was only complete recovery of the *F*-BODIPY starting material. This was a surprising result as even though the deprotection was unsuccessful, the *F*-BODIPY had appeared to react with BF_3 , according to visual inspection, before the addition of water. It is possible

that the large excess of water simply quenched the BF_3 being used to activate the *F*-BODIPY, instead of substituting at the boron centre. Therefore, the reaction was repeated but using a stoichiometric amount of water. After the addition of 1 equiv $\text{BF}_3 \cdot \text{OEt}_2$ to **3BF₂**, the reaction mixture was stirred for 10 minutes, and then 3 equiv water was added. The first 2 equiv were intended to give the dihydroxy *O*-BODIPY, and the third equiv was intended to result in hydrolysis of the covalent N–B bond, thus liberating boric acid and the parent dipyrin. Thus, upon the addition of 3 equiv water, the solution began to turn a dull yellow, suggestive of a dipyrin salt. Upon completion of the reaction, the mixture was washed with water and the organic phase was dried over Na_2SO_4 to give an orange powder. Complete characterization of this compound revealed it to be the first example of an HBF_4 salt of a dipyrin, isolated in quantitative yield (Table 10, Entry 1). ^{11}B NMR spectroscopy revealed a boron singlet at -0.65 ppm (Figure 16), indicative of the BF_4^- counter-ion which has been reported in the range of -0.5 ppm to -1.2 ppm.⁷⁸

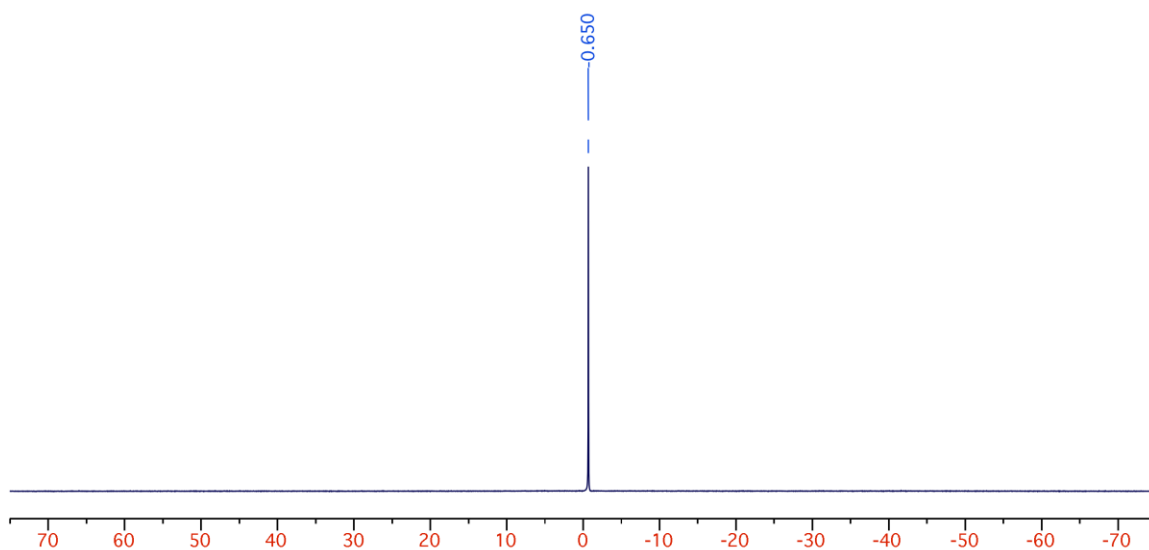
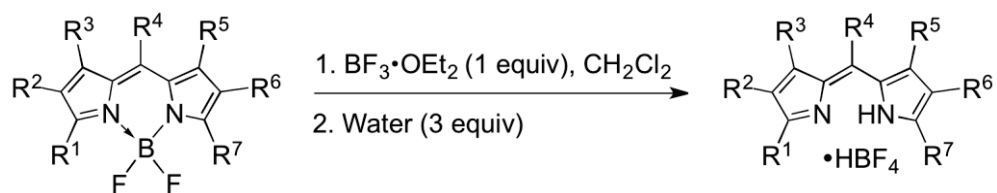


Figure 16: ^{11}B NMR of **3HBF₄** in CDCl_3

The success of this deprotection evidently shows that the stoichiometry of the added water severely alters the outcome of the methodology: excess water quenches the 1 equiv BF_3 that is used to activate the *F*-BODIPY, yet controlled amounts of water react at the boron centre of the *F*-BODIPY, by way of Lewis acid pre-activation with BF_3 .

The scope of this deprotective method was briefly explored by varying the alkyl substituents around the dipyrinato core (Table 10, entries 1-3). However, it appeared that a decreasing degree of alkyl substitution around the dipyrinato backbone resulted in decreased yields of the dipyrin HBF_4 salts. Additionally, using the meso-phenyl variant resulted in a dramatic decrease in yield (Table 10, Entries 4 and 5). In each instance where the reaction did not reach completion, the remaining starting material was recovered. The work-up of some dipyrins (entries 2-5) was different to that used for **3HBF₄**, due to the presence of unreacted *F*-BODIPY. The HBF_4 salts of these dipyrins were purified by washing the crude powder with diethyl ether in order to remove the *F*-BODIPY (highly soluble in this solvent) and leaving only pure dipyrin behind as the HBF_4 salt. These results suggest this method of deprotection of the *F*-BODIPY is chemoselective, understood when appreciating the drastic decrease in yield when using a meso-phenyl dipyrin compared to its meso-H variant. The chemoselectivity is again demonstrated in the examples whereby unsubstituted pyrrole frameworks are used. An increase in alkyl substitution around the dipyrin core results in higher yields during deprotection. It appears that the electron-donating ability of the alkyl substituents modifies the degree of activation generated by the addition of BF_3 , thus altering the degree of subsequent substitution at the boron centre by water. It is crucial that the dihydroxy *O*-BODIPY is formed effectively in order for the deprotective removal of the BF_2 moiety to be successful.



Scheme 36: Deprotection of *F*-BODIPYs with $\text{BF}_3 \cdot \text{OEt}_2$ and water

Entry	<i>F</i> -BODIPY	Product	Isolated Yield (%)
1	<p>3BF₂</p>	<p>3HBF₄</p>	>99
2	<p>2BF₂</p>	<p>2HBF₄</p>	91
3	<p>4BF₂</p>	<p>4HBF₄</p>	80
4	<p>5BF₂</p>	<p>5HBF₄</p>	45
5	<p>8BF₂</p>	<p>8HBF₄</p>	5

Table 10: Conversion of *F*-BODIPYs to dipyrin HBF_4 salts

It has been previously mentioned that the HBr salts of dipyrins are quite crystalline and, therefore, are the more commonly synthesized dipyrin HX salts.⁷ However, it appears that these new dipyrin HBF₄ salts may easily surpass the HBr analogues in terms of crystallinity. Undoubtedly, the dipyrin HBF₄ salts were very easily crystallized via the slow evaporation of solvent from a CH₂Cl₂ solution. A single crystal of **2HBF₄** was characterised by T. Stanley Cameron using X-ray crystallography (Figure 17), distinctly revealing the BF₄ counter-ion. The dipyrinato framework of the HBF₄ salt is essentially planar and the exocyclic double bond is found in the expected (*Z*)-*syn*-periplanar configuration.⁹ The planarity of this particular structure is enforced by the hydrogen bonds formed between the N-H protons and a fluoride atom on the BF₄⁻ counter-ion. The bond distances between F(4) and H(1)/H(2) are 1.854 and 1.857 Å, which is indicative of a strong hydrogen bond.⁷⁹

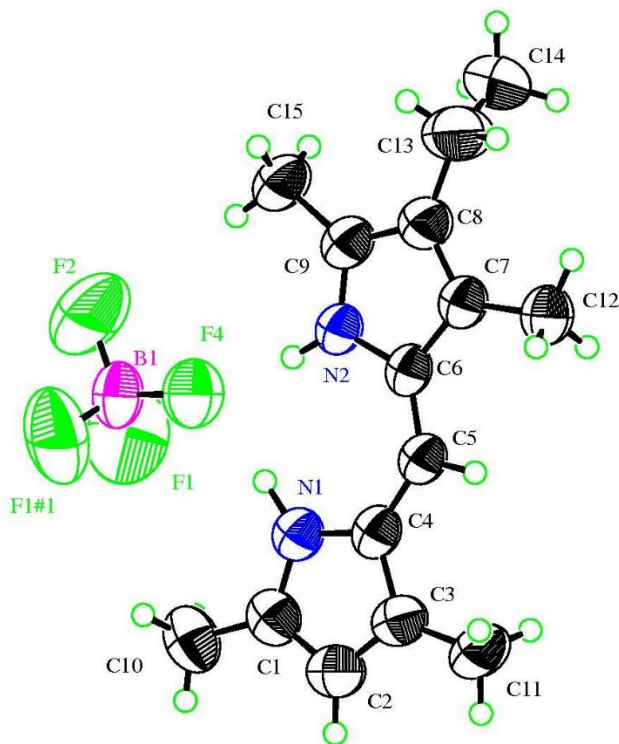
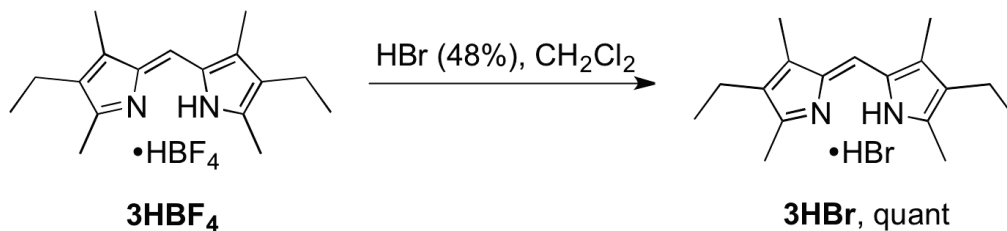


Figure 17: Ellipsoid diagram (50%, H atoms omitted) of **2HBF₄**

It should be mentioned that when the microcrystalline dipyrin HBF_4 salts were left on the bench top for several months, occasionally the loss of the BF_4^- counter ion would occur. A sample containing powdered **3HBF₄** that had been stored on the bench top for 2 months, was characterized using ^1H , ^{11}B and ^{19}F NMR experiments. While the ^1H NMR spectrum simply revealed pure dipyrin salt, the ^{11}B NMR and ^{19}F NMR spectra no longer showed the presence of the BF_4^- counter-ion. Instead, there was no signal in the ^{11}B NMR spectrum and a singlet was found at 50 ppm in the ^{19}F NMR spectrum. It is possible that the HBF_4 had decomposed over time to HF and BF_3 , forming the HF salt of the dipyrin. It was important to test the long-term stability of these compounds to open air as dipyrin HBr salts are generally quite stable over long periods of time. Therefore, it should be known if dipyrins can be stored as their HBF_4 salts without decomposition. While the powdered material appears to liberate BF_3 over time, when the salt was left in crystalline form the material remained as the pure HBF_4 salt. Since the loss of the counter-ion was witnessed, it was necessary to investigate exchange of the BF_4^- counter-ion. A solution of compound **3HBF₄** in CH_2Cl_2 was treated with aqueous HBr (48%). The mixture was stirred for 15 min and then washed with water. The organic layer was dried over Na_2SO_4 and concentrated in vacuo. The result was complete conversion of the **3HBF₄** salt to the **3HBr** salt in a quantitative yield (Scheme 37) which was confirmed using NMR. The ^{11}B and ^{19}F NMR spectra revealed there was no longer any boron or fluorine present in the sample and the ^1H NMR data matched that of **3HBr** supporting the complete conversion of **3HBF₄** to **3HBr**. The HBF_4 salts are potentially beneficial for a scenario in which the alternative HX salts are proving unsuitable for the purpose of obtaining material suitable for X-ray crystallography. There is now another option to improve the chance of obtaining

X-ray crystal structures of dipyrrens. However, if these materials are also to be prepared for long-term storage, it has also been demonstrated that the BF_4^- counter-ion can be easily exchanged for Br^- to provide HBr dipyrren salts that are suitable for storage.



Scheme 37: Exchange of BF_4^- counter-ion with Br^-

Based on the knowledge that halogen exchange occurs between *F*-BODIPYs and BX_3 ($\text{X} = \text{Cl}, \text{Br}$), it is evident that the deprotection via reaction of *F*-BODIPYs with $\text{BF}_3 \cdot \text{OEt}_2$ and stoichiometric amounts of water must clearly progress through an alternative pathway. There are no *Cl/Br*-BODIPY intermediates involved in the deprotection; instead there can only be potential exchange occurring between the fluorides of the *F*-BODIPY and the BF_3 . Given the stronger B–F bond in BF_3 versus the B–X bond in BCl_3 and BBr_3 , it is proposed that the addition of $\text{BF}_3 \cdot \text{OEt}_2$ to *F*-BODIPYs results in the activation of a B–F bond of the *F*-BODIPY (Figure 18). When there is no nucleophile present, the activation becomes terminated by the quenching of the Lewis acid during work-up, and thus quantitative recovery of the *F*-BODIPY is achieved. However, using controlled amounts of water, the water nucleophilically attacks the activated BODIPY, at boron. The result is the cleavage of the N–B bonds thus removing the BF_2 moiety and forming the BF_4^- anion as well as the formation of boric acid. To further support the concept of the activated intermediate, a nucleophile other than water was used to substitute at boron. Compound **3BF₂** was treated with 1 equiv of $\text{BF}_3 \cdot \text{OEt}_2$, followed by the addition of 2 equiv of EtMgBr .

The reaction mixture was then washed with water, dried over Na_2SO_4 and concentrated in vacuo. The reaction resulted in the complete conversion of $\mathbf{3BF}_2$ to the *C*-BODIPY $\mathbf{3BEt}_2$ (Scheme 38). It is extremely clear that the B-F bond is more susceptible to nucleophilic attack in the presence of $\text{BF}_3\cdot\text{OEt}_2$ and, as shown in Table 3, that the reaction of $\mathbf{3BF}_2$ with 2 equiv of EtMgBr alone will not reach completion at room temperature, resulting in only a 67% yield of the *C*-BODIPY.

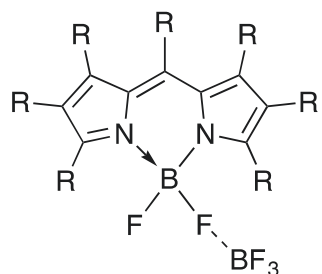
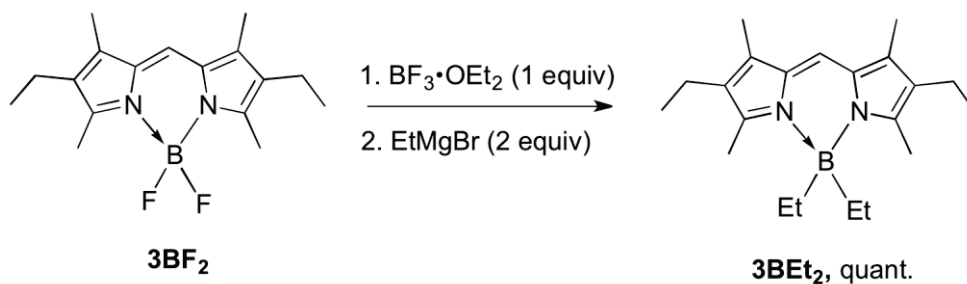


Figure 18: Proposed activation of *F*-BODIPYs of BF_3



Scheme 38: Synthesis of *C*-BODIPY from activated *F*-BODIPY

In an attempt to characterise the activated intermediate (Figure 18), a solution of $\mathbf{3BF}_2$ (10 mg, 0.033 mmol) in CDCl_3 was treated with 1 equiv (40 μL) of a 0.81 M solution of $\text{BF}_3\cdot\text{OEt}_2$ in CDCl_3 , and the mixture was analysed using ^{11}B and ^{19}F NMR spectroscopy. The spectra shown in Figure 19 clearly revealed the activation of the *F*-BODIPY boron centre. In the ^{11}B spectrum, the expected triplet of the starting material ($\mathbf{3BF}_2$) surprisingly

appeared as a rather sharp singlet at 0.76 ppm and another singlet corresponding to the BF₃ boron centre was present, as expected at 0 ppm. There was no coupling observed between boron and fluorine in either case. In the ¹⁹F NMR spectrum, the expected quartet of **3BF₂** was absent and instead a severely depressed (low intensity) and broad singlet was observed. Due to the absence of any coupling between boron and fluorine, variable temperature ¹¹B and ¹⁹F NMR spectroscopy was used to look for any exchange processes that may be occurring. It was not until the probe reached -60 °C that a significant extent of coupling between boron and fluorine was revealed. As the temperature was decreased, the ¹¹B NMR (Figure 19) spectrum E revealed that the singlet from the BF₃ ($\delta_B = 0$ ppm) remained as such but that the singlet of the *F*-BODIPY ($\delta_B = 0.76$ ppm) began to broaden until the expected triplet was seen. In the ¹⁹F NMR (Figure 20) spectra, a similar trend was witnessed as the temperature decreased. It appeared that the broad singlet at room temperature was simply the coalescence of two signals. When the sample was cooled down the intense singlet corresponding to the BF₃ ($\delta_F = 153$ ppm) appeared, as well as the quartet corresponding to the *F*-BODIPY ($\delta_F = 146$ ppm). While it is not evident in the ¹¹B NMR spectra, the ¹⁹F NMR spectra of **3BF₂** and BF₃•OEt₂ at room temperature show that, individually, these species have different chemical shifts compared to the species present in the reaction mixture. These results suggest facile room-temperature exchange of the fluorine atoms on the *F*-BODIPY with those of the BF₃ present in solution. This complements the synthetic ability for treatment of *F*-BODIPYs with BX₃ (X = Cl, Br) to result in exchange of the halogen at boron.

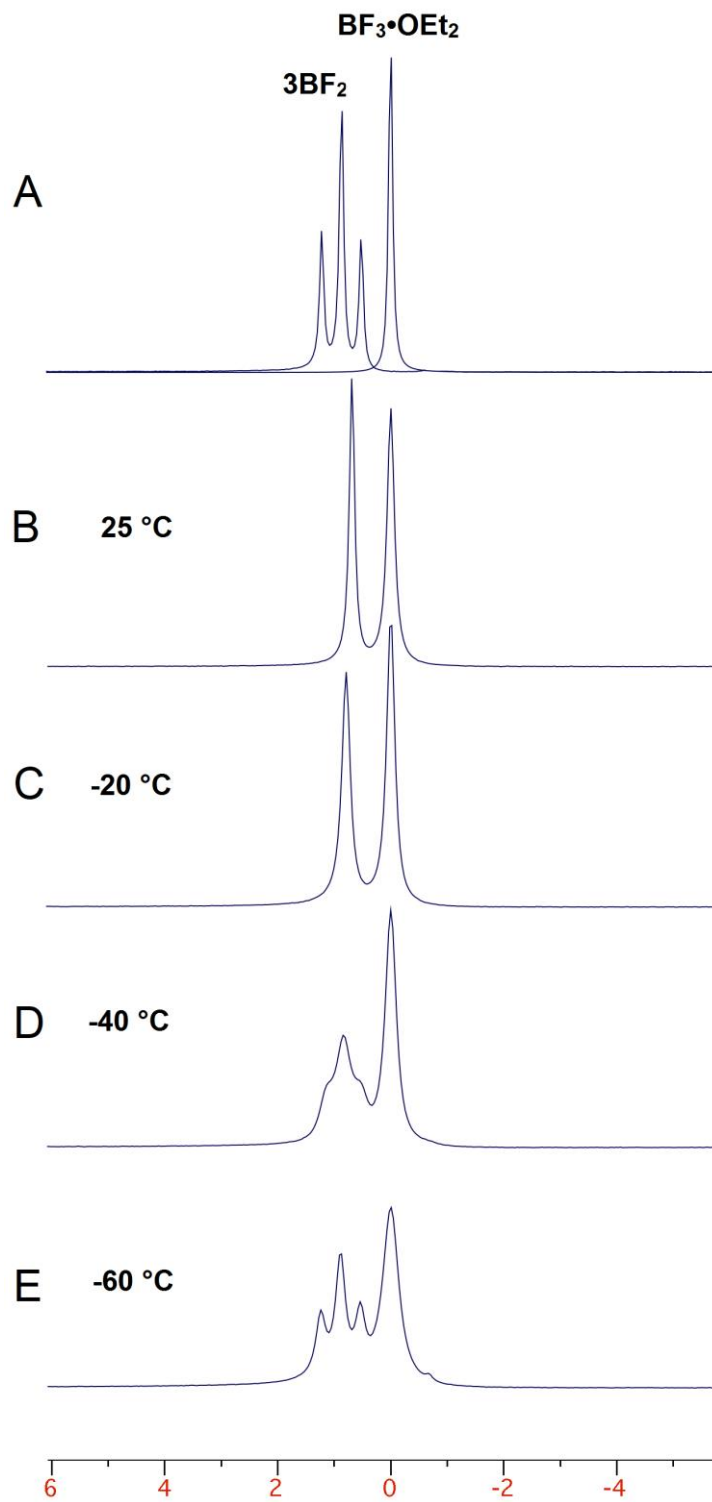


Figure 19: Variable temperature ^{11}B NMR (96 MHz) spectra B-E of 3BF_2 and $\text{BF}_3 \cdot \text{OEt}_2$. Spectrum A overlays the NMR spectra for 3BF_2 and $\text{BF}_3 \cdot \text{OEt}_2$, separately, at room temperature. All spectra were obtained using CDCl_3 as the solvent.

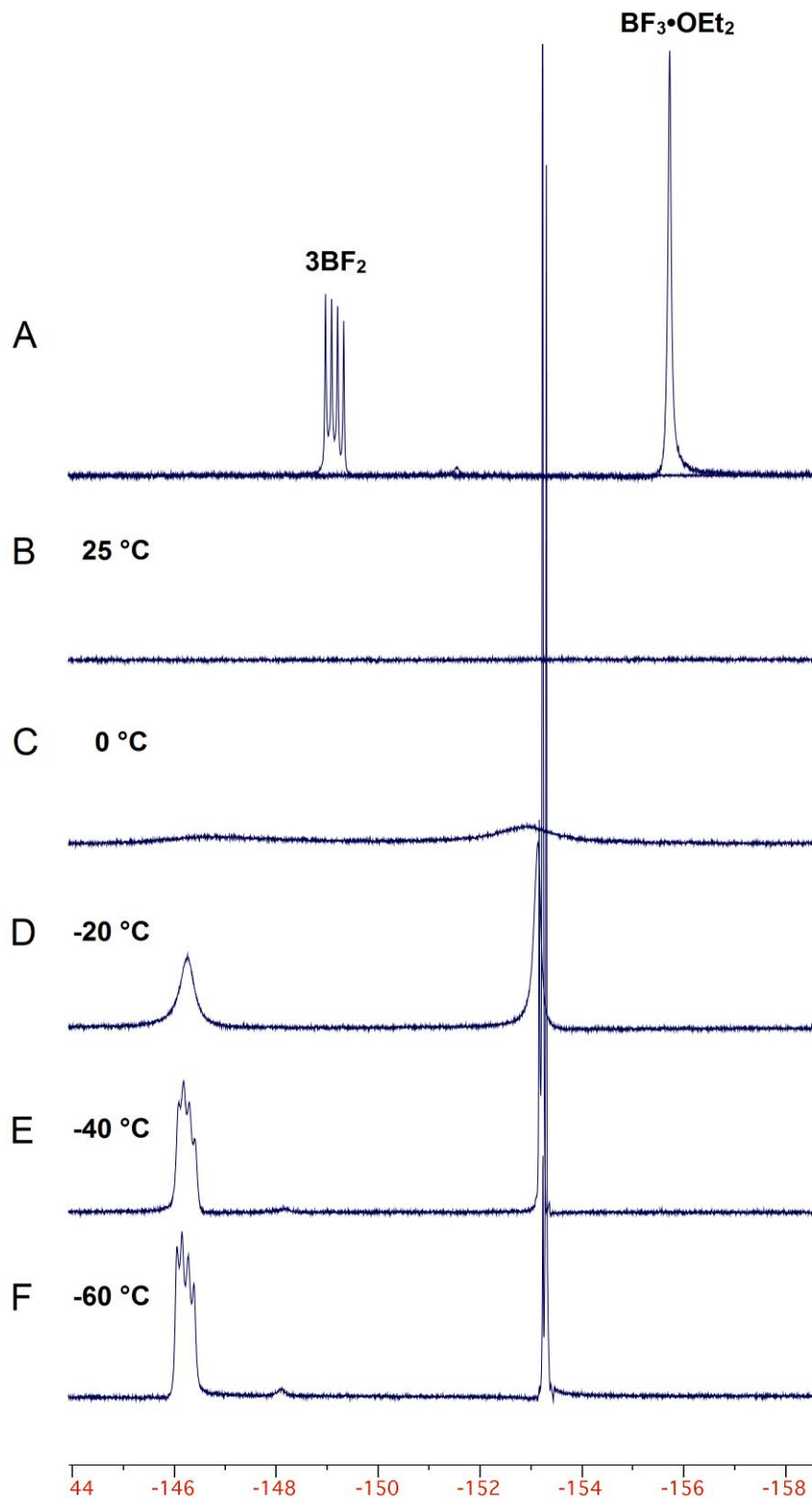
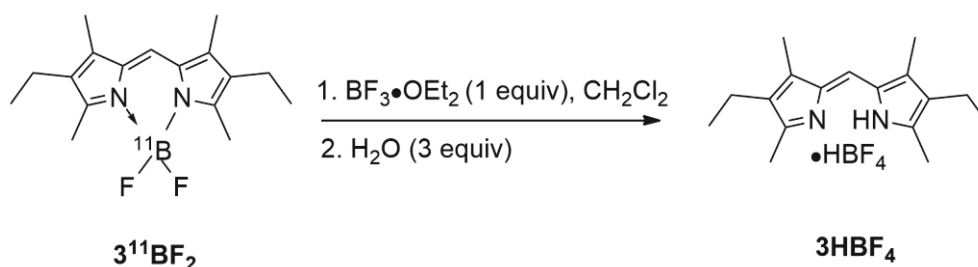


Figure 20: Variable temperature ^{19}F NMR (282 MHz) spectra B-F of 3BF_2 and $\text{BF}_3\cdot\text{OEt}_2$. Spectrum A overlays the NMR spectra for 3BF_2 and $\text{BF}_3\cdot\text{OEt}_2$, separately, at room temperature. All spectra were obtained using CDCl_3 as the solvent.

In order to probe the mechanism of the deprotection of *F*-BODIPYs using $\text{BF}_3 \cdot \text{OEt}_2$ and water even further, it was necessary to perform the deprotection using compound 3^{11}BF_2 containing the isotopically pure boron centre. It was hypothesized that the BF_3 activates the B–F bond of the *F*-BODIPY, leaving the boron centre susceptible to nucleophilic attack from water. In this scenario, it is presumed that the boron in the BF_4^- counter-ion ultimately comes from the BF_3 after removing a fluoride from the *F*-BODIPY, which is substituted with an OH^- group from water. However, recent work from Wang et al. suggests that treating an *F*-BODIPY with excess fluoride can result in the deprotection of the *F*-BODIPY to give the parent dipyrin and a BF_4^- counter-ion.⁷⁹ In this scenario, the boron centre of the BF_4^- can only come from the *F*-BODIPY. By deprotecting compound 3^{11}BF_2 , using the methodology involving $\text{BF}_3 \cdot \text{OEt}_2$ and water it can be determined whether the BF_4^- counter-ion formed contains the boron centre from the *F*-BODIPY, similar to the work from Wang et al., or from the $\text{BF}_3 \cdot \text{OEt}_2$ which has been previously hypothesized in this thesis. Therefore, 3^{11}BF_2 was subjected to the deprotection conditions as described previously and ultimately provided the dipyrin HBF_4 salt in quantitative yield as expected.



Scheme 39: Deprotection of labelled *F*-BODIPY affording an unlabelled HBF_4 salt

The material was then analyzed using high resolution mass spectrometry in negative mode to characterize the BF_4^- counter-ion. The mass spectrum revealed peaks at 86.0070 m/z and 87.0035 m/z in a relative ratio of 1:4. The presence of these two signals is

characteristic of a BF_4^- ion containing a natural boron centre, i.e., a mixture of isotopes. These results support the hypothesis that the boron centre of the HBF_4 salts originates from the $\text{BF}_3 \cdot \text{OEt}_2$ used to activate the B–F bond of the *F*-BODIPY during deprotection.

The proposed mechanism for the deprotection of *F*-BODIPYs using $\text{BF}_3 \cdot \text{OEt}_2$ and water is demonstrated in Figure 21. The *F*-BODIPY interacts with the BF_3 to form the activated intermediate in which the lone-pair on the fluoride of the BODIPY is donated to the empty p-orbital of the BF_3 . The activated boron centre of the *F*-BODIPY is now susceptible to nucleophilic attack from a molecule of water, substituting a fluoride atom of the BODIPY which ultimately forms a molecule of HBF_4 . At this stage, another molecule of water attacks the boron centre, substituting another fluoride atom and resulting in the loss of HF to form the dihydroxy *O*-BODIPY. The mechanism then follows the same path as described for the deprotection of *Cl*-BODIPYs shown in Figure 14: a molecule of water attacks the boron centre once more, resulting in the loss of boric acid and the formation of the free-base dipyrin. The dipyrin then reacts with the HBF_4 present in the reaction mixture to give the HBF_4 salt of the dipyrin.

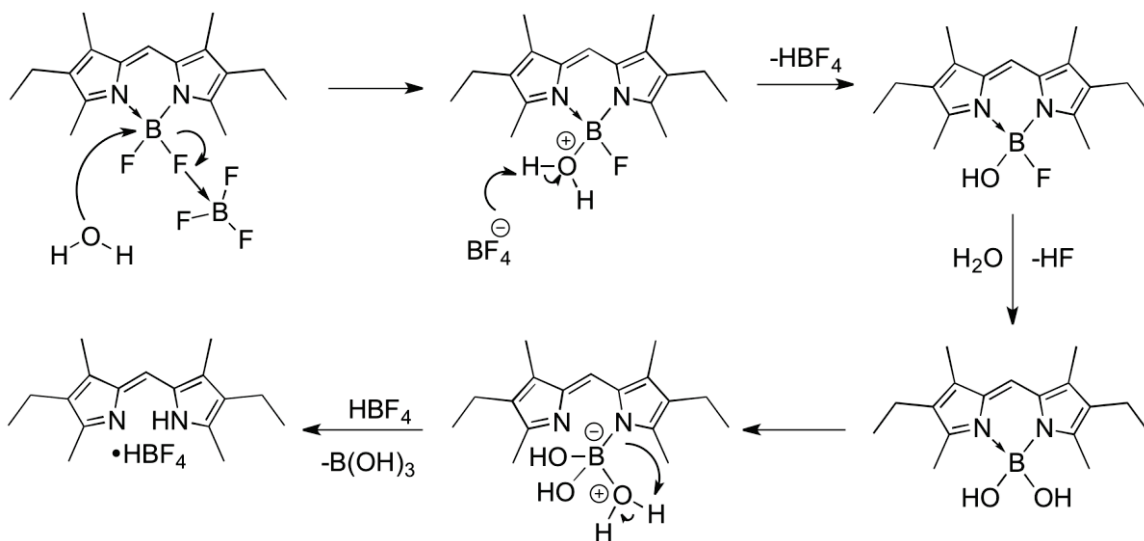


Figure 21: Proposed mechanism for the deprotection of *F*-BODIPYs using $\text{BF}_3 \cdot \text{OEt}_2$

While the formation of dipyrin HBF_4 salts using $\text{BF}_3 \cdot \text{OEt}_2$ and controlled amounts of water was rather unexpected, the result actually provides potential insight into the traditional strategy used for the synthesis of *F*-BODIPYs. As discussed in Chapter 1, *F*-BODIPYs are traditionally synthesised by reacting the dipyrin HBr salt, or free-base, with excess NEt_3 (6 equiv) and $\text{BF}_3 \cdot \text{OEt}_2$ (9 equiv). The reaction is surprisingly moisture-sensitive. With the discovery that $\text{BF}_3 \cdot \text{OEt}_2$ activates the B-F bonds of *F*-BODIPYs and renders them reactive with water, it is now evident that the formation of *F*-BODIPYs under non-anhydrous conditions is reversible, and that even the anhydrous process is vulnerable to interference by nucleophiles.⁴²

4.4 – Conclusions

In conclusion, an extremely high yielding and mild methodology was developed for the deprotection of *F*-BODIPYs using *Cl*- and *Br*-BODIPYs as *in-situ* intermediates.⁷⁶ During the development of this methodology, the first *Br*-BODIPY was isolated and characterized. The major benefit of this deprotection strategy is courtesy of the purification procedure, which simply entails an aqueous work-up without the need for further purification, such as chromatography. Using this strategy also provides the option to prepare various HX salts depending on the stability of the resulting dipyrin stemming from the substituents on the dipyrrolic framework. The deprotection of *F*-BODIPYs using water has also been demonstrated using $\text{BF}_3 \cdot \text{OEt}_2$ via the activation of the boron

centre, and these reactions provided the first HBF_4 salts of dipyrrens, which appear to be quite crystalline in nature.

Chapter 5 – Experimental

5.1 – General Experimental

All ^1H NMR (500 MHz), ^{13}C NMR (125 MHz) and ^{11}B NMR (160 MHz) spectra were recorded using a Bruker AV 500 MHz spectrometer and the ^{19}F NMR (282 MHz) spectra recorded using a Bruker AV 300 MHz spectrometer. Chemical shifts are expressed in parts per million (ppm) using the solvent signal [CDCl_3 (^1H 7.26 ppm; ^{13}C 77.16 ppm); THF-*d*8 (^1H 1.73 ppm and 3.58 ppm, ^{13}C 25.37 and 67.57 ppm)] as an internal reference for ^1H and ^{13}C . External references are used for both ^{11}B and ^{19}F NMR; $\text{BF}_3\cdot\text{OEt}_2$ for ^{11}B at 0 ppm and CFCl_3 for ^{19}F at 0 ppm. Splitting patterns are indicated as follows: br, broad; s, singlet; d, doublet; t, triplet; q, quartet; m, multiplet. All coupling constants (J) are reported in Hertz (Hz). High resolution mass spectra were obtained using TOFMS experiments operating in both positive and negative mode. Column chromatography, as indicated, was performed using 230-400 mesh ultra pure silica. Dipyrrens **2**,⁸⁰ **3**,⁸¹ **5**,⁸² **7**,³³ **8**,⁸³ **22-23**⁷⁵ were prepared using literature procedures. The free-base dipyrrens were obtained by adding concentrated ammonium hydroxide (28%) to a suspension of the HBr salt in diethyl ether. Within 15 minutes, the formation of a precipitate (NH_4Br) was observed. Distilled water was used to extract the by-products. The resulting organic fraction was dried over anhydrous Na_2SO_4 , filtered, and concentrated under reduced pressure to give the desired free-base dipyrren. Compounds were dried under vacuum before use.

5.1.1 General Procedure for Emission Measurements

The fluorescence measurements were performed using a Shimadzu RF-5301PC Spectrofluorimeter. A 10 mm quartz cuvette was used in all measurements. For the fluorescence experiments, the slit width was 3 nm for both excitation and emission. Relative quantum efficiencies of derivatives were obtained by comparing the areas under the emission spectra of the test with that of a solution of rhodamine 101 in ethanol ($\Phi_F = 0.96$) or rhodamine 6G in ethanol ($\Phi_F = 0.94$).⁸⁴ The excitation wavelength was 520 nm for rhodamine 6G, **3BCl₂** and **5BCl₂**. Quantum yields were determined using Equation 1.⁸⁵

$$\phi_X = \phi_{st} \left(\frac{I_X}{I_{st}} \right) \left(\frac{A_{st}}{A_X} \right) \left(\frac{\eta_X^2}{\eta_{st}^2} \right) \quad \text{Equation 1}$$

Where ϕ_{st} is the reported quantum yield of the standard, I is the area from the integrated emission spectra, A is the absorbance at the excitation wavelength and η is the refractive index of the solvent used. The X subscript denotes the unknown, and “st” denotes the standard.

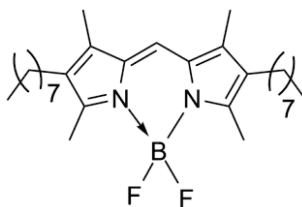
5.2 – Synthesis of Compounds

General Procedure for the Synthesis of *F*-BODIPYs (GP1)

The dipyrin HBr salt (50 mg) was dissolved in anhydrous dichloromethane (20 mL) and 2.2 equiv of solid LiHMDS was added to the solution. The reaction was stirred for two

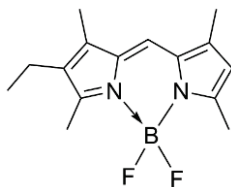
hours. A solution of $\text{BF}_3 \cdot \text{OEt}_2$ [1 equiv; 2 equiv for bis(dipyrrin)s] in anhydrous dichloromethane was then added to the reaction mixture drop-wise, and stirring was continued for another three hours. Upon completion of the reaction, the mixture was filtered over a pad of Celite, and silica if necessary, in both cases flushing with dichloromethane. The solutions were then concentrated *in vacuo* to obtain the *F*-BODIPY product.

1,3,5,7-Tetramethyl-2-octyl-8-*H*-4,4'-difluoro-bora-3a,4a-diaza-s-indacene (1BF₂)



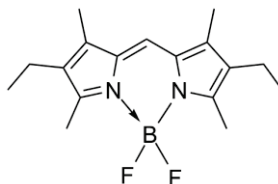
Using **GP1** and **1HBr**, compound **1BF₂** was synthesized as a bright orange solid (55 mg, quant.). δ_{H} (500 MHz, CDCl_3) 6.94 (s, 1H), 2.48 (s, 6H), 2.34 (t, $J = 7.6$, 4H), 2.15 (s, 6H), 1.44-1.26 (m, 24H), 0.89 (t, $J = 6.8$, 6H); δ_{C} (125 MHz, CDCl_3) 155.0, 137.1, 132.5, 130.4, 118.6, 32.0, 30.3, 29.7, 29.6, 29.4, 24.2, 22.8, 14.2, 12.8, 9.7; δ_{B} (160 MHz, CDCl_3) 0.90 (t, $J_{\text{B-F}} = 34$); LRMS-ESI (m/z): 495.4 $[\text{M} + \text{Na}]^+$; HRMS-ESI (m/z): $[\text{M} + \text{Na}]^+$ calcd for $\text{C}_{29}\text{H}_{47}\text{BF}_2\text{N}_2\text{Na}$ 495.3693; found 495.3709.

1,3,5,7-Tetramethyl-2-ethyl-8-*H*-4,4'-difluoro-bora-3a,4a-diaza-s-indacene (2BF₂)



Using **GP1** and **2HBr**, compound **2BF₂** was synthesized as a bright orange solid (55 mg, 91%).⁶⁶ δ_{H} (500 MHz, CDCl₃) 6.99 (s, 1H), 6.00 (s, 1H), 2.51 (s, 6H), 2.39 (q, $J = 7.5$, 2H), 2.23 (s, 3H), 2.17 (s, 3H), 1.07 (t, $J = 7.6$, 3H); δ_{C} (125 MHz, CDCl₃) 156.6, 155.2, 140.0, 137.8, 133.2, 132.9, 132.6, 119.4, 118.4, 17.4, 14.7, 14.6, 12.8, 11.4, 9.6; δ_{B} (160 MHz, CDCl₃) 0.89 (t, $J_{\text{B-F}} = 33$); LRMS-ESI (m/z): 299.2 [M + Na]⁺; HRMS-ESI (m/z): [M + Na]⁺ calcd for C₁₅H₁₉BF₂N₂Na 299.1502; found 299.1514.

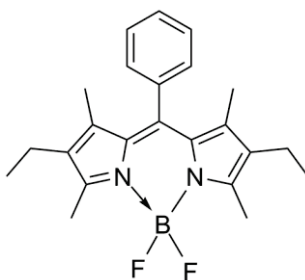
1,3,5,7-Tetramethyl-2,6-diethyl-8-H-4,4'-difluoro-bora-3a,4a-diaza-s-indacene (3BF₂)



Method 1: To a solution of free-base dipyririn **3** (50 mg, 0.20 mmol) in 10 mL of anhydrous THF, 1.1 equiv of LiHMDS (36 mg, 0.21 mmol) was added and the solution stirred for 1 h under a N₂ atmosphere. The reaction mixture went from orange to dark red upon addition of LiHMDS. Upon completion of the reaction, the solvent was removed *in vacuo* and the remaining solid was washed with hexane to remove the unreacted starting materials to obtain the purified Li complex. The resulting dipyririnato lithium salt was then stirred as a slurry in CH₂Cl₂ (10 mL) and 1 equiv of BF₃•OEt₂ (24 μ L, 0.20 mmol) was added drop-wise. The reaction was complete after 2 h and was then filtered through Celite and the solvent removed *in vacuo* to give the *F*-BODIPY **3BF₂** as a red solid (56 mg, 94%).

Method 2: Using **GP1** and **3HBr**, compound **3BF₂** was synthesized as a bright red solid (45 mg, 94%).⁶⁷ δ_{H} (500 MHz, CDCl₃) 6.93 (s, 1H), 2.49 (s, 6H), 2.36 (q, $J = 7.6$, 4H), 2.14 (s, 6H), 1.05 (t, $J = 7.6$, 6H); δ_{C} (125 MHz, CDCl₃) 154.7, 136.7, 132.5, 131.7, 118.7, 17.4, 14.7, 12.6, 9.4; δ_{B} (160 MHz, CDCl₃) 0.76 (t, $J_{\text{B-F}} = 32$). NMR data matches that previously reported.³⁷

1,3,5,7-Tetramethyl-2,6-diethyl-8-phenyl-4,4'-difluoro-bora-3a,4a-diaza-s-indacene (5BF₂)

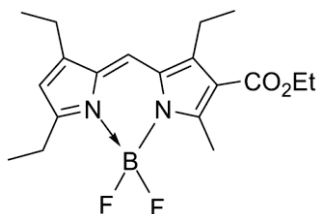


Method 1: To a solution of free-base dipyrin **5** (50 mg, 0.15 mmol) in 10 mL of anhydrous THF, 1.1 equiv of LiHMDS (28 mg, 0.17 mmol) was added and the solution stirred for 1 h under a N₂ atmosphere. The reaction mixture went from orange to dark red upon addition of LiHMDS. Upon completion of the reaction, the solvent was removed *in vacuo* and the remaining solid was washed with hexane to remove the unreacted starting materials to obtain the purified Li complex. The resulting dipyrinato lithium salt was then stirred as a slurry in CH₂Cl₂ (10 mL) and 1 equiv of BF₃•OEt₂ (19 μ L, 0.15 mmol) was added drop-wise. The reaction was complete after 2 h and was then filtered through Celite and the solvent removed *in vacuo* to give the *F*-BODIPY **5BF₂** as a red solid (50 mg, 88%).

Method 2: Using **GP1** and 1.1 equiv LiHMDS, compound **5BF₂** was synthesized from the corresponding free-base dipyrin.⁶⁸ Bright orange solid (50 mg, 88%).

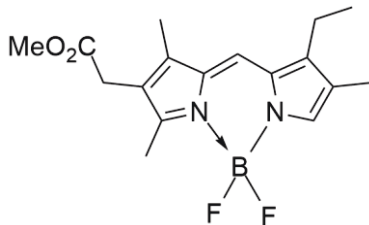
Method 3: To a solution of 5,5'-(phenylmethylene)bis(3-ethyl-2,4-dimethyl-1H-pyrrole)⁸³ (800 mg, 2.39 mmol) in anhydrous CH₂Cl₂ (80 mL) under nitrogen was added DDQ (543 mg, 2.39 mmol). The reaction mixture was stirred at room temperature for an hour before LiHMDS in anhydrous hexane (1.0 M, 7.9 mL) was added. The reaction mixture was stirred for another hour before the addition of neat BF₃•OEt₂ (0.30 mL, 2.39 mmol). After three hours the reaction mixture was filtered over Celite, flushing with dichloromethane. The filtrate was washed with 0.1 M NaOH (25 mL), 1 M HCl (25 mL) and brine (25 mL). The organic fraction was dried over Na₂SO₄ and concentrated *in vacuo*. The resulting solid was purified via filtration over a pad of silica eluting with CH₂Cl₂. Removal of the solvent *in vacuo* afforded a bright orange solid (470 mg, 52%).
 δ_{H} (500 MHz, CDCl₃) 7.37-7.40 (m, 3H), 7.17-7.21 (m, 2H), 2.45 (s, 6H), 2.21 (q, *J* = 7.5, 4H), 1.20 (s, 6H), 0.90 (t, *J* = 7.6, 6H); δ_{C} (125 MHz, CDCl₃) 150.3, 138.9, 137.8, 136.0, 135.0, 131.4, 129.8, 128.5, 128.2, 17.7, 15.0, 14.5, 11.9; δ_{B} (160 MHz, CDCl₃) 0.65 (t, *J*_{B-F} = 32). NMR data matches that previously reported.³⁷

3-Methyl-1,5,7-triethyl-2-ethylcarboxylato-8-H-4,4'-difluoro-bora-3a,4a-diaza-s-indacene (6BF₂)



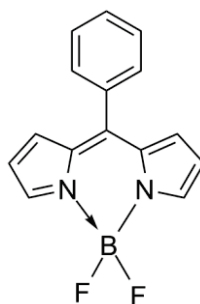
Using **GP1** and **6HBr**, compound **6BF₂** was synthesized as a bright orange solid (49 mg, 85%). δ_{H} (500 MHz, CDCl₃) 7.19 (s, 1H), 6.28 (s, 1H), 4.31 (q, $J = 7.1$, 2H), 3.00 (q, $J = 7.6$, 2H), 2.91 (q, $J = 7.5$, 2H), 2.79 (s, 3H), 2.69 (q, $J = 7.5$, 2H), 1.37 (t, $J = 7.1$, 3H), 1.32 (t, $J = 7.6$, 3H), 1.28 (t, $J = 7.6$, 3H), 1.21 (t, $J = 7.5$, 3H); δ_{C} (125 MHz, CDCl₃) 167.4, 164.6, 157.7, 151.2, 148.6, 134.6, 130.4, 121.2, 117.38, 117.35, 60.0, 22.4, 19.5, 19.4, 16.8, 14.8, 14.5, 12.6 (1C missing); δ_{B} (160 MHz, CDCl₃) 0.86 (t, $J_{\text{B-F}} = 32$); LRMS-ESI (m/z): 385.2 [M + Na]⁺; HRMS-ESI (m/z): [M + Na]⁺ calcd for C₁₉H₂₅BF₂N₂NaO₂ 385.1869; found 385.1855.

1,3,6-Trimethyl-2-(2-methoxy-2-oxoethyl)-7-ethyl-8-*H*-4,4'-difluoro-bora-3a,4a-diaza-*s*-indacene (7BF₂)



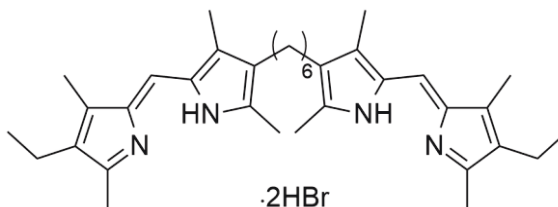
Using **GP1** and **7HBr**, compound **7BF₂** was synthesized as a bright orange solid (47 mg, 81%).⁶⁹ δ_{H} (500 MHz, CDCl₃) 7.45 (s, 1H), 7.10 (s, 1H), 3.68 (s, 3H), 3.40 (s, 2H), 2.64 (q, $J = 7.6$, 2H), 2.52 (s, 3H), 2.23 (s, 3H), 2.04 (s, 3H), 1.17 (t, $J = 7.6$, 3H); δ_{C} (125 MHz, CDCl₃) 171.0, 158.0, 144.0, 141.8, 140.8, 133.7, 132.3, 125.5, 123.1, 121.5, 52.3, 30.1, 18.1, 16.1, 13.2, 10.0, 9.9; δ_{B} (160 MHz, CDCl₃) 0.44 (t, $J_{\text{B-F}} = 32$).

8-Phenyl-4,4'-difluoro-bora-3a,4a-diaza-*s*-indacene (8BF₂)



Using **GP1** and 1.1 equiv LiHMDS, compound **8BF₂** was synthesized from the corresponding free-base dipyrin.⁷⁰ Red-orange solid (37 mg, 60%). δ_{H} (500 MHz, CDCl₃) 7.96 (brs, 2H), 7.48-7.60 (m, 5H), 6.89 (d, $J = 4.3$, 2H), 6.53 (dd, $J = 1.5, 4.3$, 2H); δ_{C} (125 MHz, CDCl₃) 147.3, 144.0, 134.9, 133.7, 131.6, 130.7, 130.4, 128.4, 118.5; δ_{B} (160 MHz, CDCl₃) 0.28 (t, $J_{\text{B-F}} = 29$); NMR data matches that previously reported.⁸⁶

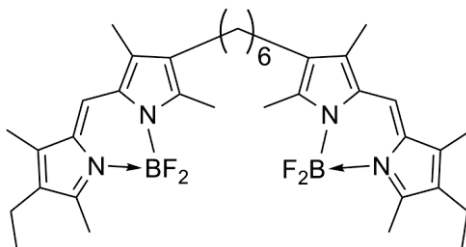
1,7-Bis(5-((*Z*)-(4-ethyl-3,5-dimethyl-2*H*-pyrrol-2-ylidene)methyl)-2,4-dimethyl-1*H*-pyrrol-3-yl)hexane dihydrobromide (12•2HBr)



Dibenzyl 4,4'-(hexane-1,7-diyl)bis(3,5-dimethyl-1*H*-pyrrole-2-carboxylate)⁴⁶ (**9**, 1.5 g, 2.8 mmol) was dissolved in THF (30 mL) along with a drop of triethylamine. 10% Pd/C (300 mg) was added to the solution, the flask was evacuated and refilled with H₂ (1 atm) and the reaction mixture then stirred overnight. The Pd/C was removed via filtration over Celite and another 300 mg of Pd/C was added to the solution. The flask was evacuated

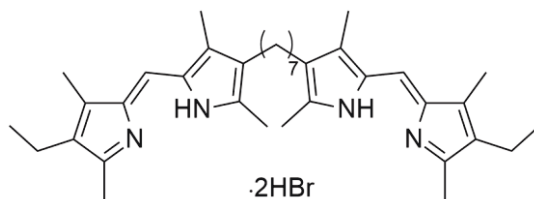
and refilled with H₂ (1 atm) once more and again stirred overnight. The Pd/C was removed via filtration over Celite and the solution was concentrated *in vacuo* to give **10** which was used in the next step without further purification. 2,4-Dimethyl-3-ethyl pyrrole-5-carboxaldehyde⁴⁷ (**11**, 848 mg, 5.61 mmol) was added to a solution of the preceding bis(pyrrole) **10** in methanol:THF (1:6, 35 mL) and the solution was degassed of oxygen by bubbling with nitrogen for 10 minutes. 48% aq. HBr (1 mL, 12 mmol) was then added drop-wise, over 5 minutes, and the reaction mixture was stirred at room temperature under nitrogen for 1 hour. The reaction mixture was then concentrated *in vacuo* until little solvent remained. Diethyl ether was then added until a copious precipitate was evident. The precipitate was collected using filtration, dissolved in dichloromethane and the solution dried over Na₂SO₄. The solution was then concentrated *in vacuo* to give **12•2HBr** as a bright orange solid (1.67 g, 92% over two steps). δ_{H} (500 MHz, CDCl₃) 9.22 (s, 2H), 6.64 (s, 2H), 2.37 (q, $J = 7.5$, 4H), 2.32 (t, $J = 8$, 4H), 2.31 (s, 6H), 2.29 (s, 6H), 2.14 (s, 6H), 2.12 (s, 6H), 1.44-1.41 (m, 4H), 1.34-1.31 (m, 4H), 1.06 (t, $J = 7.5$, 6H); δ_{C} (125 MHz, CDCl₃) 151.5, 151.4, 136.8, 136.6, 133.8, 133.5, 130.1, 128.4, 115.4, 30.5, 29.5, 24.6, 17.9, 15.0, 14.6, 14.5, 9.8, 9.6; LRMS-ESI (m/z): 539.4 [M + H]⁺; HRMS-ESI (m/z): [M + H]⁺ calcd for C₃₆H₅₁N₄ 539.4108; found 539.4099.

1,7-Bis(1,3,5,7-tetramethyl-2-ethyl-8-*H*-4,4'-difluoro-bora-3a,4a-diaza-s-indacene)hexane (12BF₂)



Using **GP1** and **12•2HBr**, and 4.4 equiv LiHMDS, compound **12BF₂** was synthesized as a bright red solid (32 mg, 54%). δ_{H} (500 MHz, CDCl₃) 6.94 (s, 2H), 2.49 (s, 6H), 2.47 (s, 6H), 2.36 (q, $J = 7.3$, 8H), 2.16 (s, 6H), 2.14 (s, 6H), 1.40 (m, 8H), 1.06 (t, $J = 7.6$, 6H); δ_{C} (125 MHz, CDCl₃) 154.9, 154.8, 137.1, 136.8, 132.5, 131.8, 130.2, 128.9, 118.7, 30.3, 29.5, 24.2, 17.4, 14.7, 12.8, 12.7, 9.7, 9.5; δ_{B} (160 MHz, CDCl₃) 0.86 (t, $J_{\text{B-F}} = 32$); LRMS-ESI (m/z): 657.4 [M + Na]⁺; HRMS-ESI (m/z): [M + Na]⁺ calcd for C₃₆H₄₈B₂F₄N₄Na 657.3983; found 657.3884.

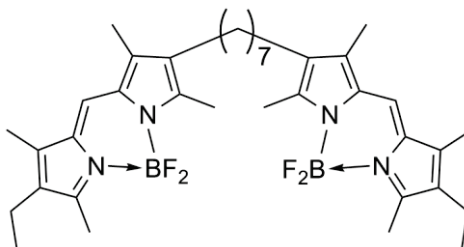
1,7-Bis(5-((*Z*)-(4-ethyl-3,5-dimethyl-2*H*-pyrrol-2-ylidene)methyl)-2,4-dimethyl-1*H*-pyrrol-3-yl)heptane dihydrobromide (15•2HBr)



Diethyl 4,4'-(heptane-1,7-diyl)bis(3,5-dimethyl-1*H*-pyrrole-2-carboxylate)⁴⁶ (**13**, 410 mg, 0.952 mmol) was added to a suspension of potassium hydroxide (481 mg, 8.57 mmol) in ethylene glycol (10 mL) and the reaction mixture was heated at 200 °C, by means of a sand bath, for one hour.⁴⁵ After cooling to room temperature, the reaction mixture was separated between ethyl acetate (30 mL) and water (30 mL). The aqueous phase was

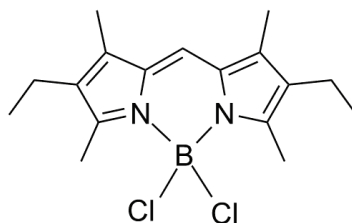
extracted with ethyl acetate (3 x 20 mL) and combined organic extracts were washed with water (50 mL) and brine (50 mL), dried over anhydrous magnesium sulfate and concentrated *in vacuo* to give 1,7-bis(2,4-dimethyl-1H-pyrrol-3-yl)heptane (**14**), which was used in the next step without further purification. 2,4-Dimethyl-3-ethyl pyrrole-5-carboxaldehyde⁴⁵ (**11**, 288 mg, 1.90 mmol) was added to a solution of the preceding bis(pyrrole) **14** in methanol:THF (1:1, 12 mL) and the solution was degassed of oxygen by bubbling with nitrogen for 10 minutes.^{73,74} 48% aq. HBr (0.4 mL, 4.60 mmol) was then added drop-wise, over 5 minutes, and the reaction mixture was stirred at room temperature under nitrogen for 18 hours. The reaction mixture was then concentrated *in vacuo* until little solvent remained. Diethyl ether was then added until a copious precipitate was evident. The precipitate was collected using filtration, washed with 10% ethyl acetate in hexanes (10 mL) followed by diethyl ether (10 mL), and then dried using a vacuum oven to give the title compound (**15•2HBr**) as a brown solid (454 mg, 67% over two steps). δ_{H} (500 MHz, CDCl₃) 12.89 (brs, 4H), 7.03 (s, 2H), 2.66 (s, 6H), 2.64 (s, 6H), 2.44-2.37 (m, 8H), 2.26 (s, 6H), 2.25 (s, 6H), 1.45-1.39 (m, 4H), 1.31-1.25 (m, 6H), 1.07 (t, $J = 7.5$, 6H); δ_{C} (125 MHz, CDCl₃) 153.9, 153.8, 141.6, 141.4, 130.7, 129.0, 126.2, 126.1, 118.7, 30.0, 29.5, 29.4, 24.0, 17.3, 14.6, 13.1, 12.9, 10.3, 10.1; LRMS-ESI (m/z): 553.3 [M + H]⁺; HRMS-ESI (m/z): [M + 2H]²⁺ calcd for C₃₇H₅₄N₄ 277.2169; found 277.2161.

1,7-Bis(1,3,5,7-tetramethyl-2-ethyl-8-*H*-4,4'-difluoro-bora-3a,4a-diaza-*s*-indacene)heptane (15BF₂)



Using **GP1** and **15•2HBr**, and 4.4 equiv LiHMDS, compound **15BF₂** was synthesized as a red solid (26 mg, 45%). δ_{H} (500 MHz, CDCl₃) 6.94 (s, 2H), 2.49 (s, 6H), 2.47 (s, 6H), 2.36 (td, $J = 7.3, 15.4$, 8H), 2.15 (s, 6H), 2.14 (s, 6H), 1.44-1.39 (m, 4H), 1.32-1.23 (m, 6H), 1.05 (t, $J = 7.6$, 6H); δ_{C} (125 MHz, CDCl₃) 155.0, 154.7, 137.1, 136.8, 132.5, 131.7, 130.3, 128.3, 118.7, 30.3, 29.6, 29.5, 24.2, 17.4, 14.7, 12.8, 12.7, 9.7, 9.5; δ_{B} (160 MHz, CDCl₃) 0.89 (t, $J_{\text{B-F}} = 33$); LRMS-ESI (m/z): 671.4 [M + Na]⁺; HRMS-ESI (m/z): [M + Na]⁺ calcd for C₃₇H₅₀B₂F₄N₄Na 671.4050; found 671.4047.

1,3,5,7-Tetramethyl-2,6-diethyl-8-phenyl-4,4'-dichloro-bora-3a,4a-diaza-*s*-indacene (3BCl₂)

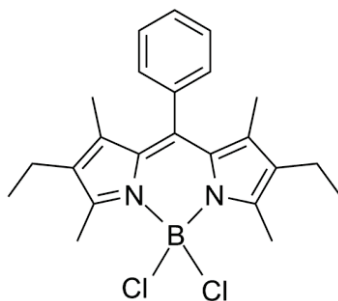


Method 1: Dipyrin **3HBr** (50 mg, 0.15 mmol) was dissolved in anhydrous THF (20 mL) and 2.2 equiv of solid LiHMDS (55 mg, 0.33 mmol) was added to the solution. The reaction was stirred for two hours. The reaction was filtered through Celite and the

solvent was removed in vacuo. The solid residue was washed with hexanes to remove any unreacted starting materials resulting in pure dipyrinato lithium salt **3Li**. The lithium salt was stirred as a slurry in toluene (20 mL) forming a yellow suspension. Boron trichloride (0.15 mL of a 1.0 M solution in hexanes, 0.15 mmol) was added drop-wise to the reaction mixture. The yellow slurry instantly changed to a red-orange solution. The reaction was stirred for an hour before filtration over Celite. The filtrate was concentrated in vacuo to give the product **3BCl₂** as a red solid (62 mg, 94%).

Method 2: Boron trichloride (0.20 mL of a 1.0 M solution in hexanes, 0.20 mmol) was slowly added to a solution of **3** (50 mg, 0.20 mmol) in anhydrous toluene (20 mL) under an N₂ atmosphere in a glovebox. The reaction mixture was stirred at room temperature for 1 h. The reaction mixture was then filtered over Celite, washed with anhydrous toluene and the filtrate was concentrated *in vacuo* to give **3BCl₂** as a red powder (65 mg, 99%). δ_{H} (500 MHz, THF-d₈) 7.34 (s, 1H), 2.69 (s, 6H), 2.43 (q, $J = 7.6$, 4H), 2.21 (s, 6H), 1.07 (t, $J = 7.6$, 6H); δ_{C} (125 MHz, THF-d₈) 157.0, 138.3, 133.7, 132.3, 120.3, 18.0, 14.6, 14.4, 9.1; δ_{B} (160 MHz, THF-d₈) 2.39 (s).

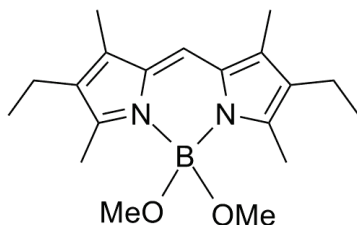
1,3,5,7-Tetramethyl-2,6-diethyl-8-phenyl-4,4'-dichloro-bora-3a,4a-diaza-s-indacene (5BCl₂)



Method 1: Dipyrin **5HBr** (50 mg, 0.12 mmol) was dissolved in anhydrous THF (20 mL) and 2.2 equiv of solid LiHMDS (45 mg, 0.27 mmol) was added to the solution. The reaction was stirred for two hours. The reaction was filtered through Celite and the solvent was removed in vacuo. The solid residue was washed with hexanes to remove any unreacted starting materials resulting in pure dipyrinato lithium salt **5Li**. The lithium salt was stirred as a slurry in toluene (20 mL) forming a yellow suspension. Boron trichloride (0.12 mL of a 1.0 M solution in hexanes, 0.12 mmol) was added drop-wise to the reaction mixture. The yellow slurry instantly changed to a red-orange solution. The reaction was stirred for an hour before filtration over Celite. The filtrate was concentrated in vacuo to give the product **5BCl₂** as a red solid (55 mg, 91%).

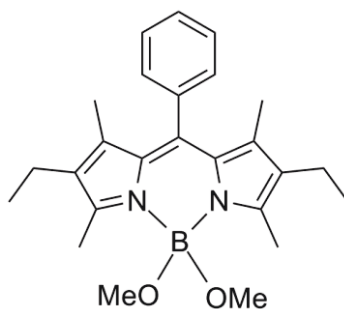
Method 2: Boron trichloride (0.15 mL of a 1.0 M solution in hexanes, 0.15 mmol) was slowly added to a solution of **5** (50 mg, 0.15 mmol) in anhydrous toluene (20 mL) under an N₂ atmosphere in a glovebox. The reaction mixture was stirred at room temperature for 1 h. The reaction mixture was then filtered over Celite, washed with anhydrous toluene and the filtrate was concentrated *in vacuo* to give **5BCl₂** as a red powder (60 mg, 99%). δ_{H} (500 MHz, THF-d₈) 7.55-7.51 (m, 3H), 7.37-7.36 (m, 2H), 2.74 (s, 6H), 2.35 (q, $J = 7.5$, 4H), 1.32 (s, 6H), 0.98 (t, $J = 7.6$, 6H); δ_{C} (125 MHz, THF-d₈) 156.4, 141.4, 139.6, 136.4, 135.1, 130.5, 130.1, 129.9, 129.3, 17.8, 14.8, 14.7, 12.0; δ_{B} (160 MHz, THF-d₈) 2.39 (s).

1,3,5,7-Tetramethyl-2,6-diethyl-8-*H*-4,4'-dimethoxy-bora-3a,4a-diaza-*s*-indacene (3B(OMe)₂)



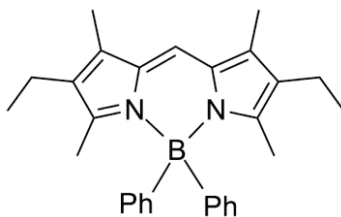
To a solution of **3BCl₂** (50 mg, 0.15 mmol) in anhydrous methanol (10 mL) was added solid sodium methoxide (52 mg, 0.95 mmol) and the reaction mixture was stirred at room temperature for 3 h in a glovebox. The reaction mixture was then removed from the glovebox, poured into water (20 mL) and extracted with ethyl acetate (20 mL). The organic layer was washed with water (2 x 20 mL) and the combined organic layers were dried over Na₂SO₄ and concentrated *in vacuo* to give **3B(OMe)₂** as an orange crystalline solid (48 mg, 99%). δ_{H} (500 MHz, CDCl₃) 6.90 (s, 1H), 2.84 (s, 6H), 2.47 (s, 6H), 2.38 (q, $J=7.5$, 4H), 2.17 (s, 6H), 1.06 (t, $J=7.5$, 6H); δ_{C} (125 MHz, CDCl₃) 154.9, 134.6, 133.8, 131.2, 118.4, 49.3, 17.5, 14.9, 12.3, 9.5; δ_{B} (160 MHz, CDCl₃) 2.66 (s); m/z ESI⁺ found 351.2214 [M+Na]⁺ calculated for C₁₉H₂₉BN₂O₂Na 351.2220.

1,3,5,7-Tetramethyl-2,6-diethyl-8-phenyl-4,4'-dimethoxy-bora-3a,4a-diaza-*s*-indacene (5B(OMe)₂)



To a solution of **5BCl₂** (50 mg, 0.12 mmol) in anhydrous methanol (10 mL) was added solid sodium methoxide (46 mg, 0.81 mmol) and the reaction mixture was stirred at room temperature for 3 h in a glovebox. The reaction mixture was then removed from the glovebox, poured into water (20 mL) and extracted with ethyl acetate (20 mL). The organic layer was washed with water (2 x 20 mL) and the combined organic layers were dried over Na₂SO₄ and concentrated *in vacuo* to give **5B(OMe)₂** as a red crystalline solid (48 mg, 99%). δ_{H} (500 MHz, CDCl₃) 7.48-7.45 (m, 3H), 7.32-7.28 (m, 2H), 2.94 (s, 6H), 2.53 (s, 6H), 2.32 (q, $J=7.5$, 4H), 1.29 (s, 6H), 1.00 (t, $J=7.5$, 6H); δ_{C} (125 MHz, CDCl₃) 154.0, 140.1, 136.6, 136.3, 132.3, 128.9 (2C), 128.6, 128.5, 49.2, 17.2, 14.8, 12.3, 11.8; δ_{B} (160 MHz, CDCl₃) 2.46 (s); m/z ESI⁺ found 427.2527 [M+Na]⁺ calculated for C₂₅H₃₃BN₂O₂Na 427.2533.

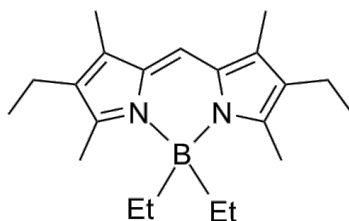
1,3,5,7-Tetramethyl-2,6-diethyl-8-H-4,4'-diphenyl-bora-3a,4a-diaza-s-indacene (3BPh₂)



Phenyl lithium (0.20 mL of a 1.8 M solution in di-*n*-butyl ether, 0.36 mmol) was slowly added to a round-bottom flask containing a solution of **3BCl₂** (61 mg, 0.18 mmol) in anhydrous THF (15 mL) at room temperature in a glovebox. The solution was allowed to stir for 1 h. The reaction mixture was then filtered through Celite and concentrated *in vacuo* to give a dark red-brown powder. The crude solid was purified over silica gel eluting with 4% EtOAc in hexanes to give **3BPh₂** as a bright orange solid (38 mg, 50%). δ_{H} (500 MHz, CDCl₃) 7.29-7.16 (m, 10H), 2.32 (q, $J=7.5$, 4H), 2.21 (s, 6H), 1.75 (s, 6H),

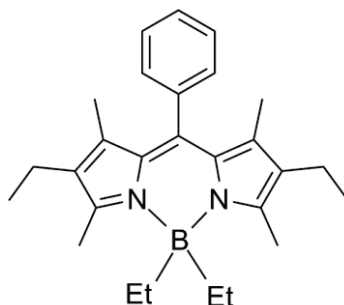
0.98 (t, $J=7.5$, 6H); δ_C (125 MHz, $CDCl_3$) 154.0, 134.1, 133.9, 133.8, 132.3, 131.6, 127.3, 125.7, 119.5, 17.7, 14.9, 14.4, 9.5; δ_B (160 MHz, $CDCl_3$) 0.18 (s).

1,3,5,7-Tetramethyl-2,6-diethyl-8-*H*-4,4'-diethyl-bora-3a,4a-diaza-*s*-indacene (3BEt₂)



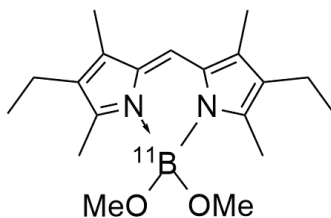
To a solution of **3BCl₂** (50 mg, 0.15 mmol) in anhydrous diethyl ether (15 mL) was added ethyl magnesium bromide (0.10 mL, 3.0 M, 0.30 mmol) and the reaction mixture was stirred at room temperature for 3 h in a glovebox. The reaction mixture was then removed from the glovebox, extracted with water (20 mL) and the layers were separated. The aqueous layer was extracted with diethyl ether (3 x 10 mL) and the combined organic layers were dried over Na_2SO_4 and concentrated *in vacuo*. Purification over silica gel eluting with 17% EtOAc in hexanes gave **3BEt₂** as a red crystalline solid (47 mg, 99%). δ_H (500 MHz, $CDCl_3$) 6.98 (s, 1H), 2.45-2.37 (m, 2x(CH₃+CH₂), 10H), 2.18 (s, 6H), 1.06 (t, $J=7.6$, 6H), 0.81 (q, $J=7.6$, 4H), 0.30 (t, $J=7.6$, 6H); δ_C (125 MHz, $CDCl_3$) 151.1, 132.6, 131.8, 131.1, 119.4, 17.9, 15.0, 13.9, 9.43, 9.40 (one signal obscured); δ_B (160 MHz, $CDCl_3$) 2.50 (s).

**1,3,5,7-Tetramethyl-2,6-diethyl-8-phenyl-4,4'-diethyl-bora-3a,4a-diaza-s-indacene
(5BEt₂)**



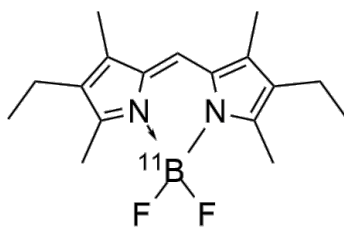
To a solution of **5BCl₂** (62 mg, 0.15 mmol) in anhydrous diethyl ether (15 mL) was added ethyl magnesium bromide (0.10 mL, 3.0 M, 0.30 mmol) and the reaction mixture was stirred at room temperature for 3 h in a glovebox. The reaction mixture was then removed from the glovebox, extracted with water (20 mL) and the layers were separated. The aqueous layer was extracted with diethyl ether (3 x 10 mL) and the combined organic layers were dried over Na₂SO₄ and concentrated *in vacuo*. Purification over silica gel eluting with 17% EtOAc in hexanes gave **5BEt₂** as a red crystalline solid (59 mg, 99%). δ_{H} (500 MHz, CDCl₃) 7.44 (brs, 3H), 7.29-7.28 (m, 2H), 2.44 (s, 6H), 2.32 (q, $J=7.1$, 4H), 1.25 (s, 6H), 0.97 (t, $J=7.1$, 6H), 0.87 (q, $J=7.3$, 4H), 0.41 (t, $J=7.0$, 6H); δ_{C} (125 MHz, CDCl₃) 150.2, 140.9, 137.7, 133.4, 132.4, 131.1, 129.0, 128.8, 128.3, 29.9, 17.6, 15.0, 14.1, 12.0, 9.6; δ_{B} (160 MHz, CDCl₃) 1.85 (s).

**1,3,5,7-Tetramethyl-2,6-diethyl-8-*H*-4,4'-dimethoxy-bora-3a,4a-diaza-s-indacene
(3¹¹B(OMe)₂)**



To a solution of **3HBr** (150 mg, 0.44 mmol) in anhydrous CH₂Cl₂ was added 2.2 equiv of LiHMDS (164 mg, 0.98 mmol). The solution changed from yellow to red with the dipyrinato lithium salt precipitating. The reaction mixture was treated with 10 equiv of ¹¹B(OMe)₃ (0.51 mL) and the precipitate dissolved as the solution became deep red. Upon completion, the reaction mixture was washed with water, dried over Na₂SO₄ and concentrated *in vacuo*. The crude material was purified over alumina eluting with 20% EtOAc in hexanes to give as a red solid **3¹¹B(OMe)₃** (74 mg, 50%). NMR data matches that previously reported.³⁷

1,3,5,7-Tetramethyl-2,6-diethyl-8-H-4,4'-difluoro-bora-3a,4a-diaza-s-indacene (3¹¹BF₂)



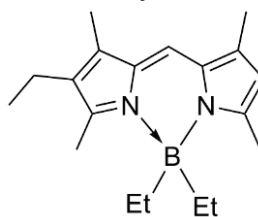
Compound **3¹¹B(OMe)₃** (50 mg, 0.16 mmol) was dissolved in anhydrous CH₂Cl₂ and treated with 2 equiv of BCl₃ (0.32 mL, 1.0 M) and stirred for 1 h, followed by the addition of 10 equiv of CsF (250 mg, 1.64 mmol). The solution stirred for another 3 h and the reaction mixture was then washed with water, dried over Na₂SO₄ and concentrated *in vacuo*. The crude product was purified over a pad of silica eluting with CH₂Cl₂ to afford **3¹¹BF₂** (16 mg, 35%). NMR data matches that previously reported.³⁷

General Procedure for the Synthesis of C-BODIPYs (GP2)

The *F*-BODIPY (50 mg) was dissolved in anhydrous dichloromethane (10 mL) and 1 equiv of BCl₃ was added drop-wise from a 1.0 M solution in anhydrous hexanes. The

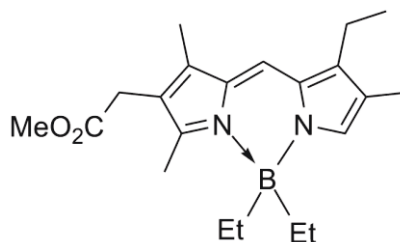
reaction was stirred for an hour to allow *in situ* formation of the *Cl*-BODIPY to occur. The *Cl*-BODIPY was then reacted with 2 equiv of EtMgBr from a 3.0 M solution in anhydrous diethyl ether and stirring was continued for another hour. Upon completion of the reaction, the mixture was washed with brine (15 mL) and the organic layer was dried over Na₂SO₄. The solution was then concentrated *in vacuo* to obtain the *C*-BODIPY product.

1,3,5,7-Tetramethyl-2-ethyl-8-*H*-4,4'-diethyl-bora-3a,4a-diaza-*s*-indacene (2BEt₂)



Using **GP2**, compound **2BEt₂** was synthesized from **2BF₂**. Bright orange solid (53 mg, 99%). δ_{H} (500 MHz, CDCl₃) 7.02 (s, 1H), 6.02 (s, 1H), 2.44-2.39 (m, 2xCH₃+CH₂, 8H), 2.25 (s, 3H), 2.19 (s, 3H), 1.06 (t, $J=7.6$, 3H), 0.81 (qd, $J=3.2, 7.6$, 4H), 0.32 (t, $J=7.6$, 6H); δ_{C} (125 MHz, CDCl₃) 153.0, 151.4, 135.2, 133.3, 133.1, 133.0, 132.0, 120.1, 118.3, 17.9, 16.3, 14.9, 14.0, 11.3, 9.4, 9.3 (one signal obscured); δ_{B} (160 MHz, CDCl₃) 2.85 (s).

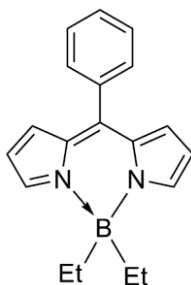
1,3,6-Trimethyl-2-(2-methoxy-2-oxoethyl)-7-ethyl-8-*H*-4,4'-diethyl-bora-3a,4a-diaza-*s*-indacene (7BEt₂)



Using **GP2**, compound **7BEt₂** was synthesized from the corresponding *F*-BODIPY.³⁷ The crude material was filtered through a plug of silica eluting with CH₂Cl₂ to isolate the product. Bright orange solid (40 mg, 75%). δ_{H} (500 MHz, CDCl₃) 7.16 (s, 1H), 7.15 (s,

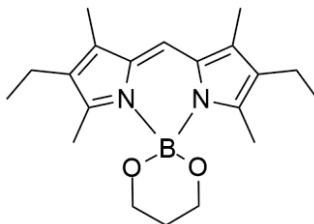
1H), 3.67 (s, 3H), 3.45 (s, 2H), 2.62 (q, $J=7.6$, 2H), 2.38 (s, 3H), 2.24 (s, 3H), 2.07 (s, 3H), 1.17 (t, $J=7.6$, 3H), 0.84 (dq, $J=7.4$, 14.5, 2H), 0.46 (dq, $J=7.4$, 14.6, 2H), 0.32 (t, $J=7.6$, 6H); δ_C (125 MHz, $CDCl_3$) 171.8, 153.4, 140.8, 139.4, 135.7, 133.4, 132.0, 124.0, 121.74, 121.71, 52.2, 30.6, 18.0, 16.4, 13.6, 10.3, 9.9, 9.0 (one signal obscured); δ_B (160 MHz, $CDCl_3$) 1.83 (s).

8-Phenyl-4,4'-diethyl-bora-3a,4a-diaza-s-indacene (8BEt₂)



Using **GP2**, compound **8BEt₂** was synthesized from **8BF₂**. Bright orange solid (53 mg, 99%). δ_H (500 MHz, $CDCl_3$) 7.61-7.59 (m, 2H), 7.57-7.45 (m, 5H), 6.85 (d, $J=4.3$, 2H), 6.54 (dd, $J=1.5$, 4.3, 2H), 0.67 (q, $J=7.3$, 4H), 0.50 (t, $J=7.3$, 6H); δ_C (125 MHz, $CDCl_3$) 146.6, 142.1, 135.2, 134.4, 130.5, 130.0, 128.2, 127.3, 117.2, 29.8, 8.9; δ_B (160 MHz, $CDCl_3$) 1.38 (s).

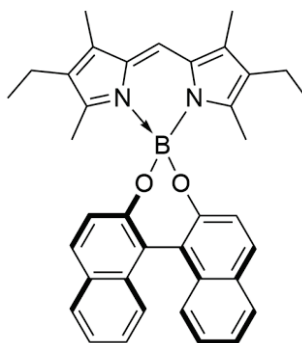
1,3,5,7-Tetramethyl-2,6-diethyl-8-*H*-4,4'-[propane-1,3-bis(olate)]-bora-3a,4a-diaza-s-indacene (17)



F-BODIPY **3BF₂** (50 mg, 0.16 mmol) was treated with 1 equiv BCl_3 (0.16 mL, 1.0 M) in anhydrous CH_2Cl_2 and the reaction mixture was stirred for 1 h. A solution of $LiO(CH_2)_3OLi$ (1 equiv) in CH_2Cl_2 was added to the reaction mixture and stirring was

continued for another three hours. The mixture was then washed with brine (15 mL) and the organic layer was dried over Na₂SO₄. The solution was then concentrated *in vacuo*. The crude material was purified over silica eluting with 50:50 hexanes:ethyl acetate. The product was isolated as an orange solid (22 mg, 40%). δ_{H} (500 MHz, CDCl₃) 6.90 (s, 1H), 4.04 (t, $J=5.8$, 4H), 2.54 (s, 6H), 2.36 (q, $J=7.6$, 4H), 2.12 (s, 6H), 1.93 (dt, $J=5.9$, 11.9, 2H), 1.02 (t, $J=7.6$, 6H); δ_{C} (125 MHz, CDCl₃) 153.7, 136.2, 133.3, 131.0, 119.0 59.9, 28.2, 17.5, 14.9, 13.5, 9.6; δ_{B} (160 MHz, CDCl₃) 1.55 (s).

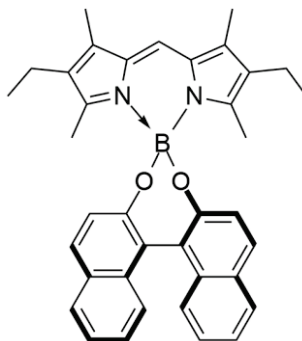
1,3,5,7-Tetramethyl-2,6-diethyl-8-*H*-4,4'-[(1,1'-binaphthalene)-2,2'-bis(olate)]-bora-3a,4a-diaza-s-indacene (18)



F-BODIPY **3BF₂** (50 mg, 0.16 mmol) was treated with 1 equiv BCl₃ (0.16 mL, 1.0 M) in anhydrous CH₂Cl₂ and the reaction mixture was stirred for 1 h. A slurry of 1 equiv (*R*)-BINOL dilithium alkoxide in CH₂Cl₂ was added to the reaction mixture and stirring was continued for another three hours. The mixture was then washed with brine (15 mL) and the organic layer was dried over Na₂SO₄. The solution was then concentrated *in vacuo*. The crude material was purified over silica pad eluting with CH₂Cl₂. The product was isolated as a red solid (90 mg, 91%). δ_{H} (500 MHz, CDCl₃) 7.84 (d, $J = 8$, 2H), 7.77 (d, $J = 8.5$, 2H), 7.32 (t, $J = 7.5$, 2H), 7.29 (d, $J = 8.5$, 2H), 7.18-7.15 (m, 4H), 7.08 (s, 1H), 2.24-2.19 (m, 10H, 2x(CH₃+CH₂)), 1.62 (s, 6H), 0.91 (t, $J = 7.6$, 6H); δ_{C} (125 MHz,

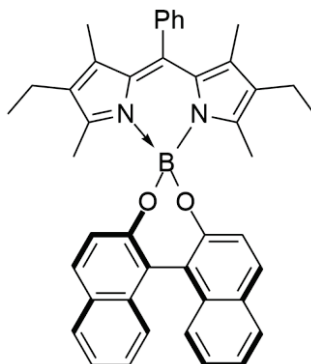
CDCl₃) 155.8, 154.7, 136.3, 133.9, 133.1, 131.9, 130.0, 129.2, 127.9, 127.2, 125.2, 124.0, 123.3, 121.7, 118.5, 17.5, 14.5, 13.5, 9.6; δ_B (160 MHz, CDCl₃) 4.58 (s).

1,3,5,7-Tetramethyl-2,6-diethyl-8-*H*-4,4'-[(1,1'-binaphthalene)-2,2'-bis(olate)]-bora-3a,4a-diaza-*s*-indacene (19)



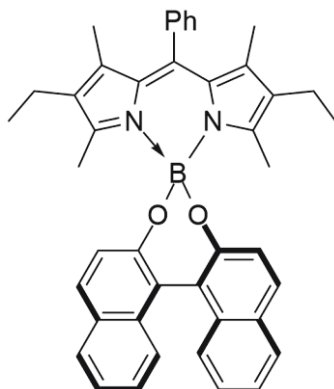
F-BODIPY **3BF₂** (50 mg, 0.16 mmol) was treated with 1 equiv BCl₃ (0.16 mL, 1.0 M) in anhydrous CH₂Cl₂ and the reaction mixture was stirred for 1 h. A slurry of 1 equiv (*S*)-BINOL dilithium alkoxide in CH₂Cl₂ was added to the reaction mixture and stirring was continued for another three hours. The mixture was then washed with brine (15 mL) and the organic layer was dried over Na₂SO₄. The solution was then concentrated *in vacuo*. The crude material was purified over silica pad eluting with CH₂Cl₂. The product was isolated as a red solid (90 mg, 91%). δ_H (500 MHz, CDCl₃) 7.84 (d, *J* = 8, 2H), 7.77 (d, *J* = 8.5, 2H), 7.32 (t, *J* = 7.5, 2H), 7.29 (d, *J* = 8.5, 2H), 7.18-7.15 (m, 4H), 7.08 (s, 1H), 2.24-2.19 (m, 10H, 2x(CH₃+CH₂)), 1.62 (s, 6H), 0.91 (t, *J* = 7.6, 6H); δ_C (125 MHz, CDCl₃) 155.8, 154.7, 136.3, 133.9, 133.1, 131.9, 130.0, 129.2, 127.9, 127.2, 125.2, 124.0, 123.3, 121.7, 118.5, 17.5, 14.5, 13.5, 9.6; δ_B (160 MHz, CDCl₃) 4.58 (s).

1,3,5,7-Tetramethyl-2,6-diethyl-8-phenyl-4,4'-[(1,1'-binaphthalene)-2,2'-bis(olate)]-bora-3a,4a-diaza-s-indacene (20)



F-BODIPY 5BF₂ (50 mg, 0.16 mmol) was treated with 1 equiv BCl₃ (0.16 mL, 1.0 M) in anhydrous CH₂Cl₂ and the reaction mixture was stirred for 1 h. A slurry of 1 equiv (R)-BINOL dilithium alkoxide in CH₂Cl₂ was added to the reaction mixture and stirring was continued for another three hours. The mixture was then washed with brine (15 mL) and the organic layer was dried over Na₂SO₄. The solution was then concentrated in vacuo. The crude material was purified over silica pad eluting with CH₂Cl₂. The product was isolated as a red solid (90 mg, 91%). δ_{H} (500 MHz, CDCl₃) 7.96-7.70 (m, 4H), 7.55-7.50 (m, 2H), 7.36-7.28 (m, 7H), 7.18-7.08 (m, 4H), 2.10 (q, J = 7.5, 4H), 1.68 (s, 6H), 1.28 (s, 6H), 0.78 (t, J = 7.5 Hz, 6H); δ_{C} (125 MHz, CDCl₃) 151.4, 134.5, 130.7, 129.9, 129.5, 128.9, 128.3, 127.9, 127.2, 126.4, 126.1, 125.6, 124.5, 123.5, 122.6, 122.1, 121.5, 117.8, 17.3, 14.5, 13.7, 12.1; δ_{B} (160 MHz, CDCl₃) 4.39 (s).

1,3,5,7-Tetramethyl-2,6-diethyl-8-phenyl-4,4'-[(1,1'-binaphthalene)-2,2'-bis(olate)]-bora-3a,4a-diaza-s-indacene (21)



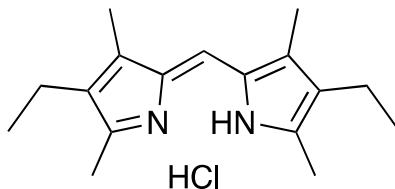
F-BODIPY **5BF₂** (50 mg, 0.16 mmol) was treated with 1 equiv BCl₃ (0.16 mL, 1.0 M) in anhydrous CH₂Cl₂ and the reaction mixture was stirred for 1 h. A slurry of 1 equiv (*S*)-BINOL dilithium alkoxide in CH₂Cl₂ was added to the reaction mixture and stirring was continued for another three hours. The mixture was then washed with brine (15 mL) and the organic layer was dried over Na₂SO₄. The solution was then concentrated *in vacuo*. The crude material was purified over silica pad eluting with CH₂Cl₂. The product was isolated as a red solid (90 mg, 91%). δ_H (500 MHz, CDCl₃) 7.96-7.70 (m, 4H), 7.55-7.50 (m, 2H), 7.36-7.28 (m, 7H), 7.18-7.08 (m, 4H), 2.10 (q, *J* = 7.5, 4H), 1.68 (s, 6H), 1.28 (s, 6H), 0.78 (t, *J* = 7.5 Hz, 6H); δ_C (125 MHz, CDCl₃) 151.4, 134.5, 130.7, 129.9, 129.5, 128.9, 128.3, 127.9, 127.2, 126.4, 126.1, 125.6, 124.5, 123.5, 122.6, 122.1, 121.5, 117.8, 17.3, 14.5, 13.7, 12.1; δ_B (160 MHz, CDCl₃) 4.39 (s).

General Procedure for the Synthesis of HX Salts, X = Cl, Br (GP3)

The *F*-BODIPY (50 mg) was dissolved in anhydrous dichloromethane (10 mL) and 1 equiv of BCl₃ (or BBr₃) was added drop-wise from a 1.0 M solution in anhydrous

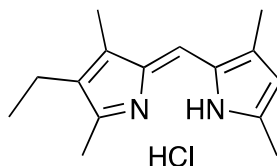
hexanes. The reaction mixture was stirred for an hour to allow *in situ* formation of the *Cl*-BODIPY (or *Br*-BODIPY). The reaction mixture was then concentrated *in vacuo*. The residue was dissolved in a mixture of acetone:water (10:1) and the solution was stirred for 10 min. The reaction mixture was extracted into dichloromethane and the organic layer was dried over Na₂SO₄. The solution was then concentrated *in vacuo* to obtain the HX salt of the dipyrin.

(*Z*)-3-Ethyl-5-((4-ethyl-3,5-dimethyl-2*H*-pyrrol-2-ylidene)methyl)-2,4-dimethyl-1*H*-pyrrole hydrochloride (3HCl)



Using **GP3**, compound **3HCl** was synthesized from **3BF₂**. Bright orange solid (48 mg, 99%). δ_H (500 MHz, CDCl₃) 13.36 (brs, 2H), 7.00 (s, 1H), 2.59 (s, 6H), 2.40 (q, *J* = 7.5, 4H), 2.24 (s, 6H), 1.05 (t, *J* = 7.5, 6H). Data matches that previously reported for this compound.⁸¹

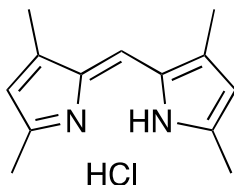
(*Z*)-2-((4-Ethyl-3,5-dimethyl-2*H*-pyrrol-2-ylidene)methyl)-3,5-dimethyl-1*H*-pyrrole hydrochloride (2HCl)



Using **GP3**, compound **2HCl** was synthesized from **2BF₂**. Bright orange solid (48 mg, 99%). δ_H (500 MHz, CDCl₃) 13.71 (brs, 2H), 7.02 (s, 1H), 6.11 (s, 1H), 2.63 (s, 3H), 2.62 (s, 3H), 2.42 (q, *J* = 7.5, 2H), 2.33 (s, 3H), 2.26 (s, 3H), 1.07 (t, *J* = 7.5, 3H); δ_C (125 MHz, CDCl₃) 155.4, 148.8, 141.9, 139.1, 131.0, 126.84, 126.82, 119.4, 116.8, 17.4,

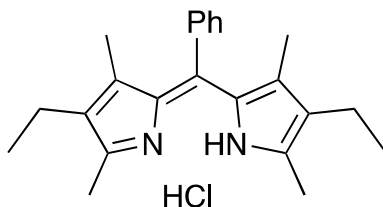
14.53, 14.51, 13.0, 12.2, 10.1. LRMS-ESI (m/z): 229.2 [M + H]⁺; HRMS-ESI (m/z): [M + H]⁺ calcd for C₁₅H₂₁N₂ 229.1699; found, 229.1691.

(Z)-2-((3,5-Dimethyl-2H-pyrrol-2-ylidene)methyl)-3,5-dimethyl-1H-pyrrole hydrochloride (4HCl)



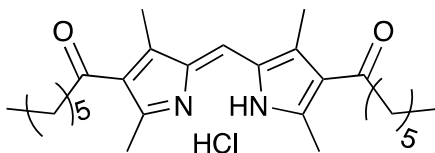
Using **GP3**, compound **4HCl** was synthesized from the corresponding *F*-BODIPY.³⁷ Bright orange solid (48 mg, 99%). δ_{H} (500 MHz, CDCl₃) 13.72 (brs, 2H), 7.03 (s, 1H), 6.13 (s, 2H), 2.62 (s, 6H), 2.32 (s, 6H). Data matches that previously reported for this compound.⁸⁷

(Z)-3-Ethyl-5-((4-ethyl-3,5-dimethyl-2H-pyrrol-2-ylidene)(phenyl)methyl)-2,4-dimethyl-1H-pyrrole hydrochloride (5HCl)



Using **GP3**, compound **5HCl** was synthesized from **5BF₂**. Bright orange solid (48 mg, 99%). δ_{H} (500 MHz, CDCl₃) 11.46 (brs, 2H), 7.55-7.41 (m, 3H), 7.26-7.25 (m, 2H), 2.58 (s, 6H), 2.33 (q, *J* = 7.5, 4H), 1.31 (s, 6H), 0.99 (t, *J* = 7.5, 6H). Data matches that previously reported for this compound.³⁷

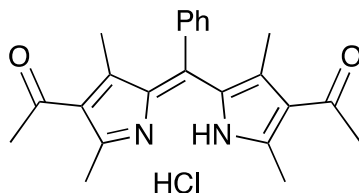
(Z)-1-(2-((4-Heptanoyl-3,5-dimethyl-1H-pyrrol-2-yl)methylene)-3,5-dimethyl-2H-pyrrol-4-yl)heptan-1-one hydrochloride (22HCl)



Using **GP3**, compound **22HCl** was synthesized from the corresponding *F*-BODIPY.⁶³

Bright orange solid (49 mg, 99%). δ_{H} (500 MHz, CDCl_3) 7.44 (s, 1H), 3.00 (s, 6H), 2.76 (t, $J = 7.2$, 4H), 2.51 (s, 6H), 1.74-1.66 (m, 4H), 1.39-1.28 (m, 12H), 0.90 (t, $J = 6.6$, 6H); δ_{C} (125 MHz, CDCl_3) 198.4, 165.7, 142.1, 136.8, 132.0, 123.1, 43.8, 31.9, 29.9, 24.2, 22.7, 17.5, 14.2, 12.4. LRMS-ESI (m/z): 425.3 $[\text{M} + \text{H}]^+$; HRMS-ESI (m/z): $[\text{M} + \text{H}]^+$ calcd for $\text{C}_{27}\text{H}_{41}\text{N}_2\text{O}_2$ 425.3163; found, 425.3147.

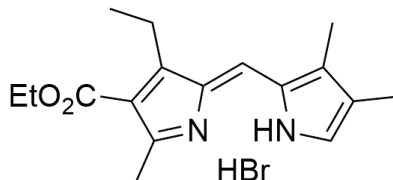
(Z)-1-(2-((4-Acetyl-3,5-dimethyl-1H-pyrrol-2-yl)(phenyl)methylene)-3,5-dimethyl-2H-pyrrol-4-yl)ethanone hydrochloride (23HCl)



Using **GP3**, compound **23HCl** was synthesized from the corresponding *F*-BODIPY.⁶³

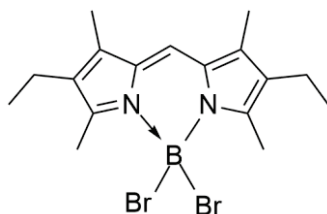
Bright orange solid (49 mg, 99%). δ_{H} (500 MHz, CDCl_3) 13.93 (brs, 2H), 7.50-7.46 (m, 3H), 7.30-7.28 (m, 2H), 2.58 (s, 6H), 2.39 (s, 6H), 1.53 (s, 6H); δ_{C} (125 MHz, CDCl_3) 196.7, 154.5, 143.7, 143.6, 137.2, 137.1, 131.0, 129.4, 129.3, 129.2, 31.8, 18.1, 14.5. LRMS-ESI (m/z): 361.2 $[\text{M} + \text{H}]^+$; HRMS-ESI (m/z): $[\text{M} + \text{H}]^+$ calcd for $\text{C}_{23}\text{H}_{25}\text{N}_2\text{O}_2$ 361.1916; found, 361.1913.

(Z)-Ethyl 2-((3,4-dimethyl-1H-pyrrol-2-yl)methylene)-3-ethyl-5-methyl-2H-pyrrole-4-carboxylate hydrobromide (24HBr)



Using **GP3**, compound **24HBr** was synthesized from the corresponding *F*-BODIPY.³⁷ Bright orange solid (55 mg, 99%). δ_{H} (500 MHz, CDCl_3) 13.73 (brs, 1H), 13.35 (brs, 1H), 7.76 (d, $J = 3.5$, 1H), 7.34 (s, 1H), 4.36 (q, $J = 7.0$, 2H), 3.07 (q, $J = 7.5$, 2H), 2.96 (s, 3H), 2.33 (s, 3H), 2.10 (s, 3H), 1.40 (t, $J = 7.0$, 3H), 1.27 (t, $J = 7.5$, 3H); δ_{C} (125 MHz, CDCl_3) 163.2, 158.6, 155.6, 144.7, 144.5, 128.9, 126.6, 125.3, 122.9, 118.2, 60.7, 19.6, 16.9, 15.6, 14.4, 10.5, 10.2. LRMS-ESI (m/z): 287.2 $[\text{M} + \text{H}]^+$; HRMS-ESI (m/z): $[\text{M} + \text{H}]^+$ calcd for $\text{C}_{17}\text{H}_{23}\text{N}_2\text{O}_2$ 287.1754; found, 287.1752.

1,3,5,7-Tetramethyl-2,6-diethyl-8-*H*-4,4'-dibromo-bora-3a,4a-diaza-s-indacene (3BBr₂)

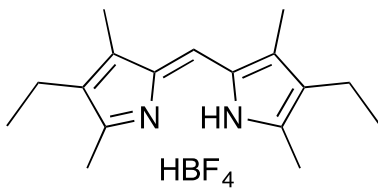


Compound **3BF₂** (50 mg, 0.16 mmol) was dissolved in anhydrous CCl_4 (10 mL) and treated with 1 equiv of BBr_3 (0.16 mL, 1.0 M). The bright orange solution became dark red/purple in colour. The solution was concentrated *in vacuo* and compound **3BBr₂** was isolated as a dark red solid (70 mg, 99%). δ_{H} (500 MHz, CDCl_3) 7.02 (s, 1H), 2.80 (s, 6H), 2.40 (q, $J = 7.5$, 4H), 2.21 (s, 6H), 1.08 (t, $J = 7.5$, 6H); δ_{C} (125 MHz, CDCl_3) 154.2, 139.6, 134.1, 131.6, 119.4, 17.4, 14.7, 14.4, 10.2; δ_{B} (160 MHz, CDCl_3) -5.89 (s).

General Procedure for the Synthesis of HBF₄ Salts (GP4)

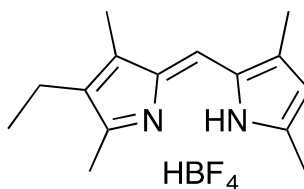
The *F*-BODIPY (50 mg) was dissolved in anhydrous dichloromethane (10 mL) and 1 equiv of BF₃·OEt₂ was added drop-wise. The reaction mixture was stirred for 10 minutes and then 3 equiv of water was added and the mixture was further stirred for 3 hours. The reaction mixture was washed with water and the organic layer dried over Na₂SO₄. The solution was concentrated *in vacuo*. The resulting solid was washed with diethyl ether to remove any unreacted *F*-BODIPY, leaving an orange powder corresponding to the HBF₄ salt of the dipyrin.

(*Z*)-3-Ethyl-5-((4-ethyl-3,5-dimethyl-2*H*-pyrrol-2-ylidene)methyl)-2,4-dimethyl-1*H*-pyrrole tetrafluoroborate (3HBF₄)



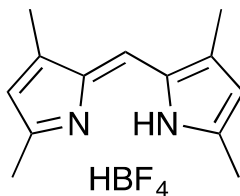
Using **GP4**, compound **3HBF₄** was synthesized from **3BF₂**. Bright orange solid (56 mg, 99%). δ_{H} (500 MHz, CDCl₃) 10.78 (brs, 2H), 7.06 (s, 1H), 2.55 (s, 6H), 2.44 (q, $J = 7.5$, 4H), 2.28 (s, 6H), 1.09 (t, $J = 7.5$, 6H); δ_{C} (125 MHz, CDCl₃) 154.3, 142.6, 131.1, 126.9, 118.9, 17.4, 14.5, 12.8, 10.2; δ_{B} (160 MHz, CDCl₃) -0.65 (s); δ_{F} (282 MHz, CDCl₃) -155.1 (s). LRMS-ESI (m/z): 87.0 [M]⁻.

(Z)-2-((4-Ethyl-3,5-dimethyl-2H-pyrrol-2-ylidene)methyl)-3,5-dimethyl-1H-pyrrole tetrafluoroborate (2HBF₄)



Using **GP4**, compound **2HBF₄** was synthesized from **2BF₂**. Bright orange solid (52 mg, 91%). δ_{H} (500 MHz, CDCl₃) 10.83 (brs, 1H), 10.73 (brs, 1H), 7.09 (s, 1H), 6.19 (s, 1H), 2.57 (s, 2 x CH₃, 6H), 2.45 (q, $J = 7.5$, 2H), 2.35 (s, 3H), 2.29 (s, 3H). 1.09 (t, $J = 7.5$, 3H); δ_{C} (125 MHz, CDCl₃) 156.1, 154.8, 146.2, 143.5, 131.7, 127.30, 127.28, 119.5, 117.4, 17.5, 14.4, 12.9, 12.3, 10.2 (1C signal missing); δ_{B} (160 MHz, CDCl₃) -0.65 (s); δ_{F} (282 MHz, CDCl₃) -155.0 (s). LRMS-ESI (m/z): 87.0 [M]⁻. A crystal suitable for X-ray crystallography was obtained from the slow evaporation of solvent from a solution of compound **35** in dichloromethane. Data for **35**: C₁₅H₂₁N₂F₄B, M = 316.15 g, dark red, block, 0.33 x 0.25 x 0.22 mm, primitive orthorhombic, Pnma (#62), a = 17.4172(8) Å, b = 7.0912(4) Å, c = 13.2491(8) Å, V = 1636.38(15) Å³, Z = 4, T = 173(1) K, $\rho = 1.283$ g cm⁻³, $\mu(\text{MoK}\alpha) = 1.068$ cm⁻¹, 10434 reflections (2620 unique, $R_{\text{int}} = 0.052$), R = 0.0595, $R_w = 0.0654$, GOF = 1.179.

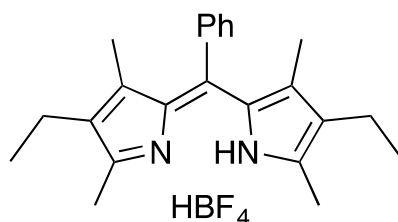
(Z)-2-((3,5-Dimethyl-2H-pyrrol-2-ylidene)methyl)-3,5-dimethyl-1H-pyrrole tetrafluoroborate (4HBF₄)



Using **GP4**, compound **4HBF₄** was synthesized from the corresponding *F*-BODIPY.³⁷ Bright orange solid (46 mg, 80%). δ_{H} (500 MHz, CDCl₃) 10.84 (brs, 2H), 7.09 (s, 1H),

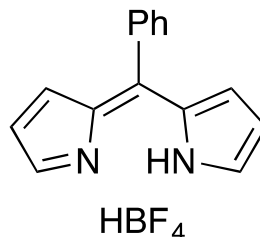
6.21 (s, 2H), 2.58 (s, 6H), 2.34 (s, 6H); δ_C (125 MHz, $CDCl_3$) 156.2, 147.4, 133.5, 127.6, 120.3, 14.5, 12.2; δ_B (160 MHz, $CDCl_3$) -0.65 (s); δ_F (282 MHz, $CDCl_3$) -154.9 (s).
LRMS-ESI (m/z): 87.0 [M]⁻.

(Z)-3-Ethyl-5-((4-ethyl-3,5-dimethyl-2H-pyrrol-2-ylidene)(phenyl)methyl)-2,4-dimethyl-1H-pyrrole tetrafluoroborate (5HBF₄)



Using **GP4**, compound **5HBF₄** was synthesized from **5BF₂**. Bright orange solid (25 mg, 45%). δ_H (500 MHz, $CDCl_3$) 9.89 (brs, 2H), 7.53-7.45 (m, 3H), 7.35-7.31 (m, 2H), 2.52 (s, 6H), 2.41 (q, $J=7.5$, 4H), 1.45 (s, 6H), 1.06 (t, $J=7.5$, 6H); δ_C (125 MHz, $CDCl_3$) 153.7, 138.5, 136.6, 135.9, 133.8, 132.2, 129.3, 129.1, 128.3, 17.5, 14.3, 12.7, 12.1; δ_B (160 MHz, $CDCl_3$) -1.01 (s); δ_F (282 MHz, $CDCl_3$) -157.4 (s). LRMS-ESI (m/z): 87.0 [M]⁻.

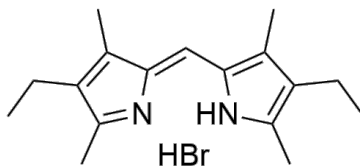
(Z)-2-(Phenyl(2H-pyrrol-2-ylidene)methyl)-1H-pyrrole tetrafluoroborate (8HBF₄)



Using **GP4**, compound **8HBF₄** was synthesized from **8BF₂**. Bright orange solid (3 mg, 5%). δ_H (500 MHz, $CDCl_3$) 8.46 (brs, 2H), 7.68 (t, $J=1.2$, 2H), 7.52-7.42 (m, 5H), 6.62 (dd, $J=4.2, 1.2$, 2H), 6.41 (dd, $J=4.2, 1.5$, 2H); δ_C (125 MHz, $CDCl_3$) 143.8, 142.7,

140.3, 137.4, 131.0, 129.5, 129.2, 127.7, 117.7; δ_B (160 MHz, $CDCl_3$) -1.00 (s); δ_F (282 MHz, $CDCl_3$) -157.0 (s). LRMS-ESI (m/z): 87.0 $[M]^-$.

(Z)-3-Ethyl-5-((4-ethyl-3,5-dimethyl-2H-pyrrol-2-ylidene)methyl)-2,4-dimethyl-1H-pyrrole hydrobromide (3HBr)



Compound **3HBF₄** (50 mg, 0.15 mmol) was dissolved in anhydrous dichloromethane (10 mL) and treated with excess (0.1 mL) aqueous HBr (48%). The resulting solution was stirred for 15 min and then washed with water. The organic layer was dried over Na_2SO_4 and concentrated *in vacuo* to give **3HBr** as a bright orange solid (49 mg, 99%). δ_H (500 MHz, $CDCl_3$) 12.87 (brs, 2H), 7.02 (s, 1H), 2.66 (s, 6H), 2.41 (q, $J = 7.5$, 4H), 2.26 (s, 6H), 1.06 (t, $J = 7.5$, 6H). Data matches that previously reported for this compound.⁷⁷

Chapter 6 – Conclusions

6.1 – Conclusions

The traditional methodology for the synthesis of *F*-BODIPY compounds involves excess NEt_3 and $\text{BF}_3 \cdot \text{OEt}_2$. While this has been the standard method used since the origin of BODIPY chemistry, it is not without its limitations. An improved methodology for the formation of *F*-BODIPYs making use of a dipyrinato lithium salt and using only 1 equiv of $\text{BF}_3 \cdot \text{OEt}_2$ has been developed. The benefits of this strategy compared to the traditional route include the absence of a $\text{BF}_3 \cdot \text{NEt}_3$ adduct, which is formed when the excess reagents are used and can hinder purification procedures, while the new methodology typically only requires filtration through Celite for an efficient purification. It also avoids the formation of scrambled by-products that can occur during the synthesis of unsymmetrical *F*-BODIPYs. Finally, the improved method has led to an increase in yields in the formation of bis(*F*-BODIPY)s.

The first *Cl*-BODIPYs were developed with the idea that they would provide easier access to substitution at the boron centre. It was found that they are in fact facile to substitute at boron, using mild conditions and short reaction times. The *Cl*-BODIPYs were initially prepared from the free-base dipyrin but can also be synthesized from the *F*-BODIPY which makes these compounds much more accessible. By converting *F*-BODIPY into *Cl*-BODIPY, it allowed for the formation of BODIPY derivatives by varying the boron substituents. This was accomplished using the *Cl*-BODIPYs as a synthetic intermediate in a one-pot procedure which afforded *O*- and *C*-BODIPYs in excellent yields, using mild reaction conditions and generally shorter reaction times than

substitution reactions at boron performed on the *F*-BODIPY directly. This methodology allowed for a direct route to the synthesis of homochiral BODIPYs by using an enantiomerically pure BINOL, to thus alter the stereochemical properties of the BODIPY by way of axial chirality. Similar chiral compounds have been synthesized previously, but this methodology is higher yielding, uses milder conditions with simpler purification procedures and requires only stoichiometric amounts of each reagent.

Studying the reactivity of the *Cl*-BODIPYs has led to the discovery that the inherent moisture sensitivity of these compounds can be utilized as a method of deprotection to completely remove the boron centre and isolate the parent dipyrin. A methodology was developed to deprotect *F*-BODIPYs using both *Cl*- and *Br*-BODIPYs as in-situ intermediates to lead to exceptionally high yields. The greatest benefit of this particular method is the ease of the purification procedure. Since the dipyrins are formed as their HX salts, only an aqueous work-up is required while all other deprotection procedures prior to this work isolated free-base dipyrins requiring chromatographic purification. Expanding this strategy for *F*-BODIPY deprotection led to a deprotection through the activation of the boron centre using $\text{BF}_3 \cdot \text{OEt}_2$ followed by treatment with water. This strategy, while not universally high yielding, has provided the first HBF_4 salts of dipyrins. The first *Br*-BODIPY was also isolated and characterized during these studies.

References

1. Piloty, O.; Stock, J.; Dormann, E., *Chem. Ber.* **1914**, *47*, 400-406.
2. Dixon, H. B. F.; Cornish-Bowden, A.; Liebecq, C.; Loening, K. L.; Moss, G. P.; Reedijk, J.; Velick, S. F.; Venetianer, P.; Vliegthart, J. F. G., *Pure Appl. Chem.* **1987**, *59*, 779-832.
3. Loudet, A.; Burgess, K., *Chem. Rev.* **2007**, *107*, 4891-4932.
4. Brunings, K. J.; Corwin, A. H., *J. Am. Chem. Soc.* **1942**, *64*, 593-600.
5. Booth, H.; Johnson, A. W.; Johnson, F.; Langdale-Smith, R. A., *J. Chem. Soc.* **1963**, 650-661.
6. Treibs, A.; Zimmer-Galler, R., *Ann.* **1963**, *664*, 140-145.
7. Wood, T. E.; Thompson, A., *Chem. Rev.* **2007**, *107*, 1831-1861.
8. Kollmannsberger, M.; Gareis, T.; Heinl, S.; Breu, J.; Daub, J., *Angew. Chem., Int. Ed. Engl.* **1997**, *36*, 1333-1335.
9. Datta, S.; Lightner, D., *Monatsh. Chem.* **2008**, *139*, 1113-1117.
10. Sheldrick, W. S.; Borkenstein, A.; Struckmeier, G.; Engel, J., *Acta Crystallogr., B* **1978**, *B34*, 329-332.
11. Laha, J. K.; Dhanalekshmi, S.; Taniguchi, M.; Ambroise, A.; Lindsey, J. S., *Org. Process Res. Dev.* **2003**, *7*, 799-812.
12. Arsenault, G. P.; Bullock, E.; MacDonald, S. F., *J. Am. Chem. Soc.* **1960**, *82*, 4384-4389.
13. MacDonald, S. F., *J. Chem. Soc.* **1952**, 4176-4184.
14. Dolphin, D., *The Porphyrins*, Academic Press, 1987.
15. Brückner, C.; Karunaratne, V.; Rettig, S. J.; Dolphin, D., *Can. J. Chem.* **1996**, *74*, 2182-2193.
16. Wagner, R. W.; Lindsey, J. S., *J. Am. Chem. Soc.* **1994**, *116*, 9759-9760.
17. Thompson, A.; Dolphin, D., *J. Org. Chem.* **2000**, *65*, 7870-7877.
18. Zhang, Y.; Thompson, A.; Rettig, S. J.; Dolphin, D., *J. Am. Chem. Soc.* **1998**, *120*, 13537-13538.
19. Hsieh, A. T. T.; Rogers, C. A.; West, B. O., *Aust. J. Chem.* **1976**, *29*, 49-54.
20. Roomi, M. W., *Tetrahedron Lett.* **1974**, 1131-1132.
21. Murakami, Y.; Matsuda, Y.; Sakata, K.; Martell, A. E., *J. Chem. Soc., Dalton Trans.* **1973**, 1729-1734.
22. Motekaitis, R. J.; Martell, A. E., *Inorg. Chem.* **1970**, *9*, 1832-1839.
23. Fergusson, J. E.; Ramsay, C. A., *J. Chem. Soc.* **1965**, 5222-5225.

24. Fergusson, J. E.; March, F. C.; Couch, D. A.; Emerson, K.; Robinson, W. T., *J. Chem. Soc.* **1971**, 440-448.
25. Brückner, C.; Zhang, Y.; Rettig, S. J.; Dolphin, D., *Inorg. Chim. Acta* **1997**, *263*, 279-286.
26. Kollmannsberger, M.; Rurack, K.; Resch-Genger, U.; Daub, J., *J. Phys. Chem. A* **1998**, *102*, 10211-10220.
27. Treibs, A.; Haerberle, N., *Liebigs Ann. Chem.* **1968**, *718*, 183-207.
28. Thoresen, L. H.; Kim, H.; Welch, M. B.; Burghart, A.; Burgess, K., *Synlett* **1998**, 1276-1278.
29. Goze, C.; Ulrich, G.; Charbonnière, L.; Cesario, M.; Prange, T.; Ziessel, R., *Chem. Eur. J.* **2003**, *9*, 3748-3755.
30. Ulrich, G.; Goze, C.; Guardigli, M.; Roda, A.; Ziessel, R., *Angew. Chem., Int. Ed.* **2005**, *44*, 3694-3698.
31. Bergström, F.; Mikhalyov, I.; Hägglöf, P.; Wortmann, R.; Ny, T.; Johansson, L. B.-Å., *J. Am. Chem. Soc.* **2002**, *124*, 196-204.
32. Metzker, M. L.; Lu, J.; Gibbs, R. A., *Science* **1996**, *271*, 1420-1422.
33. Yon-Hin, P.; Wijesekera, T.; Dolphin, D., *Can. J. Chem.* **1990**, *68*, 1867-1875.
34. Turfan, B.; Akkaya, E. U., *Org. Lett.* **2002**, *4*, 2857-2859.
35. DiCesare, N.; Lakowicz, J. R., *Tetrahedron Lett.* **2001**, *42*, 9105-9108.
36. Wagner, R. W.; Lindsey, J. S., *Pure Appl. Chem.* **1996**, *68*, 1373-1380.
37. Crawford, S. M.; Thompson, A., *Org. Lett.* **2010**, *12*, 1424-1427.
38. Ziessel, R.; Ulrich, G.; Harriman, A., *New. J. Chem.* **2007**, *31*, 496-501.
39. Tahtaoui, C.; Thomas, C.; Rohmer, F.; Klotz, P.; Duportail, G.; Y.Mely; Bonnet, D.; Hibert, M., *J. Org. Chem.* **2007**, *72*, 269-272.
40. Bröring, M.; Kruger, R.; Link, S.; Kleeberg, C.; Köhler, S.; Xie, X.; Ventura, B.; Flamigni, L., *Chem. Eur. J.* **2008**, *14*, 2976-2983.
41. Lundrigan, T.; Baker, A. E. G.; Longobardi, L. E.; Wood, T. E.; Smithen, D. A.; Crawford, S. M.; Cameron, T. S.; Thompson, A., *Org. Lett.* **2012**, *14*, 2158-2161.
42. Beh, M. H. R.; Douglas, K. I. B.; House, K. T. E.; Murphy, A. C.; Sinclair, J. S. T.; Thompson, A., *Org. Biomol. Chem.* **2016**, *14*, 11473-11479.
43. Cipot-Wechsler, J.; Ali, A. A.-S.; Chapman, E. E.; Cameron, T. S.; Thompson, A., *Inorg. Chem.* **2007**, *46*, 10947-10949.
44. Ali, A. A.-S.; Cipot-Wechsler, J.; Crawford, S. M.; Selim, O.; Stoddard, R. L.; Cameron, T. S.; Thompson, A., *Can. J. Chem.* **2010**, *88*, 725-735.
45. Fox, A.; Hartman, J. S.; Humphries, R. E., *J. Chem. Soc., Dalton Trans.* **1982**, 1275-1283.
46. Paine, J. B.; Dolphin, D., *Can. J. Chem.* **1978**, *56*, 1710-1712.

47. Jones, G.; Stanforth, S. P., *The Vilsmeier Reaction of Fully Conjugated Carbocycles and Heterocycles*. 2004.
48. Bourget-Merle, L.; Lappert, M. F.; Severn, J. R., *Chem. Rev.* **2002**, *102*, 3031-3066.
49. Vidovic, D.; Reeske, G.; Findlater, M.; Cowley, A. H., *Dalton Trans.* **2008**, 2293-2297.
50. Hudnall, T. W.; Lin, T.; Gabbai, F. P., *J. Fluorine Chem.* **2010**, *131*, 1182-1186.
51. Kim, H.; Burghart, A.; Welch, M. B.; Reibenspies, J.; Burgess, K., *Chem. Commun.* **1999**, 1889-1890.
52. Crawford, S. M., Dipyrrins, Pyrrolyldipyrrins, Prodigiosenes and Their Complexes. Ph.D. Thesis, Dalhousie University, September 2011.
53. Lundrigan, T.; Crawford, S. M.; Cameron, T. S.; Thompson, A., *Chem. Commun.* **2012**, *48*, 1003-1005.
54. Housecroft, C. E.; Sharpe, A. G., *Inorganic Chemistry*, Pearson Education Limited, Essex, 2001.
55. Ulrich, G.; Ziessel, R.; Harriman, A., *Angew. Chem., Int. Ed.* **2008**, *47*, 1184-1201.
56. Goze, C.; Ulrich, G.; Mallon, L. J.; Allen, B. D.; Harriman, A.; Ziessel, R., *J. Am. Chem. Soc.* **2006**, *128*, 10231-10239.
57. Ulrich, G.; Goze, C.; Goeb, S.; Retailleau, P.; Ziessel, R., *New J. Chem.* **2006**, *30*, 982-986.
58. Li, L.; Nguyen, B.; Burgess, K., *Bioorg. Med. Chem. Lett.* **2008**, *18*, 3112-3116.
59. Bula, M. J.; Hartman, J. S.; Raman, C. V., *Can. J. Chem.* **1975**, *53*, 326-331.
60. Gillespie, R. J.; Hartman, J. S.; Parekh, M., *Can. J. Chem.* **1968**, *46*, 1601-1610.
61. Cornet, S. M.; Dillon, K. B.; Entwistle, C. D.; Fox, M. A.; Goeta, A. E.; Goodwin, H. P.; Marder, T. B.; Thompson, A. L., *Dalton Trans.* **2003**, 4395-4405.
62. Fieldhouse, S. A.; Peat, I. R., *J. Phys. Chem.* **1969**, *73*, 275.
63. Smith, W. L., *J. Chem. Educ.* **1977**, *54*, 469-473.
64. Lerrick, R. I.; Winstanley, T. P. L.; Haggerty, K.; Wills, C.; Clegg, W.; Harrington, R. W.; Bultinck, P.; Herrebout, W.; Bennistona, A. C.; Hall, M. J., *Chem. Commun.* **2014**, *50*, 4714-4716.
65. Beer, G.; Niederal, C.; Grimme, S.; Daub, J., *Angew. Chem. Int. Ed.* **2000**, *39*, 3252-3255.
66. Zinna, F.; Bruhn, T.; Guido, C. A.; Ahrens, J.; Broring, M.; Di Bari, L.; Pescitelli, G., *Chem. Eur. J.* **2016**, *22*, 16089-16098.

67. Sanchez-Carnerero, E. M.; Moreno, F.; Maroto, B. L.; Agarrabeita, A. R.; Ortiz, M. J.; Vo, B. G.; Muller, G.; de la Moya, S., *J. Am. Chem. Soc.* **2014**, *136*, 3346-3349.
68. Ma, X.; Azeem, E. A.; Liu, X.; Cheng, Y.; Zhu, C., *J. Mater. Chem. C* **2014**, *2*, 1076-1084.
69. Haefele, A.; Zedde, C.; Retailleau, P.; Ulrich, G.; Ziessel, R., *Org. Lett.* **2010**, *12*, 1672-1675.
70. Kolemen, S.; Cakmak, Y.; Kostereli, Z.; Akkaya, E. U., *Org. Lett.* **2014**, *16*, 660-663.
71. Berova, N.; Di Bari, L.; Pescitelli, G., *Chem. Soc. Rev.* **2007**, *36*, 914-931.
72. Somani, P. R., *Chromic Materials, Phenomena and Their Technological Applications*. Applied Science Innovations Private Limited: 2010.
73. López Arbeloa, F.; Bañuelos, J.; Martínez, V.; Arbeola, T.; López Arbeloa, I., *Int. Rev. Phys. Chem.* **2005**, *24*, 339.
74. Lundrigan, T.; Thompson, A., *J. Org. Chem.* **2013**, *78*, 757-761.
75. Smithen, D. A.; Baker, A. E. G.; Offman, M.; Crawford, S. M.; Cameron, T. S.; Thompson, A., *J. Org. Chem.* **2012**, *77*, 3439-3453.
76. Lundrigan, T.; Cameron, T. S.; Thompson, A., *Chem. Commun.* **2014**, *50*, 7028-7031.
77. Chen, H.; Shen, L.; Lin, Y., *Synthetic Commun.* **2010**, *40*, 998-1003.
78. Falcone, R. D.; Baruah, B.; Gaidamauska, E.; Rithner, C. D.; Correa, N. M.; Silber, J. J.; Crans, D. C.; Levinger, N. E., *Chem. Eur. J.* **2011**, *17*, 6837-6846.
79. Wang, N.-N.; Zhang, Q.-G.; Wu, F.-G.; Li, Q.-Z.; Yu, Z.-W., *J. Phys. Chem. B* **2010**, *114*, 8689-8700.
80. Castro, A. J.; Gale, G. R.; Means, G. E.; Tertzakian, G., *J. Med. Chem.* **1967**, *10*, 29-32.
81. Tu, B.; Wang, C.; Ma, J., *Organic Preparations and Procedures International: The New Journal for Organic Synthesis* **1999**, *31*, 349-352.
82. Gabe, Y.; Urano, Y.; Kikuchi, K.; Kojima, H.; Nagano, T., *J. Am. Chem. Soc.* **2004**, *126*, 3357-3367.
83. Rohand, T.; Dolusic, E.; Ngo, T. H.; Maes, W.; Dehaen, W., *ARKIVOC* **2007**, 307-324.
84. Rurack, K., Fluorescence Quantum Yields: Methods of Determination and Standards. In *Standardization and Quality Assurance in Fluorescence Measurements I*, Resch-Genger, U., Ed. Springer Berlin Heidelberg: 2008; Vol. 5, pp 101-145.
85. Williams, A. T. R.; Winfield, S. A.; Miller, J. N., *Analyst* **1983**, *108*, 1067-1071.
86. Benniston, A. C.; Clift, S.; Harriman, A., *J. Mol. Sci.* **2011**, *985*, 346-354.

87. Sessler, J. L.; Eller, L. R.; Cho, W.-S.; Nicolaou, S.; Aguilar, A.; Lee, J. T.; Lynch, V. M.; Magda, D. J., *Angew. Chem., Int. Ed.* **2005**, *44*, 5989-5992.

Appendix A: X-ray Analysis Data

Appendix A.1 (*Z*)-2-((4-Ethyl-3,5-dimethyl-2*H*-pyrrol-2-ylidene)methyl)-3,5-dimethyl-1*H*-pyrrole tetrafluoroborate (**2HBF₄**)

A. Crystal Data for Compound **2HBF₄**

Empirical Formula	C ₁₅ H ₂₁ N ₂ F ₄ B
Formula Weight	316.15
Crystal Colour, Habit	dark red, block
Crystal Dimensions	0.33 X 0.25 X 0.22 mm
Crystal System	orthorhombic
Lattice Type	Primitive
Indexing Images	4 oscillations @ 300.0 seconds
Detector Position	127.40 mm
Pixel Size	0.100 mm
Lattice Parameters	a = 17.4172(8) Å b = 7.0912(4) Å c = 13.2491(8) Å V = 1636.38(15) Å ³
Space Group	Pnma (#62)
Z value	4
D _{calc}	1.283 g/cm ³
F ₀₀₀	664.00
μ(MoKα)	1.068 cm ⁻¹

B. Intensity Measurements for Compound 2HBF₄

Diffractionmeter	Rigaku RAXIS-UNKNOWN
Radiation	MoK α ($\lambda = 0.71070 \text{ \AA}$) graphite monochromated
Data Images	24 exposures
ω oscillation Range	75.0 - 195.0 $^\circ$
Exposure Rate	684.0 sec./ $^\circ$
Detector Position	127.40 mm
Pixel Size	0.100 mm
$2\theta_{\max}$	61.0 $^\circ$
No. of Reflections Measured	Total: 10434 Unique: 2620 ($R_{\text{int}} = 0.052$)
Corrections	Lorentz-polarization Absorption (trans. factors: 0.570 - 0.977) Secondary Extinction (coefficient: 1.39160e+002)

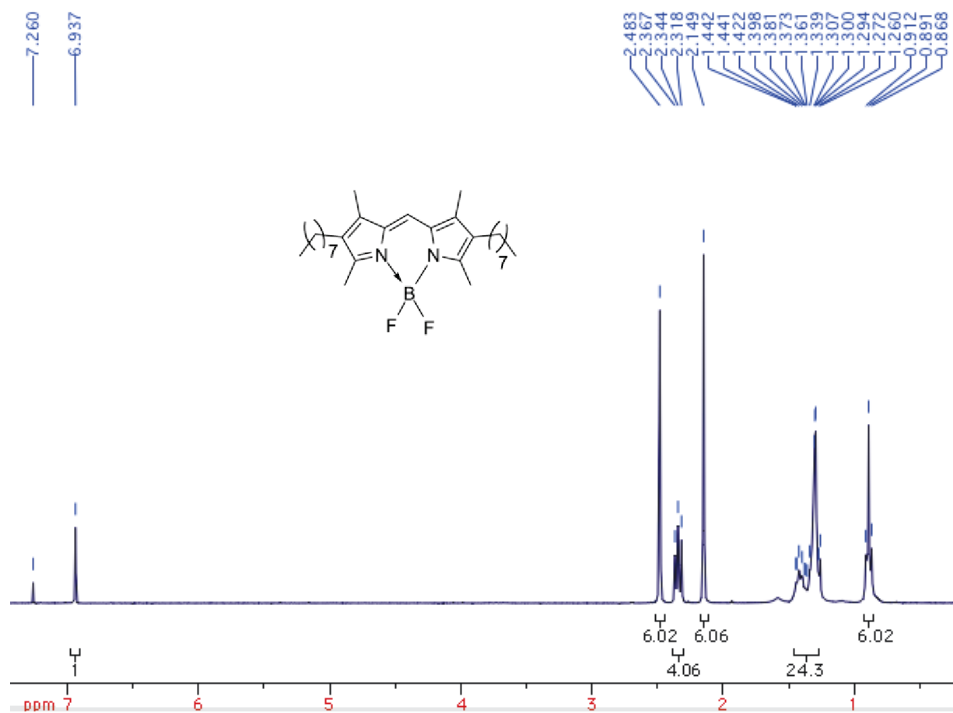
C. Structure Solution and Refinement for Compound 2HBF₄

Structure Solution	Direct Methods
Refinement	Full-matrix least-squares on F
Function Minimized	$\Sigma w (F_o - F_c)^2$
Least Squares Weights parameters	Chebyshev polynomial with 3 11.5416,-3.0509,8.4925,
$2\theta_{\max}$ cutoff	55.0°
Anomalous Dispersion	All non-hydrogen atoms
No. Observations ($I > 2.50\sigma(I)$)	1130
No. Variables	149
Reflection/Parameter Ratio	7.58
Residuals: R ($I > 2.50\sigma(I)$)	0.0595
Residuals: R _w ($I > 2.50\sigma(I)$)	0.0654
Goodness of Fit Indicator	1.179
Max Shift/Error in Final Cycle	0.000
Maximum peak in Final Diff. Map	0.17 e ⁻ /Å ³
Minimum peak in Final Diff. Map	-0.21 e ⁻ /Å ³

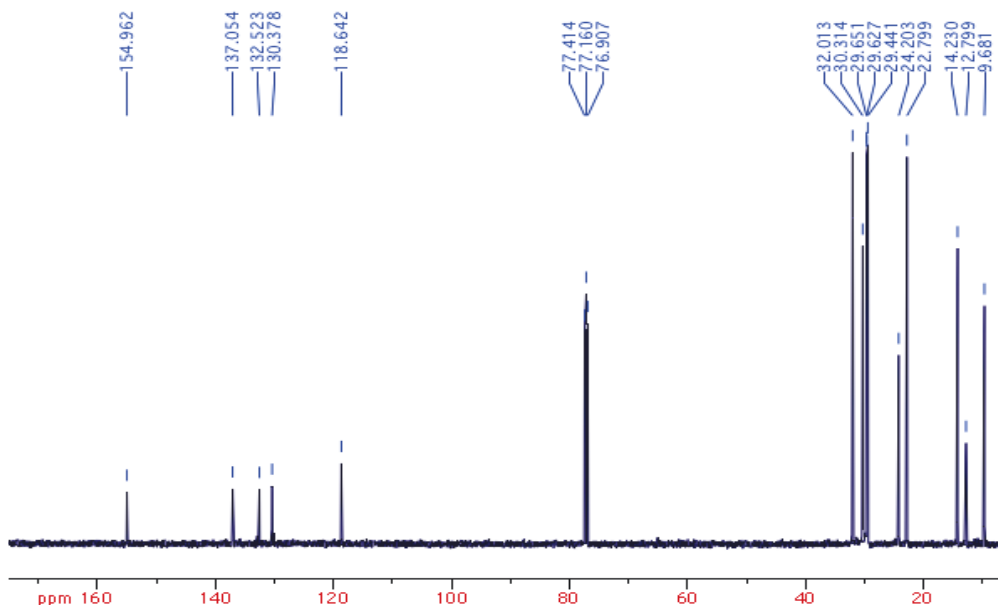
Appendix B: NMR Data for Synthesized Compounds

Appendix B.1 1,3,5,7-Tetramethyl-2-octyl-8-*H*-4,4'-difluoro-bora-3a,4a-diaza-*s*-indacene (**1BF₂**)

¹H NMR Spectrum in CDCl₃

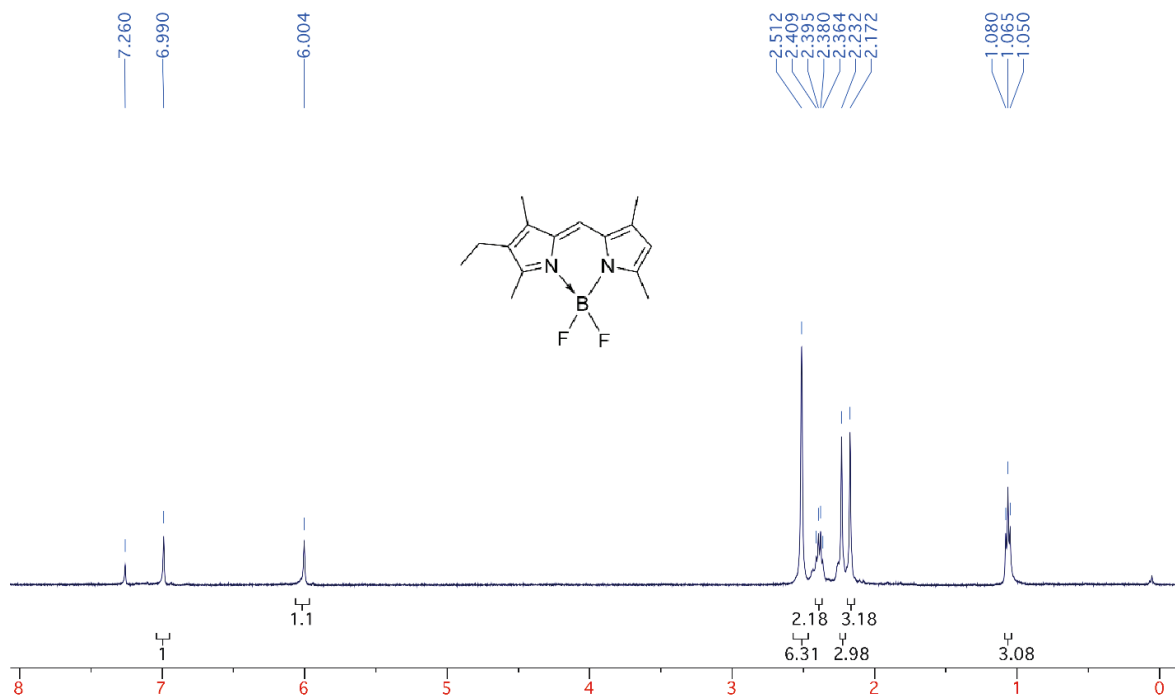


¹³C NMR Spectrum in CDCl₃

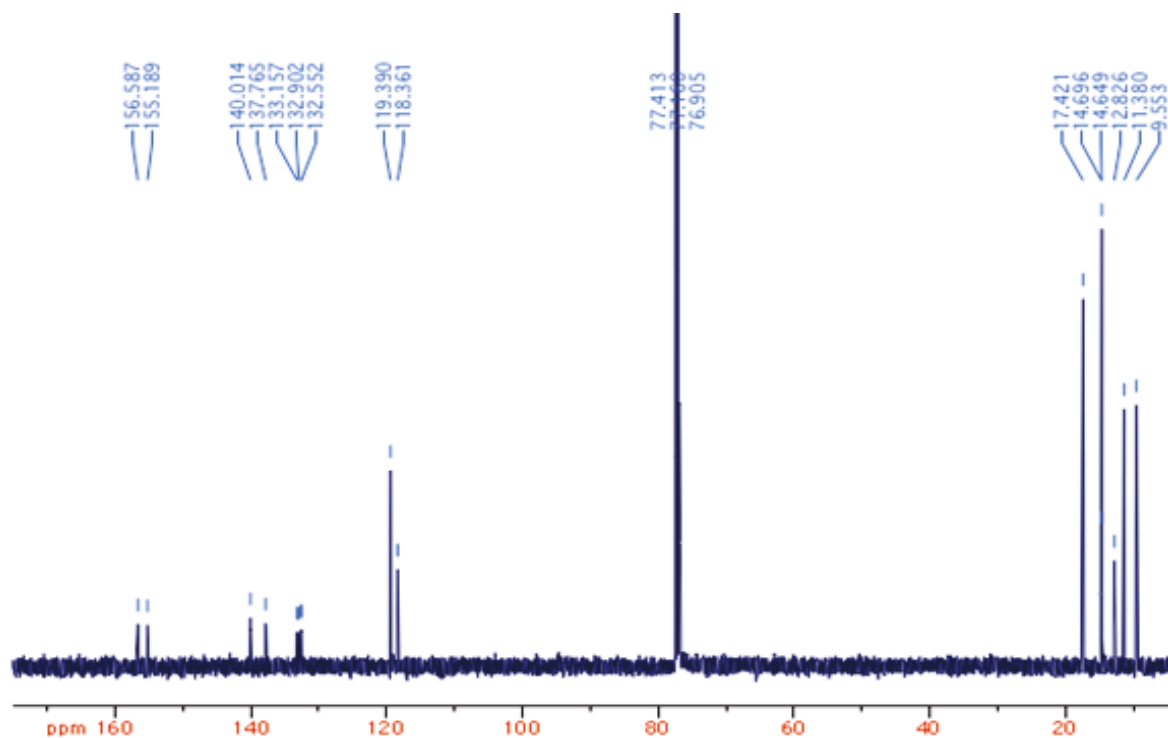


Appendix B.2 1,3,5,7-Tetramethyl-2-ethyl-8-*H*-4,4'-difluoro-bora-3a,4a-diaza-*s*-indacene (**2BF₂**)

¹H NMR Spectrum in CDCl₃

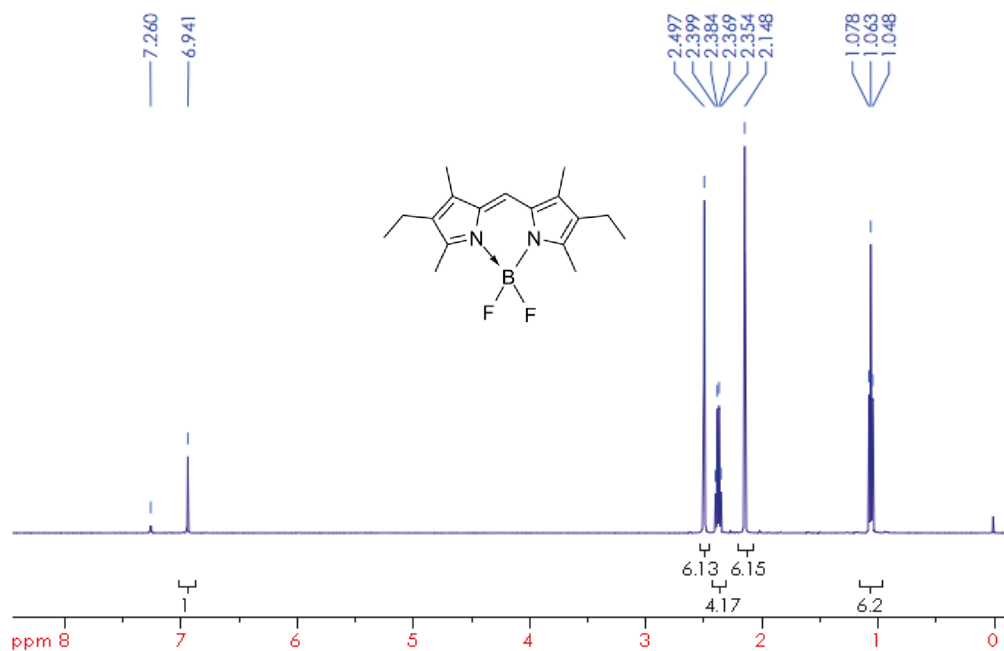


¹³C NMR Spectrum in CDCl₃

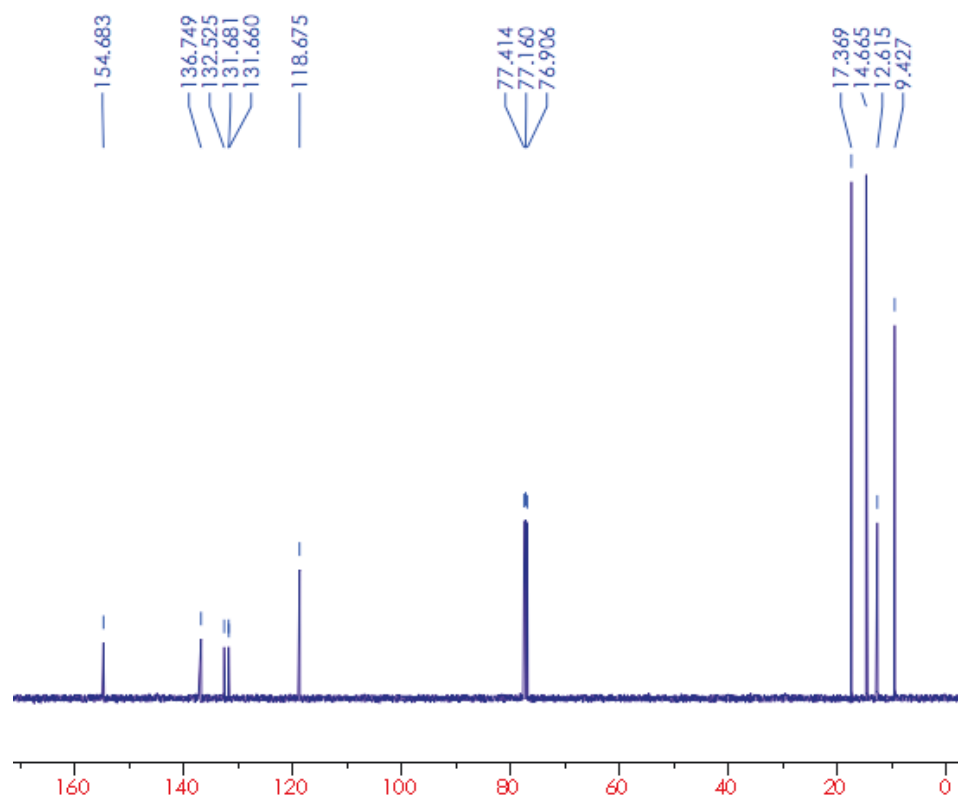


Appendix B.3 1,3,5,7-Tetramethyl-2,6-diethyl-8-*H*-4,4'-difluoro-bora-3a,4a-diaza-*s*-indacene (**3BF₂**)

¹H NMR Spectrum in CDCl₃

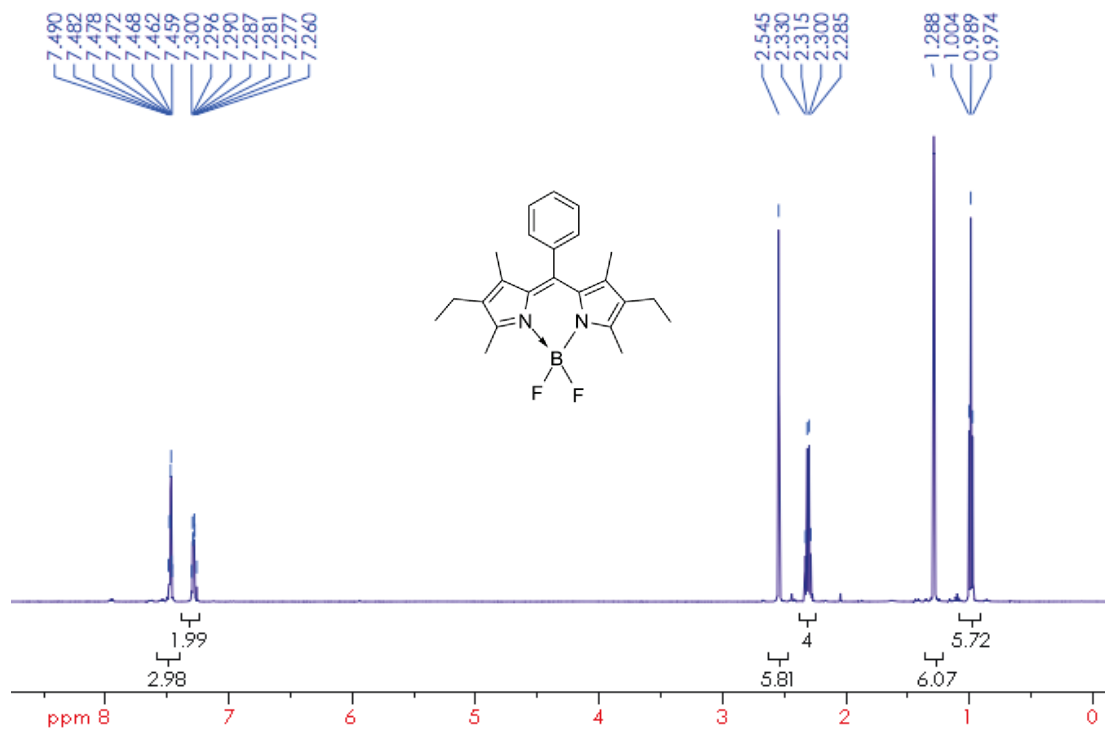


¹³C NMR Spectrum in CDCl₃

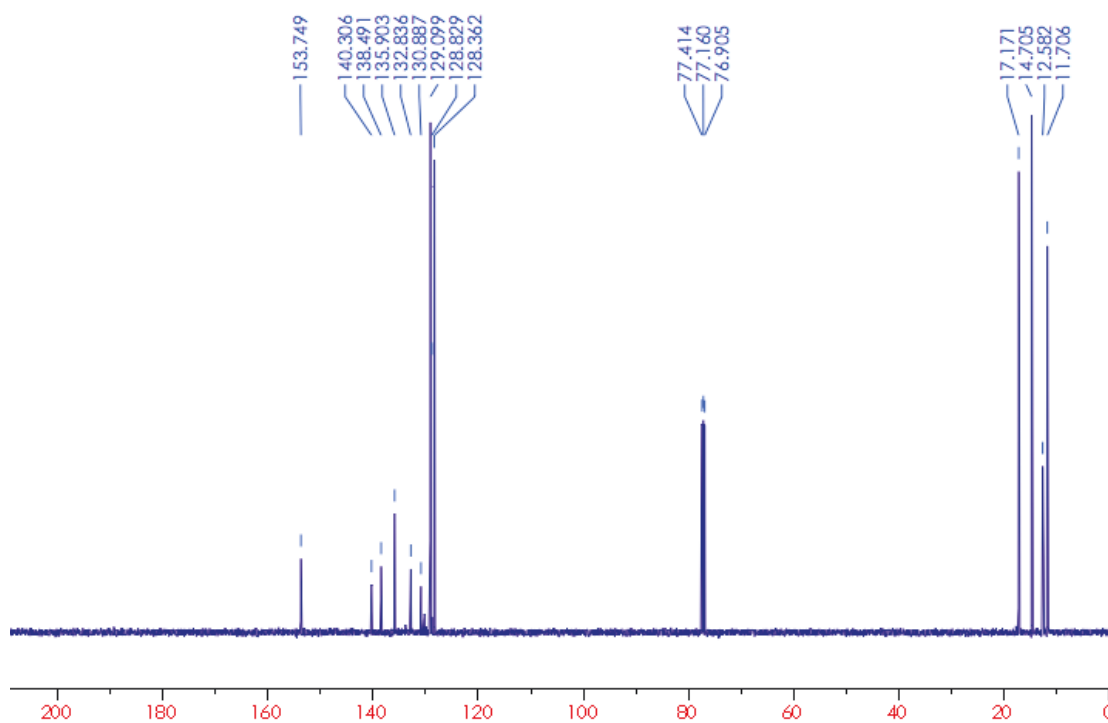


Appendix B.4 1,3,5,7-Tetramethyl-2,6-diethyl-8-phenyl-4,4'-difluoro-bora-3a,4a-diaza-s-indacene (**5BF₂**)

¹H NMR Spectrum in CDCl₃

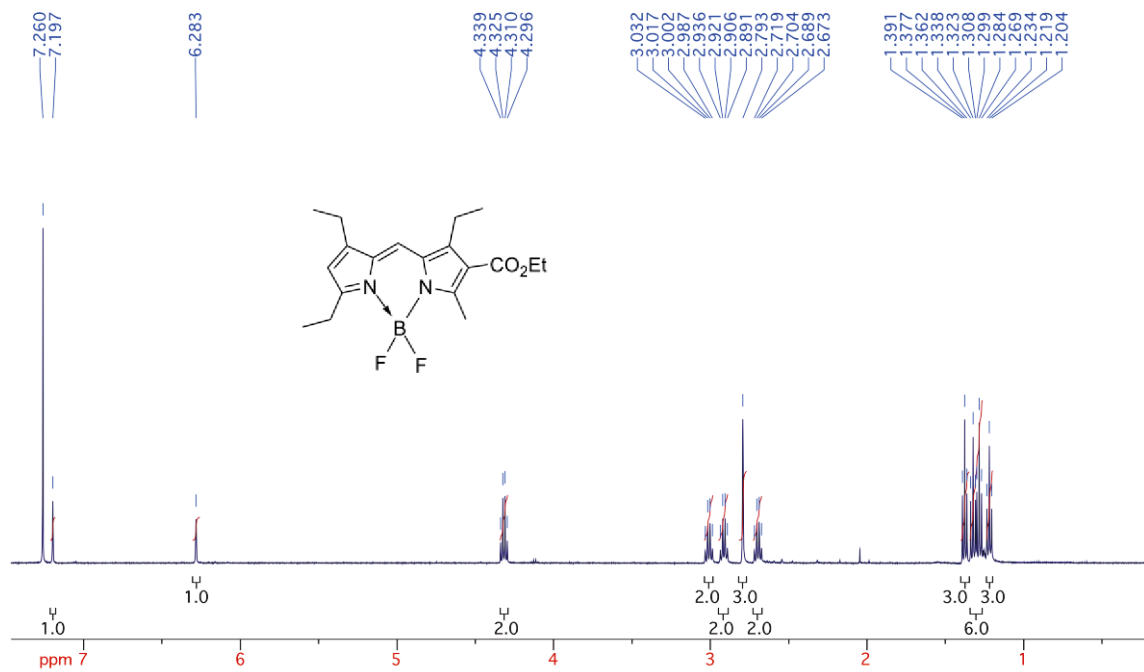


¹³C NMR Spectrum in CDCl₃

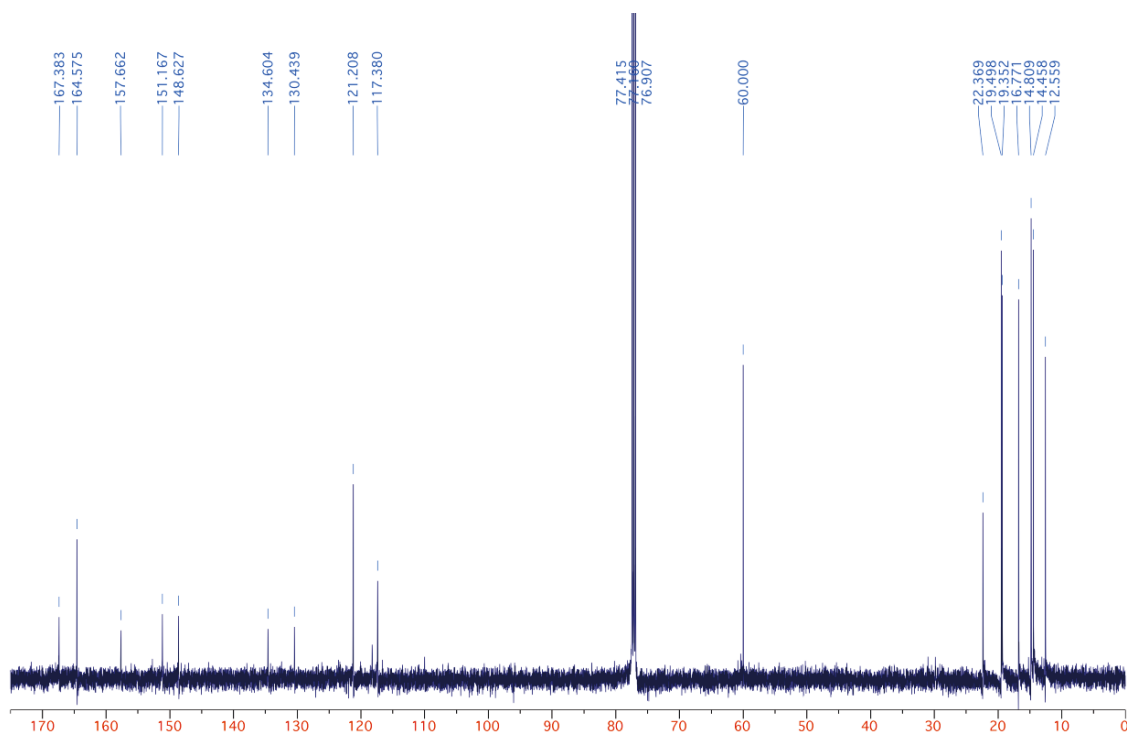


Appendix B.5 3-Methyl-1,5,7-triethyl-2-ethylcarboxylato-8-*H*-4,4'-difluoro-bora-3a,4a-diaza-*s*-indacene (**6BF₂**)

¹H NMR Spectrum in CDCl₃

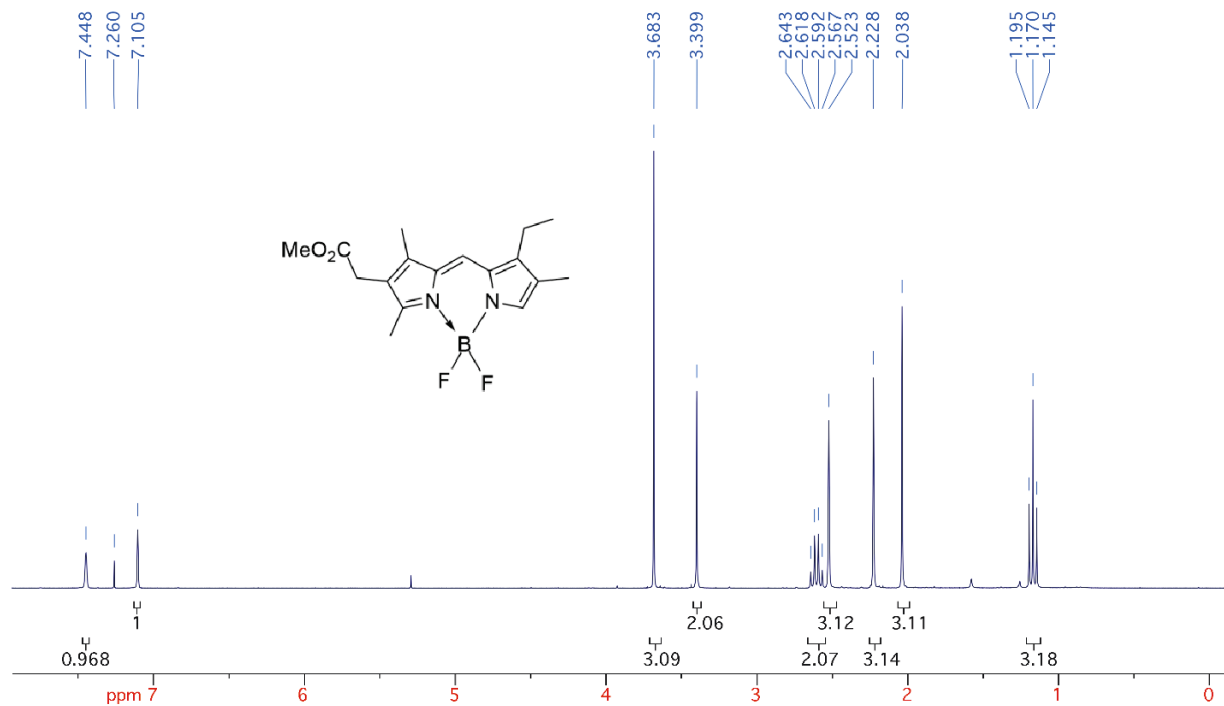


¹³C NMR Spectrum in CDCl₃

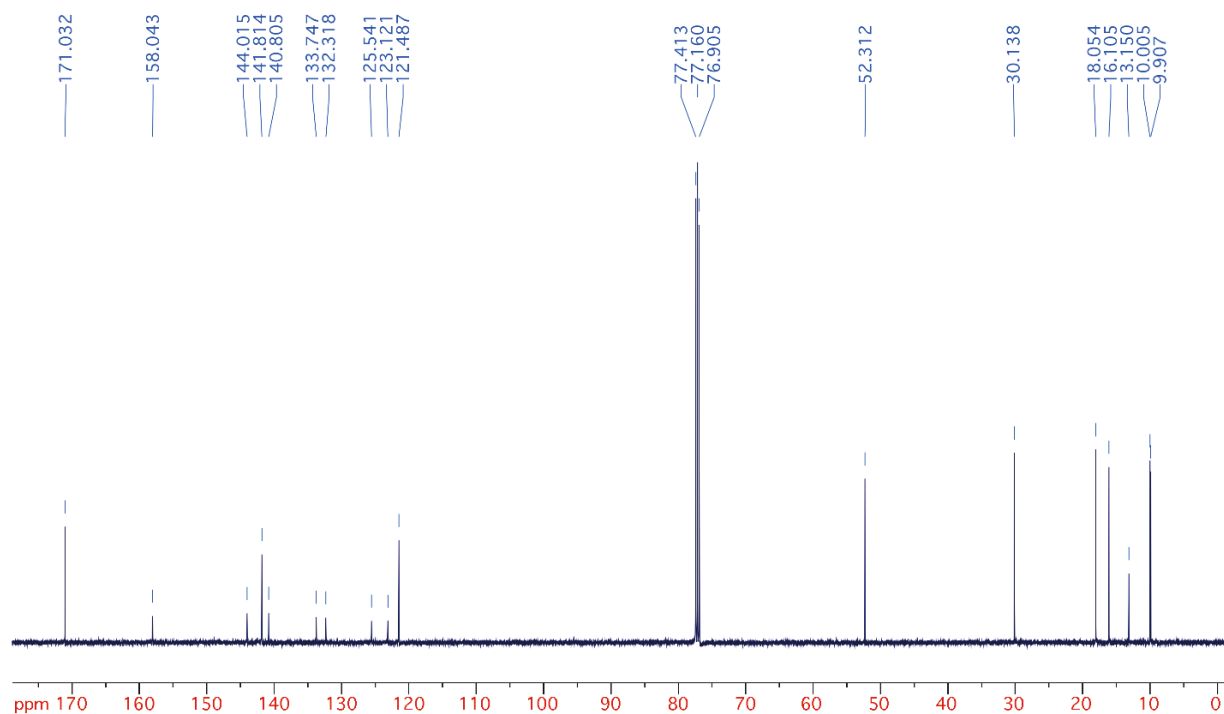


Appendix B.6 1,3,6-Trimethyl-7-ethyl-2-8-*H*-4,4'-difluoro-bora-3a,4a-diaza-*s*-indacene (7BF₂)

¹H NMR Spectrum in CDCl₃

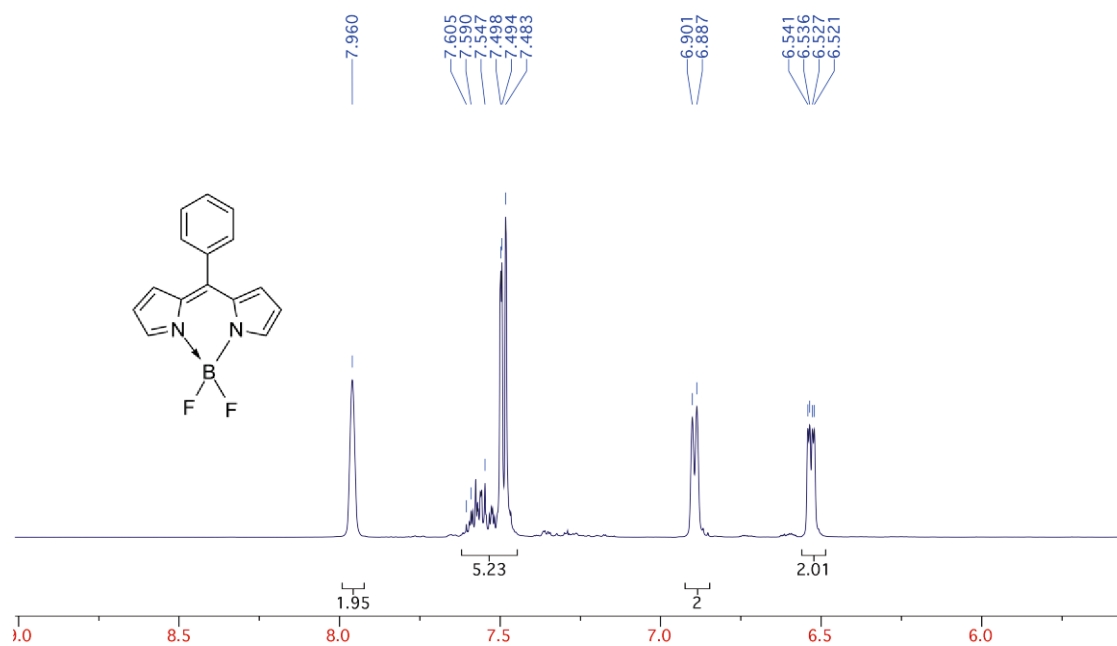


¹³C NMR Spectrum in CDCl₃

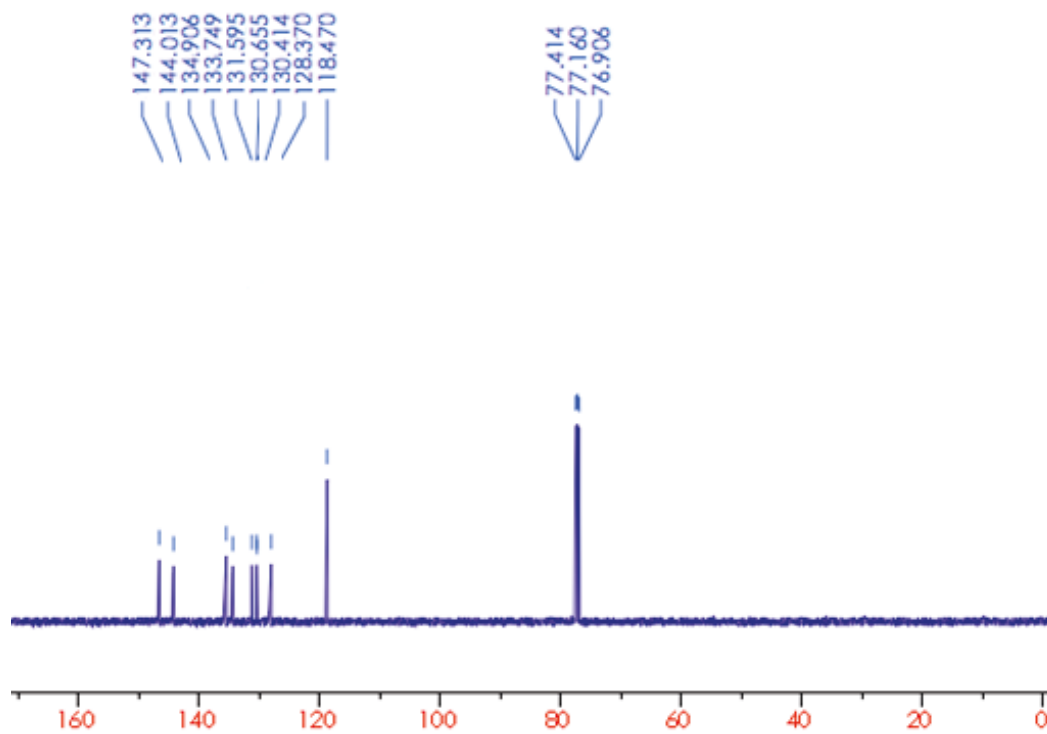


Appendix B.7 8-Phenyl-4,4'-difluoro-bora-3a,4a-diaza-s-indacene (**8BF₂**)

¹H NMR Spectrum in CDCl₃

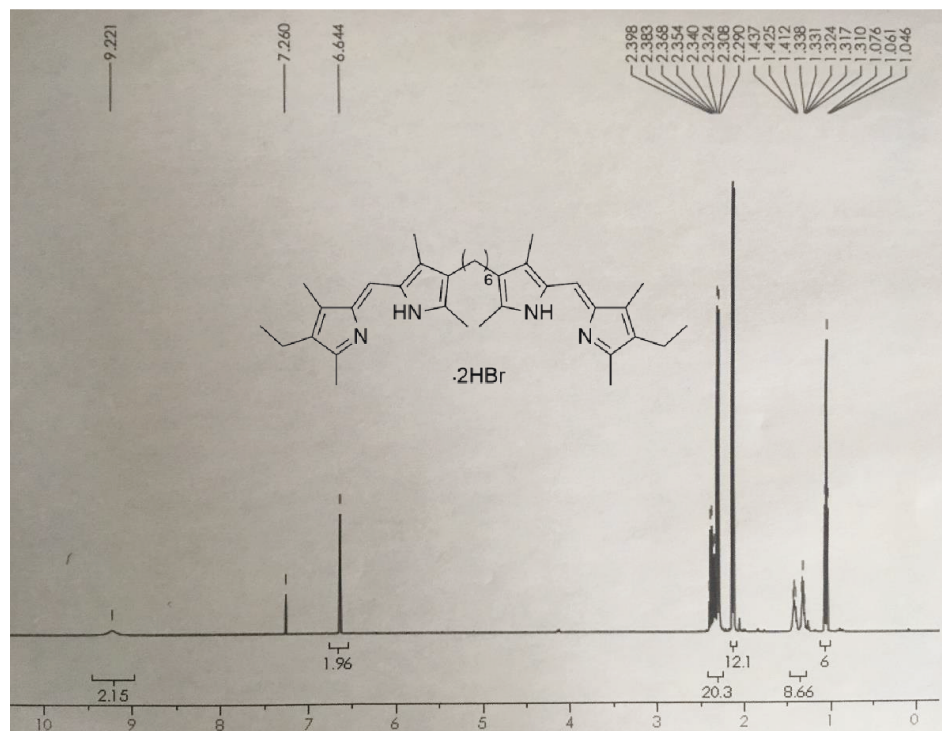


¹³C NMR Spectrum in CDCl₃

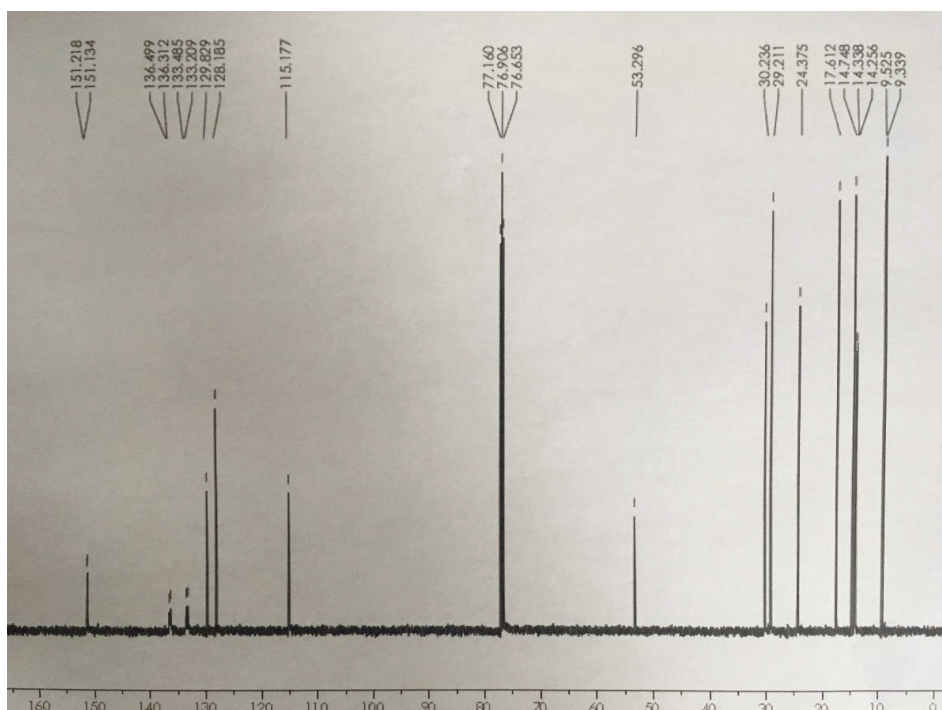


Appendix B.8 1,7-Bis(5-((*Z*)-(4-ethyl-3,5-dimethyl-2*H*-pyrrol-2-ylidene)methyl)-2,4-dimethyl-1*H*-pyrrol-3-yl)hexane dihydrobromide (**12**•2*HBr*)

¹H NMR Spectrum in CDCl₃

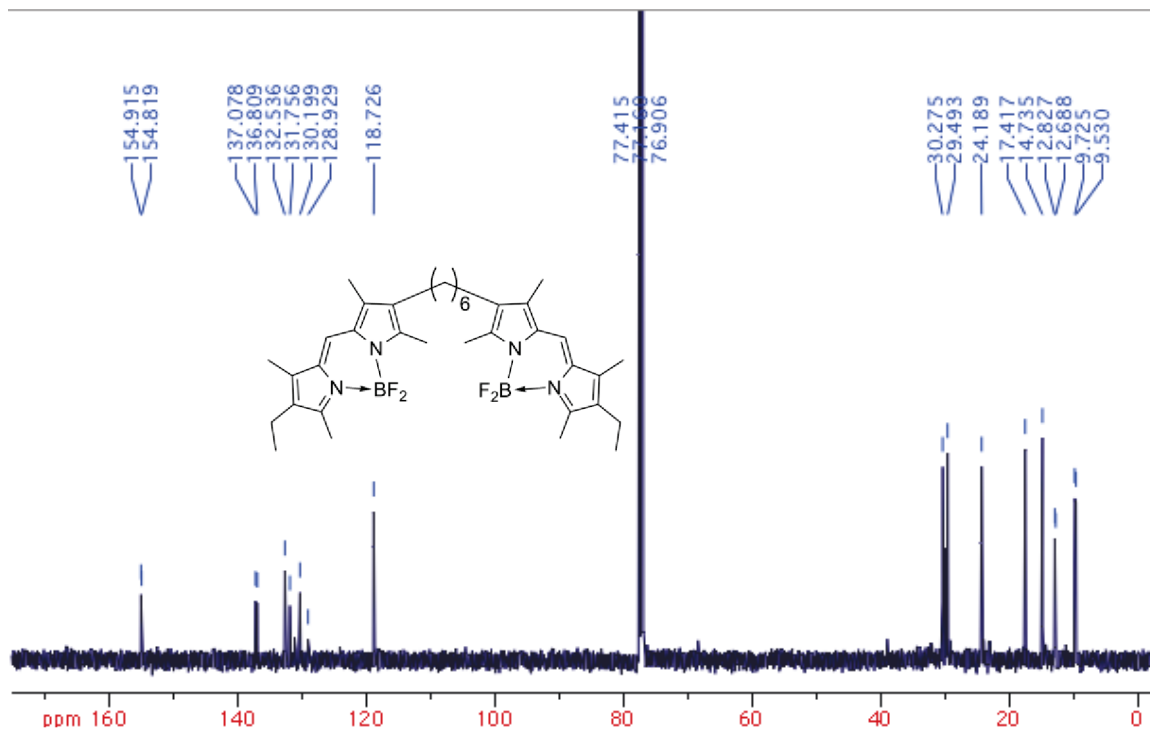


¹³C NMR Spectrum in CDCl₃



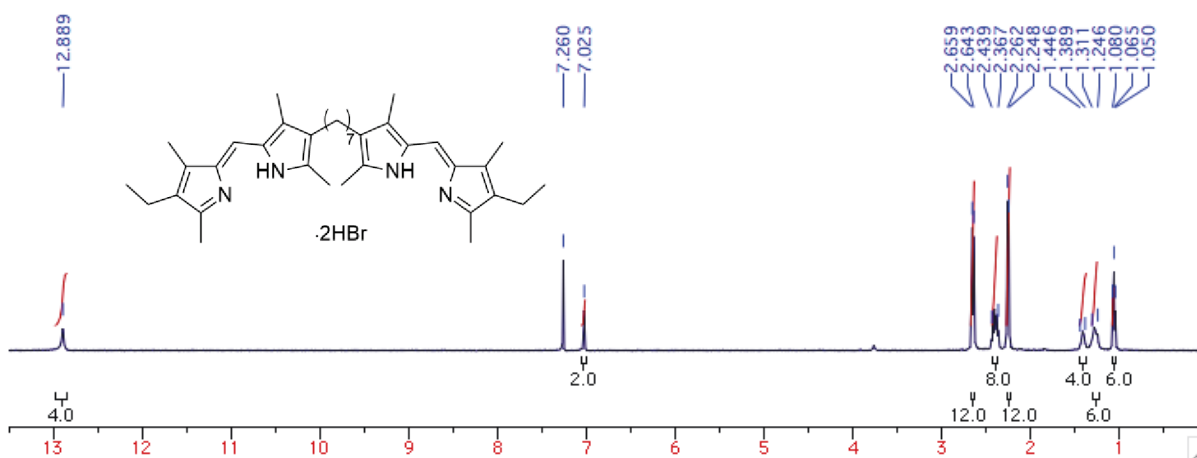
Appendix B.9 1,7-Bis(1,3,5,7-tetramethyl-2-ethyl-8-*H*-4,4'-difluoro-bora-3a,4a-diaza-*s*-indacene)hexane (**12BF₂**)

¹³C NMR Spectrum in CDCl₃

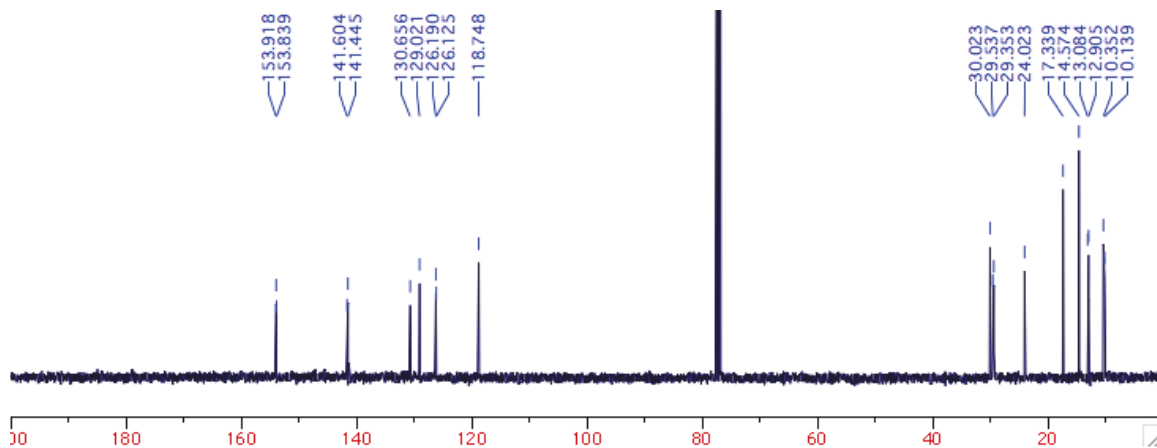


Appendix B.10 1,7-Bis(5-((*Z*)-(4-ethyl-3,5-dimethyl-2*H*-pyrrol-2-ylidene)methyl)-2,4-dimethyl-1*H*-pyrrol-3-yl)heptane dihydrobromide (**15•2HBr**)

¹H NMR Spectrum in CDCl₃

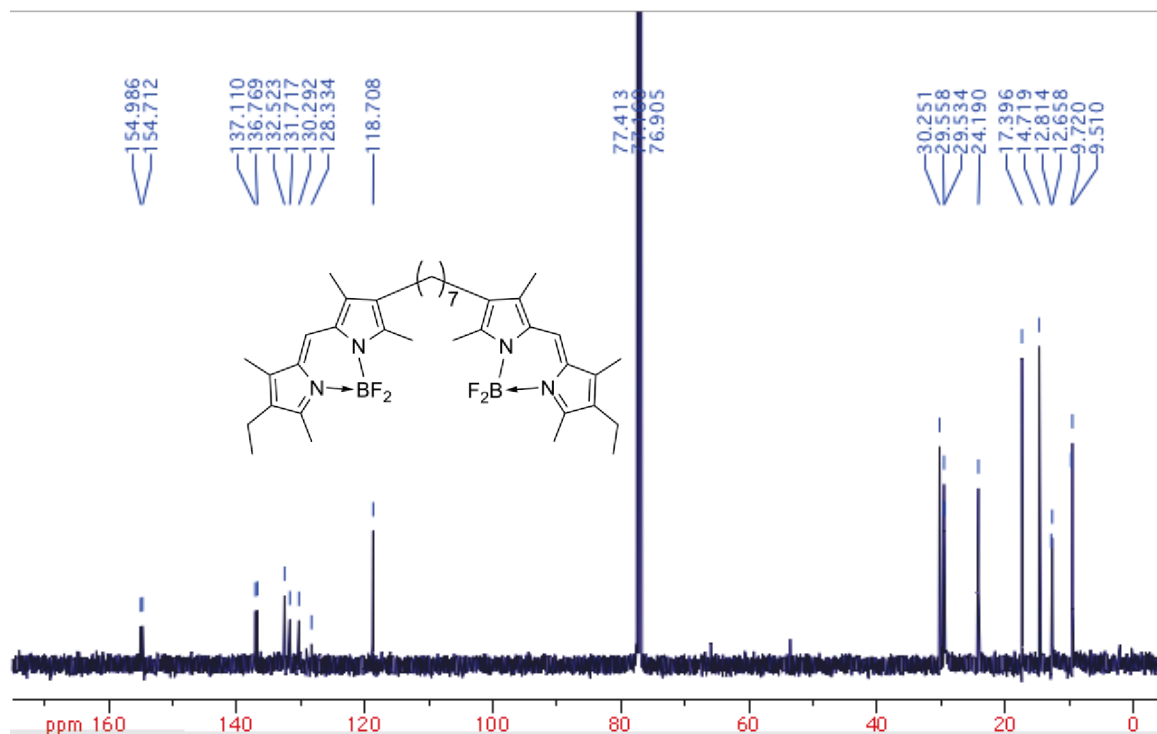


¹³C NMR Spectrum in CDCl₃



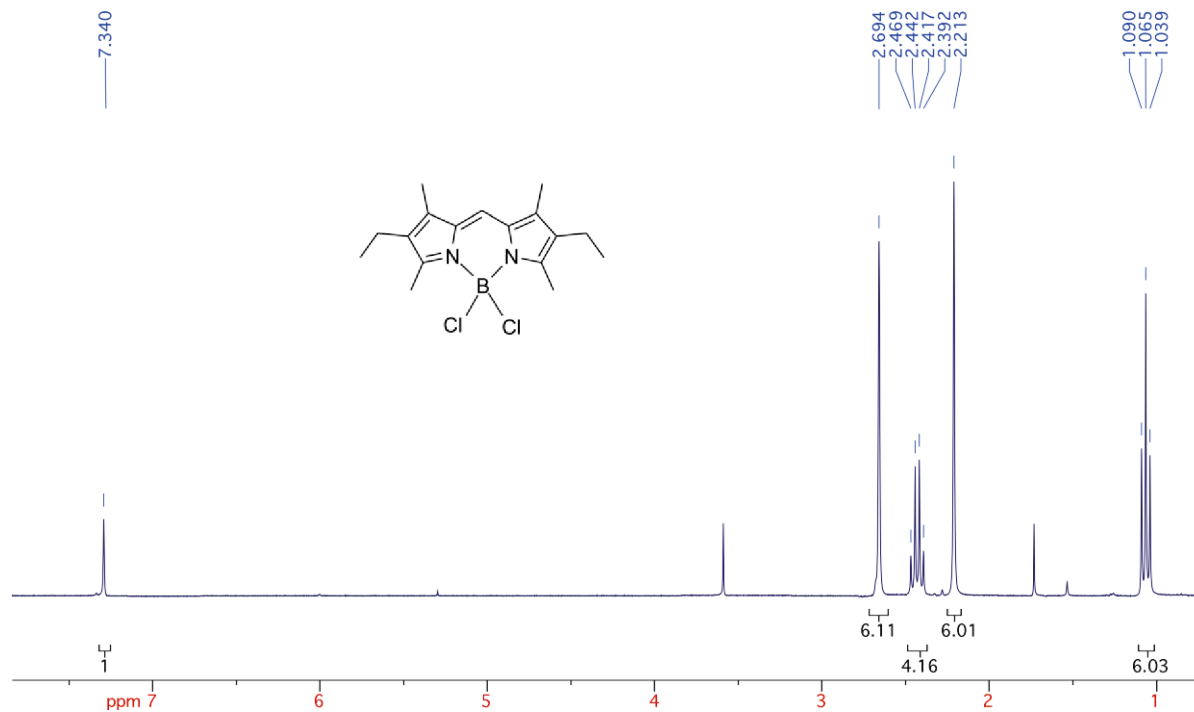
Appendix B.11 1,7-Bis(1,3,5,7-tetramethyl-2-ethyl-8-*H*-4,4'-difluoro-bora-3a,4a-diaza-*s*-indacene)heptane (**15BF₂**)

¹³C NMR Spectrum in CDCl₃

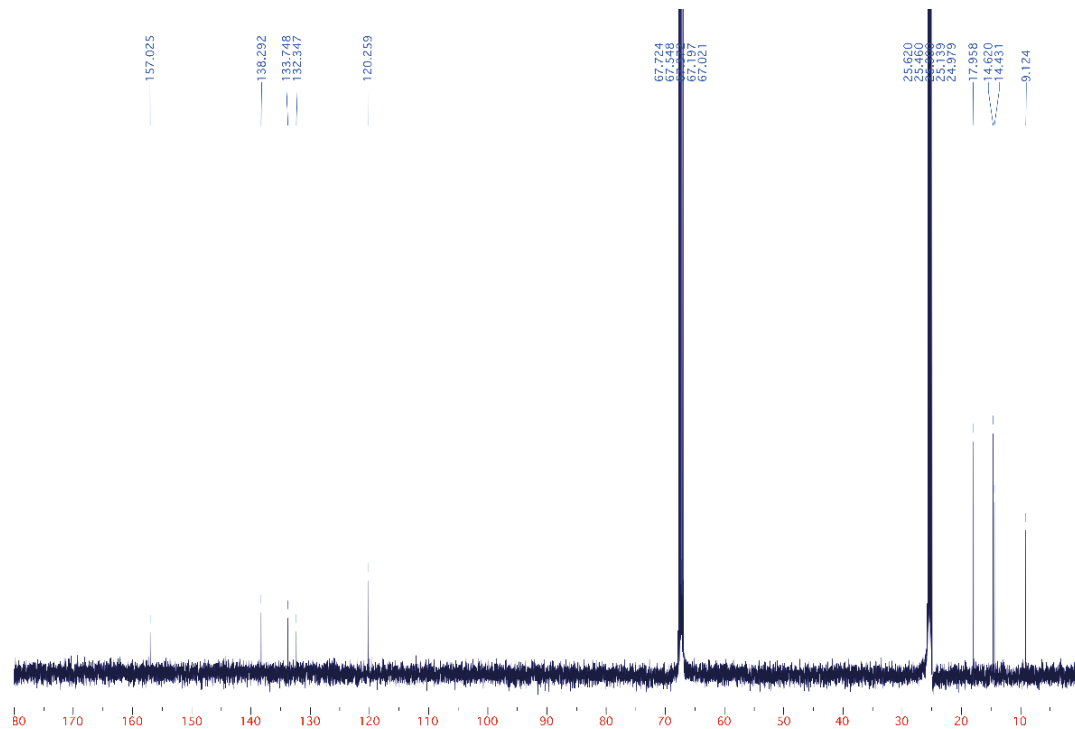


Appendix B.12 1,3,5,7-Tetramethyl-2,6-diethyl-8-phenyl-4,4'-dichloro-bora-3a,4a-diaza-*s*-indacene (**3BCl₂**)

¹H NMR Spectrum in THF-d₈

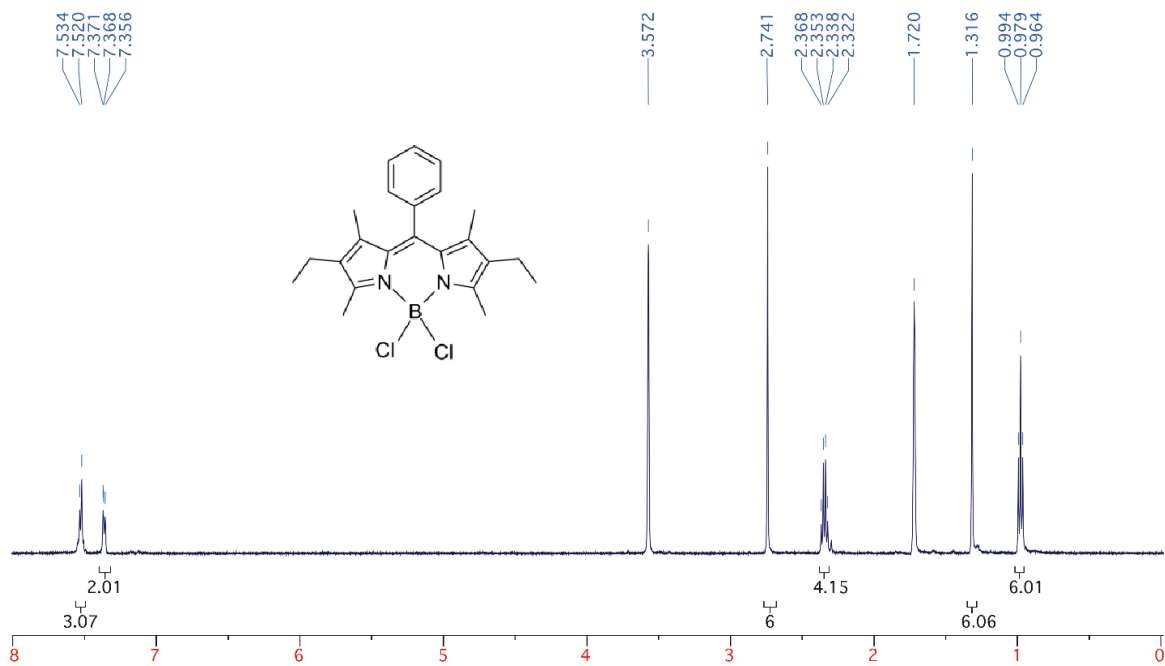


¹³C NMR Spectrum in CDCl₃

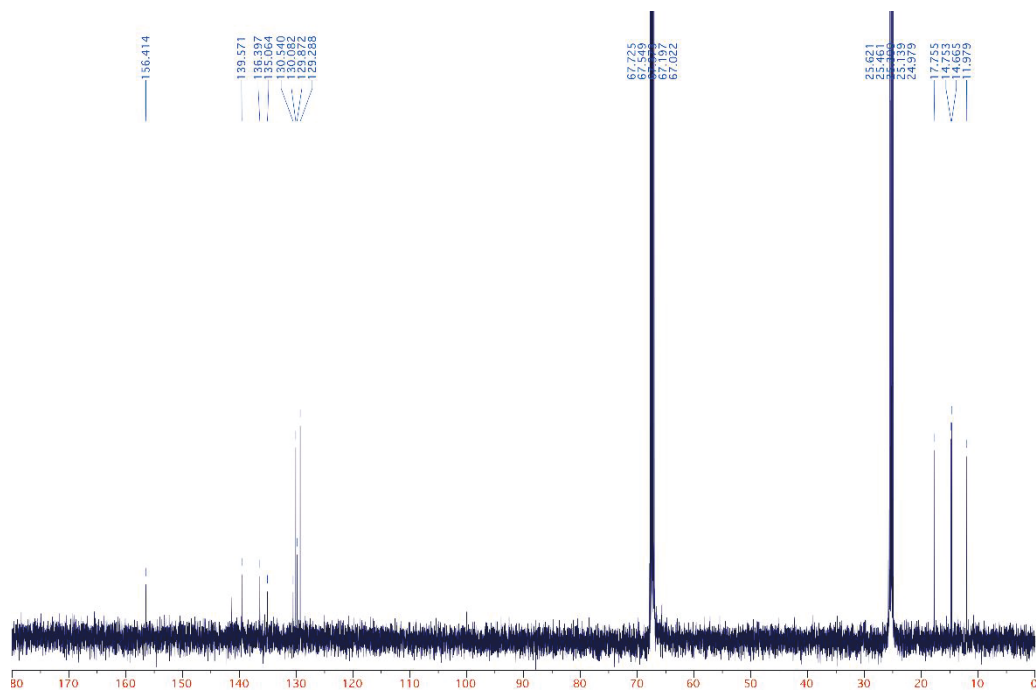


Appendix B.13 1,3,5,7-Tetramethyl-2,6-diethyl-8-phenyl-4,4'-dichloro-bora-3a,4a-diaza-*s*-indacene (**5BCl₂**)

¹H NMR Spectrum in THF-d₈

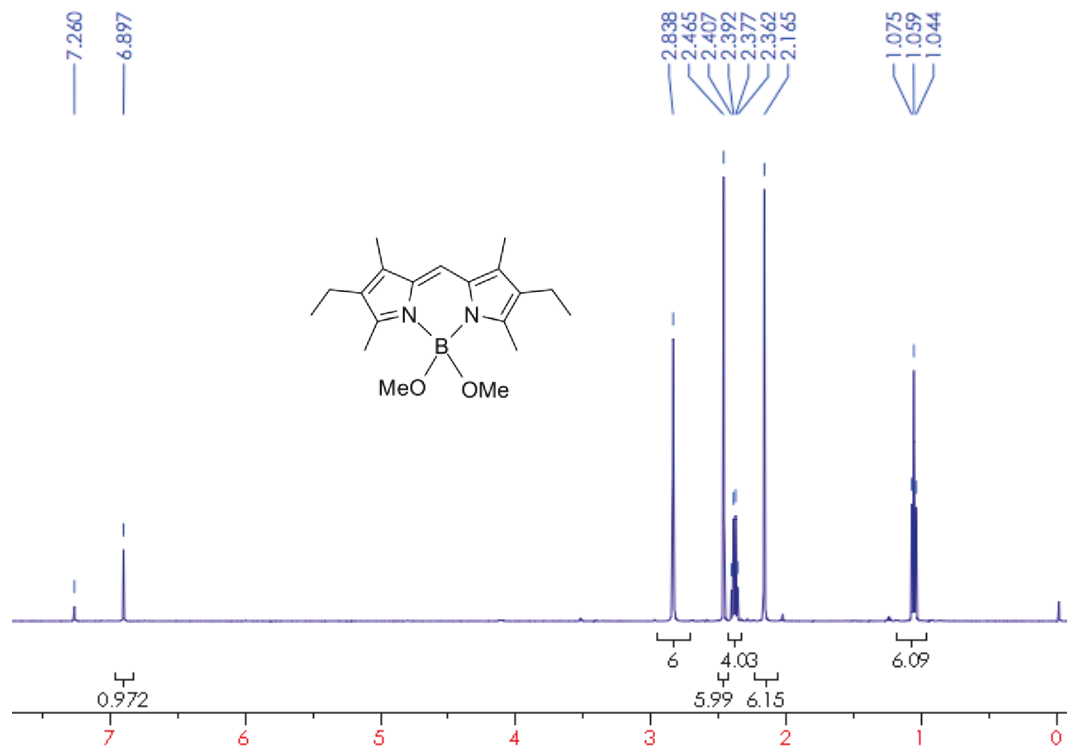


¹³C NMR Spectrum in THF-d₈

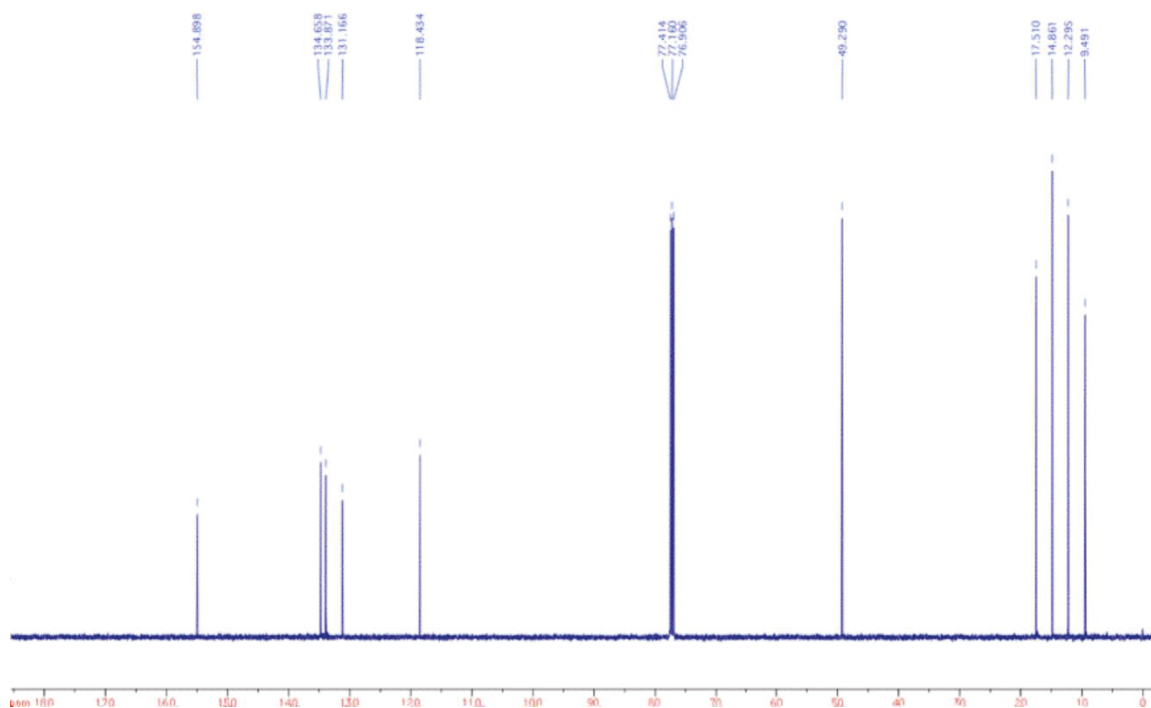


Appendix B.14 1,3,5,7-Tetramethyl-2,6-diethyl-8-*H*-4,4'-dimethoxy-bora-3a,4a-diaza-*s*-indacene (**3B(OMe)₂**)

¹H NMR Spectrum in CDCl₃

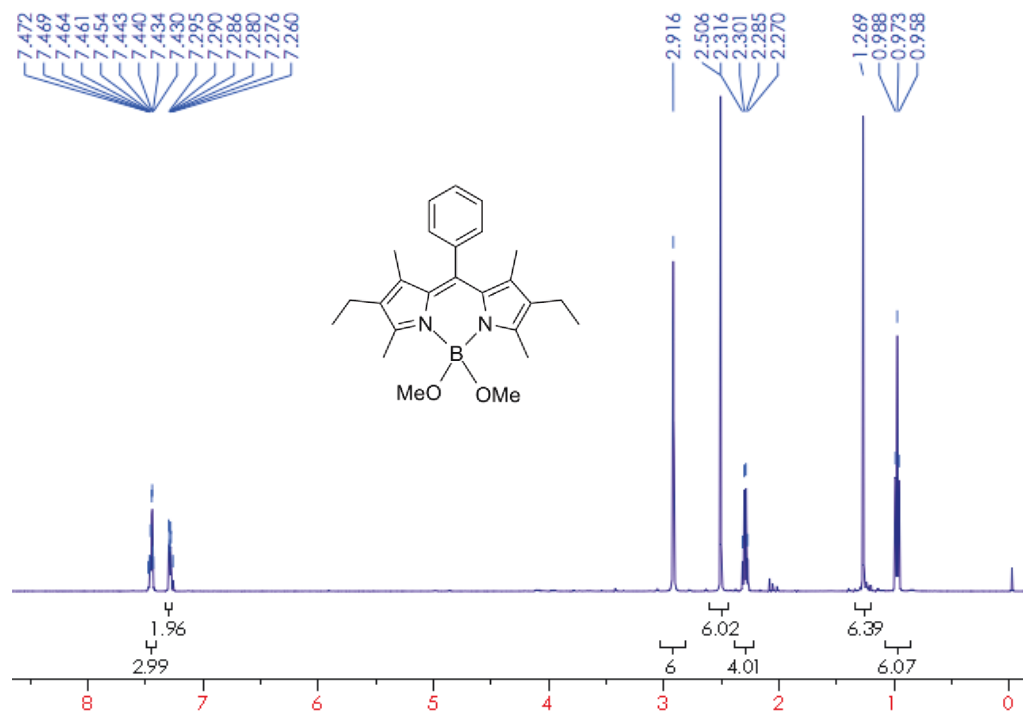


¹³C NMR Spectrum in CDCl₃

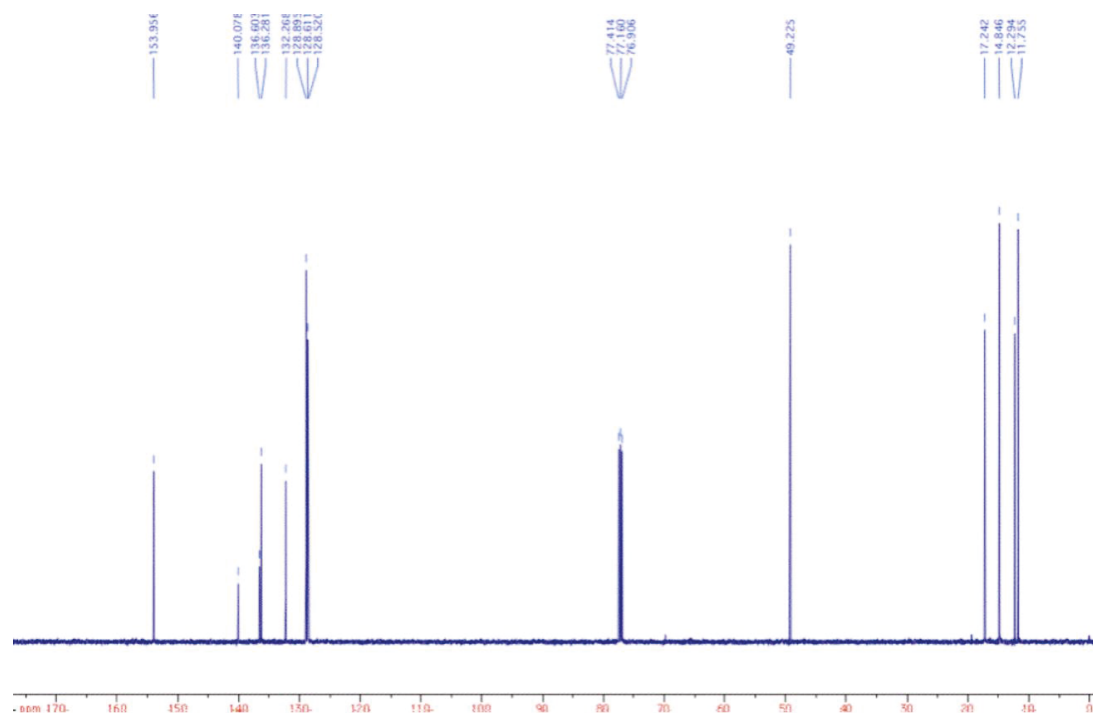


Appendix B.15 1,3,5,7-Tetramethyl-2,6-diethyl-8-phenyl-4,4'-dimethoxy-bora-3a,4a-diaza-*s*-indacene (**5B(OMe)₂**)

¹H NMR Spectrum in CDCl₃

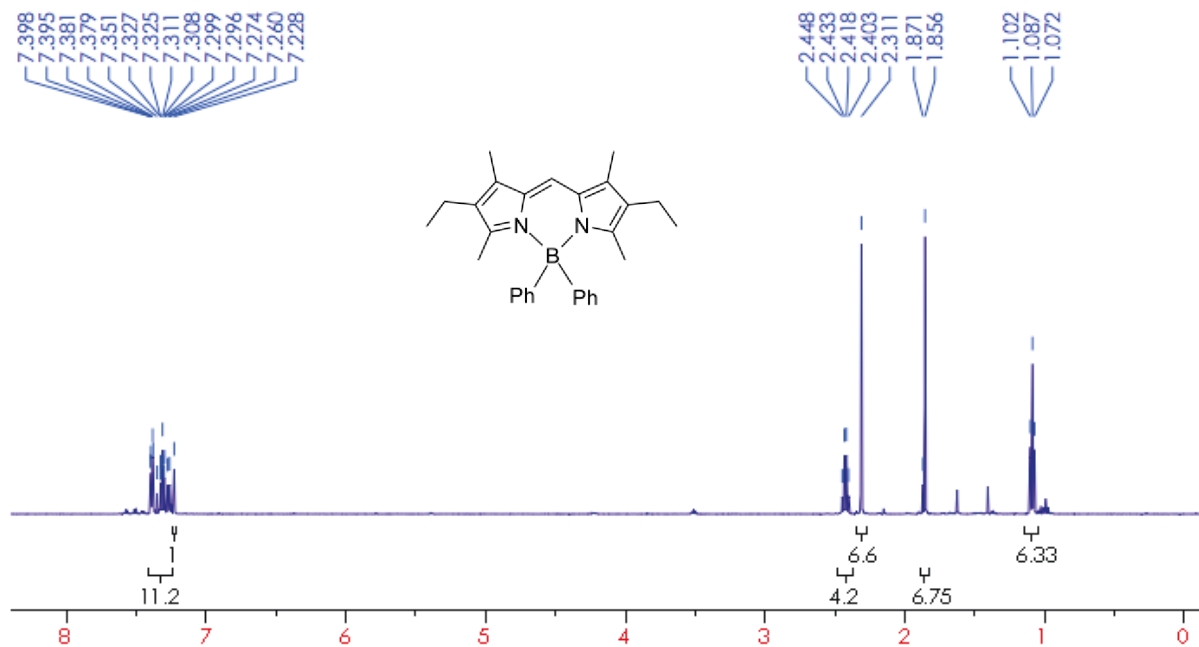


¹³C NMR Spectrum in CDCl₃

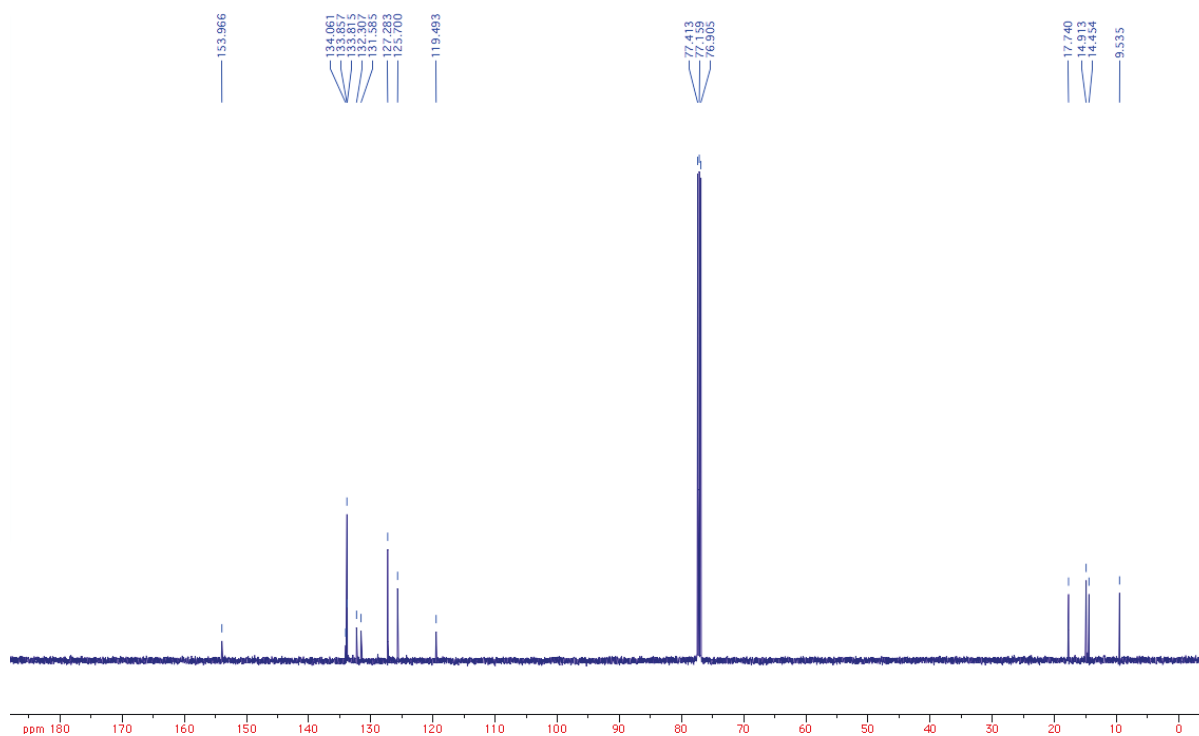


Appendix B.16 1,3,5,7-Tetramethyl-2,6-diethyl-8-*H*-4,4'-diphenyl-bora-3a,4a-diaza-*s*-indacene (**3BPh₂**)

¹H NMR Spectrum in CDCl₃

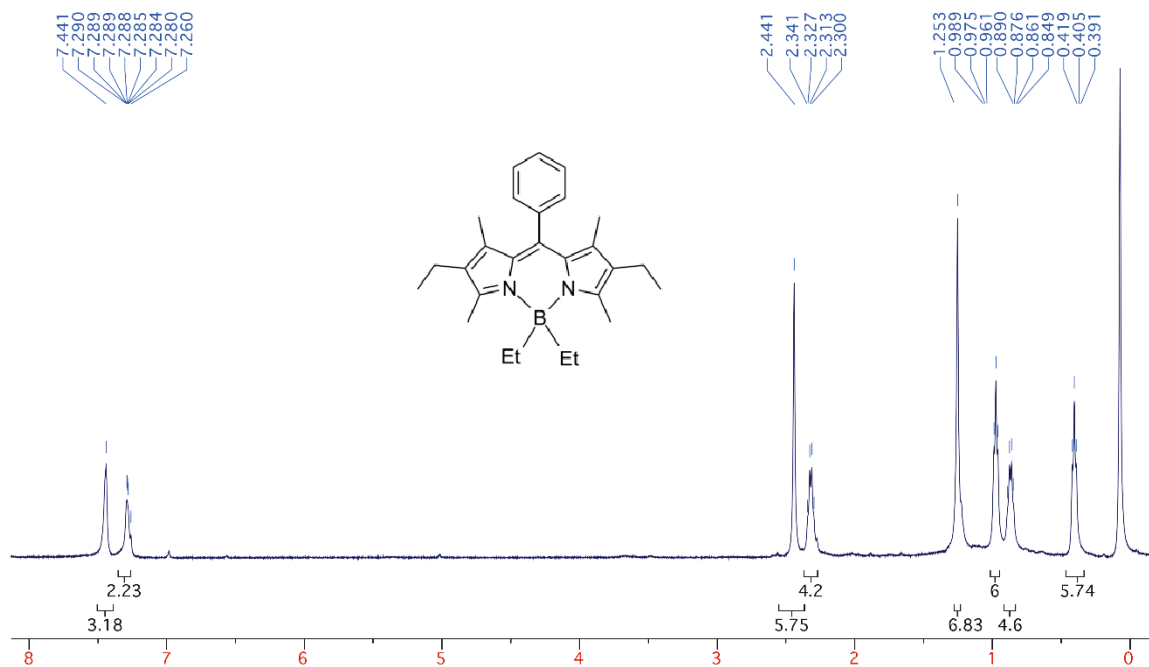


¹³C NMR Spectrum in CDCl₃

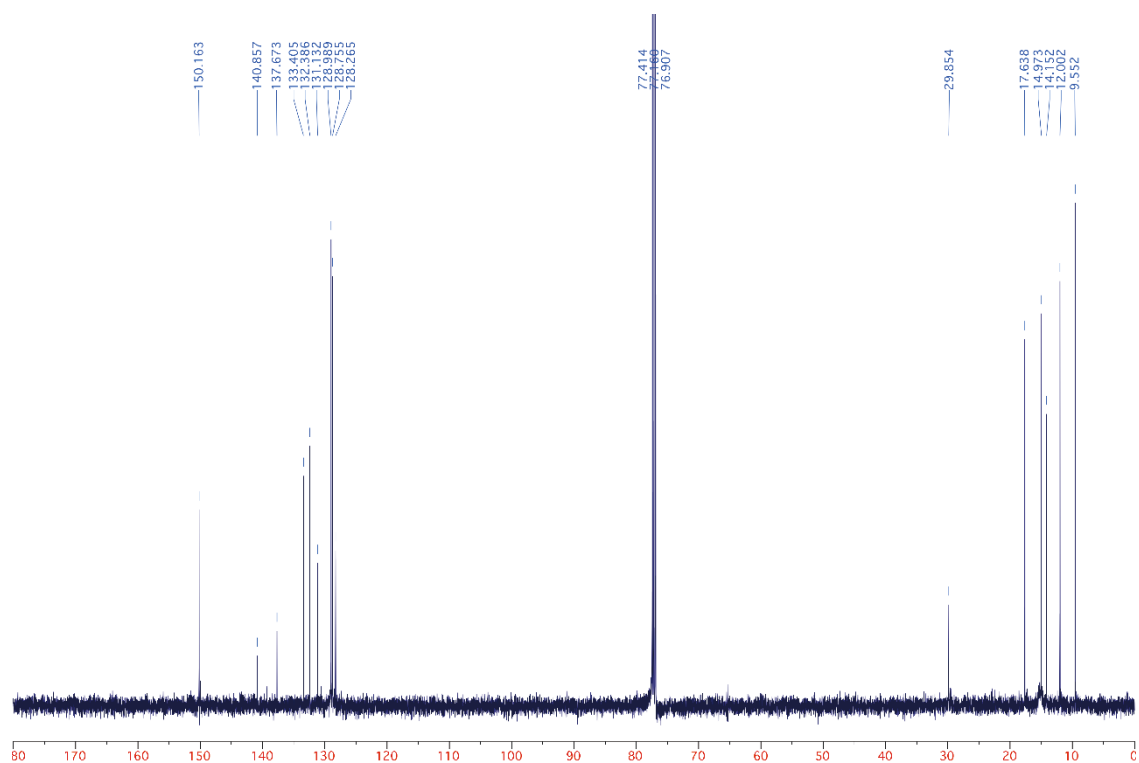


Appendix B.18 1,3,5,7-Tetramethyl-2,6-diethyl-8-phenyl-4,4'-diethyl-bora-3a,4a-diaza-*s*-indacene (**5BEt₂**)

¹H NMR Spectrum in CDCl₃

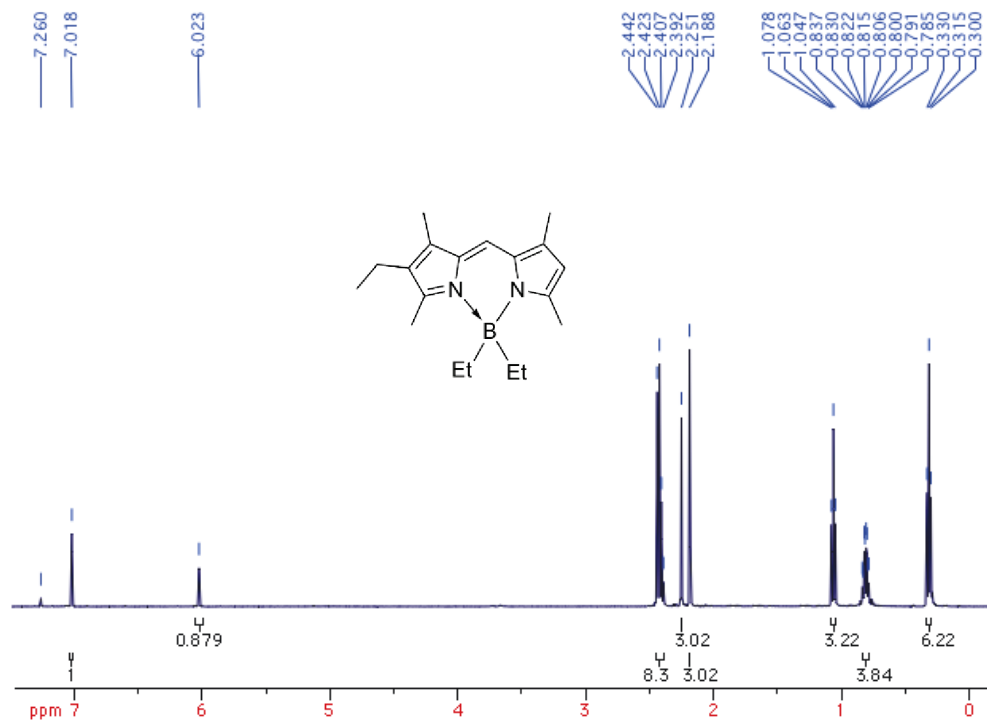


¹³C NMR Spectrum in CDCl₃

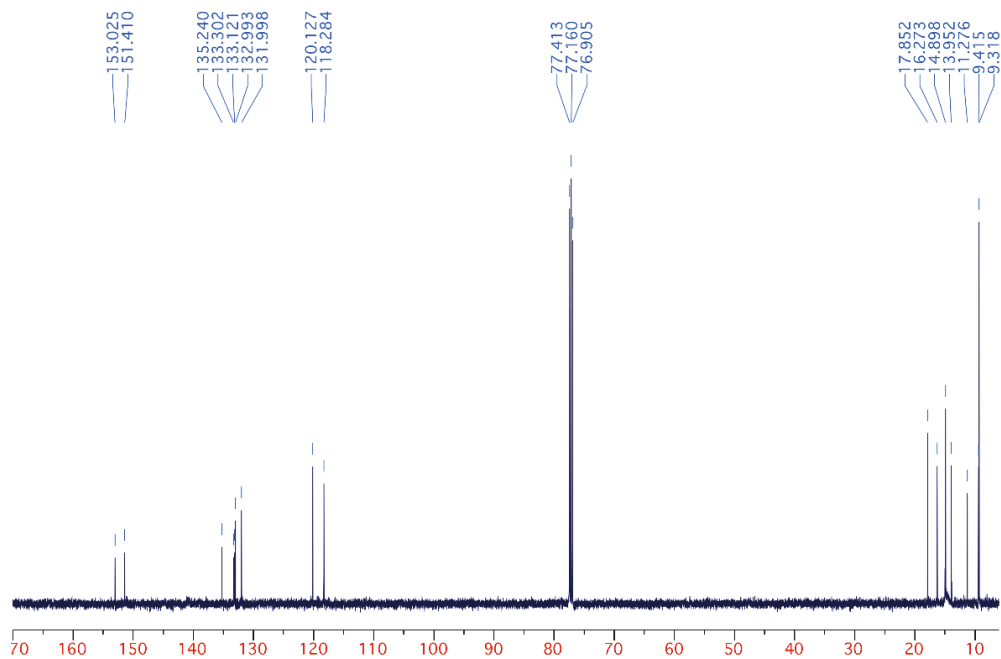


Appendix B.19 1,3,5,7-Tetramethyl-2-ethyl-8-*H*-4,4'-diethyl-bora-3a,4a-diaza-*s*-indacene (**2BEt₂**)

¹H NMR Spectrum in CDCl₃

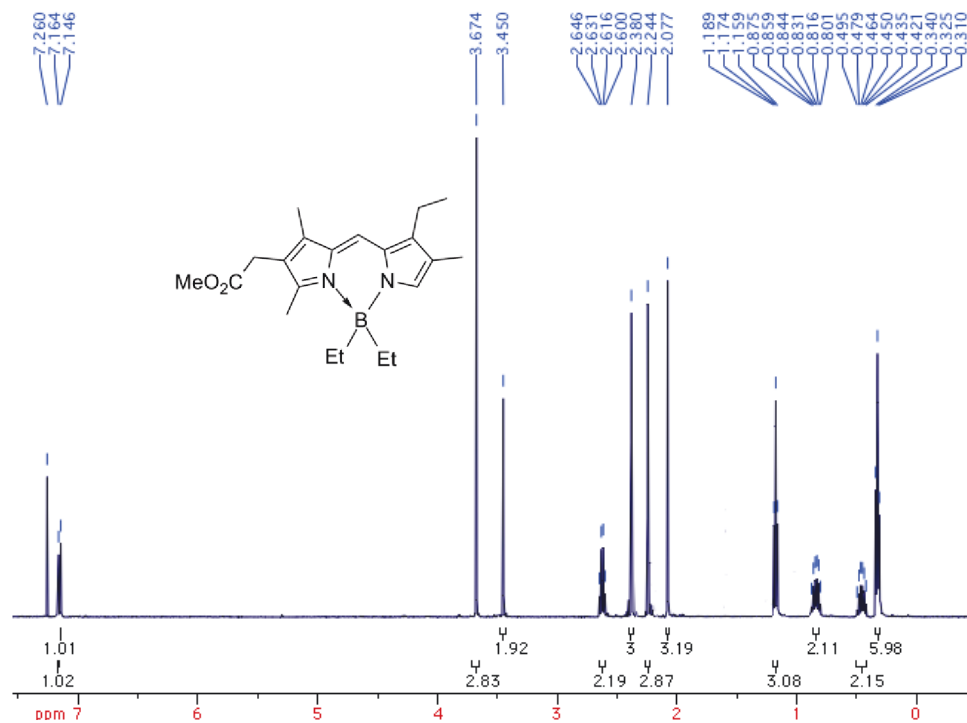


¹³C NMR Spectrum in CDCl₃

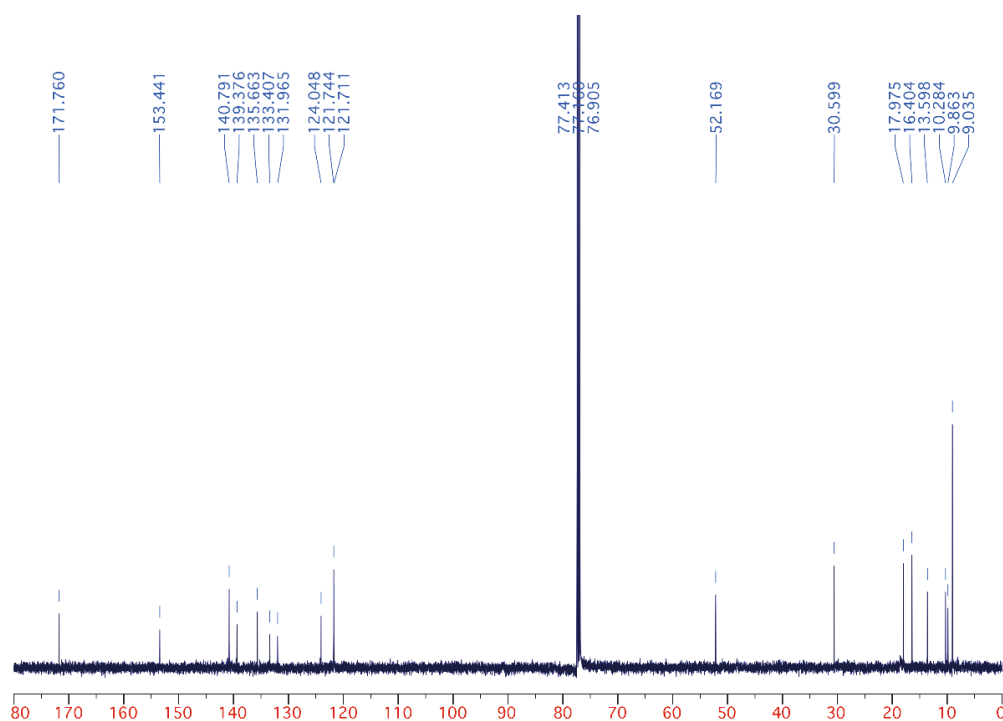


Appendix B.20 1,3,6-Trimethyl-2-(2-methoxy-2-oxoethyl)-7-ethyl-8-*H*-4,4'-diethylbora-3a,4a-diaza-*s*-indacene (**7BEt₂**)

¹H NMR Spectrum in CDCl₃

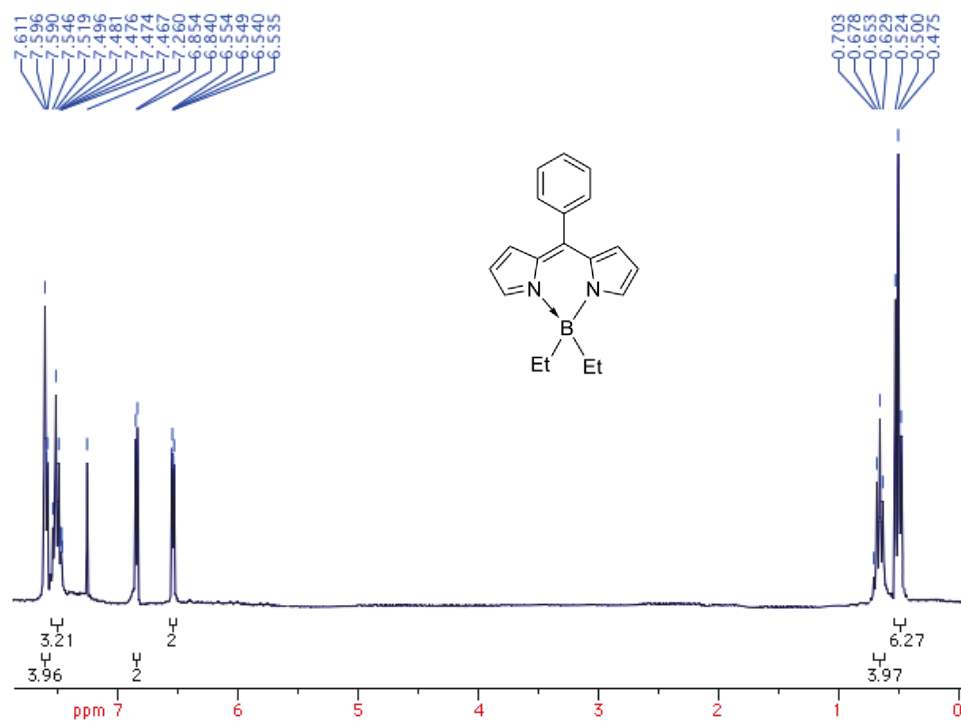


¹³C NMR Spectrum in CDCl₃

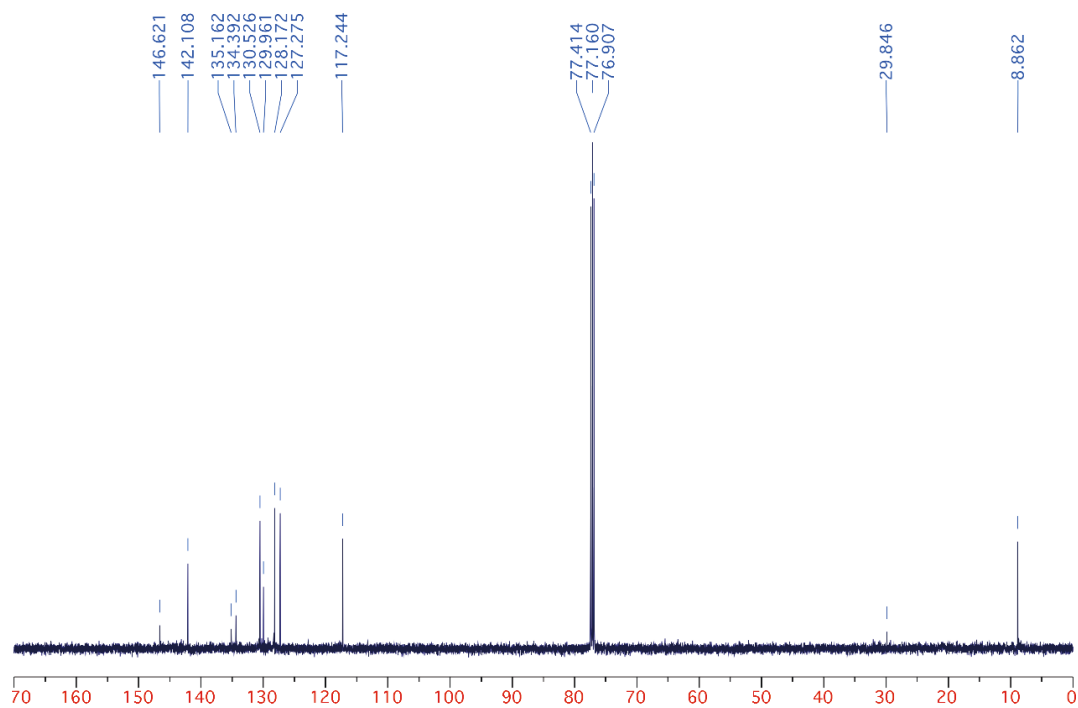


Appendix B.21 8-Phenyl-4,4'-diethyl-bora-3a,4a-diaza-s-indacene (**8BEt2**)

¹H NMR Spectrum in CDCl₃

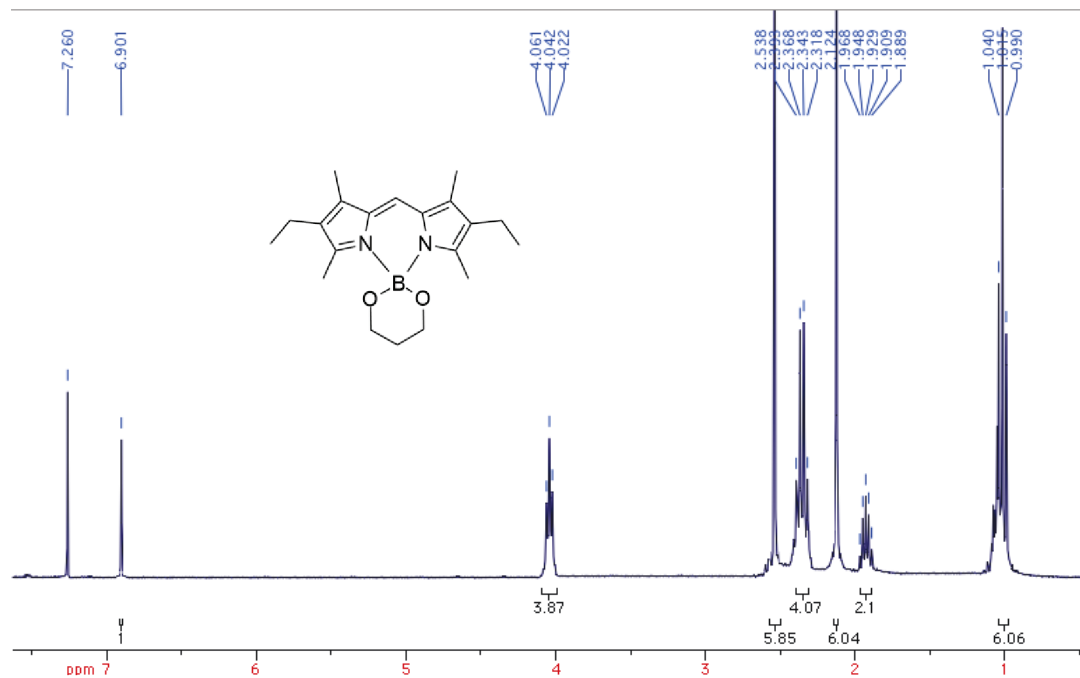


¹³C NMR Spectrum in CDCl₃

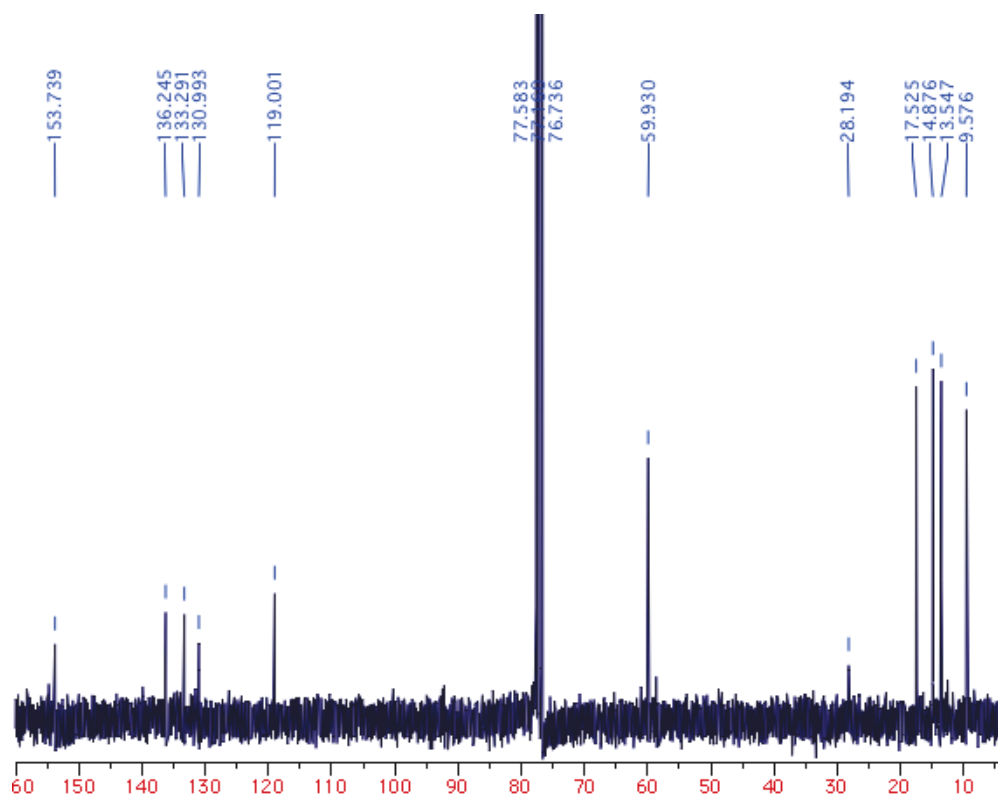


Appendix B.22 1,3,5,7-Tetramethyl-2,6-diethyl-8-*H*-4,4'-[propane-1,3-bis(olate)]-bora-3a,4a-diaza-*s*-indacene (**17**)

¹H NMR Spectrum in CDCl₃

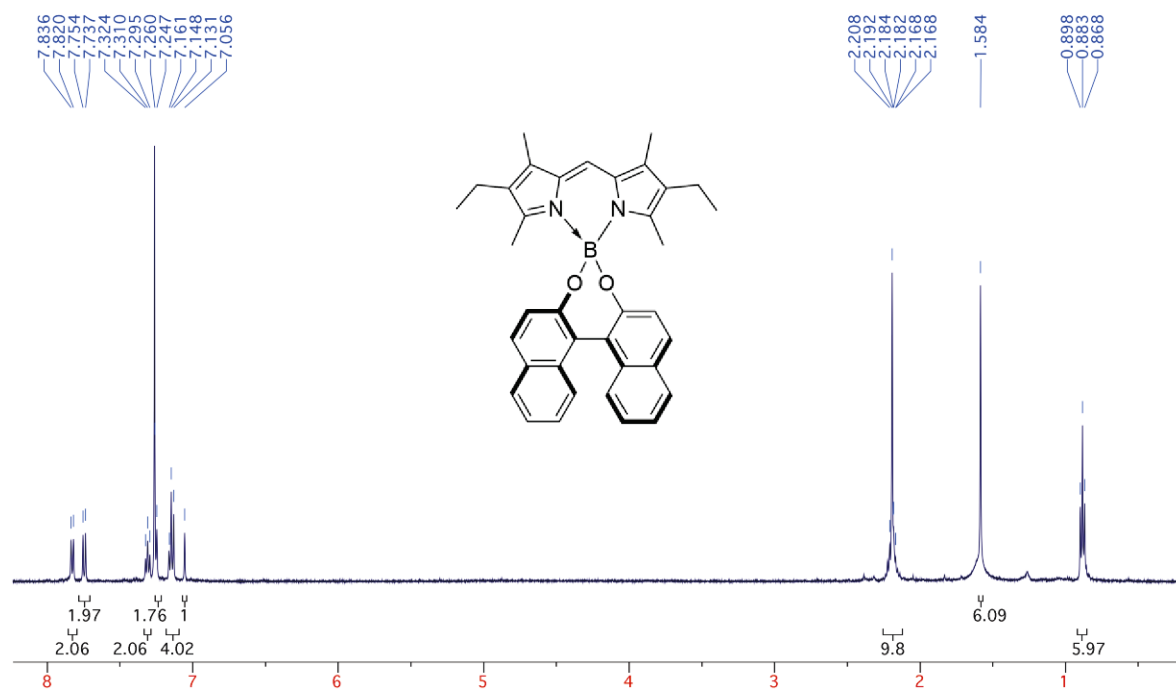


¹³C NMR Spectrum in CDCl₃

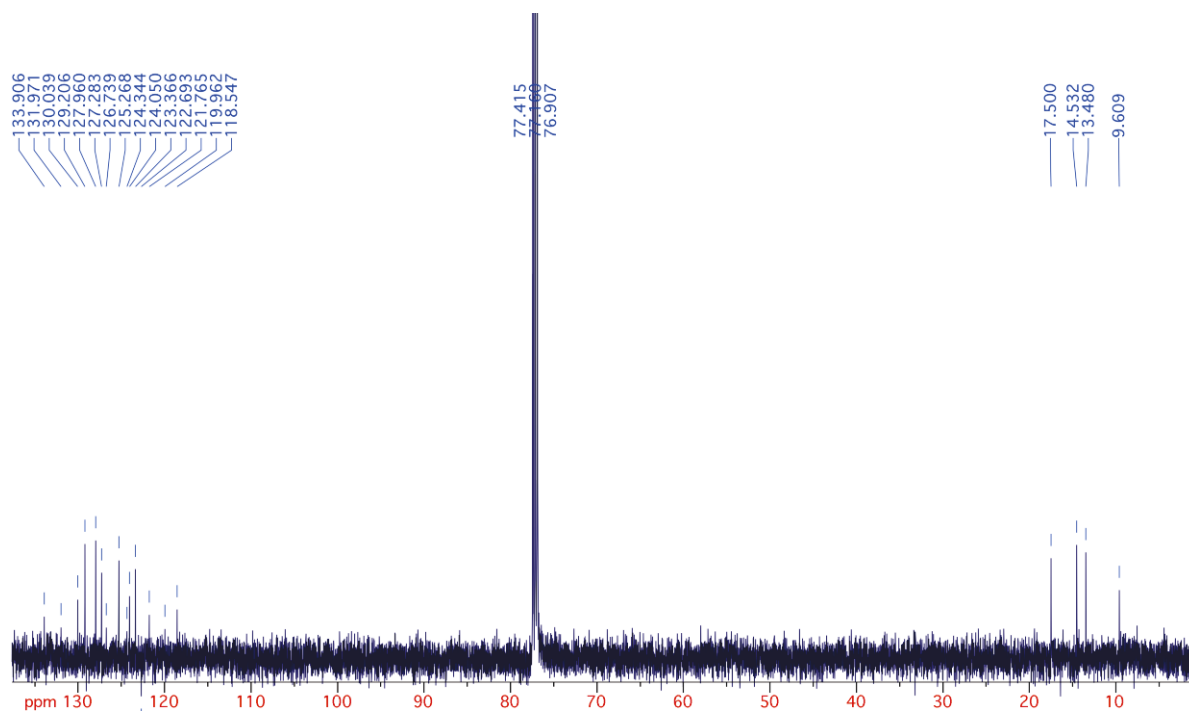


Appendix B.23 1,3,5,7-Tetramethyl-2,6-diethyl-8-*H*-4,4'-[(1,1'-binaphthalene)-2,2'-bis(olate)]-bora-3a,4a-diaza-*s*-indacene (**18**)

¹H NMR Spectrum in CDCl₃

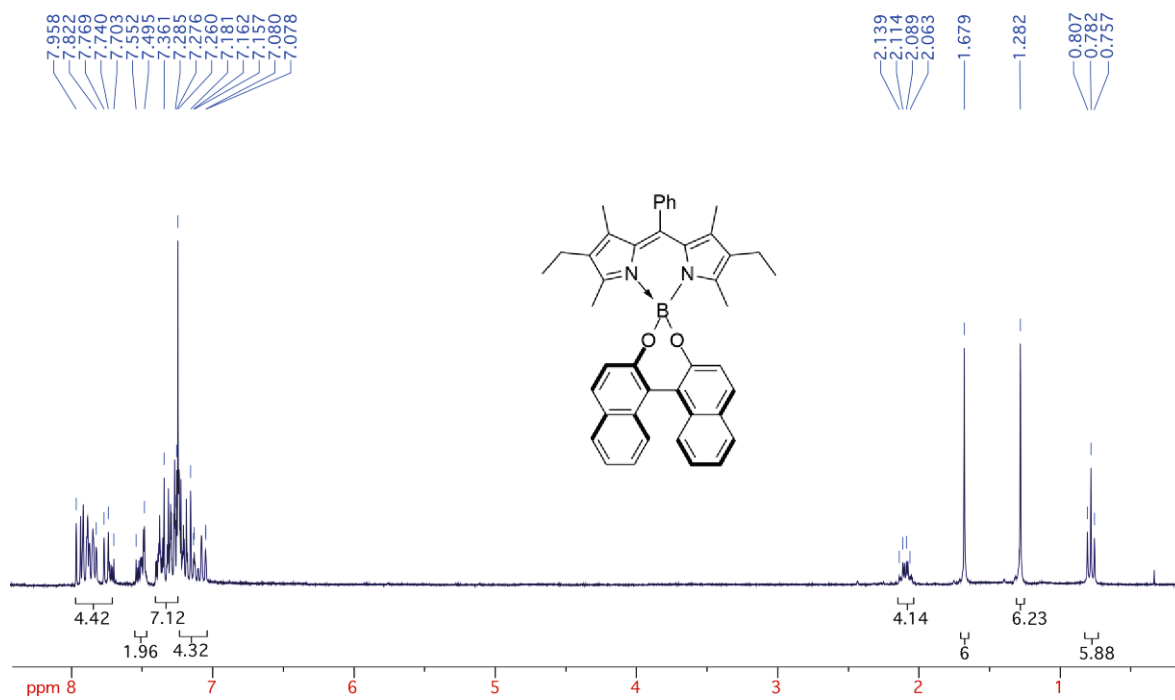


¹³C NMR Spectrum in CDCl₃

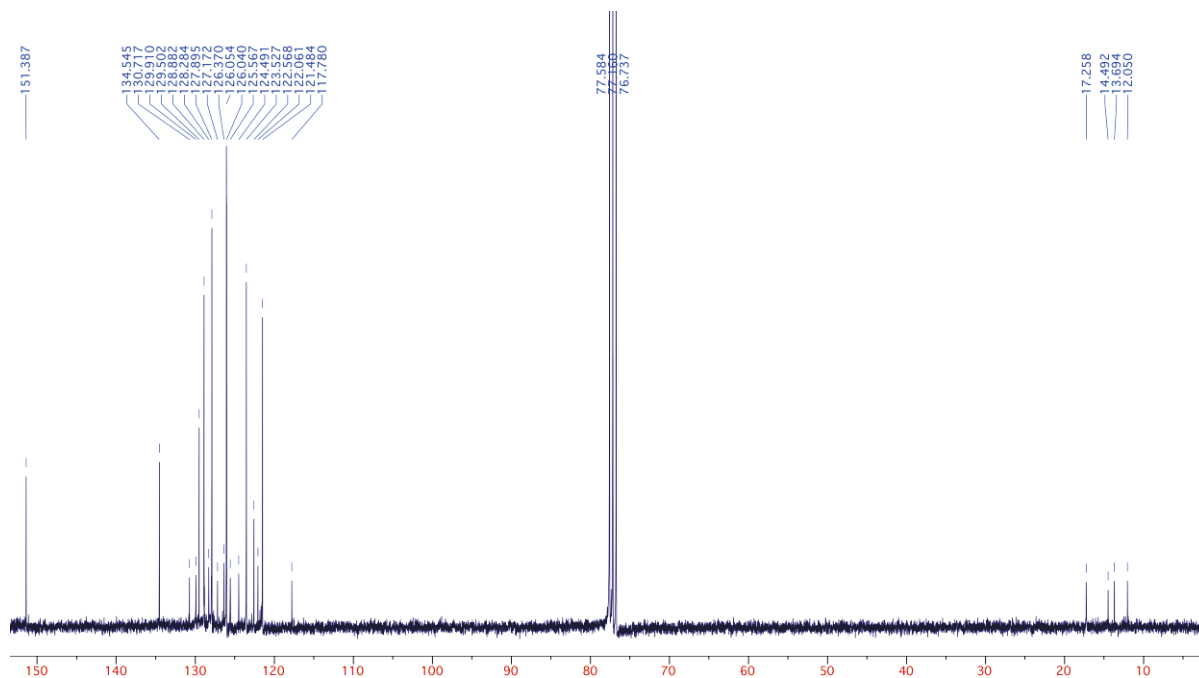


Appendix B.24 1,3,5,7-Tetramethyl-2,6-diethyl-8-phenyl-4,4'-[(1,1'-binaphthalene)-2,2'-bis(olate)]-bora-3a,4a-diaza-*s*-indacene (**20**)

¹H NMR Spectrum in CDCl₃

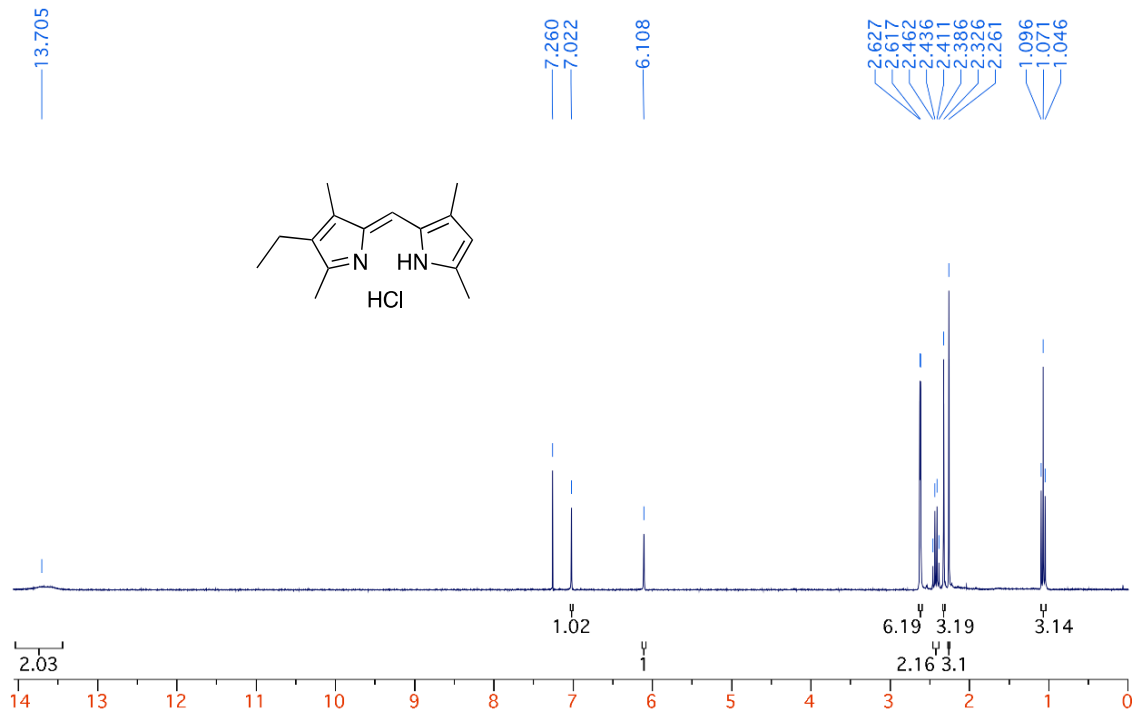


¹³C NMR Spectrum in CDCl₃

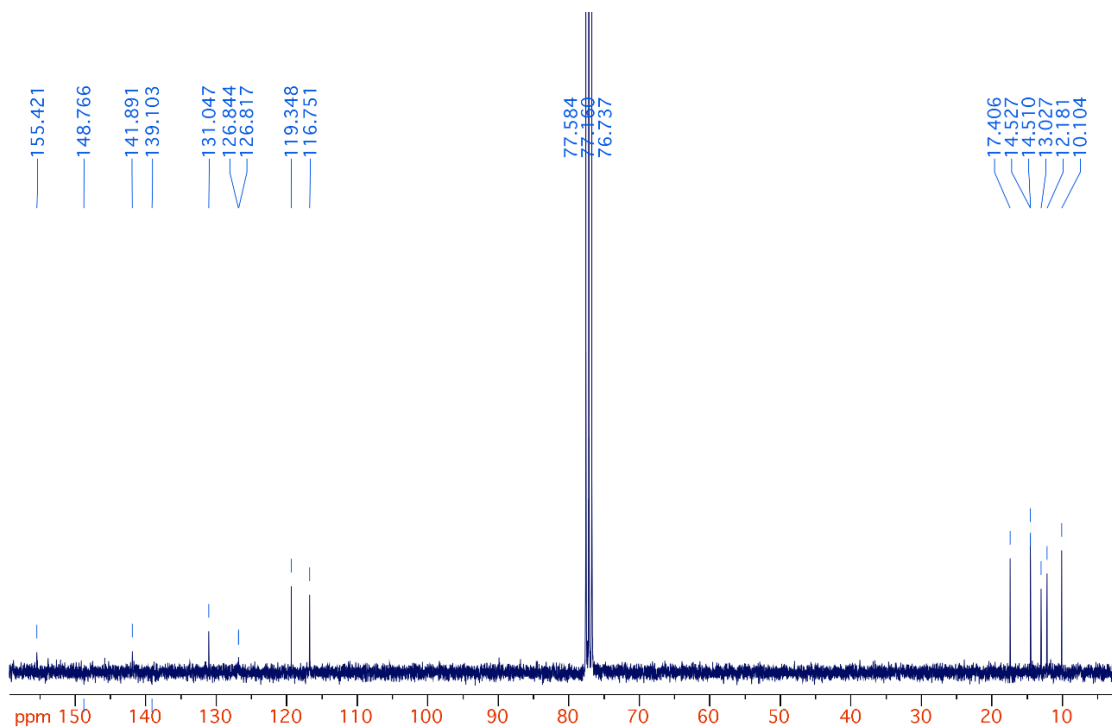


Appendix B.25 (Z)-2-((4-Ethyl-3,5-dimethyl-2*H*-pyrrol-2-ylidene)methyl)-3,5-dimethyl-1*H*-pyrrole hydrochloride (**2HCl**)

¹H NMR Spectrum in CDCl₃

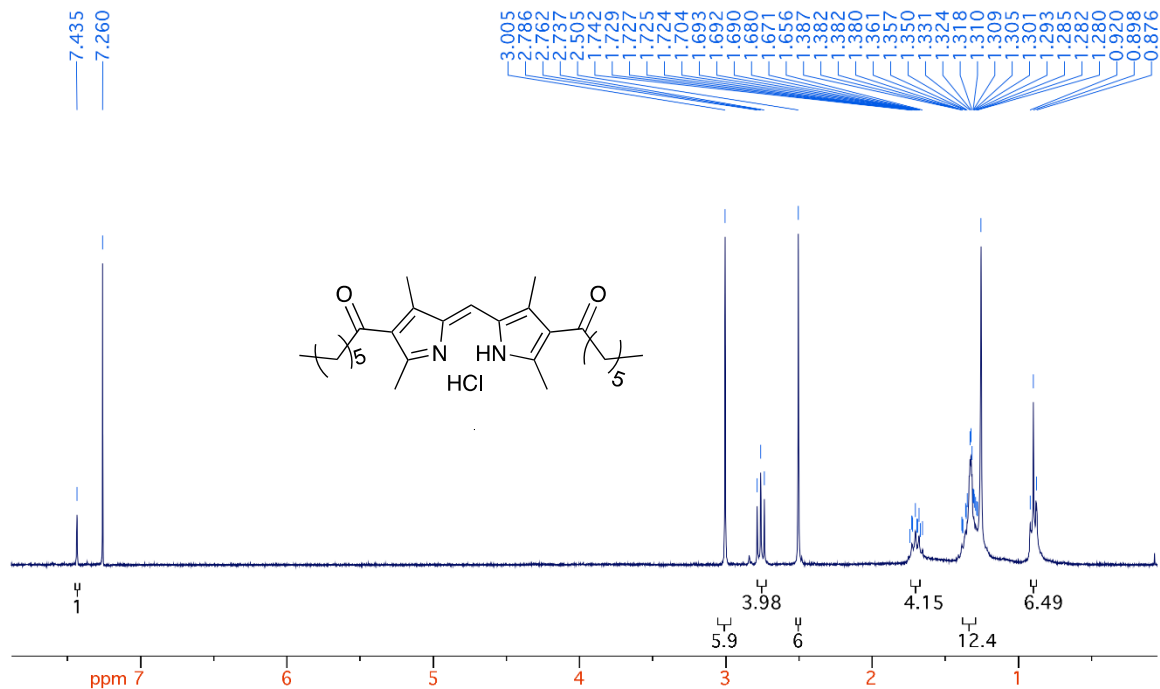


¹³C NMR Spectrum in CDCl₃

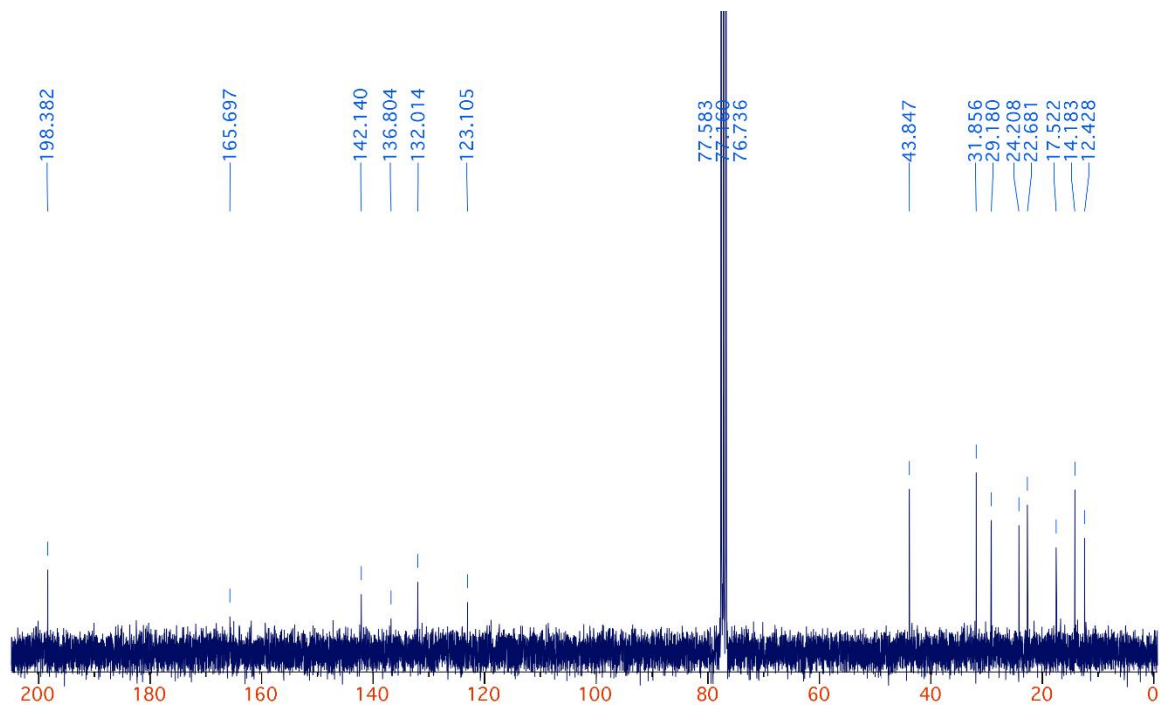


Appendix B.26 (Z)-1-(2-((4-Heptanoyl-3,5-dimethyl-1*H*-pyrrol-2-yl)methylene)-3,5-dimethyl-2*H*-pyrrol-4-yl)heptan-1-one hydrochloride (**22HCl**)

¹H NMR Spectrum in CDCl₃

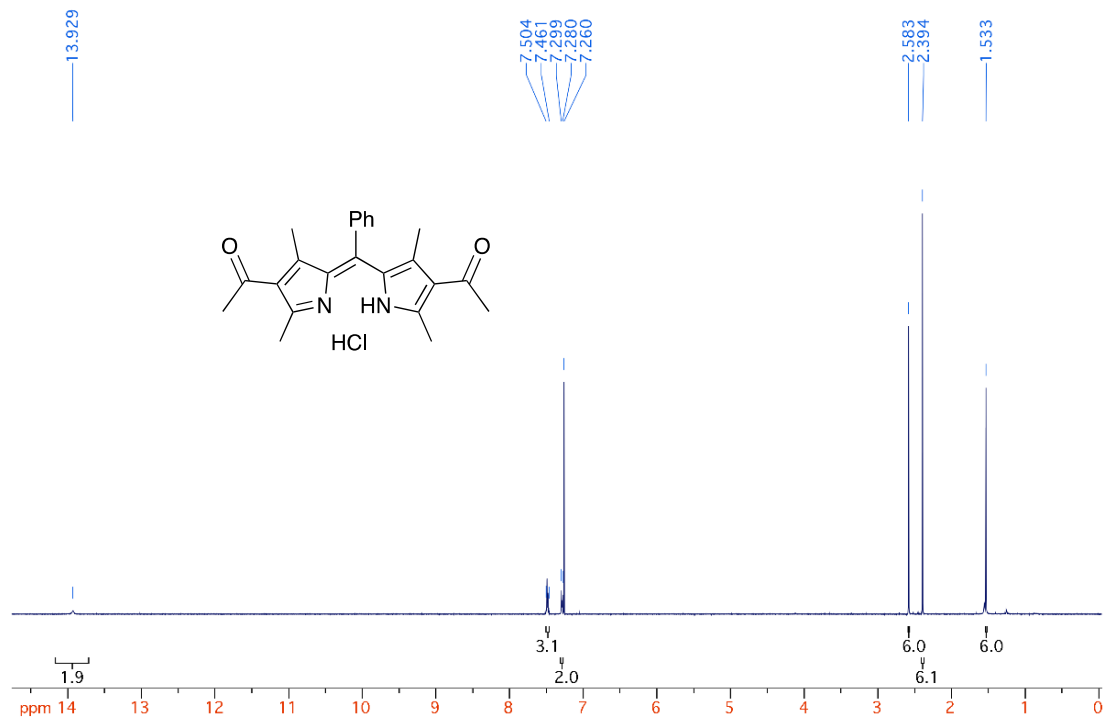


¹³C NMR Spectrum in CDCl₃

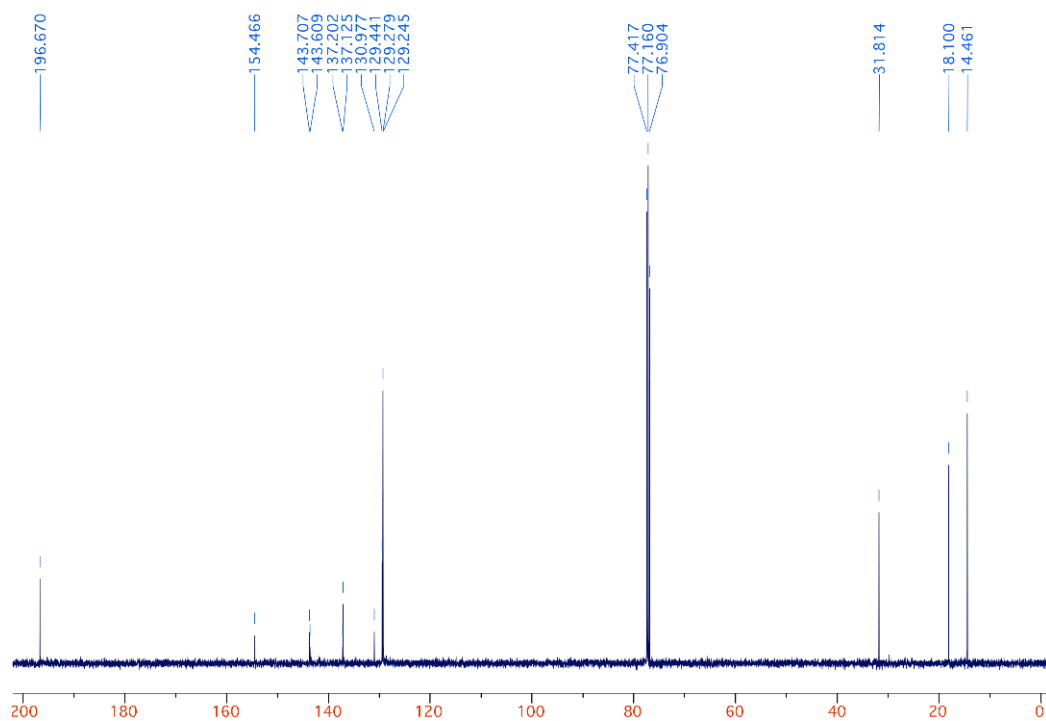


Appendix B.27 (*Z*)-1-(2-((4-Acetyl-3,5-dimethyl-1*H*-pyrrol-2-yl)(phenyl)methylene)-3,5-dimethyl-2*H*-pyrrol-4-yl)ethanone hydrochloride (**23HCl**)

¹H NMR Spectrum in CDCl₃

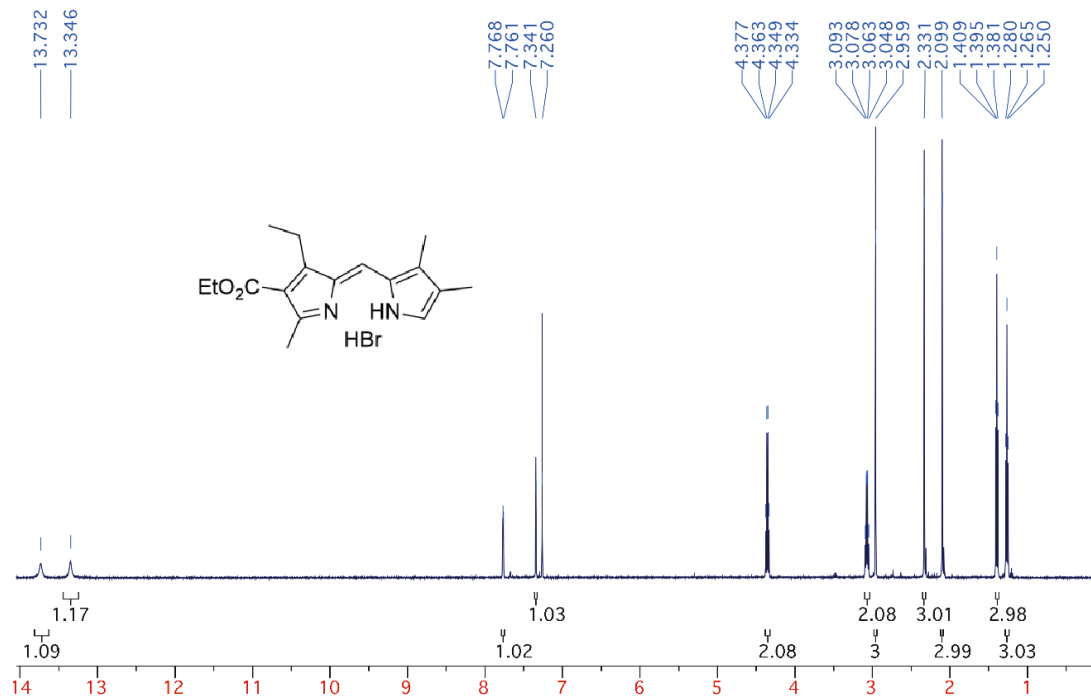


¹³C NMR Spectrum in CDCl₃

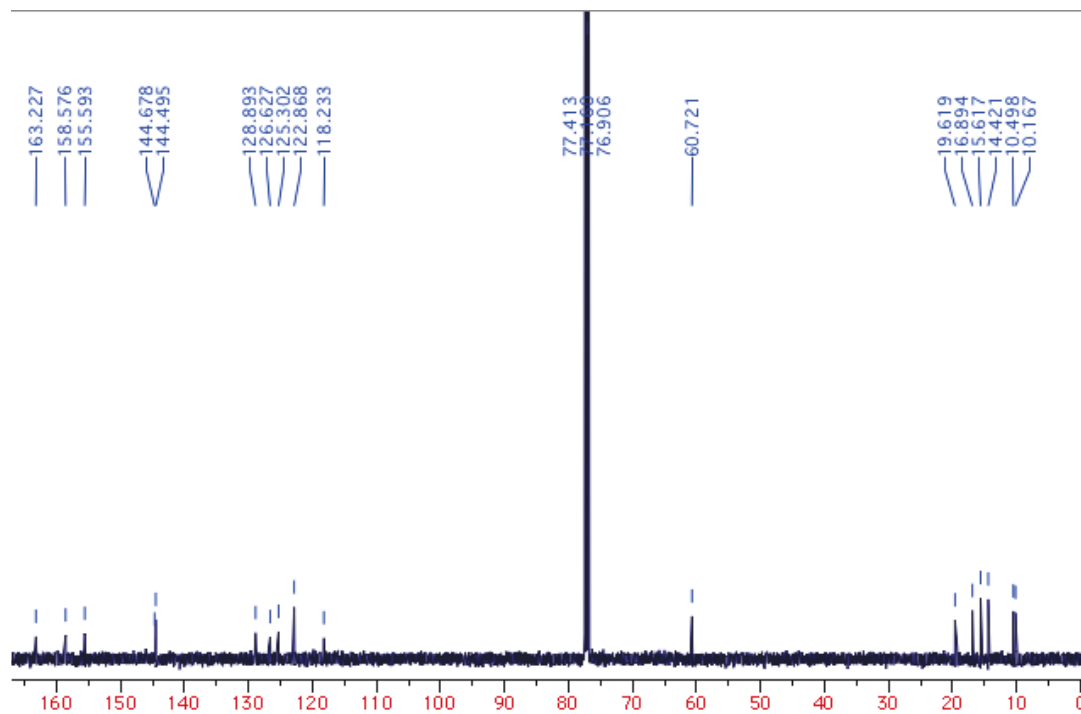


Appendix B.28 (*Z*)-Ethyl 2-((3,4-dimethyl-1*H*-pyrrol-2-yl)methylene)-3-ethyl-5-methyl-2*H*-pyrrole-4-carboxylate hydrobromide (**24HBr**)

¹H NMR Spectrum in CDCl₃

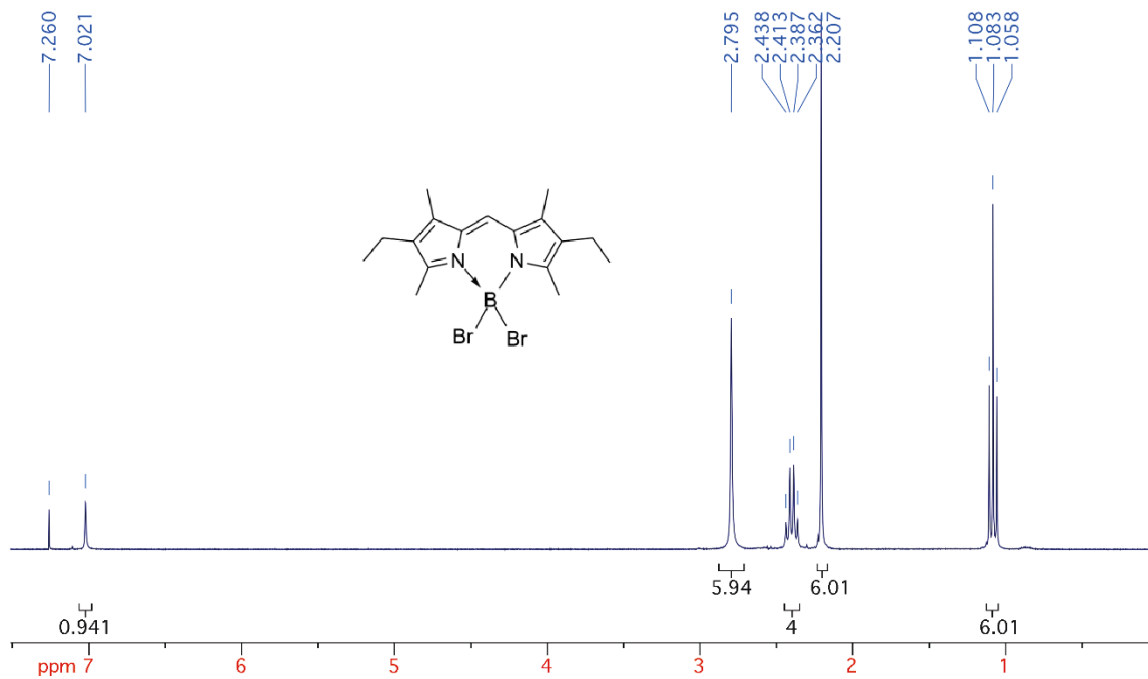


¹³C NMR Spectrum in CDCl₃

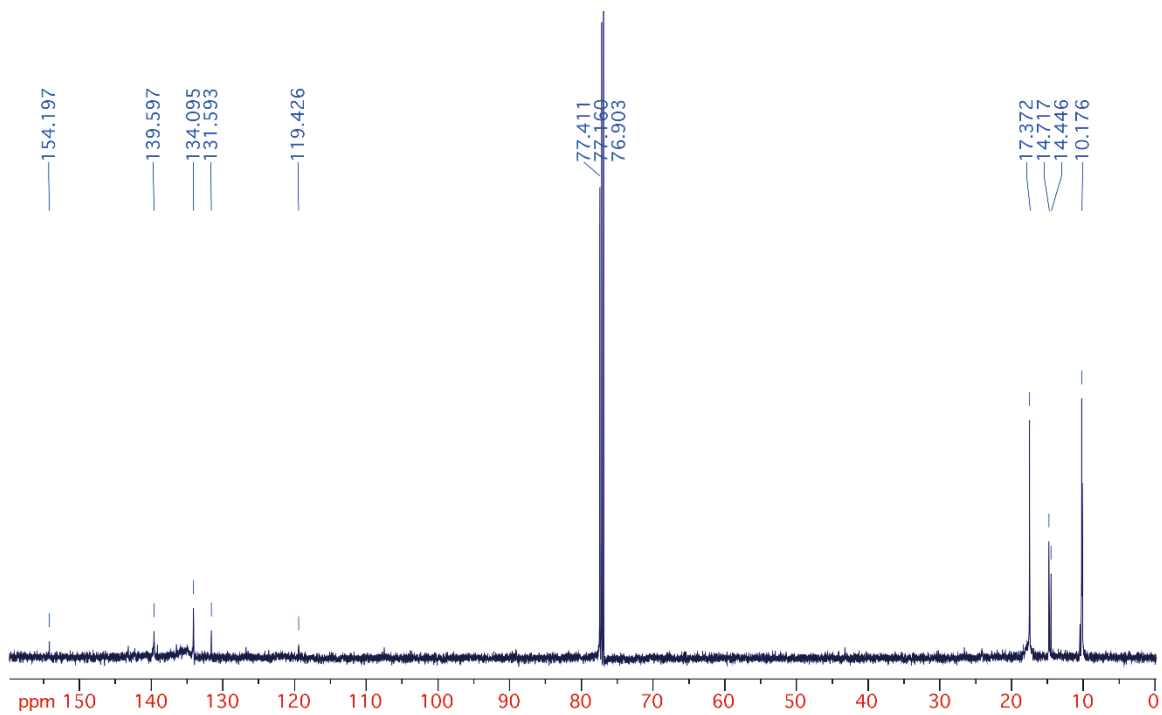


Appendix B.29 1,3,5,7-Tetramethyl-2,6-diethyl-8-*H*-4,4'-dibromo-bora-3a,4a-diaza-*s*-indacene (**3BBr₂**)

¹H NMR Spectrum in CDCl₃

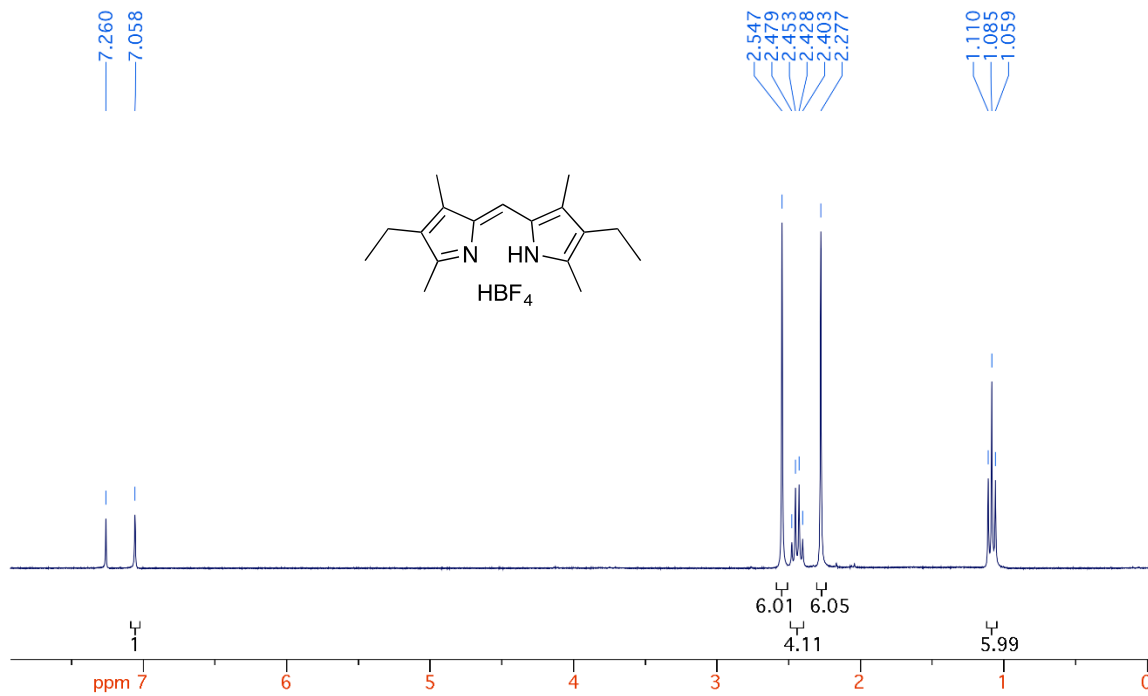


¹³C NMR Spectrum in CDCl₃

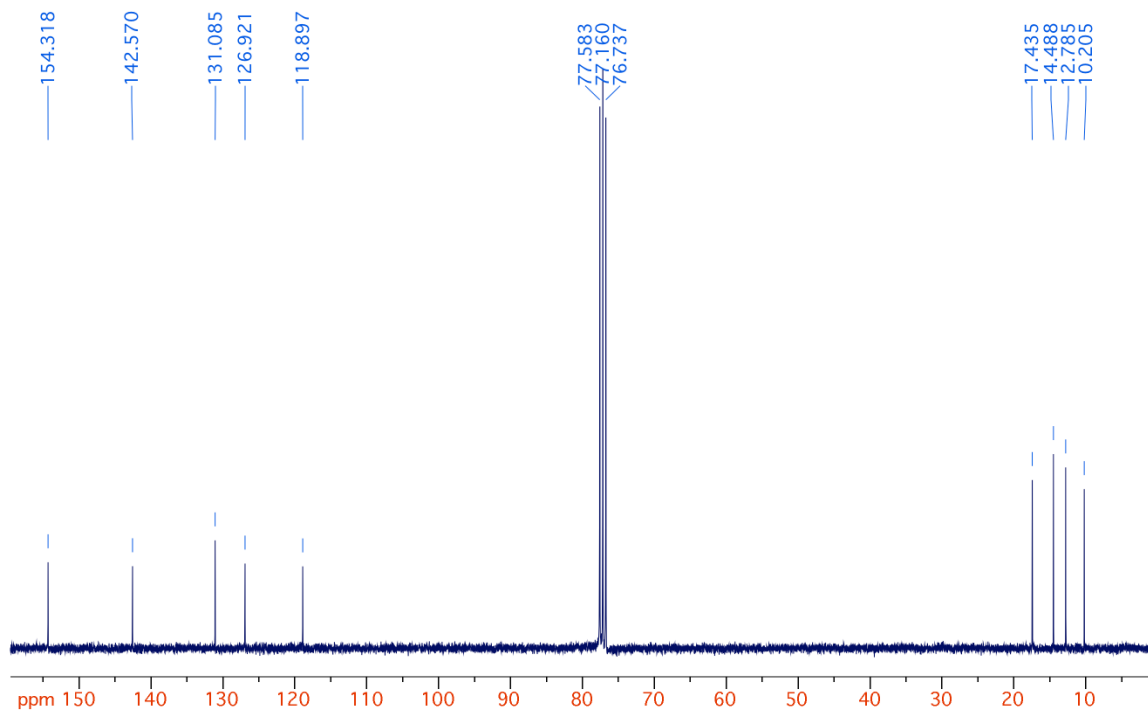


Appendix B.30 (*Z*)-3-Ethyl-5-((4-ethyl-3,5-dimethyl-2*H*-pyrrol-2-ylidene)methyl)-2,4-dimethyl-1*H*-pyrrole tetrafluoroborate (**3HBF₄**)

¹H NMR Spectrum in CDCl₃

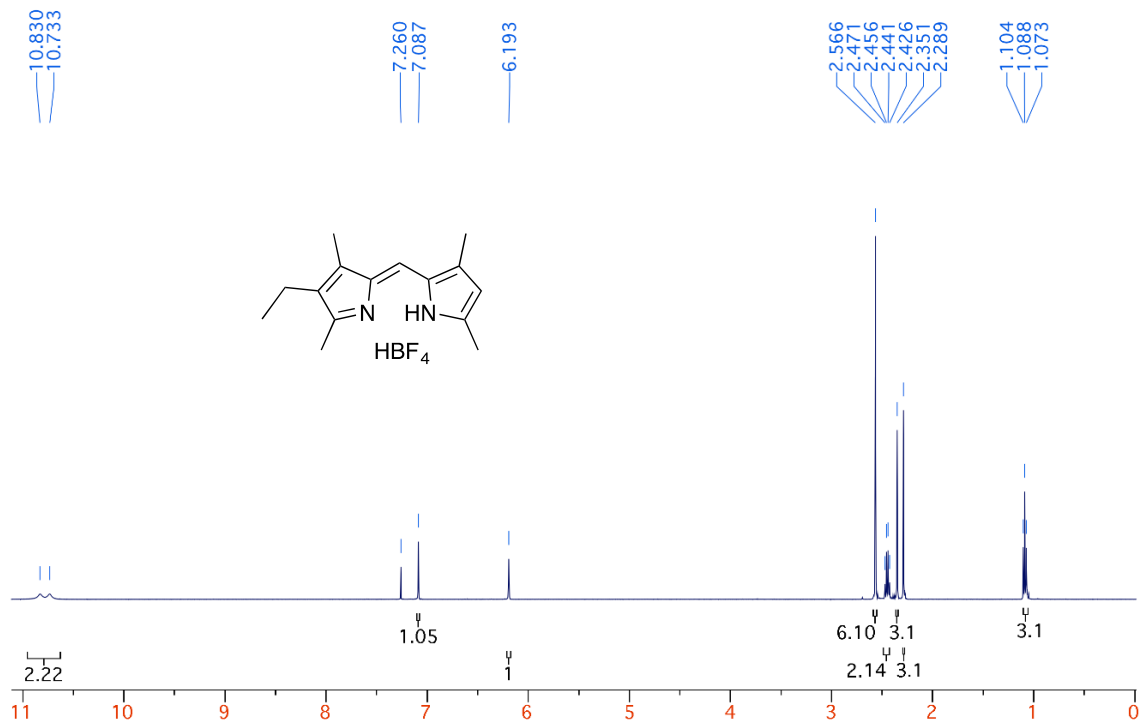


¹³C NMR Spectrum in CDCl₃

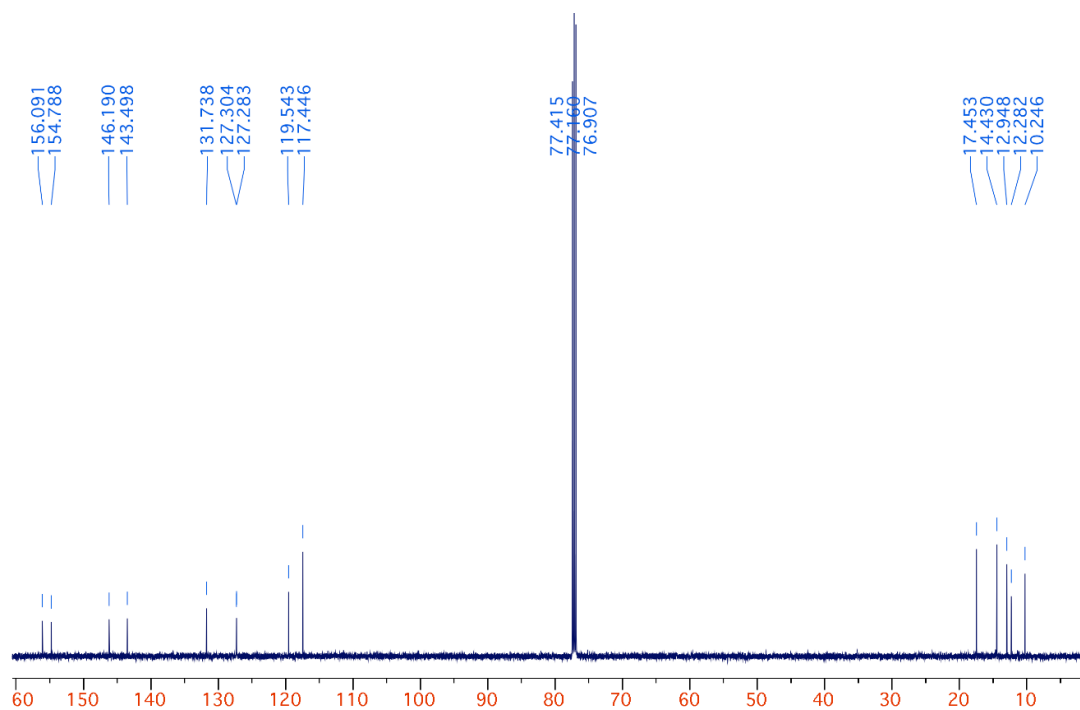


Appendix B.31 (Z)-2-((4-Ethyl-3,5-dimethyl-2*H*-pyrrol-2-ylidene)methyl)-3,5-dimethyl-1*H*-pyrrole tetrafluoroborate (**2HBF₄**)

¹H NMR Spectrum in CDCl₃

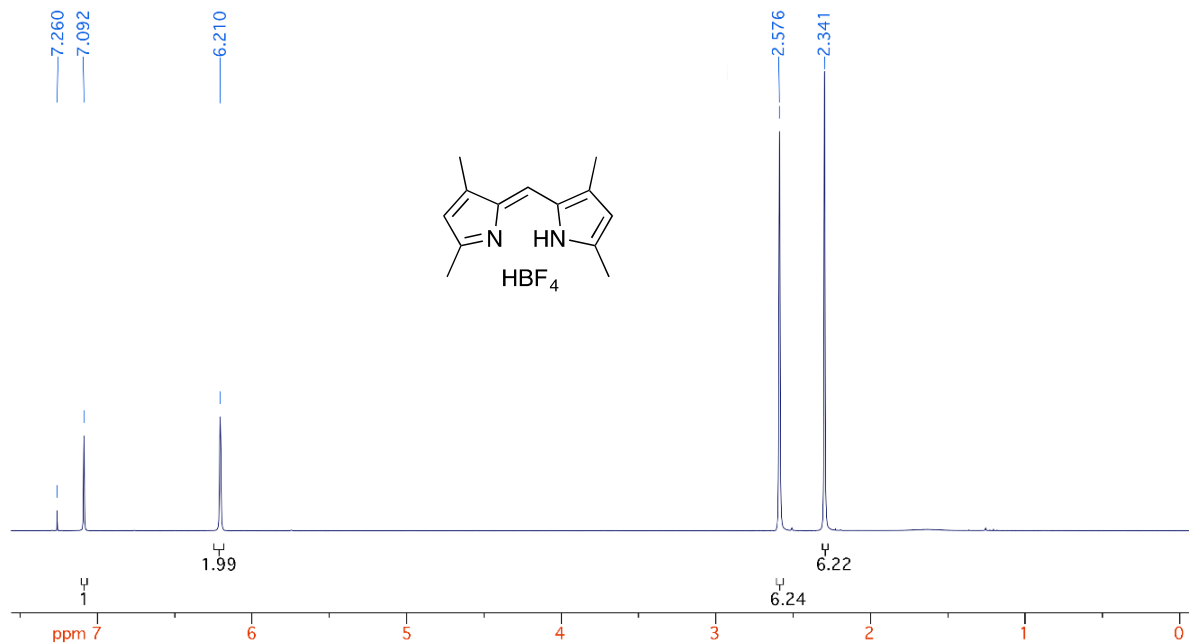


¹³C NMR Spectrum in CDCl₃

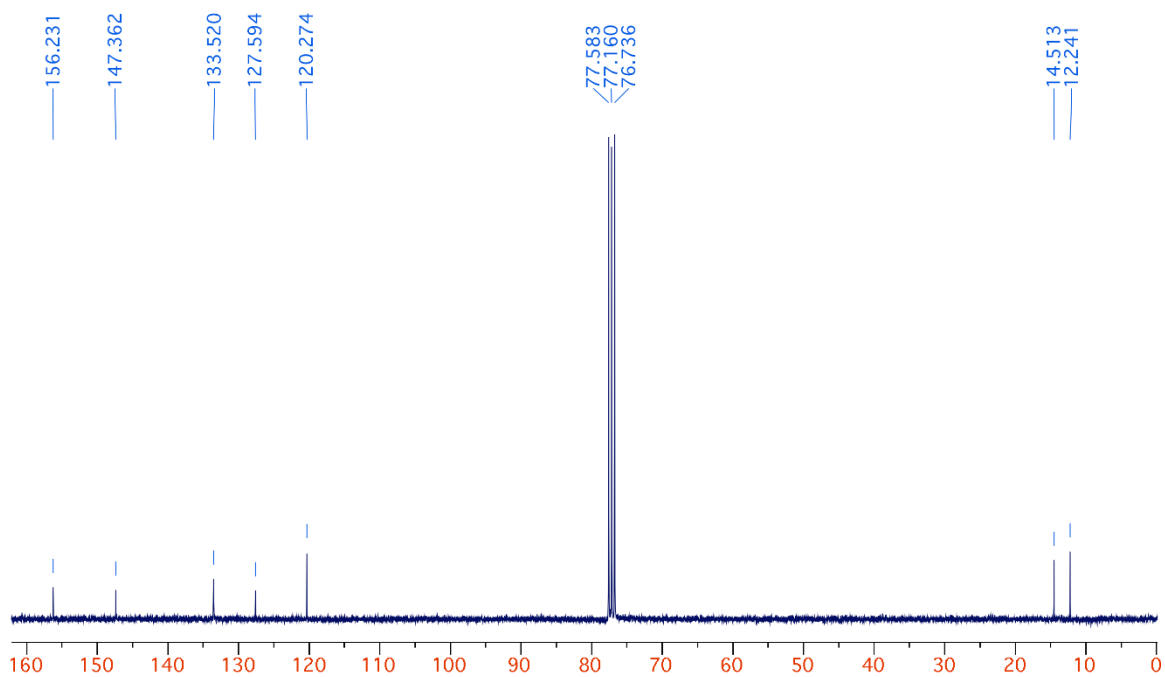


Appendix B.32 (*Z*)-2-((3,5-Dimethyl-2*H*-pyrrol-2-ylidene)methyl)-3,5-dimethyl-1*H*-pyrrole tetrafluoroborate (**4HBF₄**)

¹H NMR Spectrum in CDCl₃

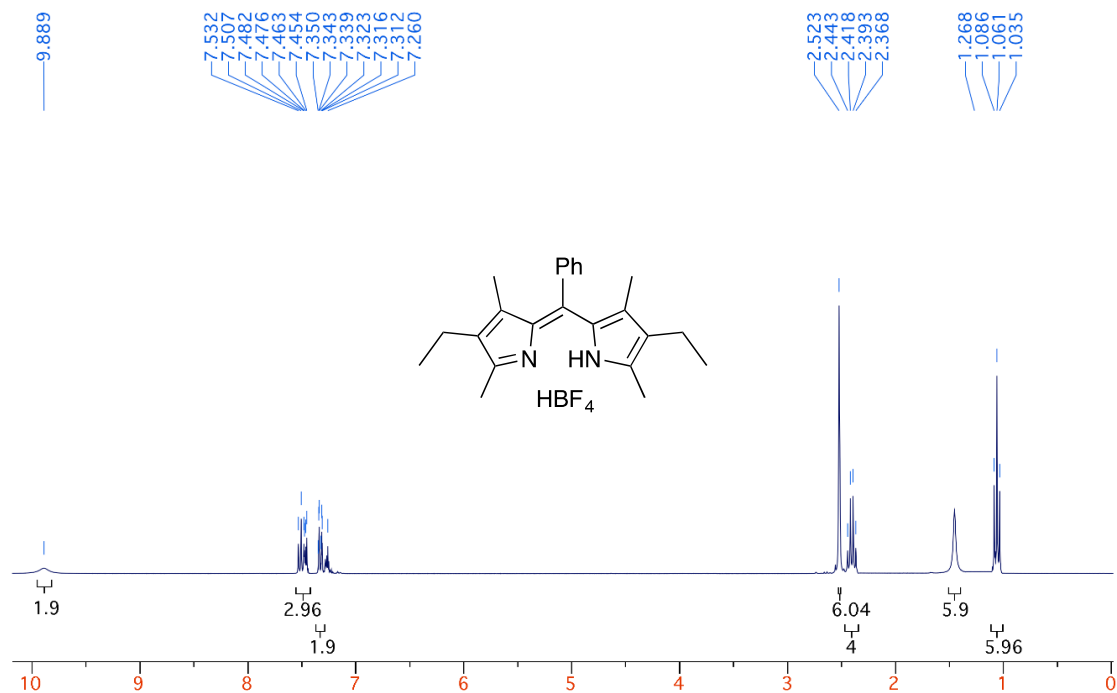


¹³C NMR Spectrum in CDCl₃

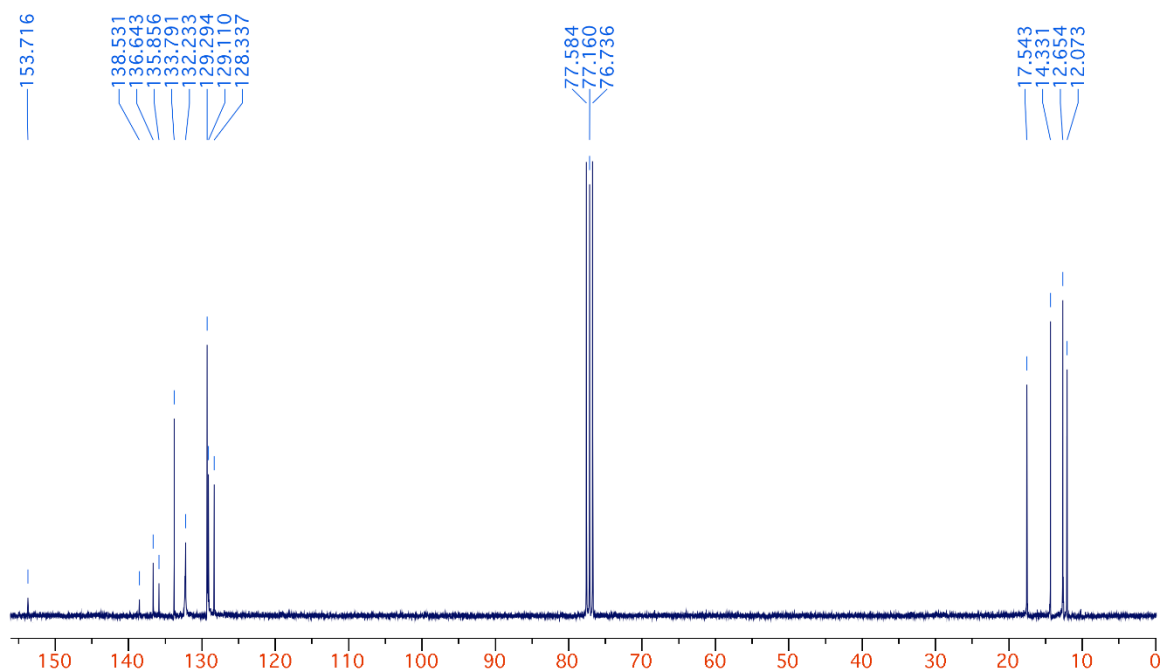


Appendix B.33 (Z)-3-Ethyl-5-((4-ethyl-3,5-dimethyl-2*H*-pyrrol-2-ylidene)(phenyl)methyl)-2,4-dimethyl-1*H*-pyrrole tetrafluoroborate (**5HBF₄**)

¹H NMR Spectrum in CDCl₃

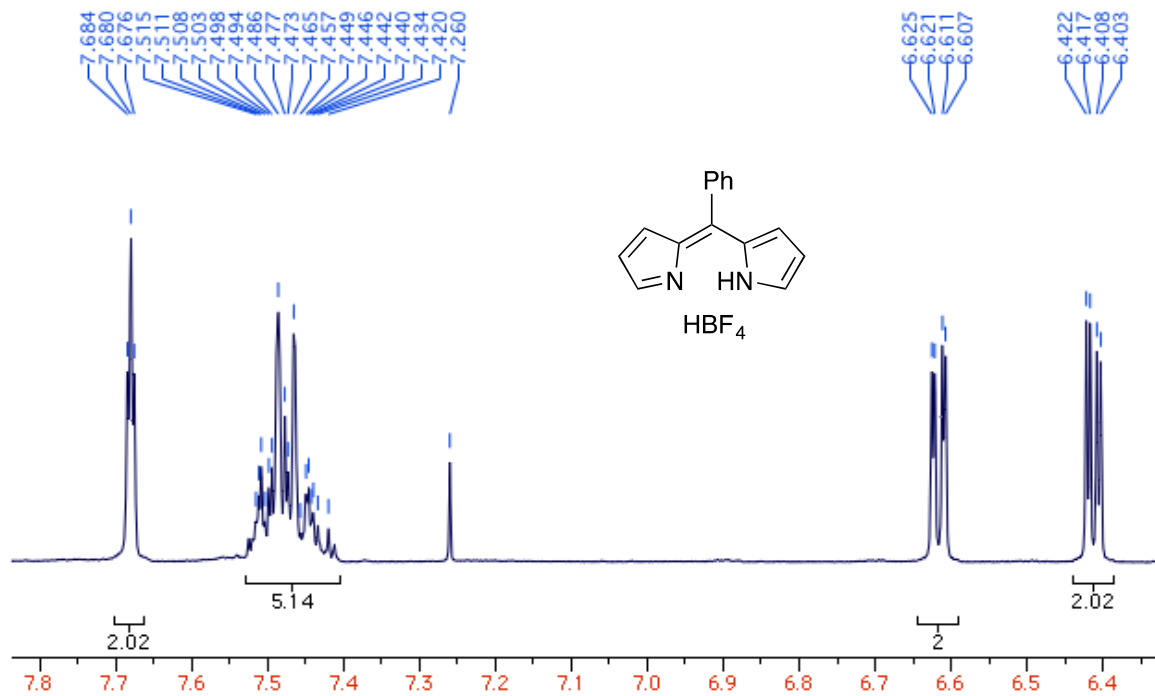


¹³C NMR Spectrum in CDCl₃



Appendix B.34 (*Z*)-2-(Phenyl(2*H*-pyrrol-2-ylidene)methyl)-1*H*-pyrrole tetrafluoroborate (**8HBF₄**)

¹H NMR Spectrum in CDCl₃



¹³C NMR Spectrum in CDCl₃

